

Universidade Federal do Rio Grande do Sul - UFRGS
Instituto de Biociências, Centro de Biotecnologia e Departamento de Botânica
Laboratório de Fisiologia Vegetal

**Caracterização de novos transportadores possivelmente envolvidos em
homeostase de Fe e Zn em plantas de arroz (*Oryza sativa L.*)**

Candidato: M. Sc. Felipe Klein Ricachenevsky

Tese submetida ao Programa
de Pós-Graduação em
Biologia Celular e Molecular
da UFRGS como requisito
parcial para a obtenção do
título de Doutor.

Orientadora: Profa. Janette Palma Fett, Ph.D.

Porto Alegre, Março de 2013

"The true value of a man is not determined by his possession, supposed or real, of Truth, but rather by his sincere exertion to get to the Truth. It is not possession of the Truth, but rather the pursuit of Truth by which he extends his powers and in which his ever-growing perfectibility is to be found. Possession makes one passive, indolent, and proud. If someone was to hold all Truth concealed in his right hand, and in his left only the steady and diligent drive for Truth, albeit with the proviso that I would always and forever err in the process, and offer me the choice, I would with all humility take the left hand"

Modified: Gotthold Ephraim Lessing, Anti-Goeze (1778)

Agradecimentos

Agradeço primeiramente à minha orientadora, Janette Palma Fett, pelo apoio e pela confiança depositada no trabalho, possibilitando que eu me deslocasse frequentemente durante o doutorado, seja para a realização de experimentos ou não. Também pela liberdade proporcionada; certamente o aprendizado seria menor se não me fosse permitido aprender com meus próprios erros. Muito obrigado por acreditar em mim.

À minha co-orientadora do estágio sanduíche, Mary Lou Guerinot, pela oportunidade de trabalhar em seu laboratório no Dartmouth College; pela confiança, dedicação e incansável apoio. O teu exemplo como cientista e mentora me faz acreditar cada vez mais que a excelência não é um feito, mas um hábito. Muito obrigado por acreditar em mim e no meu trabalho.

Ao Dr. David E. Salt, por me acolher em seu laboratório na Purdue University, e pelo constante apoio e confiança. Também pela possibilidade de realizarmos diversas análises de amostras em Purdue e em Aberdeen, o que foi indispensável para a realização deste trabalho.

Ao Arthur, pela atenção dedicada ao laboratório e estrutura associada, e por manter acessível todo o seu conhecimento. És um exemplo do que um biólogo de plantas deve saber sobre seu objeto de estudo. Um dia chego lá. Também agradeço pelo trabalho como revisor da tese.

Aos membros da comissão de acompanhamento, Dr. Augusto Schrank e Dr. Rogério Margis, pelas conversas e discussões. Também agradeço aos membros da banca examinadora, Dr. Charley Staats, Dra. Luciane Passaglia e Dra. Adriana Hemerly, por analisarem o trabalho. Aos amigos do PPGBCM, em especial ao Charley e à Lívia, sempre prontos a ajudar e a fornecer reagentes faltantes para a realização de experimentos. E à Silvia e ao Luciano, exemplos de eficiência.

Aos colegas do Laboratório de Fisiologia Vegetal, novos e antigos: a ala masculina, Raul, Ricardo, Guilherme, Vinícius, Diogo, Hélio, Júlio, Jonata; a feminina, Paloma, Karina, Naíla, Carol, Joséli, Márcia, Kelly, Lívia, Variluska, Edilena, Ariane, Joseane, Cibele, Janete, Fernanda, Anna. São tantos nesses oito anos de convívio que já nem sei quais estavam em que época, e certamente esqueci de alguns. Obrigado por

fazerem do laboratório um bom lugar para estar. Em especial, agradeço aos meus dois grandes amigos, colegas e colaboradores Raul Sperotto e Paloma Menguer: vocês foram indispensáveis nesses quatro anos. Obrigado pelo apoio em todos os aspectos, e por acreditarem e confiarem em mim. A nossa parceria ainda vai se estender por muitos tempo, tanto no trabalho quanto em churrascos.

Aos membros do Guerinot Lab, que me acolheram “como um deles” na minha estadia lá: Tracy, Maria, Sichul, Heng-Hsuan, Amanda, Jessica, Suna, Christine, Ali, Garo, Suzana. Em especial, agradeço à Tracy pela paciência para me ensinar sobre SXRF e por levar para as diferentes “beamlines”, e pela amizade. A tua dedicação em “bridge the gap” entre dois campos de pesquisa é inspiradora. Obrigado por permitir que eu aprendesse tanto contigo. Também agradeço aos membros do Salt Lab, por abrirem as portas para mim: Brett, Elena, Jessica, Prashant, Matt, Xinyuan, Daiyin, Hong-Bin.

Aos demais amigos, que por sorte são muitos e em muitos lugares, e por isso aqui resumidos: Mathias, Rafael, Tiago, Gustavo, Daniel, Luiza, Bruno, Bina, Alexandre, Márcio, Bianca, Deinha. Aos “americanos” Nat, Yan, Masha, Dea, Max, Tom, Violet e Bob, Ricky, Caroline, Britta, Susan e Carryl (e família Andersen); obrigado por me fazer sentir em casa mesmo longe de casa.

À minha família, sempre sensacional. Obrigado pelo apoio e pelo carinho, vocês são inestimáveis. Em família incluo meus sogros, por me ajudarem o tempo todo e muito mais do que eu poderia pedir. Ao meu irmão, Rafael, por ter entrado na minha vida e me ensinado o quanto ela pode ser simples. Ao meu pai, por estar sempre ao meu lado, pelo apoio e amor incondicionais, e por me compreender e estimular. Te amo muito, pai.

À minha mãe, que sempre me estimulou a seguir a carreira acadêmica; que acreditava que formação e conhecimento eram os bens mais importantes; e que cada um deveria dar seu máximo em qualquer atividade. Ela certamente estaria feliz nesse momento. Te amo muito, mãe.

E por último, agradeço à minha melhor amiga, namorada, noiva, esposa, Andréa. Teu carinho e suporte está em meio a todo esse trabalho, e em cada momento desde que te conheci. Obrigado por estar ao meu lado, sempre. Te amo demais, Wendy.

Obrigado!

Instituições onde o trabalho foi desenvolvido:

- Laboratório de Fisiologia Vegetal da Universidade Federal do Rio Grande do Sul, RS, Brasil.
- *Salt Lab, Purdue University*, Indiana, Estados Unidos.
- *Guerinot Lab, Dartmouth College*, Estados Unidos.
- *National Synchrotron Light Source (NSLS), Brookhaven National Laboratory (BNL)*, New York, Estados Unidos.
- *Stanford Synchrotron Radiation Lightsource (SSRL), Stanford University*, California, Estados Unidos.
- *Advanced Photon Source (APS), Argonne National Laboratory*, Illinois, Estados Unidos.

Fontes Financiadoras:

- Conselho Nacional de Desenvolvimento Científico e Tecnológico (CNPq)
- Coordenação de Aperfeiçoamento de Pessoal de Nível Superior (CAPES)
- *The National Science Foundation (NSF)*, USA.
- *The National Institutes of Health (NIH)*, USA.
- *The Department of Energy (DOE)*, USA.

Índice

Resumo	1
Abstract	2
Lista de Abreviaturas	3
Introdução Geral	6
1. Arroz	7
2. Nutrição mineral (Fe e Zn) em humanos	8
2.1 Importância de Fe em humanos.....	8
2.2 Importância de Zn em humanos.....	10
3. Homeostase de Fe em plantas	12
3.1 Absorção de Fe nas raízes.....	13
3.2 Transporte radial e carregamento do xilema	15
3.3 Transporte de Fe na parte aérea e remobilização por meio de carregamento do floema.....	18
3.4 Transporte de Fe para as sementes.....	20
4. Homeostase de Zn em plantas	23
4.1 Absorção de Zn nas raízes.....	25
4.2 Transporte radial e carregamento do xilema.....	26
4.3 Transporte de Zn na parte aérea e remobilização por meio de carregamento do floema.....	28
4.4 Transporte de Zn para as sementes.....	29
5. Transportadores da família ZIP (ZRT/IRT - Zinc-Regulated/ Iron-Regulated Transporter)	30
6. Biofortificação de grãos de arroz	31
7. Linhagens de <i>Arabidopsis thaliana</i> Rice Full-length Over-expressors (FOX)	34
8. As técnicas de <i>inductively coupled plasma</i> (ICP-MS) e <i>synchrotron X-ray fluorescence</i> (SXRF) no estudo do ionoma de plantas	35
8.1 Uso de ICP-MS no estudo do ionoma de plantas e o <i>ionomicsHub</i>	35
8.2 Uso de SXRF no estudo na homeostase de metais em plantas.....	36

9. Tricomas.....	38
Objetivos.....	40
1. Objetivo Geral.....	41
2. Objetivos específicos.....	41
 Capítulo 1: “ZINC-INDUCED FACILITATOR-LIKE family in plants: lineage-specific expansion in monocotyledons and conserved genomic and expression features among rice (<i>Oryza sativa</i>) paralogs”	42
 Abstract.....	43
1. Background.....	43
2. Results.....	44
 2.1 ZIFL genes in plants.....	44
2.2 ZIFL proteins are a distinct family of MFS transporters.....	45
2.3 ZIFL gene expansion is lineage specific.....	45
2.4 ZIFL paralogs are unequally distributed in the rice genome.....	46
2.5 OsZIFL genes organization is highly conserved.....	46
2.6 Protein motif composition reveals a variable region in the ZIFL family.....	49
2.7 Expression of OsZIFL genes in rice vegetative and reproductive organs.....	51
2.8 The Fe-deficiency element IDE1 is enriched in promoters of OsZIFL genes.....	51
2.9 Zn-excess and Fe-deficiency regulate OsZIFL expression mainly in rice roots.....	53
2.10 OsZIFL duplicated pairs are co-expressed in specific plant organs and in response to stresses.....	55
 3. Discussion.....	56
3.1 ZIFL expansion through segmental duplication.....	56
3.2 Sequence and expression analyses suggest new functional sites in OsZIFL proteins and insights about duplicated gene pairs.....	57
3.3 Expression of OsZIFL genes is involved in the partially overlapping pathways of Zn-excess and Fe-deficiency responses.....	58
 4. Conclusions.....	59
 5. Methods.....	59

5.1 Plant material and treatments.....	59
5.2 Sequence retrieval and databases.....	59
5.3 Alignments and phylogenetic analyses.....	60
5.4 Exon-intron determination, motif finding and promoter analysis.....	60
5.5 Genevestigator.....	60
5.6 RNA extraction and cDNA synthesis.....	61
5.7 Quantitative RT-PCR and data analysis.....	61
5.8 Statistical analyses.....	61
6. References.....	62
Capítulo 2: “Elemental profiling of rice FOX lines leads to characterization of a new Zn transporter and uncovers a function for Zn accumulation in trichomes of <i>Arabidopsis thaliana</i>”.....	77
Abstract.....	79
1. Background.....	80
2. Results.....	82
2.1 Rice FOX lines selection.....	82
2.2 Elemental analysis of Rice FOX lines.....	83
2.3 OsZIP7 can complement yeast cells defective in Zn uptake.....	84
2.4 OsZIP7 is localized to the plasma membrane in <i>A. thaliana</i> protoplasts.....	84
2.5 Expression of OsZIP7 in <i>Arabidopsis</i> leads to enhanced Zn sensitivity and disruption of Zn root-to-shoot partitioning.....	84
2.6 Seeds of plants expressing OsZIP7 accumulate more Zn.....	85
2.7 OsZIP7 constitutive expression leads to alteration in Zn dynamic accumulation in leaves.....	86
2.8 High resolution SXRF imaging of trichomes suggest extracellular Zn localization in trichome cells.....	87
2.9 Variations in leaf Zn concentration change accumulation at the base of trichomes in <i>A. thaliana</i> natural accessions.....	88
3. Discussion.....	88
3.1 Coupling Rice FOX lines and ionomics profiling is a fast method for molecular characterization of metal-related genes from rice.....	89
3.2 OsZIP7 is a Zn influx plasma membrane transporter.....	89
3.3 Zn accumulates at the base of trichomes in <i>A. thaliana</i> , possibly at the extracellular space.....	91
3.4 Trichomes might have a role in metal detoxification.....	92
4. Materials and Methods.....	94

4.1 Plant materials and growth conditions.....	95
4.2 Elemental analyses by ICP-MS.....	95
4.3 Protoplast preparation and subcellular localization.....	96
4.4 Yeast mutants complementation.....	97
4.5 Preparation of samples for high-resolution two-dimensional SXRF raster scanning of trichomes.....	97
4.6 Synchrotron X-Ray Fluorescence (SXRF).....	99
4.7 Statistical analyses.....	100
5. References.....	102
6. Legends to Figures.....	120
7. Legends to Supplemental Figures.....	122
 Considerações Finais.....	 139
 1. Utilizando <i>A. thaliana</i> para transferir conhecimento de uma planta modelo para uma planta cultivada.....	 140
2. A nomenclatura <i>OsZIFL4</i> deve ser adotada em detrimento à <i>TOM1</i>.....	141
3. As proteínas ZIFL possivelmente possuem funções no efluxo de moléculas da família NA/DMA em plantas de arroz.....	142
4. O uso de linhagens FOX permite a identificação de genes envolvidos na homeostase de metais de maneira rápida.....	143
5. Localização e dinâmica de acúmulo de Zn em tricomas de <i>A. thaliana</i> indicam um novo mecanismo de detoxificação em não-hiperacumuladores.....	144
 Referências Gerais.....	 146
 Apêndice 1: Artigos publicados no período do doutorado fora do escopo da tese.....	 171
 Apêndice 2: Artigos submetidos no período do doutorado fora do escopo da tese.....	 172
 Apêndice 3: Curriculum vitae resumido.....	 173

Lista de Figuras e Tabelas

Introdução Geral.....	6
Figura 1. Estratégias para a captação de Fe a partir do solo.....	15
Figura 2. Via de biossíntese de fitossideróforos (PS) da família do ácido mugineico.....	19
Figura 3. Representação esquemática do processamento dos grãos de arroz.....	22
Figura 4. Possíveis etapas limitantes para o acúmulo de metais nos grãos.....	32
Capítulo 1: “ZINC-INDUCED FACILITATOR-LIKE family in plants: lineage-specific expansion in monocotyledons and conserved genomic and expression features among rice (<i>Oryza sativa</i>) paralogs”.....	42
Figure 1. ZIFL family sequence signatures.....	46
Figure 2. Phylogenetic tree showing the relationships between ZIFL protein sequences.....	47
Table 1. Rice ZIFL sequence identity at the amino acid level.....	48
Figure 3. Genomic alignment obtained with the GATA tool using 100 kb regions containing rice or <i>S. bicolor</i> ZIFL genes.....	48
Figure 4. Exon-intron gene organization of rice <i>OsZIFL</i> genes.....	49
Table 2. Conserved motifs found in ZIFL protein sequences.....	49
Figure 5. Motifs in ZIFL protein sequences identified with the MEME tool.....	50
Figure 6. Expression of <i>OsZIFL</i> genes in roots, culms and leaves during vegetative growth and flag leaves and panicles during reproductive growth, evaluated by qPCR.....	52
Figure 7. Localization of CATGC and IDE1-like boxes in rice OsZIFL gene promoters.....	53
Figure 8. Gene expression in roots of rice plants submitted for 3 days to 0.5 µM of Zn (control, white bars) or 200 µM of Zn (Zn ⁺ , gray bars), evaluated by qPCR.....	54
Figure 9. Gene expression in leaves of rice plants submitted for 3 days to 0.5 µM of Zn (control, white bars) or 200 µM of Zn (Zn ⁺ , gray bars), evaluated by qPCR.....	54

Figure 10. Gene expression in roots of rice plants submitted for 7 days to control (100 µM Fe ⁺³ -EDTA, white bars) or Fe-deficiency (no Fe added, gray bars), evaluated by qPCR.....	55
Figure 11. Gene expression in leaves of rice plants submitted for 7 days to control (100 µM Fe ⁺³ -EDTA, white bars) or Fe-deficiency (no Fe added, gray bars), evaluated by qPCR.....	55
Figure 12. <i>OsZIFL2</i> , <i>OsZIFL3</i> , <i>OsZIFL5</i> , <i>OsZIFL7</i> , <i>OsZIFL10</i> , <i>OsZIFL12</i> and <i>OsZIFL13</i> gene expression data obtained using Genevestigator, and based on Affymetrix specific probes.....	56
Figure 13. <i>OsZIFL2</i> , <i>OsZIFL3</i> , <i>OsZIFL5</i> , <i>OsZIFL7</i> , <i>OsZIFL10</i> , <i>OsZIFL12</i> and <i>OsZIFL13</i> gene expression data obtained using Genevestigator, and based on Affymetrix specific probes.....	56
Additional File 1. <i>ZIFL</i> gene sequence information.....	65
Additional File 2. Previously unannotated <i>ZIFL</i> genes.....	68
Additional File 3. Phylogenetic trees of <i>ZIFL</i> and MFS_1 proteins.....	69
Additional File 4. Conserved residues found in <i>ZIFL</i> protein sequences.....	70
Additional File 5. Chromosomal positions of <i>ZIFL</i> genes.....	73
Additional File 6. Alignment of <i>OsZIFL</i> protein sequences.....	74
Additional File 7. Probes used in Genevestigator analyses and evaluation of specificity of rice <i>ZIFL</i> Affymetrix® microarray probes.....	75
Additional File 9: Gene-specific primers used for quantitative RT-PCR.....	76
Capítulo 2: “Elemental profiling of rice FOX lines leads to characterization of a new Zn transporter and uncovers a function for Zn accumulation in trichomes of <i>Arabidopsis thaliana</i>”.....	77
Table 1. Ionomics profile of Rice FOX lines.....	115
Table 2. Natural accession of <i>A. thaliana</i> used in this work.....	116
Supplemental Table 1. Rice FOX lines used in this work.....	117
Supplemental Table 2. Primers used in this work.....	119

Figure 1. The OsZIP7-OE lines accumulate higher Zn in leaves.....	124
Figure 2. Functional complementation of yeast mutant strains.....	125
Figure 3. Subcellular localization of OsZIP7-YFP construct in <i>A. thaliana</i> mesophyll protoplast after transient transformation.....	126
Figure 4. <i>A. thaliana</i> OsZIP7-OE lines show higher sensitivity to excessive Zn.....	127
Figure 5. OsZIP7-OE lines show changes in Zn root to shoot translocation.....	128
Figure 6. Seeds of OsZIP7-OE lines show higher abundance of Zn.....	129
Figure 7. 2D SXRF leaf maps of Col-0, OsZIP7-OE and <i>glabrous-1</i> mutant.....	130
Figure 8. Quantification of Zn total abundance in individual trichomes of maps from leaves.....	131
Figure 9. High resolution 2D SXRF maps of fresh individual trichomes.....	132
Figure 10. High resolution SXRF maps of resin-embedded, sectioned trichomes.....	133
Figure 11. Zn abundance in trichomes of <i>A. thaliana</i> accessions with contrasting total leaf Zn concentrations.....	134
Figure 12. Correlation of the percentage of the total Zn in trichomes with mean Zn counts in whole leaf of Arabidopsis accessions.....	135
Supplemental Figure 1. Metal concentrations in shoots and roots of Col-0 and OsZIP7-OE plants.....	136
Supplemental Figure 2. Metal concentrations in seeds of Col-0 and OsZIP7-OE plants.....	137
Supplemental Figure 3. High resolution 2D SXRF maps of fresh individual trichomes.....	138

Resumo

O arroz é uma das monoculturas mais importantes no mundo, sendo alimento diário para cerca de metade da população mundial. No entanto, o grão de arroz é pobre em micronutrientes como Fe e Zn, os dois minerais mais comumente deficientes na dieta humana. Em plantas, tanto Fe quanto Zn devem ser absorvidos do solo, distribuídos e armazenados na planta, de forma que suas concentrações sejam mantidas em níveis suficientes, porém não tóxicos. A compreensão dos mecanismos e proteínas envolvidas na manutenção da homeostase de Fe e Zn em plantas tem o potencial de beneficiar a agricultura, melhorando o uso dos micronutrientes pelas plantas, assim como indicar abordagens que visam à biofortificação dos grãos, aumentando a qualidade nutricional dos mesmos. Neste trabalho, foi identificada e caracterizada em nível genômico uma nova família de genes, *ZINC-INDUCED FACILITATOR LIKE* (*ZIFL*), incluindo a organização no genoma, análises de sequências e regulação da expressão gênica em arroz. Demonstramos que a família *ZIFL* passou por um processo de expansão na linhagem das monocotiledôneas, e caracterizamos as duplicações dos genes *ZIFL* de arroz, assim como a sua regulação em resposta a variações nas concentrações de Fe e Zn. Em um segundo trabalho, analisamos o perfil ionômico de linhagens de *Arabidopsis thaliana* expressando genes de arroz, e identificamos um novo transportador de Zn localizado na membrana plasmática, OsZIP7. As linhagens de *A. thaliana* expressando OsZIP7 são sensíveis ao excesso de Zn, e têm a dinâmica do acúmulo de Zn na base dos tricomas em folhas alterada. Com base nessas observações, nós demonstramos que os tricomas acumulam Zn no apoplasto, possivelmente ligado à parede celular, e que esse acúmulo depende da concentração de Zn nas folhas. Por último, propomos que a localização de Zn em tricomas seja parte de um mecanismo para detoxificação de excesso do metal em *A. thaliana*, uma planta não-hiperacumuladora de metais. Nossas observações podem servir de base para estudos da família *ZIFL* em plantas, e demonstram a utilidade de técnicas para o estudo da ionômica combinadas com expressão heteróloga em *A. thaliana*. Nosso trabalho descreve novos genes com potencial para o melhoramento de plantas e biofortificação.

Abstract

Rice is one of the most important cultures in the world, with nearly half of the population eating rice every day. However, the rice grain is very poor in micronutrientes such as Fe and Zn, the two minerals most often deficient in the human diet. In plants, both Fe and Zn should be acquired from the soil, distributed and stored within the plant, and their concentrations should be maintained in sufficient but non-toxic levels. Understanding the mechanisms and proteins involved in Fe and Zn homeostasis in plants has the potential to benefit agriculture, improving the use of micronutrientes by plants, as well as indicate approaches for grain biofortification to increase their nutritional quality. In this work, we identified e characterized at the genomic level a new family of proteins, *ZINC-INDUCED FACILITATOR LIKE* (*ZIFL*), including their organization in the genome, sequence analyses and gene expression regulation in rice. We demonstrated that the *ZIFL* family underwent an expansion process in the monocot lineage, and characterized the duplication of *ZIFL* genes in rice as well as their regulation in response to variations in Fe and Zn concentrations. In another work, we analyzed the ionomics profile of *Arabidopsis thaliana* lines expressing rice genes, and identified a new plasma membrane Zn transporter, OsZIP7. *A. thaliana* lines expressing *OsZIP7* are sensitive to Zn excess, and the dynamics of Zn accumulation at the base of their leaf trichomes is altered. Based on those observations, we show that trichomes accumulate Zn in the apoplast, possibly bound to the cell wall, and that this accumulation is dependent on the Zn leaf concentration. At last, we propose that the localization of Zn in trichomes is part of a mechanism for excessive Zn detoxification in the metal non-hyperaccumulator *A. thaliana*. Our observations could be the base for new studies with the *ZIFL* family in plants, and also show the usefulness of combining ionomics techniques with heterologous expression in *A. thaliana*. Our work describes new genes with potential for plant breeding and biofortification.

Lista de abreviaturas

- AES – *atomic emission spectroscopy* (espectroscopia de emissão atômica)
- AHA – *arabidopsis H⁺-pump ATPase* (ATPase bombeadora de H⁺ de Arabidopsis)
- ATP – *adenosine triphosphate* (trifosfato de adenosina)
- CAX – *calcium exchangers* (permutadores de cálcio)
- CDF – *cation diffusion facilitator* (facilitador da difusão de cátions)
- cDNA – *complementary DNA* (DNA complementar)
- CPC – CAPRICE
- DMA – *deoxymugineic acid* (ácido desoximugineico)
- DMAS – *deoxymugineic acid sintase* (ácido desoximugineico sintase)
- DMT – *divalent metal transporter* (transportador de metal divalente)
- EGL – *ENHANCER OF GLABRA* (proteína acentuadora de *glabra*)
- ETC – ENHANCER OF TRY
- FER – *ferritin* (ferritina)
- FOX - *full-length cDNA over-expressors* (linhagens que super-expressam cDNAs completos)
- FPN – *ferroportin* (ferroportina)
- FRD – *ferric-reductase defective* (defectivo em redutase férrica)
- FRDL – *ferric-reductase defective like* (semelhante a defectivo em redutase férrica)
- FRO – *ferric reductase oxidase* (redutase oxidase férrica)
- GL – *GLABRA/GLABROUS* (proteína/mutante glabro)
- HBED - *N,N'-di(2-hydroxybenzyl)-ethylenediamine-N,N'-diacetic acid monohydrochloride hydrate* (N,N'-di(2-hidroxibenzil)-etilenodiamina-N,N' - hidrato de ácido diacético monoidroclorado)
- HCP – *heme-carrier protein* (proteína carreadora de heme)
- HMA – *heavy metal associated* (associado a metais pesados)
- ICP – *inductively coupled plasma* (plasma indutivamente acoplado)
- IDS – *iron deficiency-specific clone* (clone específico de deficiência de ferro)
- IRT – *iron-regulated transporter* (transportador regulado por ferro)
- MES – *2-(N-morpholino)-ethanesulfonic acid* (ácido 2-(N-morfolino)-etanosulfônico)

MFS – *major facilitator superfamily* (superfamília de facilitadores majoritários)

MIT – *mitochondrial iron transporter* (transportador de ferro de mitocôndria)

MS – *mass spectrometry* (espectrometria de massa)

MT – *metalothionein* (metalotioneína)

MTP – *metal tolerance protein* (proteína de tolerância a metais)

MYA – *millions of year ago* (milhões de anos atrás)

NA – *nicotianamine* (nicotianamina)

NAAT – *nicotianamine aminotransferase* (nicotianamina aminotransferase)

NAC – fator de transcrição NAC (NAM/ATAF/CUC)

NAM – *non-apical meristem* (meristema não-apical)

NAS – *nicotianamine synthase* (nicotianamina sintase)

NK – *natural killer cells* (célula extermínadora natural)

NRAMP – *natural resistance-associated macrophage protein* (proteína de macrófago associada à resistência natural)

OES – *optical emission spectroscopy* (espectroscopia de emissão óptica)

PCR – *plant cadmium resistance* (resistência a cadmio em plantas)

PCS – *phytochelatin synthase* (sintase de fitoquelatina)

PEZ – *Phenolics Efflux Zero* (efluxo de fenólicos zero)

PIC – *permease in chloroplast* (permease de cloroplasto)

PS – *phytosiderophore* (fitossideróforos)

RFP – *red fluorescent protein* (proteína fluorescente vermelha)

RT-PCR – *reverse transcriptase polymerase chain reaction* (transcrição reversa seguida de reação em cadeia da polimerase)

SAM – *S-adenosyl-methionine* (S-adenosil-metionina)

SAMS – *S-adenosyl-methionine synthetase* (S-adenosil-metionina sintetase)

SUT – *sucrose transporter* (transportador de sacarose)

SXRF – *synchrotron X-ray fluorescence* (fluorescência de raios-X baseada em sincrotron)

T-DNA – *transfer DNA* (DNA de transferência)

TOM – *Transporter of Mugineic Acid Family* (transportador da família do ácido mugineico)

TRY – TRIPTYCHON

TTG – TRANSPARENT TESTA GLABRA

VIT – *vacuolar iron transporter* (transportador vacuolar de ferro)

WT – *wild type* (tipo selvagem)

XRF – *X-ray fluorescence* (fluorescência de raios-X)

YFP – *yellow fluorescent protein* (proteína fluorescente amarela)

YS – *yellow stripe*

YSL – *yellow stripe-like* (semelhante *yellow stripe*)

ZIF – *Zinc Induced Facilitator* (facilitador induzido por zinco)

ZIFL – *Zinc Induced Facilitator-Like* (semelhante ao facilitador induzido por zinco)

ZIP – *zinc-regulated/iron-regulated transporter* (transportador zinco-regulado/ ferro-regulado)

ZnT – *Zn transporter* (transportador de Zn)

ZRT – *zinc-regulated transporter* (transportador regulado por zinco)

Introdução Geral

1. Arroz

O arroz (*Oryza sativa* L.) é uma das três monoculturas mais importantes no mundo juntamente com milho (*Zea mays*) e trigo (*Triticum aestivum*). Considerando-se área plantada, o arroz aparece em terceiro, com 159 milhões de hectares; e em segundo quando considerada a produção, com 696 milhões de toneladas (FAO – Food and Agriculture Organization; <http://faostat.fao.org>). Os países com maior produção e também os maiores consumidores estão localizados no continente asiático. Por exemplo, países como China e Índia consomem respectivamente 29,4% e 23,3% do arroz produzidos no mundo. Segundo dados de 2009, foram consumidos 146 gramas de arroz por pessoa por dia (g/pessoa/dia) em média no mundo (FAO - <http://faostat.fao.org>). Nesse contexto, estima-se que grãos de arroz sejam a base da alimentação de cerca de metade da população mundial (Wang et al 2012).

O Brasil é o nono maior produtor de arroz, e o maior fora do continente asiático, seguido pelos Estados Unidos. Em média, são consumidos 95 g/pessoa/dia no país, colocando o Brasil como o 55º maior consumidor (FAO - <http://faostat.fao.org>). Cerca de 60% da produção brasileira provém do Rio Grande do Sul (IBGE 2012), onde diversos municípios baseiam sua economia na produção orizícola, principalmente na metade sul do estado.

O arroz também é considerado uma planta-modelo para estudos em monocotiledôneas. Possui o menor genoma entre as plantas cultivadas, entre 398 a 466 Mb na região eucromática (Goff et al 2002, Yu et al 2002, IRGSP 2005), cerca de 3,7 vezes maior que o genoma da planta-modelo *Arabidopsis thaliana* (*Arabidopsis Genome Initiative* 2000). Também estão disponíveis os genomas completamente sequenciados de ambas as variedades *indica* e *japonica* (Yu et al 2002, IRGSP 2005). A comunidade científica tem à disposição diversos recursos para caracterização funcional de genes de arroz: bancos contendo cerca de 40.000 cDNAs completos, tanto da variedade *indica* quanto *japonica* (Kikuchi et al 2003, Liu et al 2007, Tanaka et al 2008); bibliotecas de mutantes por inserção de T-DNA, transposons ou retrotransposons e por mutagênese induzida por radiação ou agentes químicos (Wang et al 2012); ferramentas para análise da expressão e co-expressão de transcritos (Jung et al 2008; Sato et al 2012a e 2012b),

bases de dados de proteômica (Helmy et al 2011) e interatômica (Gu et al 2011), e grande quantidade de informação sobre cultivares e variabilidade genética da espécie *Oryza sativa* (Huang et al 2012). Baseado na abundância de recursos, a comunidade científica planeja caracterizar a função de todos os genes de arroz até o ano de 2020 (Zhang et al 2008).

Apesar de sua importância para a dieta, o grão de arroz é pobre em nutrientes como ferro (Fe) e zinco (Zn), sendo o cereal com as concentrações mais baixas, e que apresenta a variabilidade genética mais restrita para melhoramento convencional desta característica (Kennedy e Burlingame 2003, Pfeiffer et al 2008). As deficiências de Fe e Zn em humanos afetam cerca de 30% da população mundial, sendo as duas principais deficiências minerais conhecidas (Gómez-Galera 2010). Dietas baseadas principalmente em cereais, comuns em países e populações pobres, aumentam os riscos de desnutrição, indicando que esforços para a melhoria da qualidade nutricional de grãos são necessários. Em 2008 o *Copenhagen Consensus* (<http://www.copenhagencoensus.com/>) listou as soluções para problemas mundiais de maior custo-benefício. Fortificações de alimentos com Zn e Fe foram consideradas em primeiro e terceiro lugar, enquanto a biofortificação foi considerada em quinto. Biofortificação consiste na produção de variedades capazes de acumular quantidades maiores de nutrientes nas suas partes comestíveis, com impacto positivo na nutrição humana, de maneira que não seja necessário qualquer processamento ou a adição *a posteriori* destes nutrientes. Para exemplificar o custo-benefício dessa abordagem, estima-se que a cada dólar gasto para corrigir a desnutrição infantil para Zn, a economia futura será de 17 dólares (<http://www.copenhagencoensus.com/>). Sendo assim, o estudo da homeostase de Fe e Zn em arroz visando à biofortificação de grãos é uma alternativa interessante, tanto devido à importância da cultura no contexto mundial quanto à maior disponibilidade de ferramentas para o entendimento dos mecanismos de absorção, transporte e armazenamento de nutrientes minerais na planta.

2. Nutrição mineral (Fe e Zn) em humanos

2.1 Importância de Fe em humanos

A deficiência de Fe é considerada um dos 10 principais problemas de saúde da atualidade (Gómez-Galera et al 2010). Calcula-se que dois bilhões de pessoas sofram de deficiência nutricional de Fe, totalizando cerca de 30% da população mundial (<http://www.who.int/nutrition/topics/ida/en/index.html>). O Fe é um componente essencial da hemoglobina e da mioglobina, tendo papel no transporte, armazenagem tecidual transitória e utilização de oxigênio. Também está presente em moléculas de citocromo, participando da cadeia de transporte de elétrons em mitocôndrias e de reações de degradação e detoxificação de compostos no fígado (McDermid e Lönnerdal 2012).

O Fe é absorvido na membrana apical dos enterócitos por meio do transportador de Fe⁺² DMT1 (*divalent metal transporter 1*; Mims e Prchal 2005). O Fe ligado a grupo heme também pode ser internalizado pelo transportador específico HCP1 (*Heme-Carrier Protein 1*; Shayegui et al 2005), sendo liberado pela ação da heme-oxigenase lisossomal (Anderson e McLaren 2012; McDermid e Lönnerdal 2012). Após a absorção, o Fe pode ser armazenado na holoproteína ferritina, capaz de armazenar até 4500 átomos de Fe, ou exportado para células adjacentes pela ação do transportador de efluxo localizado nas membranas basolaterais, FPN (Ferroportina, Anderson e McLaren 2012; McKie et al 2000). Após o efluxo, o transporte de Fe entre tecidos ocorre por meio da proteína carreadora transferrina, a qual é reconhecida por receptores específicos e internalizada, fazendo o descarregamento de Fe nas células (McDermid e Lönnerdal 2012). O peptídeo hepcidina é sintetizado pelo fígado em resposta a variações nas concentrações de Fe circulantes ou sinais inflamatórios, e se liga a ferroportina nos enterócitos, degradando-a. Assim, a hepcidina regula a distribuição de Fe a partir dos enterócitos, e consequentemente a absorção de Fe a partir da dieta (McDermid e Lönnerdal 2012).

A deficiência de Fe em humanos está associada a prejuízo do sistema immune, assim como menor capacidade de trabalho para o indivíduo (Anderson e McLaren 2012). Quando severa, pode acarretar em fadiga generalizada, anemia, taquicardia, além de problemas de desenvolvimento cognitivo e comportamental na infância (McDermid e Lönnerdal 2012). A toxidez por excesso de Fe é observada em pessoas com desordens genéticas associadas ao metabolismo de Fe. A hemocromatose tipo 1 (*HFE hereditary hemochromatosis*) é uma doença autossômica recessiva que resulta no aumento na absorção intestinal de Fe. O Fe em excesso se deposita nos tecidos, podendo levar a

necrose tecidual, cirrose e outras complicações (McDermid e Lönnerdal 2012). A ingestão de suplementos de Fe de forma inadequada também pode levar a sintomas de toxidez, incluindo vômito, diarréia, tonturas, podendo levar à morte (McDermid e Lönnerdal 2012).

Em média, um adulto apresenta em torno de 2 g de Fe na forma de hemoglobina, enquanto uma pequena quantidade é armazenada em transferrina e outras proteínas (Gómez-Galera et al 2010). Quantidades consideráveis de Fe são recicladas pela degradação de eritrócitos senescentes. Ainda assim, a homeostase depende da regulação da absorção de Fe proveniente da dieta. Este pode ser Fe ligado a grupos heme ou Fe não-heme, sendo o primeiro mais facilmente absorvido que o segundo. Enquanto o Fe-heme é mais comum em dietas ricas em proteína animal, como carnes e peixes, o Fe não heme é mais rico em alimentos de origem vegetal. A absorção de Fe também é inibida por compostos mais comumente presentes em vegetais, como taninos, polifenóis e fitato (McDermid e Lönnerdal 2012). Em países em desenvolvimento, a dieta é normalmente baseada em grãos como arroz, milho e trigo, com menor consumo de alimentos ricos em Fe, aumentando o risco de deficiência de Fe nessas populações.

2.2 Importância de Zn em humanos

Estimativas conservadoras sugerem que 25% da população mundial esteja sob risco de deficiência de Zn, enquanto outras indicam que até 2 bilhões de pessoas apresentam a condição (Maret e Sandstead 2006; Gómez-Galera et al 2010). Estima-se que 10% das proteínas codificadas pelo genoma humano sejam capazes de ligar Zn (Andreini et al 2006). O Zn é essencial para o desenvolvimento e função de células mediadoras da imunidade inata, assim como para as células NK (*natural killer*), macrófagos e neutrófilos. Processos como a fagocitose e a produção de citocinas são afetados pela deficiência de Zn, assim como a proliferação de células T e B (Prasad 2012). Recentemente, o Zn foi associado também com a maturação de óócitos durante a ovulação, demonstrando a importância do mineral para a reprodução (Kim et al 2011). Manifestações de deficiência de Zn severa incluem dermatites, alopecia (perda de cabelos), diarréia, desordens psiquiátricas e neuro-sensoriais, perda de peso, infecções

recorrentes devido a disfunções do sistema imune, hipogonadismo em homens, úlcera e, se não for tratada, pode levar à morte (Prasad 2012). Além de baixa absorção, a deficiência de Zn pode ocorrer em decorrência de diarréia, doenças hepáticas e renais crônicas e diabetes (Prasad 2003).

O Zn também tem sido descrito como importante na sinalização celular, especialmente associado à atividade de neurotransmissores (Fukada et al 2011). São descritos dois tipos de sinalização: o inicial, independente de atividade transcricional, onde variações na concentração de Zn são percebidas por proteínas presentes no citoplasma, iniciando ou continuando cascatas de sinalização; e o tardio, dependente de transcrição *de novo*, onde transportadores e proteínas ligadoras de Zn são sintetizadas (Fukada et al 2011).

As concentrações intracelulares de Zn são controladas por transportadores de influxo da família ZIP (*Zinc-Regulated/ Iron-Regulated Transporter*) e transportadores de efluxo da família ZnT (*Zn Transporter*; também conhecidos como CDF – *Cation Diffusion Facilitator* – ou MTP – *Metal Tolerance Protein* – em plantas; ver seção 4) (Fukada et al 2011). O genoma humano apresenta 14 genes ZIP e 9 genes ZnT (Fukada e Kambe 2011). Em geral, proteínas ZIP transportam Zn para dentro do citoplasma, enquanto proteínas ZnT retiram Zn do citoplasma, seja para o meio extracelular ou para o interior de organelas (Fukada e Kambe 2011).

Diversos transportadores de Zn de humanos foram caracterizados, e alguns polimorfismos foram associados a doenças quando presentes. ZIP4 é expresso em enterócitos e a proteína se localiza na membrana apical, tendo papel fundamental na absorção intestinal de Zn (Fukada e Kambe 2011). A acrodermatite enteropática, doença causada por baixa absorção de Zn no intestino, está ligada a mutações no transportador ZIP4 (Küry et al 2002, Wang et al 2002). O Zn extracelular também é captado por ZIP8 e ZIP14 na membrana apical, enquanto ZIP5 está localizado na membrana basolateral. Os transportadores ZIP1 a ZIP6, 8, 10, e 14 são todos localizados na membrana plasmática. Interessantemente, camundongos nocaute para ZIP1, ZIP2 e ZIP3 são sensíveis à deficiência de Zn durante a gestação (Dufner-Beattie et al 2005, Dufner-Beattie et al 2006). Mutações no gene ZIP13 foram associadas a uma forma da síndrome de Ehlers-Danlos, relacionada a problemas na síntese do colágeno (Fukada et al 2008). Já mutações

na sequência codificante do transportador de efluxo para o meio extracelular ZnT1 são letais em camundongos. Outro transportador com função conhecida, Znt8 é expresso especificamente em células β das ilhotas de Langherans no pâncreas, tendo função no transporte de Zn para grânulos, onde o metal é co-precipitado com insulina para armazenagem, estando relacionado com a diabetes (Lemaire et al 2009).

3. Homeostase de Fe em plantas

O Fe é o quarto elemento mais abundante da crosta terrestre, sendo o metal de transição mais abundante nos organismos vivos. Sua ampla utilização se deve a características químicas que permitem a formação de ligações com átomos doadores de elétrons como oxigênio, nitrogênio e enxofre (S), permitindo sua ligação a proteínas como grupos heme, grupamentos Fe-S e também como Fe não-heme (Barker e Pilbeam 2007). O Fe existe em dois estados de oxidação sob pH fisiológico – os íons ferroso (Fe^{+2}) e férrico (Fe^{+3}), o que o torna um eficiente doador e acceptor de elétrons. Em plantas, o Fe exerce funções críticas em reações redox da fotossíntese e respiração devido à sua presença em proteínas envolvidas em transporte de elétrons em cloroplastos e mitocôndrias (Briat et al 2007). Também está envolvido na síntese da clorofila, fixação do nitrogênio e síntese de DNA. Algumas enzimas de plantas que contêm Fe são citocromos, catalase, peroxidases, ferredoxina, ferro-superóxido dismutase, aconitase e lipoxigenases (Marschner, 1995).

Apesar de abundante, o Fe é geralmente pouco disponível para as plantas, devido à sua baixa solubilidade em solos com condições aeróbicas e pH neutro ou básico. Nessas condições, o Fe^{+3} é o estado de oxidação mais comum, e forma polímeros de óxido-hidróxidos altamente insolúveis. A concentração de Fe nessas condições é de aproximadamente 10^{-14} a 10^{-17} M, sendo que o ideal para que as plantas se desenvolvam adequadamente é entre 10^{-4} e 10^{-9} M (Guerinot e Yi, 1994). Considerando que 1/3 dos solos cultiváveis são do tipo calcário, a deficiência de Fe é um grande problema para a agricultura. Plantas sob deficiência de Fe também apresentam prejuízo no desenvolvimento, além de sintomas facilmente detectáveis como inibição do crescimento e clorose (deficiência de clorofila) nas folhas jovens (Barker e Pilbeam, 2007). Devido a

sua importância para a fotossíntese, a maior parte do Fe celular está localizada nos cloroplastos, e a deficiência de Fe leva a decréscimo nas taxas fotossintéticas e mudanças na estrutura dos cloroplastos (Spiller e Terry 1980; Terry e Low 1982; Marschner 1995). A deficiência de Fe também altera a composição de lipídios e proteínas e reduz a capacidade de transporte nos tilacóides (Spiller e Terry, 1980; Nishio et al, 1985), além de diminuir a concentração de ATP nas folhas (Arulanantham et al, 1990). Todos esses efeitos são observados com maior intensidade nas folhas jovens (Marschner 1995). Nas raízes, a deficiência de Fe causa inibição do alongamento, aumento no diâmetro da zona apical e formação de pelos radiculares em maior quantidade (Santi e Schmidt 2008, Santi e Schmidt 2009).

No entanto, ambientes alagados caracterizam-se por apresentar baixas concentrações de oxigênio (anoxia) e baixo pH, o que facilita a redução do Fe^{+3} para Fe^{+2} , mais solúvel. Assim, o mineral torna-se disponível em concentrações elevadas, podendo levar à toxidez por excesso de Fe (Sahrawat et al 2000). O cultivo do arroz no RS é principalmente por irrigação em solos alagadiços, o que favorece a toxidez por Fe. O Fe é tóxico devido à sua capacidade de catalisar a formação da espécie reativa de oxigênio hidroxila ($\text{OH}\bullet$) através da reação de Haber-Weiss, que é a soma da redução do Fe^{+3} pelo ânion superóxido (O_2^-) e a reação de Fenton (Briat 2002). Os principais sintomas de toxidez por excesso de Fe são: o bronzeamento das folhas (inicialmente as mais velhas), retardo no crescimento, baixa produtividade de sementes ou grãos, esterilidade, e em casos mais severos, morte da planta (Sahrawat 2000). Logo, tanto a manutenção dos níveis intracelulares de Fe quanto o armazenamento do Fe em formas não-tóxicas devem ser controlados para o correto desenvolvimento das plantas (Morrissey e Guerinot 2009).

3.1 Absorção de Fe nas raízes

As plantas apresentam diferentes estratégias para aquisição de Fe a partir da rizosfera. Dicotiledôneas e monocotiledôneas não-gramíneas utilizam a estratégia I (Figura 1A, Sperotto et al 2012a), baseada na redução de Fe, e que consiste em três etapas distintas: (1) extrusão de prótons por meio de próton-ATPases, acidificando a

rizosfera e aumentando a solubilidade de Fe⁺³ (e.g. AtAHA2, *Arabidopsis H⁺-pump ATPase*; Santi e Schmidt 2009); (2) redução de Fe⁺³ para Fe⁺² por redutases férricas extracelulares ligadas à membrana plasmática (e.g. AtFRO2, *Ferric Reductase Oxidase*; Robinson et al 1999); e (3) absorção de Fe⁺² pelas células epidérmicas das raízes por transportadores transmembrana (e.g. AtIRT1, *Iron-Regulated Transporter*; Eide et al 1996).

Já as gramíneas utilizam a estratégia II (Figura 1B, Sperotto et al 2012a), baseada em quelação, consistindo em duas etapas: (1) secreção de fitosideróforos (PS; *phytosiderophores*) na rizosfera, que quelam Fe⁺³, formando o complexo Fe(III)-PS; e (2) absorção do complexo Fe(III)-PS pelas células epidérmicas por transportadores específicos da família YS (*Yellow Stripe*; Curie et al 2001, Murata et al 2006, Inoue et al 2009, Lee et al 2009a).

Tanto a rota de biossíntese de PS quanto as enzimas envolvidas são conhecidas (Figura 2). Inicialmente, a caracterização molecular das enzimas envolvidas na biossíntese de PS foi feita em cevada: S-adenosil-metionina sintetase (SAMS; *S-adenosyl-methionine synthetase*; Takizawa et al 1996); nicotianamina sintase (NAS; *nicotianamine synthase*; Higuchi et al 1999); nicotianamina aminotransferase (NAAT; *nicotianamine aminotransferase*; Takahashi et al 1999); ácido desoximugineico sintase (DMAS; *deoxymugineic acid synthase*; Bashir et al 2006) e as dioxigenases IDS2 (Okumura et al 1994; Nakanishi et al 2000) e IDS3 (Nakanishi et al 1993, Nakanishi et al 2000). Posteriormente, os genes ortólogos de arroz e milho foram identificados e caracterizados (Higuchi et al 2001, Inoue et al 2003, Mizuno et al 2003, Kobayashi et al 2005, Bashir et al 2006). Em geral, os genes de síntese de PS são induzidos por deficiência de Fe (Kobayashi et al 2005). Dependendo da espécie de gramínea, diferentes PS são produzidos: espécies mais sensíveis à deficiência de Fe, como arroz e milho, secretam predominantemente ácido desoximugineico (DMA; *deoxymugineic acid*), enquanto espécies mais resistentes, como cevada e centeio, secretam formas hidroxiladas de PS (Römheld e Marschner 1990).

Inicialmente, acreditava-se que a secreção de PS ocorria por fusão de vesículas à membrana plasmática (Nishizawa and Mori 1987, Sakaguchi et al 1999, Negishi et al 2002, Mizuno et al 2003). No entanto, recentemente foi descrito o transportador

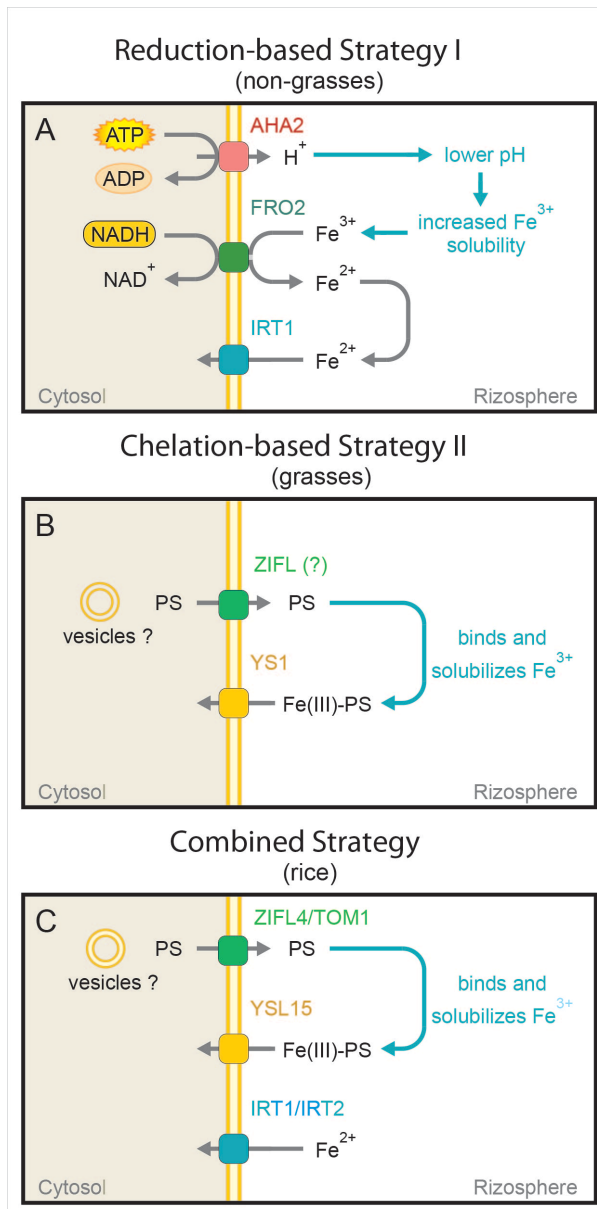


Figura 1. Estratégias para a captação de Fe a partir do solo. (A) Estratégia I, baseada em redução. Próton-ATPases (AHA2) secretam prótons e acidificam a rizosfera, aumentando a solubilidade de Fe⁺³. Fe⁺³ solúvel é reduzido pela redutase de membrana (FRO2) e o Fe⁺² é absorvido pelo transportador específico (AtIRT1). (B) Estratégia II, baseada em quelação. Fitosideróforos (PS) são sintetizados, e então secretados na rizosfera por OsZIFL4/TOM1. PS quelam Fe⁺³, e o complexo Fe(III)-PS é absorvido pelo transportador específico (YS1). (C) Estratégia combinada. Apesar de poderem captar Fe⁺³, plantas de arroz também podem captar Fe⁺² devido à presença de transportadores IRT1/IRT2. Figura modificada de Sperotto et al (2012a).

OsZIFL4/TOM1 (*Zinc Induced Facilitator-Like/ Transporter of Mugineic Acid family*), responsável pela secreção de DMA a partir das raízes de arroz para a rizosfera (Nozoye et al 2011, Ricachenevsky et al 2011). O gene *OsZIFL4/TOM1* faz parte de uma família multigênica, composta por 13 membros em arroz (Ricachenevsky et al 2011). Apesar do primeiro trabalho descrevendo a função de *OsZIFL4/TOM1* ter sido publicado por Nozoye et al (2011) e ter utilizado o nome TOM1, a proteína descrita apresenta similaridade com um transportador anteriormente nomeado com *AtZIF1* (*Zinc Induced Facilitator*; Haydon and Cobbett et al 2007) de *Arabidopsis thaliana*. Como a nomenclatura deve fazer referência à primeira proteína descrita na família, o nome a ser utilizado na literatura deve ser *OsZIFL4* (Ricachenevsky et al 2011).

Após a secreção, PS se liga a Fe^{+3} , formando o complexo Fe(III)-PS, o qual é absorvido por transportadores da família *Yellow Stripe-Like* (YSL, Curie et al 2001). O primeiro membro descrito da família foi o transportador ZmYS1 de milho. Plantas com perda de função de ZmYS1 apresentam deficiência de Fe constitutiva, mesmo quando cultivadas em condições de suficiência de Fe. A clorose intervenal, característica de deficiência de Fe, resulta em um padrão fenotípico de listras amarelas nas folhas, daí o nome do mutante que levou à identificação de ZmYS1 (Curie et al 2001). Posteriormente, ortólogos de ZmYS1 foram descritos em cevada (HvYS1; Murata et al 2006) e arroz (OsYSL15; Inoue et al 2009 e Lee et al 2009a).

Apesar de ser uma planta de estratégia II, o genoma do arroz apresenta um ortólogo funcional de *AtIRT1*, *OsIRT1* (Ishimaru et al 2006, Lee e An 2009). Conforme descrito anteriormente, AtIRT1 é o transportador para aquisição de Fe^{+2} após a redução em plantas de estratégia I, e surpreendentemente OsIRT1 possui função similar (Ishimaru et al 2006). Com base nesse dado, foi sugerido que arroz apresenta estratégia I e II combinada (Figura 1C), pois é capaz de captar tanto Fe^{+3} ligado a PS quanto Fe^{+2} (Ishimaru et al 2006). Em solos aeróbicos, de pH alcalino ou neutro, o estado de oxidação mais comum é o Fe^{+3} ; já em solos anaeróbicos e de pH ácido, como quando o arroz é cultivado em condições de alagamento, o estado de oxidação mais comum é o Fe^{+2} (Sahrawat 2000). Portanto, a capacidade de absorver Fe^{+2} pode ser uma adaptação de plantas de arroz às condições de alagamento (Ishimaru et al 2006). Tanto atividade de redutase quanto acidificação da rizosfera, comuns em plantas de estratégia I, estão

ausentes em raízes de arroz (Ishimaru et al 2006). Em comparação com outras gramíneas, o arroz secreta concentrações relativamente baixas de PS, sugerindo uma menor dependência desse sistema para aquisição de Fe (Mori et al 1991). O mutante com perda de função do gene *OsNAAT1* (cuja função na rota de síntese de PS está mostrado na Figura 2), enzima-chave na síntese de PS, tem o crescimento prejudicado em meio de cultivo contendo Fe^{+3} como fonte de Fe. No entanto, o mesmo mutante cresce normalmente quando Fe^{+2} está presente no meio (Cheng et al 2007). Em outro trabalho, foi demonstrado que quando a estratégia I é complementada em plantas de arroz por uma construção contendo uma redutase férrica sob controle do promotor de *OsIRT1*, as plantas de arroz transgênicas são mais resistentes à deficiência de Fe em condições de cultivo aeróbicas, pois passam a ser capazes de reduzir Fe^{+3} por meio do transgene e absorver Fe^{+2} utilizando a proteína OsIRT1 endógena (Ishimaru et al 2007). Esses dados suportam a hipótese de que arroz apresenta uma estratégia de aquisição de Fe que combina a estratégia II com parte da estratégia I. Apesar disso, as contribuições relativas de cada estratégia em condições de campo ainda não foram determinadas (Sperotto et al 2012a).

3.2 Transporte radial e carregamento do xilema

Após a entrada no simplasto, o Fe é translocado radialmente nas raízes até o estelo, onde deve ser carregado no xilema para translocação até a parte aérea via corrente transpiratória. Apesar de ser aceito que, uma vez dentro do simplasto, o Fe se desloca livremente até seu efluxo para dentro do xilema por um transportador no estelo, ainda não existem evidências de que este modelo esteja correto. A importância relativa de cada camada longitudinal para a captação de metais ainda não foi determinada. Em *Arabidopsis thaliana*, a atividade do promotor de *AtIRT1* em resposta a deficiência de Fe é restrita às células das camadas mais externas, principalmente na epiderme e pelos radiculares (Vert et al 2002). Já em arroz, o promotor de *OsIRT1* é expresso tanto na epiderme quanto no córtex (Ishimaru et al 2006), indicando que OsIRT1 pode desempenhar papel na absorção também nas camadas longitudinais mais internas das raízes. Outro exemplo de contribuição tipo celular-específico é o transportador de efluxo

expresso no estelo, PEZ1 (*Phenolics Eflux Zero 1*), o qual secreta ácido protocatecúico e ácido caféico no apoplasto para solubilizar Fe^{+3} precipitado no apoplasto (Ishimaru et al 2011).

Uma vez no estelo, o Fe é carregado no xilema através do transportador de efluxo ferroportina (AtFPN1), descrito em *Arabidopsis thaliana* (Morrissey et al 2009). No xilema, o Fe é provavelmente translocado para a parte aérea via corrente transpiratória, complexado com citrato. O transportador AtFRD3 medeia o efluxo de citrato para o xilema, sendo necessário para a translocação de Fe para a parte aérea e posterior entrada nas células foliares (Rogers e Guerinot 2002, Green e Rogers 2004, Durrett et al 2007). O ortólogo de arroz para AtFRD3, OsFRDL1, também é necessário para a correta translocação de Fe para a parte aérea (Yokosho et al 2009), porém ainda não foi descrito um ortólogo de AtFPN1 em arroz. Recentemente, foi demonstrada pela primeira vez a presença do complexo Fe(III)-citrato no xilema em condições fisiológicas em plantas de tomate, confirmando a necessidade de citrato para a correta translocação (Rellán-Álvarez et al 2010).

3.3 Transporte de Fe na parte aérea e remobilização por meio de carregamento do floema

Pouco se sabe sobre genes envolvidos na captação de Fe pela membrana das células foliares. Sugere-se que AtFRO6, um parálogo de AtFRO2 (redutase de membrana envolvida na absorção de Fe nas raízes), poderia estar envolvido em uma etapa de redução na membrana de células na parte aérea (Jeong et al 2008, Li et al 2011). Uma vez absorvido, cerca de 80% do Fe presente em folhas se encontra nos cloroplastos. Duas proteínas foram implicadas na captação de Fe em cloroplastos de *Arabidopsis thaliana*: AtFRO7, localizada na face extracelular do cloroplasto, reduzindo Fe^{+3} para Fe^{+2} (Jeong et al 2008); e PIC1, um possível transportador de Fe^{+2} do citoplasma para dentro do cloroplasto (Duy et al 2007, Duy et al 2011). Em arroz, também foi descrito o primeiro transportador mitocondrial de Fe, OsMIT1 (Bashir et al 2011). Porém, não há relatos sobre ortólogos dos genes AtFRO7 ou PIC1. O Fe pode ser remobilizado a partir da parte

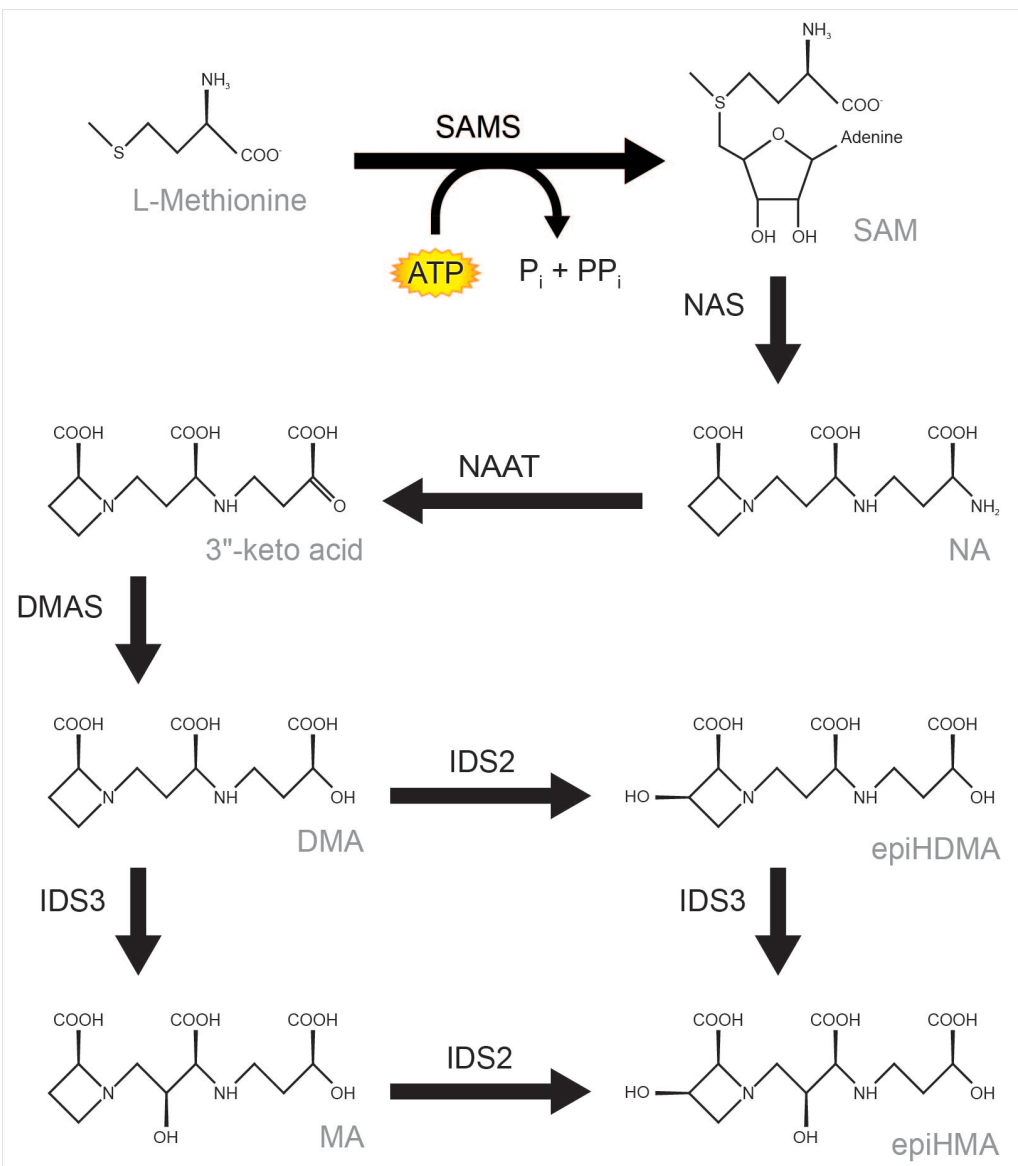


Figura 2. Via de biossíntese de fitossideróforos (PS) da família do ácido mugineico. L-metionina é adenilada pela S-adenosilmetionina sintetase (SAMS), que consome ATP e forma S-adenosil-metionina (SAM). A nicotianamina sintase (NAS) combina três moléculas de SAM para formar a nicotianamina (NA). A nicotianamina aminotransferase (NAAT) catalisa a transferência do grupo amino e forma o intermediário 3-ceto-ácido, que é reduzido pela ácido desoximugineico sintase (DMAS) para formar o ácido desoximugineico (DMA). As dioxigenases IDS2 e IDS3 catalisam diferentes etapas de hidroxilação para formar outros PS. Figura de Sperotto et al (2012a).

aérea em diferentes situações, incluindo a translocação para sementes durante o desenvolvimento reprodutivo (Sperotto et al 2012b). Utilizando os mutantes de ervilha (*Pisum sativum*) *brz* (*bronze*) e *dgl* (*degenerated leaflets*), ambos hiperacumuladores de Fe, foi demonstrado que o Fe deve ser quelado antes de ser carregado via floema durante a remobilização (Grusak 1994, Zhang et al 2007). A nicotianamina (NA), um dos precursores na síntese de PS e de presença ubíqua em plantas, é o quelante de metais mais provável no transporte de Fe no floema, uma vez que forma complexos estáveis com vários metais em pH alcalino (Koike et al 2004, Curie et al 2009).

OsYSL2, parólogo mais similar a OsYSL15 no genoma de arroz, é expresso especificamente em floema e transporta Fe(II)-NA (Koike et al 2004). O silenciamento de OsYSL2 leva ao acúmulo de Fe nas raízes e diminui a translocação de Fe para a parte aérea, indicando que OsYSL2 pode ter função no transporte de Fe (Ishimaru et al 2010). Tanto parte aérea quanto sementes apresentam concentrações de Fe mais baixas em plantas onde OsYSL2 não é expresso, enquanto raízes apresentam concentrações mais altas. Curiosamente, a super-expressão de OsYSL2 causa uma distribuição de Fe semelhante, provavelmente criando um dreno nas raízes e impedindo a translocação. Quando OsYSL2 é expresso sob controle de um promotor de sacarose sintase, altamente ativo em células do floema, as concentrações de Fe em sementes aumentam, indicando que o transporte de Fe ligado a NA via floema é importante para a remobilização de metais para as sementes (Ishimaru et al 2010). Em *Arabidopsis thaliana*, as proteínas AtYSL1 e AtYSL3, parcialmente redundantes, também parecem ter função na remobilização de metais, especialmente durante o processo de senescência (Waters et al 2006).

3.4 Transporte de Fe para as sementes

Apesar do grande interesse da comunidade científica em entender como o Fe é transportado para as sementes em desenvolvimento, principalmente do ponto de vista da saúde pública, e das diversas abordagens já testadas para aumentar a concentração de metais no grão maduro de arroz (Sperotto et al 2012a; ver seção 6 - Biofortificação), ainda entendemos pouco sobre como as plantas translocam metais para as sementes, e

principalmente quais são as etapas limitantes para obtermos sucesso no melhoramento da qualidade nutricional dos grãos. O grão maduro de arroz apresenta diferentes tipos celulares: retirando-se as duas brácteas (a palea e a lema), a cariopse ou arroz marrom (conhecido como arroz “integral”; Figura 3) apresenta camadas mais externas, como a aleurona, que cobrem o endosperma rico em amido, e o embrião, ligado ao endosperma pelo escutelo (<http://www.knowledgebank.irri.org/rkb/rice-milling/contributions-and-references-milling/glossary/86.html>). O polimento do arroz marrom resulta na perda das camadas mais externas e do embrião, resultando no chamado arroz branco, mais comumente comercializado, que é constituído basicamente do endosperma. Interessantemente, as camadas de aleurona, subaleurona e o embrião contêm as maiores concentrações de Fe (e Zn) do grão maduro (Johnson et al 2011). Dessa forma, é necessário não apenas entender como a planta capta Fe nas raízes ou remobiliza Fe dos tecidos vegetativos para o grão, mas também compreender, no nível molecular, quais fatores determinam a localização dos metais nesses tipos celulares. Assim, será possível elaborar estratégias para aumentar as concentrações de metais especificamente no endosperma.

Em trigo, foi descrito um fator de transcrição da família NAC, NAM-B1, que controla a senescência durante o desenvolvimento (Uauy et al 2006). NAM-B1 é um pseudogene em cultivares modernas, mas é funcional em ancestrais selvagens do trigo. Sua expressão é detectada especialmente em folhas-bandeira, a folha imediatamente adjacente à panícula, e que é a folha que mais contribui com fotoassimilados, e possivelmente micronutrientes, para a semente em desenvolvimento (Abou-khalifa et al 2008, Waters et al 2009). Quando ativo, NAM-B1 acelera a senescência, o que aumenta a remobilização de Fe e Zn a partir da folha-bandeira e resulta em concentrações em torno de 30% mais altas nos grãos maduros (Uauy et al 2006, Waters et al 2009). Em arroz, o fator de transcrição NAC mais similar a NAM-B1 não apresenta a mesma função (Distelfeld et al 2012). Um possível candidato a ortólogo funcional é o gene *OsNAC5*, cuja expressão em folhas-bandeira é positivamente correlacionada com concentrações de Fe (e Zn) em grãos maduros de diferentes cultivares de arroz, e é associado com o processo de senescência (Sperotto et al 2009, Sperotto et al 2010).

Recentemente, foi demonstrado que a remobilização de Fe a partir de tecidos vegetativos não é absolutamente necessária, mas sim dependente do *status* nutricional da

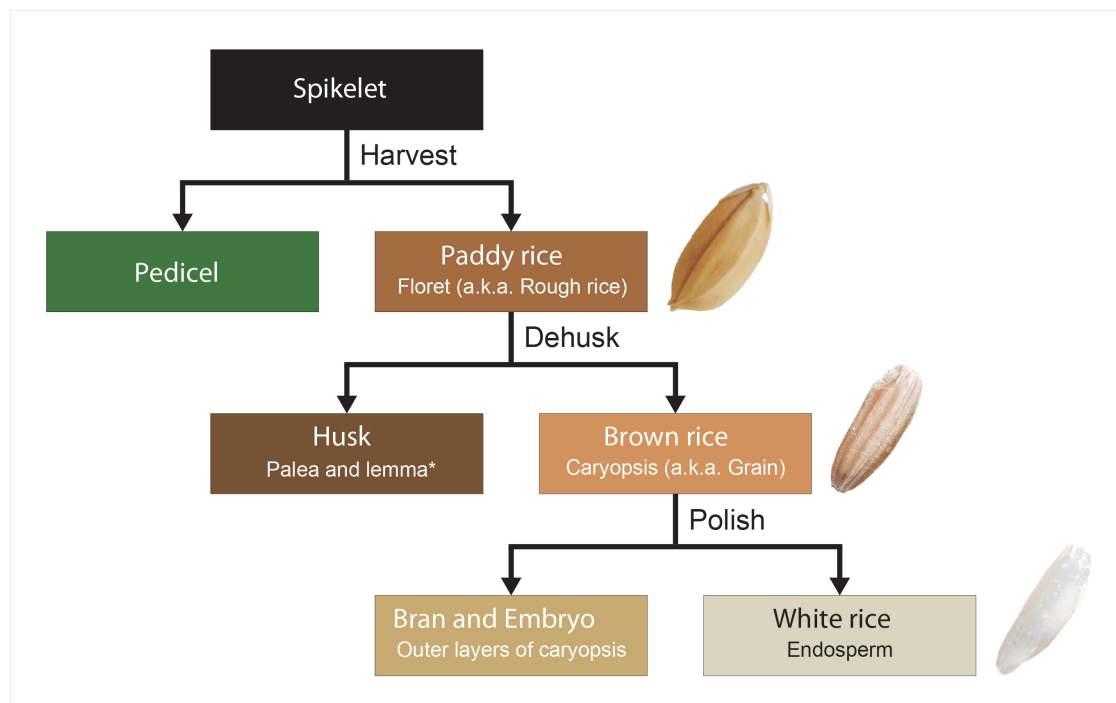


Figura 3. Representação esquemática do processamento dos grãos de arroz. As panículas sustentam as espiguetas, que são compostas pelo pedicelo e pelo florete. Durante a colheita, o florete é removido e então chamado de “paddy rice”, ou semente madura. A casca, composta da pálea e da lema e estruturas associadas, cobre a cariopse, denominada arroz marrom, grão ou arroz integral. Normalmente o arroz é polido para remover as camadas externas da cariopse e o embrião, o que resulta no arroz branco composto basicamente do endosperma. Figura de Sperotto et al (2012a).

planta: em baixas concentrações de Fe, a remobilização aumenta em importância relativa, enquanto a captação *de novo* nas raízes contribui mais para a concentração final no grão maduro quando a planta se encontra em condições de suficiência de Fe (Sperotto et al 2012b). Estes resultados estão de acordo com o que foi descrito em *Arabidopsis thaliana* (Waters et al 2008a). Outro trabalho recente demonstrou que os transportadores vacuolares de Fe OsVIT1 e OsVIT2 (*Vacuolar Iron Transporter*) exercem papel importante nas folhas-bandeira no controle da remobilização de Fe para os grãos (Zhang et al 2012). Em plantas com perda da função de *OsVIT1* ou *OsVIT2*, o Fe deixa de ser

armazenado nos vacúolos das células foliares em folhas-bandeira, aumentando a translocação para o grão via floema. Mutações nesses transportadores também resultam em alterações na localização de Fe no grão de arroz, especialmente na região do embrião (Zhang et al 2012). A perda de função do ortólogo de *Arabidopsis thaliana* também levou à alteração da distribuição de Fe: quando *AtVITI* é mutado, o Fe se localiza na face abaxial dos cotilédones, juntamente com manganês (Mn), enquanto em sementes de plantas do tipo-selvagem o Fe é visto em associação com o sistema pró-vascular (Kim et al 2006).

Tanto em arroz quanto em *A. thaliana*, diversos genes-candidatos foram identificados como possivelmente ligados às concentrações de Fe e outros metais nos grãos (Waters et al 2008b, Sperotto et al 2010). Porém, poucos trabalhos descrevem a função desses genes. As proteínas vacuolares codificadas pelos genes altamente similares AtNRAMP3 e AtNRAMP4 tem como função transportar Fe do vacúolo para o citoplasma, especialmente durante a germinação (Lanquar et al 2005). Já o transportador de Fe AtOPT3 tem função importante na translocação de Fe para as sementes, uma vez que mutantes *atopt3* acumulam Fe em outros tecidos mas tem concentração diminuída em sementes (Stacey et al 2008). No entanto, os ortólogos desses genes em arroz ou outras plantas de interesse agronômico ainda não foram caracterizados.

4. Homeostase de Zn em plantas

O Zn é um componente essencial de várias proteínas, sendo necessário para a manutenção da estrutura de mais de 300 enzimas e 2000 fatores de transcrição (Prasad 2012). É o segundo metal de transição mais abundante em organismos vivos, apresenta alta afinidade por uma ampla variedade de ligantes e pode adotar diversas geometrias em coordenação com outros átomos, sendo por isso extremamente flexível. Em condições biológicas, seu estado redox (+2) não é alterado e, portanto, o Zn não participa de reações de transferência de elétrons. Por isso, em comparação com outros metais de transição como Fe e Cu, o uso de Zn em macromoléculas é mais seguro em proximidade com macromoléculas como ácidos nucléicos (Sinclair e Krämer 2012). É o único metal representado em todas as seis classes de enzimas (Broadley et al 2007), e mais de setenta

metaloproteínas contendo Zn já foram identificadas (Barak e Helmke 1993), entre elas: a álcool desidrogenase, a anidrase carbônica, a cobre-zinco-superóxido dismutase, a fosfatase alcalina, a fosfolipase, a carboxipeptidase e a RNA polimerase (Marschner 1995).

O papel do Zn como componente estrutural de diversas enzimas o torna um elemento crucial para processos metabólicos em plantas, tais como fotossíntese, formação de sacarose e amido, síntese protéica, manutenção da integridade da membrana, metabolismo de auxina e reprodução (Marschner 1995; Barker w Pilbeam 2007). Uma das funções mais conhecidas do Zn está relacionada com a regulação da expressão gênica: a maior classe de proteínas ligantes de Zn é a daquelas que contêm domínios do tipo dedos de zinco, e são dependentes do metal para reconhecer seqüências de DNA específicas e ativar a transcrição de genes (Alberts et al 1998; Brown 2006).

Em geral, as plantas exibem sintomas de deficiência de Zn quando as concentrações na parte aérea são mais baixas que $15\text{-}20 \mu\text{g.g}^{-1}$ de peso seco (Marschner 1995, Sinclair e Krämer 2012). Os sintomas incluem redução da produção de biomassa, clorose foliar, maior ramificação da parte aérea, baixa fertilidade floral e início prematuro da senescência (Sinclair e Krämer 2012). Várias mudanças bioquímicas também podem ser relacionadas à deficiência de Zn: redução da atividade fotossintética, produção de radicais livres, diminuição da síntese protéica, redução dos níveis de auxinas, entre outras (Marschner 1995).

Entretanto, o excesso de Zn também é prejudicial, levando a sintomas como inibição do alongamento radicular e clorose nas folhas jovens (Marschner, 1995). Embora a concentração total de Zn em células eucarióticas seja estimada na ordem de $100 \mu\text{M}$, as concentrações internas de Zn livre estão abaixo da escala nanomolar, e em *Escherichia coli*, abaixo da fentomolar (Cousins 2006, Sinclair e Krämer 2012), indicando a necessidade de manter o Zn intracelular quelado e/ou compartmentalizado. O Zn é capaz de competir pelos sítios de ligação de proteínas que contenham metais de menor afinidade, em particular o Fe^{+2} e o Mg^{+2} , que apresentam raio iônico similar ao do Zn^{+2} , levando a uma deficiência induzida desses outros metais. De fato, diferentes abordagens demonstraram que alguns efeitos de concentrações altas de Zn podem ser mitigados por aumento concomitante nas concentrações de Fe (Shanmugam et al 2011,

Shanmugam et al 2012). Em geral, as plantas desenvolveram diferentes estratégias para lidar com concentrações excessivas de Zn: a exclusão, na qual a entrada nas raízes é impedida ou minimizada por meio de restrição de disponibilidade do metal no solo ou inibição da expressão de transportadores de aquisição; e a tolerância, baseada na detoxificação ou compartmentalização de Zn, permitindo o acúmulo do metal nos tecidos da planta de maneira não-tóxica (Lin e Aarts 2012). Interessantemente, algumas espécies que crescem em solos contaminados contendo altas concentrações de Zn desenvolveram mecanismos de hiperacumulação, sendo observados até 1% Zn/ massa seca em folhas (revisado por Krämer 2010).

4.1 Absorção de Zn nas raízes

Em comparação à aquisição de Fe nas raízes, pouco se sabe sobre os mecanismos de captação de Zn. Até o momento, não foi descrito um transportador de alta afinidade de Zn dedicado à absorção nas raízes a partir da rizosfera. Apesar de amplamente caracterizado como o principal transportador de Fe nas raízes de *Arabidopsis thaliana*, AtIRT1 é pouco específico, sendo capaz de transportar outros metais divalentes como Mn⁺², Co⁺², Cd⁺² e Zn⁺² (Eide et al 1996, Korshunova et al 1999, Rogers et al 2000, Connolly et al 2002). Assim, esses metais são captados do solo quando a planta é submetida à deficiência de Fe. De fato, as concentrações de Mn⁺², Co⁺², Cd⁺² e Zn⁺² aumentam em folhas de plantas sob deficiência de Fe até mesmo quando nenhuma alteração na concentração de Fe é observada (Baxter et al 2008a). De maneira similar, quando *OsIRT1* é super-expresso em plantas de arroz, as concentrações de Cd e Zn também aumentam em raízes, partes aéreas e grãos (Lee e An 2009). Esses resultados indicam que, embora não seja o transportador de Zn majoritário nas raízes, a contribuição de AtIRT1 (e OsIRT1) para a aquisição primária de Zn deve ser considerada na manutenção de níveis fisiológicos do metal.

No entanto, a captação indevida durante a resposta à deficiência de Fe leva a elevação rápida da concentração de Zn em raízes, sendo potencialmente tóxica. Em *A. thaliana*, o transportador vacuolar AtMTP3 é responsável por detoxificar esse Zn em excesso para dentro do vacúolo (Arrivault et al 2006). *AtMTP3* é expresso em células

epidérmicas e corticais e é induzido por deficiência de Fe, tendo um padrão de expressão similar ao de AtIRT1 (Arrivault et al 2006). Já o parólogo AtMTP1, também um transportador vacuolar de Zn, tem função geral na tolerância ao excesso de Zn, sendo expresso tanto em raízes quanto em parte aérea de forma constitutiva (Kobae et al 2004, Desbrosses-Fonrouge et al 2005 Kawachi et al 2009). Embora mutantes com perda de função tanto de AtMTP1 quanto de AtMTP3 tenham maior sensibilidade a concentrações excessivas de Zn, os papéis fisiológicos das proteínas são distintos: AtMTP3 retém Zn em excesso nas raízes, impedindo a toxidez na parte aérea, durante a resposta a deficiência de Fe; já AtMTP1 detoxifica Zn em excesso na célula, tanto em raízes quanto em parte aérea, de forma constitutiva (Kobae et al 2004 Desbrosses-Fonrouge et al 2005, Arrivault et al 2006, Kawachi et al 2009). Em arroz, foi descrita uma proteína ortóloga ao par de parálogos AtMTP1/AtMTP3. Apesar de ser demonstrado que OsMTP1 está envolvido na homeostase de Zn, os resultados desse trabalho são controversos, afirmando que a proteína está localizada na membrana plasmática e que poderia atuar no efluxo de Zn da célula (Yuan et al 2012). Uma vez que esses resultados não são consistentes com outros, a função de OsMTP1 ainda deve ser elucidada (Lan et al 2012, Menguer et al, submetido).

Outro gene importante para a compartmentalização de Zn em excesso em *Arabidopsis thaliana* é o transportador *ZINC-INDUCED FACILITATOR 1* (*AtZIF1*). A proteína vacuolar AtZIF1 é necessária para a tolerância ao excesso de Zn, e sua expressão é induzida por deficiência de Fe e excesso de Zn (Haydon and Cobbett 2007). No entanto, AtZIF1 não transporta metais para dentro do vacúolo, mas sim o quelante nicotianamina (NA; Haydon et al 2012). Especula-se que AtZIF1 poderia atuar em conjunto com AtMTP3, o primeiro transportando NA e o segundo transportando Zn para dentro do vacúolo, impedindo que a concentração vacuolar de Zn livre seja danosa (Haydon et al 2012, Sinclair e Krämer 2012).

4.2 Transporte radial e carregamento do xilema

Assim como para Fe, acredita-se que o transporte radial de Zn ocorra pelo simplasto: uma vez dentro das células da epiderme ou córtex, o Zn circula livremente até

as células do pericílio, onde transportadores de efluxo carregam o metal no xilema (Sinclair e Krämer 2012). No entanto, o mutante de *A. thaliana* *enhanced suberin 1* (*esb1*), que contém maior quantidade de suberina depositada no apoplasto da endoderme, apresenta redução nas concentrações de Ca, Mn e Zn na parte aérea (Baxter et al 2009). Esses resultados sugerem que Ca, Mn e Zn são transportados radialmente via apoplasto nas raízes, e não via simiplasto (Baxter et al 2009). Outro trabalho também sugere que Zn chegue até o xilema nas raízes via apoplasto (White et al 2002), indicando que a contribuição relativa de cada via para o transporte radial de Zn (e de outros elementos) deve ser elucidada.

Os principais transportadores para o carregamento do xilema são proteínas da família HMA (*Heavy Metal Associated*). Em *Arabidopsis thaliana*, o par de parálogos AtHMA2 e AtHMA4 tem funções redundantes, e são responsáveis pelo efluxo de Zn do pericílio para ao xilema, tendo papel fundamental na translocação de Zn para a parte aérea. Duplo-mutantes *athma2athma4* têm crescimento prejudicado, alta concentração de Zn em raízes e redução em parte aérea (Eren and Arguello 2004, Hussain et al 2004, Verret et al 2005). Em arroz, OsHMA2 tem função similar na translocação de Zn (Nocito et al 2011, Satoh-Nagasawa et al 2012, Takahashi et al 2012). Interessantemente, existem três cópias ortólogas do gene *HMA4* no genoma da Brassicaceae hiperacumuladora de Zn *Arabidopsis halleri*, que foram descritos como produtos de dois eventos de duplicação subsequentes (Hanikenne et al 2008). A triplicação de *HMA4*, assim como modificações em elementos *cis* do seu promotor que permitem expressão constitutiva, estão diretamente envolvidas no surgimento da característica de hiperacumulação nessa espécie (Hanikenne et al 2008, Sinclair e Krämer et al 2012).

Outro transportador com função no efluxo de Zn do pericílio para o xilema é a proteína PLANT CADMIUM RESISTANCE 2 (AtPCR2). Mutantes com perda de função de AtPCR2 apresentam fenótipo similar ao duplo mutante *athma2athma4*, com aumento da concentração de Zn nas raízes e redução da concentração em parte aérea (Song et al 2010). Sua função, porém, não é redundante à de HMA2 e HMA4. Baseado no fato de sua expressão ser observada tanto no pericílio quanto na epiderme, sugere-se que AtPCR2 tenha mais de uma função, sendo importante em condições de deficiência de Zn para aumentar a translocação das raízes para a parte aérea, mas também em excesso

de Zn, onde faria o efluxo de Zn da epiderme para a rizosfera (Song et al 2010). No entanto, existem poucas evidências para a função no efluxo de Zn. Não foram caracterizados gene homólogos a *AtPCR2* em arroz ou outras gramíneas.

4.3 Transporte de Zn na parte aérea e remobilização por meio de carregamento do floema

Uma vez no xilema, o Zn é levado à parte aérea pelo fluxo de massa da transpiração. Pouco se sabe sobre como as células adjacentes ao xilema captam Zn na parte aérea, e como este é distribuído entre os diferentes tipos celulares. Sugere-se que tricomas e células epidérmicas em particular acumulem as concentrações mais altas de Zn (Sinclair e Krämer 2012). No entanto, trabalhos com hiperacumuladores de Zn mostram que, enquanto *Noccaea caerulescens* acumula Zn apenas nas células da epiderme, *Arabidopsis halleri* acumula altas concentrações tanto em tricomas quanto em células do mesófilo (Küpper et al 1999, Küpper et al 2000), indicando que pode haver variação no mecanismo de estocagem de Zn excedente em folhas (ver Capítulo 2). Apesar disso, considera-se que os vacúolos sejam o principal sítio de armazenamento de Zn nas folhas, principalmente devido à atividade de MTP1 (Sinclair e Krämer 2012). Em suporte a essa hipótese, foi observada uma correlação positiva entre as concentrações totais de Zn em folhas de diferentes ecotipos de *Arabidopsis thaliana* e a expressão em nível de mRNA de *AtMTP1* (Conn et al 2012). Ainda assim, o papel relativo de cada tipo celular na homeostase de Zn em folhas, especialmente em *Arabidopsis thaliana*, não está elucidado.

A remobilização de Zn a partir das folhas pelo floema é claramente descrita em trigo (Erenoglu et al 2011). Evidências apontam que NA é responsável por quiciar Zn no floema, permitindo assim o transporte de longa distância (Klatte et al 2009, Haydon et al 2012, Deinlein et al 2012). Em arroz, foi recentemente demonstrado que Zn(II)-NA é a forma majoritária de Zn no floema (Nishiyama et al 2012). No entanto, apesar de ter sido demonstrado que AtYSL1 e AtYSL3 de *A. thaliana* são necessários para a remobilização de Zn durante a senescência, nenhum transportador YSL (ou de outra família gênica) testado até o momento apresentou atividade de transporte de Zn(II)-NA (Curie et al 2009).

4.4 Transporte de Zn para as sementes

Embora as concentrações de Fe e Zn em diferentes órgãos sejam reguladas por transportadores distintos, as concentrações de ambos os metais em grãos maduros apresentam correlação positiva, indicando que mecanismos similares podem alocá-los para as sementes em desenvolvimento (Uauy et al 2006, Sperotto et al 2009). O fator de transcrição de trigo NAM-B1, quando não-funcional, diminui o acúmulo de Zn nos grãos, assim como de Fe (Uauy et al 2006). Conforme já descrito, o possível ortólogo funcional de arroz OsNAC5 também pode ter efeito na remobilização de Zn, uma vez que é observada correlação positiva entre o nível de expressão de *OsNAC5* e a concentração final de Zn nos grãos de diferentes cultivares (Sperotto et al 2009). Além disso, foi demonstrado que a remobilização de Zn a partir das folhas-bandeira, assim como das folhas não-bandeira superiores, contribui significativamente para as concentrações finais de Zn no grão (Yoneyama et al 2010).

Os transportadores vacuolares de arroz OsVIT1 e OsVIT2 também transportam Zn, ao contrário do seu ortólogo de *Arabidopsis thaliana* AtVIT1 (Kim et al 2006, Zhang et al 2012). Assim, mutantes com perda de função em qualquer um dos dois genes VIT de arroz apresentam redução da concentração de Zn nos grãos maduros, uma vez que as duas proteínas permitem o armazenamento de Zn (e Fe) nos vacúolos das folhas bandeiras, tornando-os menos disponíveis para remobilização (Zhang et al 2012). Além disso, como mutações nos genes VIT causam alteração na localização de Fe no grão, é possível que esses mutantes apresentem diferenças na localização de Zn, embora não tenham sido feitas análises para comprovar essa hipótese (Zhang et al 2012).

Outra família gênica que parece estar envolvida na localização de Zn em sementes é a das metalotioneínas (MT). MTs são proteínas de sequência primária curta, ricas em resíduos de cisteínas, inicialmente descritas pela sua capacidade em quelar e detoxificar Cd. Porém, se sabe que MT também se ligam a outros metais, incluindo Zn (Cobbett and Goldsbrough 2002). Em plantas, as MTs são subdivididas em quatro subtipos, e as do tipo 4 tem maior afinidade por Zn (Guo et al 2008). Em *A. thaliana*, *AtMT4a* e *AtMT4b* são expressos em embriões, e a super-expressão ou silenciamento de cada um leva ao

aumento e à diminuição da concentração de Zn nas sementes, respectivamente (Ren et al 2012). Em arroz, transcritos de *OsMT1a* acumulam-se em resposta a tratamento com excesso de Zn, e plantas super-expressando *OsMT1a* apresentam concentrações mais altas de Zn, tanto em folhas quanto em grãos (Yang et al 2009).

5. Transportadores da família ZIP (ZRT/IRT - Zinc-Regulated/ Iron-Regulated Transporter)

O primeiro membro da família ZIP a ser descrito foi o transportador de Fe AtIRT1 de *A. thaliana*, seguido pelos transportadores de Zn ZRT1 e ZRT2 de levedura (*Saccharomyces cerevisiae*; Eide et al 1996, Zhao e Eide 1996a, Zhao e Eide 1996b). AtIRT1, conforme já comentado, apresenta afinidade por Zn^{+2} , além de Fe^{+2} e outros cátions divalentes (Korshunova et al 1999). Os parálogos de AtIRT1, AtIRT2 e AtIRT3, também transportam Zn^{+2} . Porém, tanto para AtIRT1 quanto para AtIRT2 não existem evidências que indiquem função na homeostase de Zn *in planta* (Eide et al 1996, Vert et al 2001, Connolly et al 2002, Vert et al 2002). Já AtIRT3 tem transcritos acumulados em resposta à deficiência de Zn, enquanto as espécies hiperacumuladoras de Zn *A. halleri* e *N. caeruleascens* apresentam quantidades dos transcritos dos respectivos ortólogos constitutivamente altas (Becher et al 2004; Talke et al 2006; van de Mortel et al 2006, Lin et al 2009). Além disso, a super-expressão de AtIRT3 leva ao aumento da concentração de Zn em parte aérea de plantas de *A. thaliana*, indicando uma função na homeostase de Zn (Lin et al 2009).

Vários ZIPs foram descritos como tendo capacidade de transporte de Zn em diferentes espécies de plantas. Os transportadores de *A. thaliana* AtZIP1, AtZIP2 e AtZIP3 são capazes de transportar Zn quando transformados em leveduras (Grotz et al 1998). Na leguminosa *Medicago truncatula*, outras três proteínas, MtZIP1, MtZIP5 e MtZIP6, transportam Zn (López-Millán et al 2004), enquanto em soja (*Glycine max*), GmZIP1 foi descrito como um transportador de Zn específico de nódulos (Moreau et al 2002). Já as proteínas de arroz OsZIP1, OsZIP3, OsZIP4, OsZIP5 e OsZIP8 transportam Zn quando expressos heterologamente em leveduras (Ramesh et al 2003; Ishimaru et al 2005; Ishimaru et al 2007; Lee et al 2010a; Lee et al 2010b; Yang et al 2009). Destes,

OsZIP4 é um dos mais estudados: é induzido por deficiência de Zn tanto em raízes quanto em parte aérea, e seu promotor tem atividade associada com o floema e meristemas (Ishimaru et al 2005). A super-expressão de *OsZIP4* em arroz resulta no aumento da concentração de Zn em raízes, porém em redução das concentrações na parte aérea e em grãos (Ishimaru et al 2007). Resultados similares foram obtidos com *OsZIP5* and *OsZIP8* (Lee et al 2010a, Lee et al 2010b). Apesar de se especular que *OsZIP4* tenha papel na translocação de Zn da raiz para a parte aérea, ainda é necessário um conjunto maior de evidências para corroborar essa hipótese (Ishimaru et al 2007). Ainda assim, é interessante notar que poucos dados funcionais de ZIPs *in planta* foram obtidos até o momento.

6. Biofortificação de grãos de arroz

A biofortificação é definida como o aumento das concentrações biodisponíveis de nutrientes nas partes comestíveis de plantas antes da colheita (White and Broadley 2005). Tentativas de biofortificar o grão de arroz com Fe e Zn utilizando técnicas de melhoramento clássico têm enfrentado dificuldades, principalmente devido à baixa variabilidade nas concentrações de Fe e Zn no germoplasma de arroz, diferente do que se observa em trigo e milho (Kennedy e Burlingame 2003, Pfeiffer et al 2008). São consideradas cinco possíveis etapas limitantes para que tentativas de biofortificação sejam bem sucedidas: (1) absorção nas raízes; (2) carregamento no xilema; (3) remobilização de metais das folhas e carregamento do floema; (4) descarregamento nos grãos; e (5) força de dreno dos grãos (Figura 4).

Inicialmente, a maior parte das tentativas visava aumentar a concentração de Fe no endosperma de grãos de arroz por meio do aumento da força de dreno do tecido. Para isso, foram utilizadas construções que continham o gene da ferritina controlado por um promotor endosperma-específico (Goto et al 1999, Lucca et al 2001, Vasconcelos et al 2003, Drakakaki et al 2005, Qu et al 2005). A ferritina é uma proteína composta por 24 subunidades, em uma estrutura capaz de armazenar Fe de forma segura e biodisponível, pois pode ser liberado dependendo da demanda celular (Arosio et al 2009). Apesar do relativo sucesso, com aumento de até 3 vezes na concentração de Fe em endosperma,

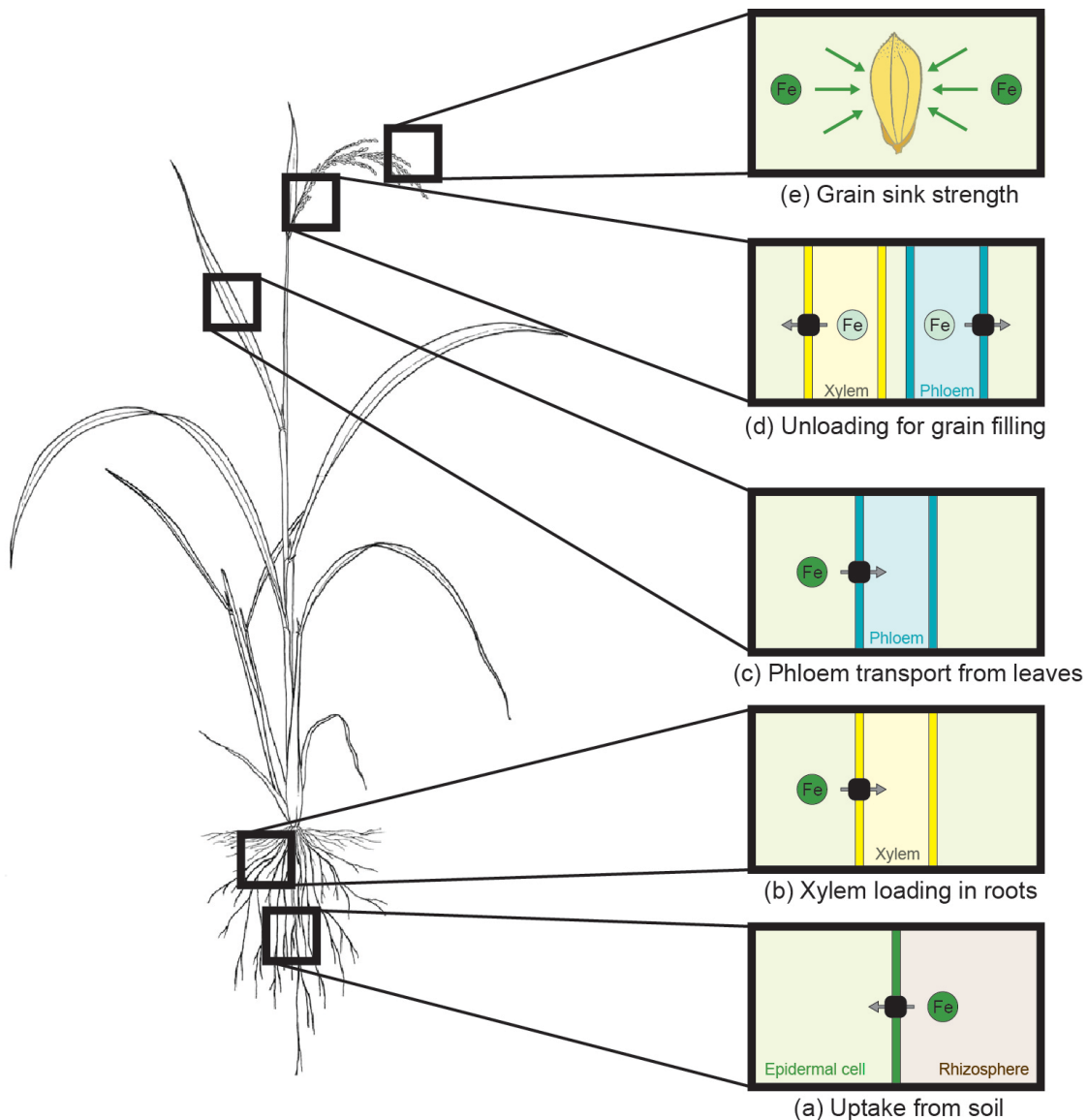


Figura 4. Possíveis etapas limitantes para o acúmulo de metais nos grãos. (A) Aquisição a partir do solo pelas raízes. (B) Carregamento do xilema pelas raízes para translocação para a parte aérea. (C) Transporte nas folhas através do floema durante o enchimento do grãos. (D) Carregamento do grão. (E) Força de dreno do grão. Figura de Sperotto et al (2012a). Imagem da planta de arroz gentilmente cedida por Nicholas Polato, Cornell Rice Program; e utilizada com permissão pela base de dados Gramene (http://www.gramene.org/species/oryza/rice_illustrations.html).

percebeu-se que esse aumento era menor do que o aumento dos níveis de expressão da proteína ferritina, 10 vezes maior. Assim, concluiu-se que o simples incremento da demanda de Fe no endosperma não era suficiente para aumentar a concentração de maneira significativa, indicando que outras etapas-chave deveriam ser identificadas (Qu et al 2005, Sperotto et al 2012).

Pelo menos dois trabalhos mostram relativo sucesso quando mais de um transgene é inserido no genoma da planta. Wirth et al (2009) utilizaram expressão específica de ferritina em endosperma e expressão constitutiva de *AtNAS1* concomitantemente. Além disso, foi incluída uma terceira construção contendo uma fitase, também controlada por promotor endospema-específico (Wirth et al 2009). A fitase tem por finalidade degradar o fitato, considerado um anti-nutriente devido à sua capacidade de se ligar a metais e torná-los não-disponíveis para absorção pelos enterócidos no intestino humano (Reddy et al 1996). No entanto, apesar do aumento na concentração de Fe no endosperma ser cerca de 6 vezes, os valores ainda estão longe do indicado para ter algum efeito na nutrição humana (Wirth et al 2009, Sperotto et al 2012). Mais recentemente, outro trabalho também utilizou uma estratégia multigênica: um cassete contendo o gene da ferritina sob controle de dois diferentes promotores endosperma-específicos; um gene da enzima NAS sob controle do promotor constitutivo da actina; e o gene *OsYSL2* sob controle de um promotor endosperma-específico e também sob controle do promotor de *SUT1*, ativo em panículas e grãos imaturos, totalizando cinco diferentes unidades de transcrição inseridas, mais marcadores de seleção (Masuda et al 2012). Mais uma vez, observou-se aumentos das concentrações de Fe de quatro a seis vezes em comparação com plantas não transformadas, porém com valores de concentração similares ao observado anteriormente (Wirth et al 2009, Masuda et al 2012). Apesar dos valores absolutos não representarem um ganho significativo na qualidade nutricional dos grãos, esses trabalhos foram relativamente bem-sucedidos em utilizar conhecimento adquirido para elaborar estratégias de biofortificação.

Diversos trabalhos observaram alterações nas concentrações de Fe e Zn quando genes foram mutados ou super-expressos, porém poucos tiveram resultados com potencial para a biofortificação. A ativação por *activation-tagging* dos genes *OsNAS2* e *OsNAS3* causou aumentos de cerca de duas vezes nas concentrações de Fe e Zn. Testes

demostraram que, quando alimentados com o arroz transgênico, camundongos absorveram maiores quantidades de Fe e Zn (Lee et al 2009b, Lee et al 2011). A super-expressão de genes NAS também se mostrou uma estratégia bem-sucedida: no melhor resultado até o momento descrito na literatura, Johnson et al (2011) mostraram aumentos de 2 a 4 vezes nas concentrações de Fe quando os genes *OsNAS1*, *OsNAS2* ou *OsNAS3* são super-expressos independentemente em plantas de arroz. Nesse caso os valores de concentração estão acima do que é considerado necessário para ter impacto na nutrição humana. Porém, nenhum teste de biodisponibilidade para absorção foi conduzido com essas plantas, assim como não se tem dados sobre a estabilidade da construção e do fenótipo após múltiplas gerações (Johnson et al 2011).

7. **Linhagens de *Arabidopsis thaliana* Rice Full-length Over-expressors (FOX)**

Uma grande quantidade de informação foi obtida com o sequenciamento do genoma do arroz (Goff et al 2002, Yu et al 2002, IRGSP 2005). Ainda assim, é necessário entender a função de cada gene para que seja possível transformar esse conhecimento em cultivares mais produtivas e/ou com características consideradas superiores (Zheng et al 2008). Apesar da grande quantidade de recursos para a caracterização de genes em arroz, *A. thaliana* apresenta vantagens na facilidade de trabalho, principalmente se considerarmos tempo de geração, espaço necessário para cultivo, rapidez no crescimento, etc. Para utilizar essa vantagem e acelerar a identificação de genes importantes de arroz, plantas de *A. thaliana* tiveram cDNAs de arroz inseridos em seu genoma por meio de transformação com *Agrobacterium tumefaciens*, gerando 23.000 linhagens FOX independentes (Kondou et al 2009). Cada linhagem teve o cDNA inserido sequenciado, e sementes T2 dessas linhagens foram disponibilizadas publicamente por meio da base de dados RiceFOX (<http://ricefox.psc.riken.jp/>; Sakurai et al 2011). Trabalhos foram realizados para encontrar genes envolvidos na resistência a *Pseudomonas syringae* (Dubouzet et al 2011), metabolismo de nitrogênio (Albinsky et al 2010), tolerância a estresse (Yokotani et al 2009), além de caracterização de genes

específicos (Anders et al 2012). No entanto, nenhum trabalho utilizou essa ferramenta para a busca e caracterização de genes que regulam o ionoma (ver abaixo).

8. As técnicas de *inductively coupled plasma* (ICP-MS) e *synchrotron X-ray fluorescence* (SXRF) no estudo do ionoma de plantas

8.1 Uso de ICP-MS no estudo do ionoma de plantas e o *ionomicsHub*

A técnica analítica de ICP tem por finalidade ionizar átomos em uma amostra para detecção, utilizando para isso um plasma, um gás no qual os átomos estão presentes no estado ionizado. Para a detecção, pode-se utilizar tanto a emissão óptica espectroscópica (*optical emission spectroscopy* – ICP-OES; o mesmo que *atomic emission spectroscopy* – ICP-AES), quanto a espectrometria de massas (*mass spectrometry* – ICP-MS) (Salt et al 2008). Embora já consagradas na química analítica, técnicas de ICP passaram a ser amplamente usadas para análise de amostras biológicas, especialmente a partir da possibilidade de análises *high-throughput* (Lahner et al 2003, Salt et al 2008). A ionômica (*ionomics*), ou estudo dos elementos presentes em um organismo, tem por objetivo compreender como a concentração, localização e especiação desses elementos são reguladas e controladas pelos seres vivos (Salt et al 2008). O desenvolvimento do campo ocorreu de forma concomitante com ferramentas analíticas de bioinformática, estatística e, mais recentemente, genética, como microarranjos de DNA, sequenciamento de genomas e bancos de mutantes e germoplasmas, além da diminuição dos custos de análise (Salt et al 2008). Como exemplo, recentemente o ionoma completo de *Saccharomyces cerevisiae* foi analisado, utilizando linhagens mutantes, super-expressororas, ou mutantes diplóides em heterozigose, para todos os genes conhecidos da levedura (Yu et al 2012).

Em plantas, a ionômica ganhou espaço a partir do trabalho de Lahner et al (2003), que possibilitou comparação do perfil ionômico entre diferentes grupos amostrais, incluindo 18 elementos distintos (Li, B, Mg, P, S, K, Ca, Mn, Fe, Co, Ni, Cu, Zn, As, Rb, Sr, Mo, Cd), em grande número de populações de mutantes de *Arabidopsis thaliana* (cerca de 6.000; Lahner et al 2003). Após, diversos trabalhos utilizaram o

conceito para identificar genes que controlam o ionoma, tanto em *screenings* de mutantes de perda de função quanto em populações naturais de *A. thaliana*, e em cultivares de arroz (Baxter et al 2008b, Baxter et al 2009, Morrissey et al 2009, Atwell et al 2010, Buescher et al 2010, Chao et al 2012, Baxter et al 2012, Norton et al 2012). É interessante notar que trabalhos envolvendo variedades genéticas permitem a identificação de genótipos envolvidos na variação fenotípica observada no ionoma. É possível, portanto, explorar outro conjunto de genes, que não necessariamente seriam identificados utilizando-se um único ecótipo ou cultivar contendo mutações de perda de função.

Foi criado um espaço virtual para a divulgação e compartilhamento dos dados gerados pela comunidade científica envolvida no estudo do ionoma, o *Ionomics Hub* (iHub; www.ionomicshub.org), visando a homogeneização na análise, comparação e publicação dos resultados, além de possibilitar a meta-análise dos mesmos (Baxter et al 2007). Atualmente, o iHub hospeda dados provenientes de projetos envolvendo *Arabidopsis thaliana* (172.811 amostras analisadas), arroz (26.268) e soja (6.872), está construindo as bases de dados de milho e canola, e ainda possui uma para *Saccharomyces cerevisiae* (51.550 amostras analisadas, Yu et al 2012). Por serem públicos, os dados do iHub já estão sendo utilizados para a geração e teste de hipóteses por grupos não necessariamente colaboradores e gerando publicações (Conn et al 2012), demonstrando a utilidade desse tipo de iniciativa.

8.2 Uso de SXRF no estudo na homeostase de metais em plantas

Apesar de ICP-MS (e ICP-OES) ser considerada a técnica de excelência para quantificação, ela apresenta a desvantagem de não possibilitar a obtenção de qualquer informação quanto à localização espacial dos elementos. Para isso, técnicas envolvendo fluorescência de raios-X baseadas em radiação sincrotron (SXRF – *synchrotron X-ray fluorescence*) apresentam-se como alternativa, ainda que com menor acuidade na quantificação e *throughput*. XRF é o resultado da emissão de radiação de um átomo após excitação e absorção de raios-X de alta energia. A radiação, ou fluorescência, é característica do átomo do qual ela foi emitida, podendo então ser utilizada para detectar

e quantificar elementos específicos em misturas complexas (Salt et al 2008). Quando a radiação síncrotron é utilizada para gerar os raios X, é possível focalizá-los em áreas micrométricas e até sub-micrométricas devido à grande quantidade de energia, permitindo a análise tanto da distribuição quanto da concentração de elementos múltiplos, com limites de detecção bastante baixos. Técnicas de SXRF passaram a ser aplicadas tanto para mapeamento em duas dimensões, assim como em três dimensões nos casos de tomografia SXRF e SXRF confocal, permitindo a análise de amostras praticamente sem necessidade de preparo (Salt et al 2008, Donner et al 2012).

As aplicações de SXRF para o estudo do ionoma de plantas, especialmente em associação com técnicas de genética molecular, estão apenas começando a ser exploradas. Muitos trabalhos utilizaram SXRF para descrever a localização de elementos em plantas hiperacumuladoras, como Co e Ni em *Alyssum murale* (Tappero et al 2007) e Zn em *Arabidopsis halleri* (Sarret et al 2009) e Se em *Stanleya pinnata* e *Astragalus bisulcatus* (Freeman et al 2012), assim como a distribuição de Fe, Zn, As e Se em arroz (Carey et al 2011, Johnson et al 2011, Carey et al 2012) e As e Se em feijão-caupí (*Vigna unguiculata*; Kopittke et al 2012a, Kopittke et al 2012b). Esses trabalhos mostram a localização quantitativa de elementos, porém não utilizam abordagens genéticas para possibilitar a identificação dos genes determinantes para a localização.

Em um trabalho pioneiro, a tomografia SXRF ajudou a descrever a função do gene AtVIT1 de *A. thaliana* (Kim et al 2006). Sementes do mutante *vit1*, que não possui cópia funcional do gene *AtVIT1* (ver seção 3.4), apresentam alteração na distribuição de Fe em comparação com o tipo selvagem. Curiosamente, a concentração de Fe é a mesma, demonstrando um caso em que o fenótipo do mutante não poderia ser identificado apenas pela quantificação de Fe (i.e., por ICP-MS), sendo necessária a informação espacial (Kim et al 2006). Posteriormente, mutantes de *A. thaliana* com perda de função nos transportadores de Ca CAX1 e CAX3 foram analisados, identificando o papel das proteínas no acúmulo de Ca em sementes (Punshon et al 2012). Em arroz, o mapeamento em 2D de sementes de plantas super-expressando *OsNAS2* demonstrou que o aumento na concentração de Fe e Zn observado por ICP-OES está diretamente associado a aumento da abundância de ambos os metais nas camadas de aleurona, sub-aleurona e no endosperma, este último o tecido ideal para acúmulo de nutrientes no grão de arroz

visando a biofortificação (Johnson et al 2011). Portanto, o uso de técnicas de SXRF ainda é pequeno no estudo da regulação do ionoma, porém apresenta grande potencial.

9. Tricomas

Os tricomas são protuberâncias formadas na camada mais externa da epiderme, tomando formas bastante distintas. Atuam principalmente como barreiras física e química contra herbívoros e patógenos, além de proteger a planta contra a radiação UV-B, altas temperaturas e a perda de água (Wagner et al 2004). Os tricomas são bastante utilizados na taxonomia, e dependendo de sua função, podem ser classificados em glandulares e não-glandulares (Tissier 2012).

Os tricomas glandulares variam não apenas na forma, mas também quanto aos metabólitos secretados, desde óleos e açúcares até metais, havendo interesse comercial em alguns desses produtos de secreção (Sarret et al 2006, Weinhold e Baldwin 2011, Tissier 2012). Tricomas glandulares estão presentes em cerca de 30% das plantas vasculares, e têm função como obstáculos para o movimento pela superfície da epiderme e/ou captura de predadores e como fonte de metabólitos secundários voláteis, não voláteis e proteínas que repelem ou são tóxicos para herbívoros (Laue 2000, Simmons et al 2004, Cardozo 2008, Shepherd e Wagner 2007, Schilmiller et al 2010). Em tabaco, a excreção de Zn e Cd por tricomas glandulares é conhecida, ocorrendo quando os metais estão em concentrações elevadas, na forma de cristais contendo Ca (Sarret et al 2006, Isaure et al 2010).

Já os tricomas não-glandulares são amplamente estudados como modelo para o entendimento da diferenciação celular não-programada e formação de padrões, uma vez que a determinação de quais células da epiderme irão se desenvolver como tricomas ocorre através de sinais entre células vizinhas previamente equivalentes, porém não randômica (An et al 2011, Grebe 2012). Devido à disponibilidade de ferramentas, o desenvolvimento e a estrutura dos tricomas de *A. thaliana* são os mais conhecidos. Os tricomas de *A. thaliana* se desenvolvem a partir de uma única célula da epiderme, que para de se dividir, aumenta em tamanho e continua replicando seu DNA, num processo

conhecido como endoreplicação. Cada célula de tricoma pode passar por dois a três ciclos de endoreplicação, atingindo até 8N (Marks 1997, Grebe 2012).

Algumas proteínas que controlam a diferenciação do tricoma e a inibição do processo de células adjacentes são conhecidas. O complexo ternário, formado pelos fatores de transcrição GLABRA1 (GL1), GLABRA3(GL3) ou ENHANCER OF GLABRA3 (EGL3), com TRANSPARENT TESTA GLABRA1 (TTG1), promove a expressão de GLABRA2 (GL2) que, por sua vez, controla a diferenciação da célula em tricoma (Ishida et al 2008). Em contrapartida, o complexo composto pelas proteínas CAPRICE (CPC), TRPTYCHON (TRY), ENHANCER OF TRY AND CPC 1 (ETC1) ou ETC2, é formado na própria célula em diferenciação, e se move a partir dela para as células vizinhas, onde compete com GL1 pela ligação à GL3/EGL3, inibindo a ativação do complexo GL1-GL3/ELG3-TTG1. Assim, a célula que está se diferenciando em tricoma inibe as células adjacentes que permanecem com identidade de célula epidérmica (An et al 2011, Grebe et al 2012).

A relação entre tricomas e acúmulo de metais já foi observada em diversas plantas, como, Pb, Zn e Cd em *Nicotiana tabacum* (Martell 1974, Sarret et al 2006, Isaure et al 2010), Cd em *Brassica juncea* (Salt et al 1995), Mn em *Helianthus annuus* (Blamey et al 1986), Ni nas hiperacumuladoras de Ni *Alyssum lesbiacum* e *Alyssum murale* (Krämer et al 1997, Küpper et al 2001, Tappero et al 2007), Zn e Cd em *Arabidopsis halleri* (Hokura et al 2006, Sarret et al 2009) e Zn em *Arabidopsis lyrata* (Sarret et al 2009). Considerando tricomas não-glandulares, um estudo comparando a hiperacumuladora *A. halleri* e com a não-hiperacumuladora *A. lyrata* indicou que provavelmente o sítio de hiperacumulação em *A. halleri* são as células do mesófilo, que detoxificariam o Zn em excesso para dentro do vacúolo por meio de transportadores MTP1, excluindo os tricomas como sítios importantes para a detoxificação em hiperacumuladores (Sarret et al 2009, Shahzad et al 2010). Em *A. thaliana*, também não-hiperacumuladora de metais, foi observado acúmulo de Cd e Mn em tricomas (Ager et al 2003, Isaure et al 2006). Porém, até o momento, tanto a função quanto o mecanismo de controle desse acúmulo em tricomas não-glandulares em plantas permanece desconhecido.

Objetivos

1. Objetivo Geral

Identificar novos genes potencialmente envolvidos com a homeostase de Fe e Zn em plantas de arroz visando contribuir para o entendimento da homeostase de metais em plantas.

2. Objetivos Específicos

- Identificar sequências similares ao gene *AtZIF1* no genoma de arroz e de outras plantas com genoma sequenciado;
- Caracterizar os genes semelhantes a *AtZIF1* no genoma de arroz quanto à organização gênica, genômica e expressão em resposta a estresses de deficiência de Fe e excesso de Zn;
- Analisar linhagens de *A. thaliana* expressando genes de arroz (FOX lines) utilizando ICP-MS para determinação do perfil ionômico das mesmas, em comparação com plantas tipo selvagem;
- Caracterizar funcionalmente genes que alteram o perfil ionômico de *A. thaliana*, por meio de expressão em linhagens levedura mutantes para o transporte de Fe e Zn, e por meio da expressão transiente em protoplastos para determinar a localização subcelular;
- Caracterizar as linhagens com perfil ionômico alterado em concentrações não-ótimas de metais no meio de cultura (i.e., deficiência ou excesso);
- Utilizar técnicas de SXRF para caracterizar as linhagens com perfil ionômico alterado;

Capítulo 1

**Artigo publicado no periódico *BMC Plant Biology*
(Fator de Impacto JCR 2011 = 3.45)**

RESEARCH ARTICLE

Open Access

ZINC-INDUCED FACILITATOR-LIKE family in plants: lineage-specific expansion in monocotyledons and conserved genomic and expression features among rice (*Oryza sativa*) paralogs

Felipe K Ricachenevsky¹, Raul A Sperotto¹, Paloma K Menguer², Edilena R Sperb², Karina L Lopes², Janette P Fett^{1,2*}

Abstract

Background: Duplications are very common in the evolution of plant genomes, explaining the high number of members in plant gene families. New genes born after duplication can undergo pseudogenization, neofunctionalization or subfunctionalization. Rice is a model for functional genomics research, an important crop for human nutrition and a target for biofortification. Increased zinc and iron content in the rice grain could be achieved by manipulation of metal transporters. Here, we describe the ZINC-INDUCED FACILITATOR-LIKE (*ZIFL*) gene family in plants, and characterize the genomic structure and expression of rice paralogs, which are highly affected by segmental duplication.

Results: Sequences of sixty-eight *ZIFL* genes, from nine plant species, were comparatively analyzed. Although related to MSF_1 proteins, *ZIFL* protein sequences consistently grouped separately. Specific *ZIFL* sequence signatures were identified. Monocots harbor a larger number of *ZIFL* genes in their genomes than dicots, probably a result of a lineage-specific expansion. The rice *ZIFL* paralogs were named *OsZIFL1* to *OsZIFL13* and characterized. The genomic organization of the rice *ZIFL* genes seems to be highly influenced by segmental and tandem duplications and concerted evolution, as rice genome contains five highly similar *ZIFL* gene pairs. Most rice *ZIFL* promoters are enriched for the core sequence of the Fe-deficiency-related box IDE1. Gene expression analyses of different plant organs, growth stages and treatments, both from our qPCR data and from microarray databases, revealed that the duplicated *ZIFL* gene pairs are mostly co-expressed. Transcripts of *OsZIFL4*, *OsZIFL5*, *OsZIFL7*, and *OsZIFL12* accumulate in response to Zn-excess and Fe-deficiency in roots, two stresses with partially overlapping responses.

Conclusions: We suggest that *ZIFL* genes have different evolutionary histories in monocot and dicot lineages. In rice, concerted evolution affected *ZIFL* duplicated genes, possibly maintaining similar expression patterns between pairs. The enrichment for IDE1 boxes in rice *ZIFL* gene promoters suggests a role in Zn-excess and Fe-deficiency up-regulation of *ZIFL* transcripts. Moreover, this is the first description of the *ZIFL* gene family in plants and the basis for functional studies on this family, which may play important roles in Zn and Fe homeostasis in plants.

Background

Duplications are recurrent in the evolutionary history of plant genomes. Whole genome duplications (or polyploidy) are described for dicotyledons and monocotyledons [1-4]. It is estimated that the incidence of

polyploidy in angiosperms is 30-80%, and ploidy changes may represent about 24% of speciation events [5]. Duplication generates two copies of each gene, and the fate of duplicated genes was first described by Ohno: one copy should maintain the ancient function and another copy should lose function (pseudogenization) or gain a new function (neofunctionalization) [6]. This model was improved, giving rise to the duplication-degeneration-complementation (DDC) model, where the duplicated

* Correspondence: jpfett@cbiot.ufrgs.br

¹Centro de Biotecnologia, Universidade Federal do Rio Grande do Sul, Av. Bento Gonçalves 9500, P.O.Box 15005, Porto Alegre, 91501-970, Brazil
Full list of author information is available at the end of the article

copies can have complementary functions that resemble the ancestral gene's function (subfunctionalization) [7]. The DDC model's predictions are believed to be more accurate than the previous model, since loss-of-function changes in regulatory regions are more likely to occur than gain-of-function mutations [7]. Other improvements of the basic model for duplicated gene retention, involving buffering of crucial functions via conversion and crossing-over, were recently proposed [8,9].

Due to repetitive genome duplications, plants are likely to harbor relatively larger gene families, as compared to animal genomes [10]. It is well established that one whole-genome duplication occurred in the cereal lineage, estimated 70 million years ago (MYA), preceding the radiation of the major cereal clades by 20 million years or more [3,11]. Recently, comparing the genomic sequences of rice (*Oryza sativa*) and *Sorghum bicolor*, it was demonstrated that an early duplication occurred in the monocot lineage [4]. The duplication blocks cover at least 20% of the cereals transcriptome [4]. It was also shown that expression divergence between duplicate genes is significantly correlated with their sequence divergence [12]. After duplication, gene pairs rapidly diverge, and only a small fraction of ancient gene pairs do not show expression divergence [12]. However, for some genomic segments, concerted evolution homogenizes homologous sequences through unequal crossing-over and gene conversion, changing the estimated duplication age and gene divergence [9,13-15].

Rice was first described as having 18 duplicated segments which cover 65.7% of its genomic sequence, and several individual gene duplications [16]. More recent estimates account for 29 duplications in the rice genome, including 19 minor blocks that overlap with 10 major blocks [17]. A duplication block between chromosomes 11 and 12 has been extensively characterized in rice and other cereals, although the age of its birth is still controversial [9,14,15,18,19]. Rice is a model for cereal genomic and genetics studies, due to the availability of the genome sequences from two varieties, extensive gene annotation, and mutant resources [20-24]. Rice is also a major staple food, feeding nearly half of the world's population. However, it is a poor source of minerals such as iron (Fe) and zinc (Zn), the two mineral elements most commonly lacking in human diets [25,26]. Metal homeostasis in plants has been extensively studied in recent years, with a special focus on the transition metals Zn and Fe [27-29]. Thus, rice emerges both as a model species for physiological and molecular studies and as a candidate for biotechnological improvement aiming at Zn and Fe biofortification [30-32].

Both Zn and Fe are essential to mineral nutrition of plants. Zn has a key role in gene expression, cell development and replication, while Fe is necessary for

photosynthesis, electron transport and other redox reactions [33]. Although essential, both can be toxic when in excess [34-37]. Several transporters involved in uptake and translocation inside the plant were described for Fe and Zn [35,38-43].

The ZINC-INDUCED FACILITATOR 1 gene (*AtZIF1*), described by Haydon and Cobbett, belongs to a new family of transporters, with three members in *Arabidopsis thaliana*: *AtZIF1* (AT5G13740), *AtZIFL1* (AT5G13750) and *AtZIFL2* (AT3G43790) [34]. The *AtZIF1* transporter is clearly involved in Zn homeostasis, as the loss-of-function *atzif1* mutant has altered Zn distribution and its transcription is up-regulated by Zn-excess [34]. Importantly, *AtZIF1* proteins are expressed in the tonoplast, and probably are involved in transport of Zn, Zn and a ligand or a ligand alone, to the vacuole [34]. Besides *AtZIF1*, only one similar protein had been previously characterized: the maize (*Zea mays*) Zm-mfs1, which is induced by infection by the pathogens *Cochliobolus heterostrophus* and *C. carbonum* and to ultraviolet light [44]. This gene is highly expressed in the *Les9* disease lesion mimic background and in plant tissues engineered to express flavonoids or the avirulence gene *avrRvx* [44]. Both *AtZIF1* and Zm-mfs1 are part of the Major Facilitator Superfamily (MFS), which comprises the largest superfamily of secondary transport carriers found in living organisms and is subdivided in at least 29 families [45]. More recently, *AtZIF1* and *AtZIFL1* were described as quantitative trait loci (QTL) candidates for Zn concentrations in *Arabidopsis* seeds [46]. In barley (*Hordeum vulgare*), microarray analyses revealed that a *ZIF1-like* gene is expressed in the aleurone layer of seeds and its transcription increases in the embryo upon foliar Zn application [47]. Therefore, it is possible that *ZIFL* genes are involved in Zn translocation to the seeds.

In this work, we describe the ZIF-like (ZIFL) family of transporters. We identified 68 family members from plants and reconstructed their phylogenetic relationships. We also analyzed in detail the organization of *ZIFL* genes in the rice (*Oryza sativa*) genome: the motif composition, genomic organization, and promoter sequences. We analyzed the expression of *OsZIFL* genes in different plant organs and developmental stages, as well as in response to different stresses. This is the first attempt to describe the *ZIFL* gene family in plants, and the first expression analysis of these genes in rice.

Results

ZIFL genes in plants

We first used the *AtZIF1*, *AtZIFL1* and *AtZIFL2* sequences to query genomic databases to determine the distribution of this gene family among plant species. Two dicots, *Vitis vinifera* and *Populus trichocarpa*, one bryophyte, *Physcomitrella patens*, one lycophyte, *Selaginella moellendorffii*,

and four monocots, *Sorghum bicolor*, *Brachypodium distachyon*, *Oryza sativa* and *Zea mays* had their genomes screened for *ZIFL* genes. All sequences found through this search plus the three *Arabidopsis* sequences were used to generate a Hidden Markov Model (HMM) profile to iteratively search the same genomes (see Methods). The final dataset consists of 66 genes coding for proteins already annotated (Additional File 1) and two unannotated proteins from *Zea mays* (Additional File 2).

All organisms queried contain *ZIFL* sequences, with predicted protein sequences ranging from 289 to 557 amino acids and an average of 468.4 amino acids per protein. All gene sequences begin with an initiation codon and end with a stop codon, except for the protein PpZIFL1, which lacks a small N-terminal portion (about 50 amino acids) and was included in the analyses. The overall structure contains 11 to 12 predicted transmembrane (TM) domains (Additional File 1 and Additional File 2), found in 63% of the proteins in our dataset. Fourteen putative proteins are predicted to have 10 TM domains, and 11 proteins have seven to nine TM domains (Additional File 1 and Additional File 2).

Dicot species have a small number of *ZIFL* gene copies, with *V. vinifera* and *P. trichocarpa* showing five and four paralogs of *ZIFL* in their genomes, similar to the three members of the *Arabidopsis* *ZIFL* gene family [34]. Conversely, monocot species show a higher number of *ZIFL* genes, with *S. bicolor* having the highest number of members (14), followed by rice (13), *B. distachyon* (10) and *Z. mays* (10). *P. patens* and *S. moellendorffii* harbor two and seven *ZIFL* genes, respectively. Clearly, monocot species have a higher number of *ZIFL* family paralogs than dicots. The seven *ZIFL* genes found in *S. moellendorffii* seem to be closely related and not originated from the same expansion which originated the monocot *ZIFL* genes.

***ZIFL* proteins are a distinct family of MFS transporters**

The *ZIFL* proteins are all part of the Major Facilitator Superfamily (MFS) clan of transporter proteins (Pfam number CL0015), composed by 22 families. They show similarity to the MFS_1 family (Pfam number PF07690), which is the largest family within the MFS clan. We used the MFS_1 HMM profile to isolate the MFS_1 proteins from all dicot and monocot genomes analyzed in this work. Phylogenetic trees reconstructing the evolutionary history of MFS_1 and *ZIFL* proteins for each species were generated using the neighbor-joining method (Additional File 3). We observed that in all cases the *ZIFL* proteins clustered in a separate group from all other MFS_1 members. This result could be an indication that *ZIFL* is a distinct family of MFS transporters.

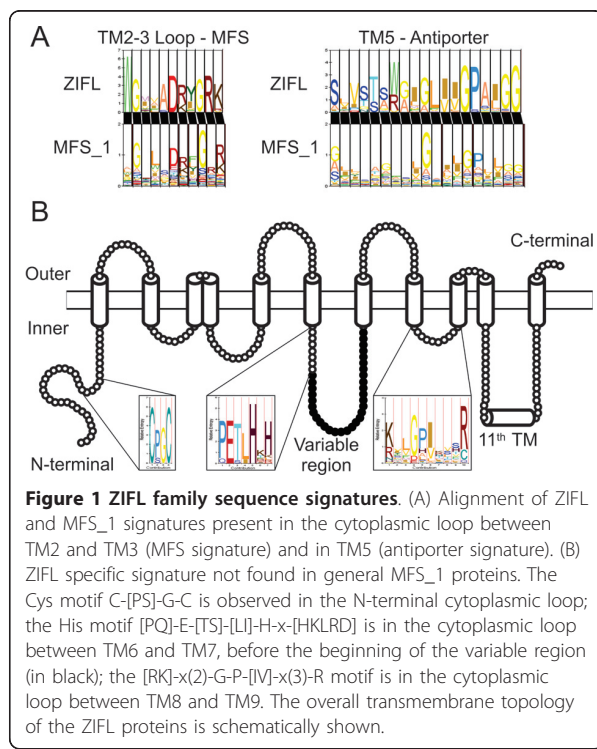
Simmons et al suggested that sequences similar to Zm-mfs1 (ZmZIFL5 in Additional File 1 and throughout

this work) could be a distinct group of MFS proteins found in plants [44]. This was based on comparison of signature sequences of nine plant sequences to bacterial and fungal MFS sequences. To confirm this hypothesis, we searched for signatures in the *ZIFL* HMM profile and aligned them to the MFS_1 HMM profile. We found the canonical MFS signature, located in the cytoplasmic loop between TM2 and TM3, as well as the antiporter signature in TM5 (Figure 1A). When aligning these signatures to the MFS_1 HMM profile, we noticed that the *ZIFL* MFS signature G-x(3)-D-[RK]-x-G-R-[RK] has a conserved tryptophan (W) before the first glycine position, which is not observed in MFS_1 (Figure 1A). The antiporter signature, S-x(8)-G-x(3)-G-P-x(2)-G-G, is also slightly different, having preference for serine in the first position, instead of glycine, as observed by Simmons et al (Figure 1A) [44]. The presence of these conserved positions indicates that *ZIFL* transporters share structural and functional similarities with MFS antiporters, although they show specific features that are not common to other MFS proteins.

The *ZIFL* sequences also show signatures that are not shared with MFS_1 proteins. The conserved positions in the loop between TM8 and TM9, [RK]-x(2)-G-P-[IV]-x(3)-R, previously reported by Simmons et al, were confirmed in our dataset with a few changes (Figure 2B) [44]. Importantly, we found two new conserved signatures that are specific for the *ZIFL* proteins. One of them is a cysteine (Cys)-containing motif C-[PS]-G-C in the cytoplasmic N-terminal loop of *ZIFL* proteins, and the second one is a histidine (His)-containing motif [PQ]-E-[TS]-[LI]-H-x-[HKL RD] in the cytoplasmic loop between TM6 and TM7, before the beginning of a variable region (Figure 2B; see below). From our dataset of 68 *ZIFL* proteins, 58 have the Cys motif, with only three proteins showing a serine residue in the second position instead of a proline (Additional File 4). For the histidine motif, 61 *ZIFL* proteins have the conserved residues (Additional File 4). From these, 45 have the most conserved residues P-E-T-L-H-x-H, while the other 16 *ZIFL* members contain the same motif with no more than one residue substitution (Additional File 4). Considering that the MFS_1 family has 56,680 proteins with very low overall similarity between them, and that *ZIFL* proteins share both high similarity and unique signatures, we suggest that *ZIFL* proteins comprise a distinct family of transporters.

***ZIFL* gene expansion is lineage specific**

To address the hypothesis of a lineage specific expansion of *ZIFL* genes in monocot species, we generated an alignment using the amino acid sequences of the 68 *ZIFL* genes found and reconstructed the phylogenetic relationships of these protein sequences using two



methods: neighbor-joining and bayesian analysis (Figure 2). Although some nodes are not in agreement comparing the two methods, our bootstrap values and posterior probabilities support all the major nodes of the tree, indicating that the reported group relationships are reliable (Figure 2).

Proteins from bryophyte and lycophyte species grouped together, with paralogs from each species in a separate cluster. The ZIFL proteins from dicots also formed a distinct group (Figure 2). However, there was no clear separation into sub-groups of orthologous sequences within the dicots group (Figure 2). Species-specific gene duplications are observed in *Arabidopsis* (AtZIFL1 and AtZIFL1), *V. vinifera* (VvZIFL2 and VvZIFL3; VvZIFL4 and VvZIFL5) and *P. trichocarpa* (PtZIFL1 and PtZIFL4) (Figure 2).

The ZIFL paralogs from monocot species were grouped in three distinct groups, named Monocot I, Monocot II and Monocot III. All three ZIFL protein groups from the monocots contain paralogs from the four species included in our analysis. The Monocot I group contains 17 ZIFL proteins, while the Monocot II and Monocot III groups contain 15 proteins each (Figure 2). Both the number of sequences found in monocot species and the tree topology strongly suggest that the ZIFL gene family experienced an expansion in the monocot lineage, and that the last common ancestor of the monocots already had ZIFL paralogs of the three

groups (Figure 2). Thus, the split of the four monocot species used in this work probably occurred after the expansion of the ZIFL family observed in monocots, and this expansion is not shared with other plant lineages.

ZIFL paralogs are unequally distributed in the rice genome

The identification of the ZIFL gene chromosome locations revealed that they are not evenly distributed in the rice genome, but rather arranged in clusters (Additional File 5). The same trend is observed in *S. bicolor* and *B. distachyon*, but not in *Z. mays* (Additional File 5). Rice ZIFL genes were named ZIFL1 to 13 based on their genomic locations. Two ZIFL genes, OsZIFL1 and OsZIFL2 are located in chromosome 1, and OsZIFL3 is located in chromosome 7. OsZIFL4, OsZIFL5, OsZIFL6, OsZIFL7 and OsZIFL8 are found in chromosome 11, while OsZIFL9, OsZIFL10, OsZIFL11, OsZIFL12 and OsZIFL13 are located in chromosome 12. Interestingly, the ZIFL genes arranged in tandem in chromosomes 11 and 12 are closely related, with OsZIFL4 being very similar to OsZIFL9 (92% of identity), OsZIFL5 to OsZIFL10 (95%), OsZIFL6 to OsZIFL11 (82%), OsZIFL7 to OsZIFL12 (85%) and OsZIFL8 to OsZIFL13 (73%) (Table 1). We used the GATA tool to align the 100 kb regions that include OsZIFL genes in chromosomes 11 and 12 (hereafter Os11 and Os12; Figure 3A). The regions of chromosomes 11 and 12 where these genes are located have already been described as a recent segmental duplication in the rice genome, what would explain the high number of matches between these regions (Figure 3A) [18,48]. However, the same duplication was recently found in *S. bicolor*, indicating that this segmental duplication is ancient to the split of these species [14,15]. We observed that *S. bicolor* chromosomes 5 and 8 (hereafter Sb05 and Sb08), which are homologous to rice chromosomes 11 and 12 (Os11 and Os12), harbor three and two ZIFL genes, respectively (Figure 3B) [14]. An incomplete sequence related to ZIFL is also found in chromosome 8 (Sb08g001390; Figure 3B). It is possible to observe that an inversion has occurred when comparing the orientation of ZIFL regions in Sb05 and Sb08 (Figure 3B). The alignment between rice and *S. bicolor* homologous chromosomes Os11 with Sb05 and Os12 with Sb08 demonstrate that the *S. bicolor* ZIFL region in Sb08 is inverted, since the alignment of Os11 with Sb05 is in direct orientation (Figure 3C) while the alignment of Os12 with Sb08 is in reverse (Figure 3D). Therefore, although in homologous regions, the ZIFL gene cluster in Sb08 is differentially oriented in relation to rice.

OsZIFL genes organization is highly conserved

We aligned the genomic and coding sequence (CDS) of each ZIFL gene from rice and determined the exon-intron organization (Figure 4). The exon sizes of each

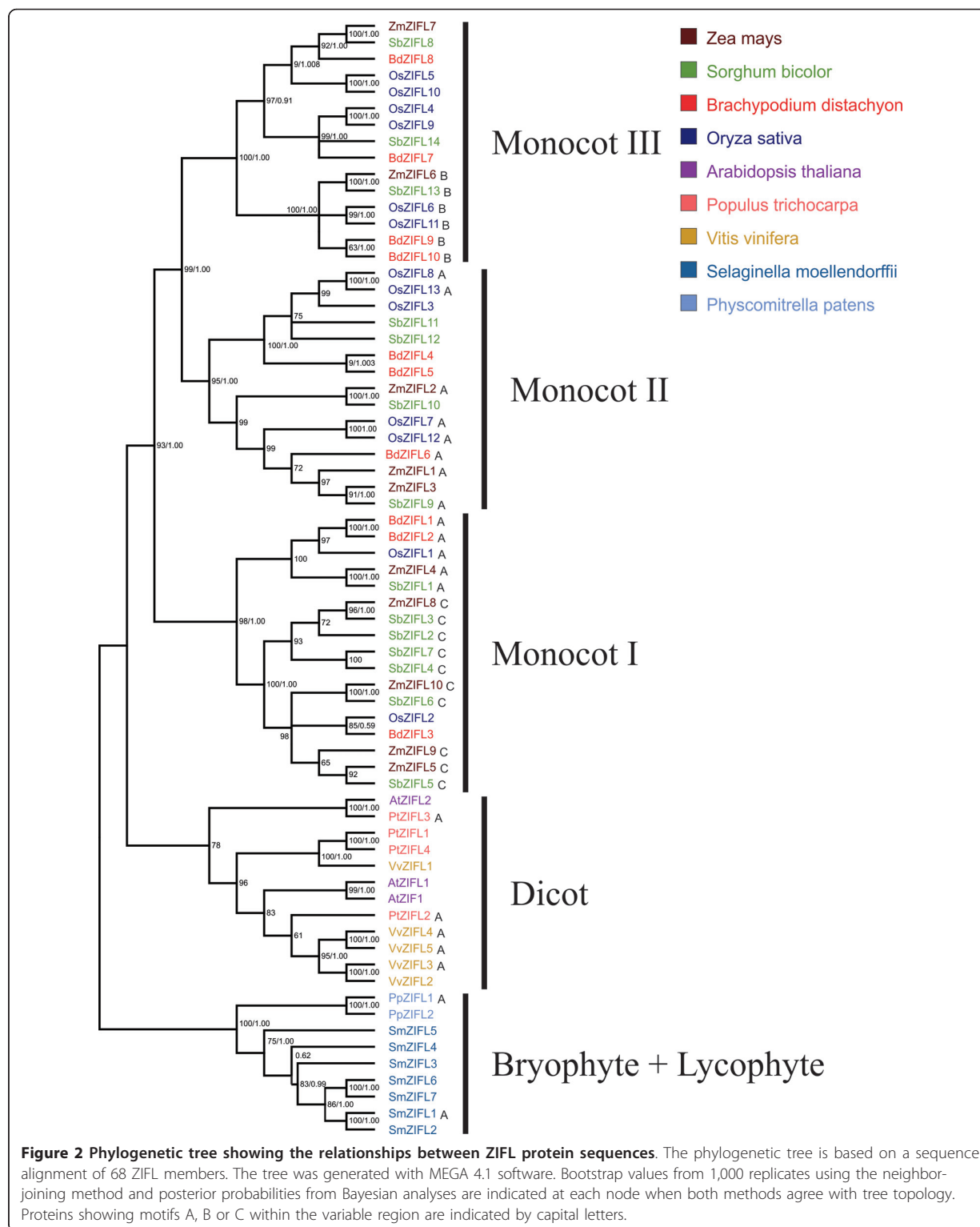
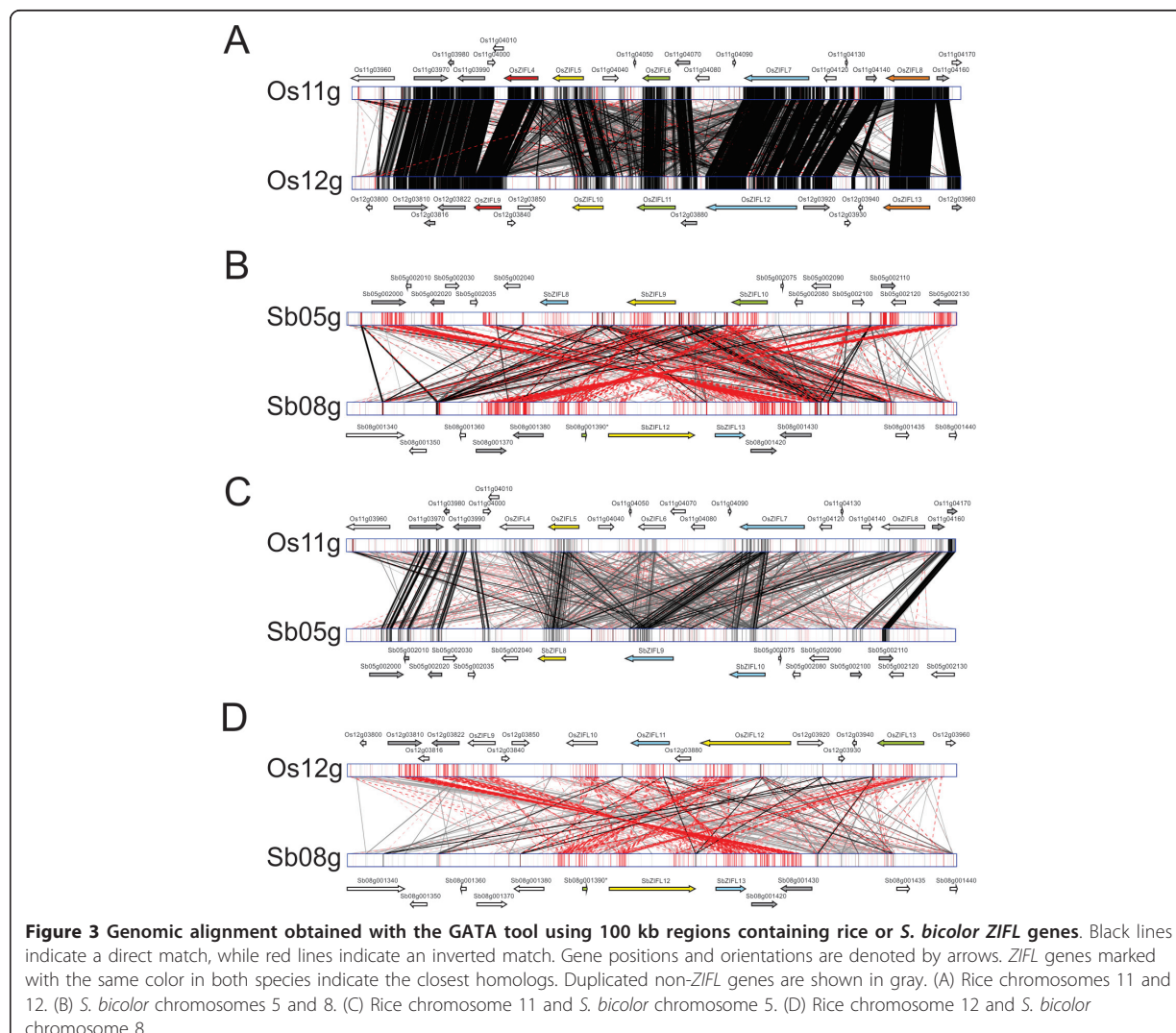
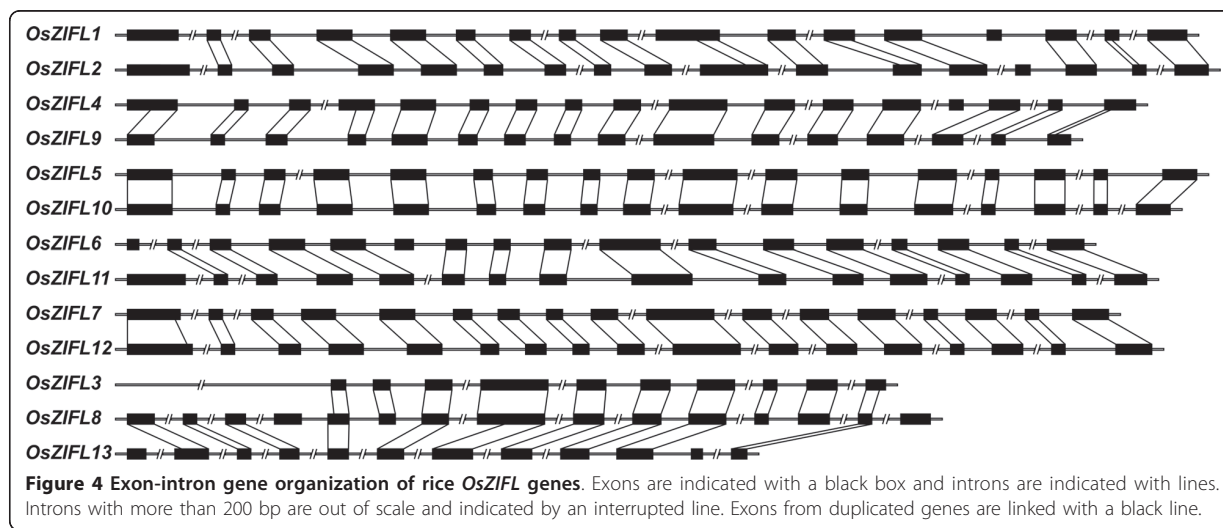


Table 1 Rice ZIFL sequence identity at the amino acid level

	OsZIFL1	OsZIFL2	OsZIFL3	OsZIFL4	OsZIFL5	OsZIFL6	OsZIFL7	OsZIFL8	OsZIFL9	OsZIFL10	OsZIFL11	OsZIFL12
OsZIFL2	57											
OsZIFL3	44	44										
OsZIFL4	53	53	49									
OsZIFL5	55	55	50	74								
OsZIFL6	51	52	46	66	69							
OsZIFL7	51	52	43	56	58	50						
OsZIFL8	48	47	60	54	54	48	47					
OsZIFL9	54	55	44	92^a	72	60	53	49				
OsZIFL10	55	52	48	72	95^a	68	57	53	70			
OsZIFL11	47	49	42	61	62	82^a	49	44	59	62		
OsZIFL12	54	54	56	62	66	58	86^a	61	62	65	54	
OsZIFL13	40	37	40	39	40	35	48	73^a	39	40	39	47

^a Rice ZIFL gene pairs from chromosomes 11 and 12.





gene pair, *OsZIFL4-OsZIFL9*, *OsZIFL5-OsZIFL10*, *OsZIFL6-OsZIFL11*, *OsZIFL7-OsZIFL12* and *OsZIFL8-OsZIFL13* are nearly identical, with very few variations in sequences. We observed that *OsZIFL1* and *OsZIFL2* are probably originated from duplication, since they share a similar exon-intron organization. However, their amino acid sequences are only 57% identical (Table 1). This duplication probably occurred in the common ancestor of monocots, as orthologs from *S. bicolor*, *B. distachyon* and *Z. mays* were found for both *OsZIFL1* and *OsZIFL2* (Figure 2). *OsZIFL3* is suggested to be originated from a partial duplication of the *OsZIFL8-OsZIFL13* pair last common ancestor (Figures 2 and 4), and shares more identities to *OsZIFL8* sequence (60%) than to *OsZIFL13* (40%). Thus, it is clear that duplications were of major importance in the ZIFL family expansion in rice,

especially the segmental duplication observed in chromosomes 11 and 12.

Protein motif composition reveals a variable region in the ZIFL family

We aligned the 13 rice ZIFL proteins and observed that they share large similarity (Additional File 6 and Table 1). To search for functional sites shared by OsZIFL putative proteins, we used MEME (<http://meme.nbcr.net/>) to identify conserved motifs in their amino acid sequences [49]. We found eleven motifs shared by almost all 13 OsZIFL proteins, with few exceptions (Table 2, Figure 5A). Seven motifs matched the general MFS_1 motif in InterProScan (<http://www.ebi.ac.uk/Tools/InterProScan/>) (motifs 1, 2, 4, 5, 6, 7 and 9), while four showed no hits (motifs 3, 8, 10, and

Table 2 Conserved motifs found in ZIFL protein sequences

Motif	Width	Assign	Amino acid sequence
1	50	MFS ^a	NWPLMSSIIILYCVFSFHDAMAYSEIFSLWAESDRKYGGFSSEDVGQVLA
2	50	MFS ^a	QPAEKYPNVFSEKSFGRFPYFLPCLCISVFAAVLISCIWLPTLHKHK
3	41	No hit	LPISSLFPFLYFMIRDLHVAKREEDIGFYAGFGVASYMIGR
4	50	MFS ^a	LQNNAVPQDQRGTANGIATTAMSFFKAIAPIAGAGVLFSWAQKRQHAAFFP
5	50	MFS ^a	GASLLVYQLFIYPWVHKVLPINNSRIAIALSIPILCTYPFMTHLSGPWL
6	50	MFS ^a	RFLLGALNGMLGPIAKSIEVCRPEHQALGLSIVSTAWGIGLVGVPAIGG
7	29	MFS ^a	PVIVFSIFSWFNTLFLSTKYWMATT
8	21	No hit	HDGCPGCAMERRKEEHKGIPY
9	15	MFS ^a	ASIFWGIVADRIGRK
10	28	No hit	GDQMVFMLNVTEVIGMLTFKPFLAVP
11	21	No hit	VLNIAASMMKNNLAVTIITGTN
A ^b	21	No hit	NSVEALEEHLMDPNEEENENE
B ^b	15	No hit	IKRIKELPSQQAYWD
C ^b	11	No hit	EELEAQVGGSN

^aMFS (Major Facilitator Superfamily Antiporter)

^bAnalysis performed with whole set of ZIF proteins (68 sequences)

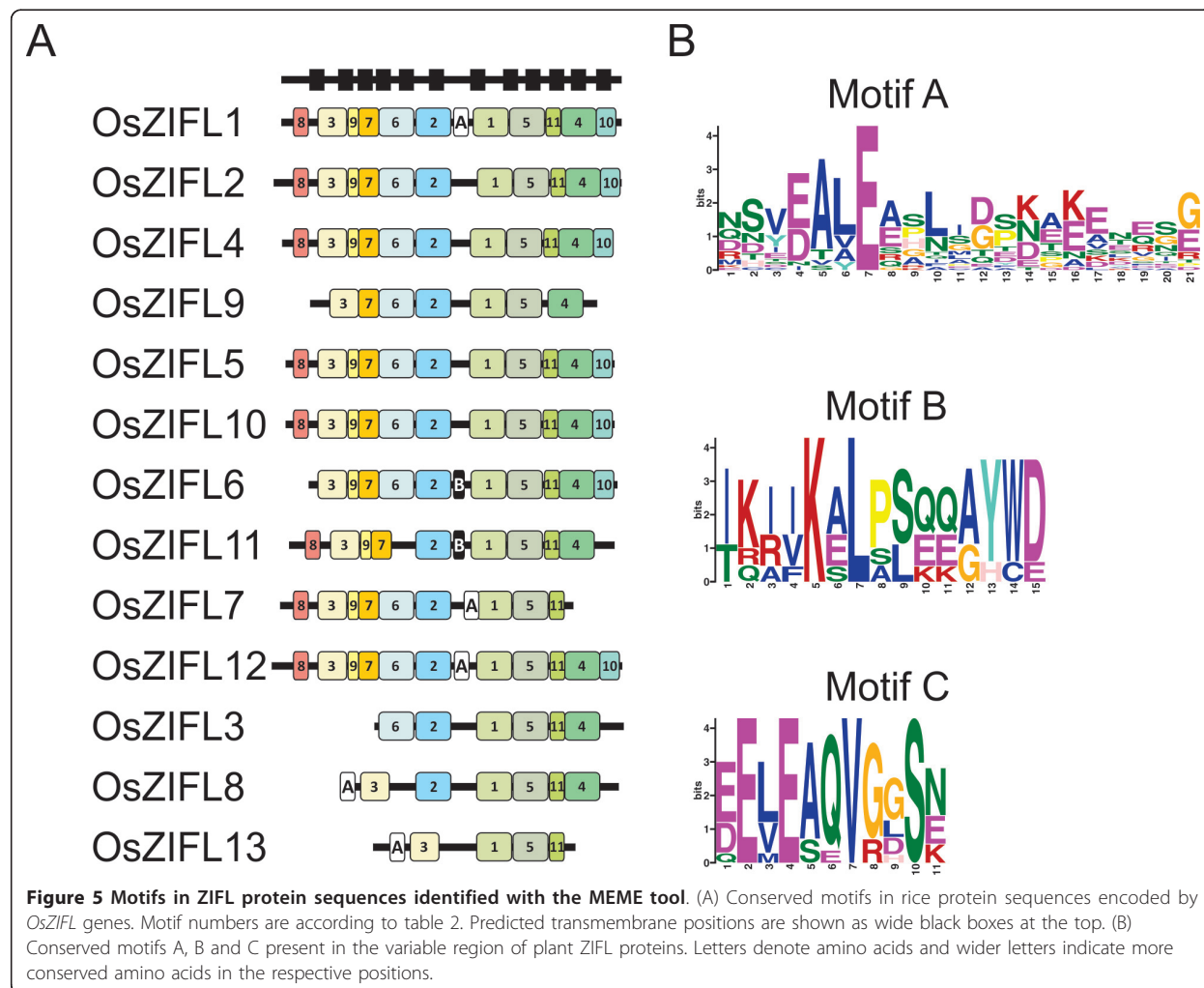


Figure 5 Motifs in ZIFL protein sequences identified with the MEME tool. (A) Conserved motifs in rice protein sequences encoded by *OsZIFL* genes. Motif numbers are according to table 2. Predicted transmembrane positions are shown as wide black boxes at the top. (B) Conserved motifs A, B and C present in the variable region of plant ZIFL proteins. Letters denote amino acids and wider letters indicate more conserved amino acids in the respective positions.

11) (Table 2). The ZIFL signatures Cys motif and His motif are located within the motif 8 and motif 2, respectively (Table 2).

OsZIFL1, *OsZIFL2*, *OsZIFL4*, *OsZIFL5*, *OsZIFL10* and *OsZIFL12* have all eleven motifs, while the duplicated pair *OsZIFL8*-*OsZIFL13* and their duplicated copy in chromosome 7 (*OsZIFL3*) lack several motifs (Figure 5A). Some of these motifs are located in regions predicted to be transmembrane (Figure 5A, black boxes at the top). Further characterization is needed to determine if the duplicated rice ZIFL genes are becoming pseudogenes or acquiring new functions.

The *OsZIFL4* duplicated copy *OsZIFL9* lacks the N-terminal motif 8 and the C-terminal motif 10; *OsZIFL6* lacks motif 8 and its duplicated copy *OsZIFL11* lacks motif 6 and motif 10; the duplicated pair *OsZIFL7* and *OsZIFL12* only differ by the C-terminal motifs 4 and 10, which are absent in *OsZIFL7* (Figure 5A). These differences suggest a divergence process between duplicated

pairs. Moreover, it is clear that the central motifs are more conserved than those located at the N- and C-terminal regions of *OsZIFL* proteins (Figure 5A).

We also observed a variable region between motifs 1 and 2 which did not show significant pattern conservation in *OsZIFL* proteins (Figure 5A). This region is located between transmembrane regions 6 and 7 (considering 12 TM proteins) and is a cytoplasmic loop according to Conpred II predictions (Figure 1B). The variable region is preceded by the conserved His motif P-E-T-L-H-x-H (Figure 1B). Variable regions are found in transporters and could be involved in transport or sensing functions [50,51]. The whole set of 68 ZIFL proteins used in this work was submitted to MEME analysis to find any conserved motifs specifically in the variable region. Three motifs were found in this region and named motifs A, B and C (Table 2; Figure 5B). None matched any known motif in the InterPro database (Table 2). We indicated proteins that contain each motif

in our phylogenetic tree (Figure 2) and showed their positions in rice ZIFL protein sequences (Figure 5A). Rice ZIFL proteins contain motifs A and B in their variable region, but not motifs C.

Motif A is present in proteins from the Monocot I, Monocot II, Dicot and Bryophyte-Lycophyte groups (Figure 1). This motif shows low amino acid conservation (Figure 5B). The negatively charged glutamic acid (E) residue in the seventh position of the motif is the most conserved residue. Conserved negatively charged residues are also found in the fourth position (glutamic or aspartic acid, E or D). Between these positions, two non-polar residues, alanine (A) and leucine (L) are also conserved (Figure 5B). Other positions containing a positively-charged residue of lysine (K), a negatively charged glutamic acid (E), and residues of leucine (L) and glycine (G), although less conserved, are present (Figure 5B). Charged positions could be involved in transporter specificity, as already described for cation diffusion facilitator (CDF) proteins [52]. Motif B is shared only by a sub-group of six proteins from monocot II (Figure 2). The fifth and seventh positions of this motif contain one positively charged residue and one hydrophobic residue, lysine (K) and leucine (L) (Figure 4B). Polar residues of serine (S), glutamine (Q) and tyrosine (Y), non-polar tryptophan (W) and proline (P) are also observed (Figure 4B). The motif C is common to 10 proteins from the Monocot I group (Figure 2), and is similar to motif A, showing the two glutamic acids (E) separated by one instead of two non-polar residues (Figure 5B). However, since only a small number of proteins share motifs B and C, we should be cautious on making assumptions about the functionality of conserved amino acids found in these motifs, as their conservation could be an effect of phylogenetic relatedness and not of evolutionary constraints.

Importantly, it is possible to observe the high divergence of the variable region even when comparing these three motifs. The variability is much higher in this region than in the whole sequence of ZIFL proteins, as MEME analysis revealed several motifs shared by all the 68 ZIFL proteins (data not shown). Therefore, these motifs in the cytoplasmic loop could be involved in specific functions of different ZIFL proteins.

Expression of OsZIFL genes in rice vegetative and reproductive organs

We analyzed the expression levels of OsZIFL transcripts in several rice organs by qPCR, including roots, culms and shoots (vegetative tissues); flag-leaves and whole panicles (reproductive tissues), both during R3 (panicle exertion), R5 (grain filling) and R7 (grain dry down) stages (Figure 6). Throughout our qPCR experiments, OsZIFL1, OsZIFL6, OsZIFL8, OsZIFL11 and OsZIFL13 transcripts were not

detected or were detected below a confidence threshold for analysis. The expression levels of OsZIFL genes varied considerably, with some genes reaching higher expression levels (*OsZIFL2* and *OsZIFL4*, Figures 6A and 6C) and others showing very low expression (*OsZIFL3*, *OsZIFL9*, *OsZIFL5* and *OsZIFL7*; Figures 6B, 6D, 6E and 6G). *OsZIFL2* and *OsZIFL3*, although not resultant of a duplication event, share a similar pattern of expression: both are more expressed in leaves and also accumulate in the later stages of flag-leaf development, reaching the highest levels in R7 (Figures 6A and 6B).

When analyzing gene pairs, we observed that *OsZIFL4* is almost specifically expressed in roots, showing only little expression in panicles during the R7 stage (Figure 6C), while its duplicated copy *OsZIFL9* is not expressed in vegetative tissues nor in flag-leaves, but is detected at low levels in panicles during R5 and at higher levels during R7 (Figure 6D). Transcripts from the *OsZIFL5*-*OsZIFL10* pair show similar patterns of expression, especially when considering the reproductive organs flag-leaves and panicles (Figures 6E and 6F). *OsZIFL5* and *OsZIFL10* are both induced from R3 to R5 in flag-leaves, maintaining high levels at R7. In panicles, they are also induced from R3 to R5, although *OsZIFL10* transcript levels are further induced from R5 to R7 (Figures 6E and 6F). In vegetative tissues, *OsZIFL5* levels are higher in roots, while *OsZIFL10* is more expressed in shoots (Figures 6E and 6F).

The genes from the *OsZIFL7*-*OsZIFL12* pair also show similar expression patterns in the organs analyzed. *OsZIFL7* is more expressed in culms and leaves, accumulates from R3 to R5 in flag-leaves and decreases its expression from R3 to R5 during panicle development (Figure 6G). The *OsZIFL12* transcript accumulates in leaves and also increases from R3 to R5 in flag-leaves and decreases from R3 to R5 in panicles (Figure 6H). Taken together, our gene expression data demonstrates that, even after duplication and divergence, most *OsZIFL* genes still share similar expression patterns in rice organs within gene pairs.

The Fe-deficiency element IDE1 is enriched in promoters of OsZIFL genes

To investigate the presence of conserved *cis*-elements in promoter regions of *OsZIFL* genes, we used the POCO tool [53]. This approach consisted in comparing the -1,500 to +1 regions of *OsZIFL* genes to several random samples of promoters from the entire *Arabidopsis* genome with the same size (each sample composed of 13 promoters). If a *cis*-element is more often found in the promoters of *OsZIFL* genes than in a random set of promoters, this *cis*-element is enriched in these sequences. The POCO analysis revealed that the sequence CATGC is enriched in our promoter set when

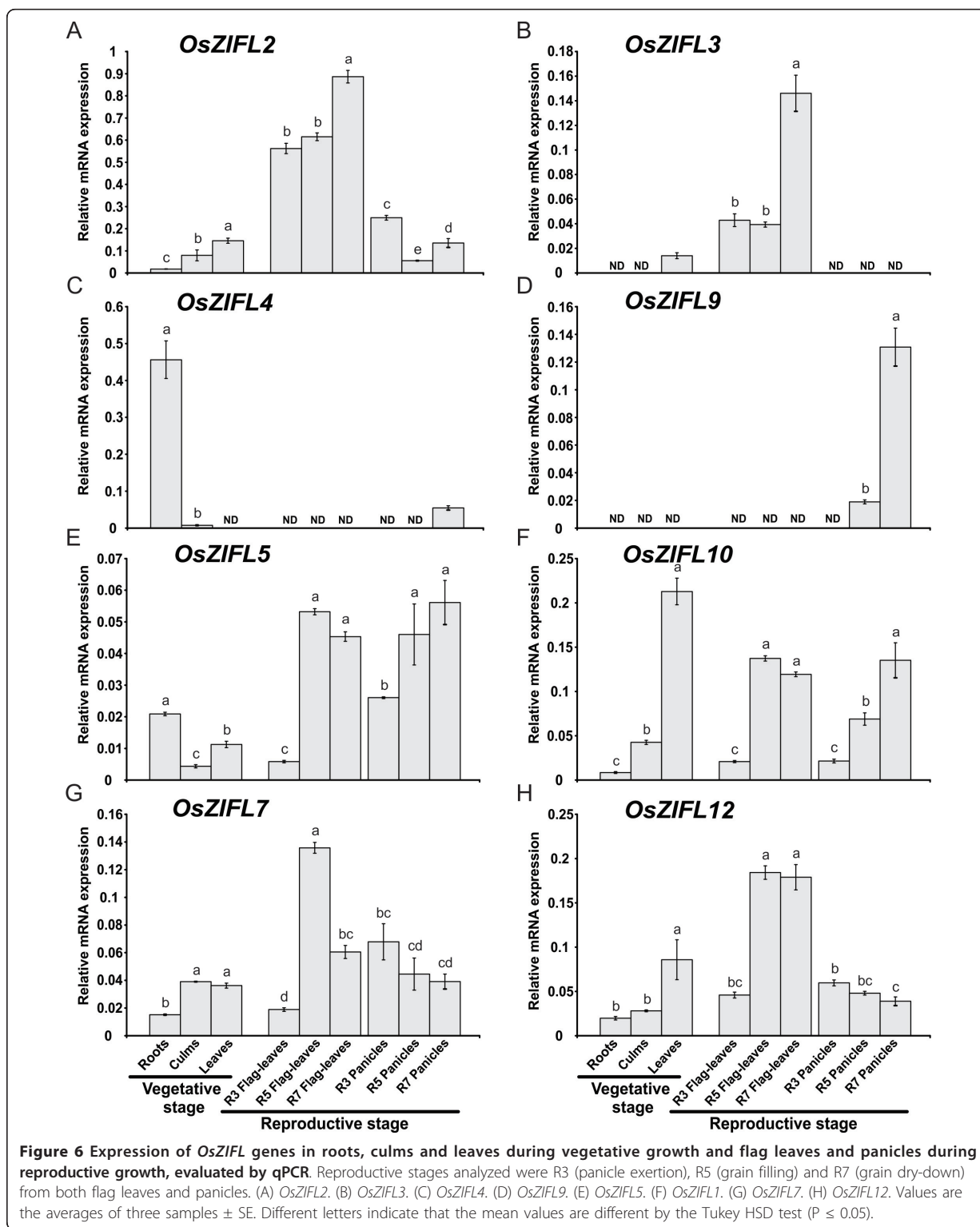


Figure 6 Expression of *OsZIFL* genes in roots, culms and leaves during vegetative growth and flag leaves and panicles during reproductive growth, evaluated by qPCR. Reproductive stages analyzed were R3 (panicle exertion), R5 (grain filling) and R7 (grain dry-down) from both flag leaves and panicles. (A) *OsZIFL2*. (B) *OsZIFL3*. (C) *OsZIFL4*. (D) *OsZIFL9*. (E) *OsZIFL5*. (F) *OsZIFL10*. (G) *OsZIFL7*. (H) *OsZIFL12*. Values are the averages of three samples \pm SE. Different letters indicate that the mean values are different by the Tukey HSD test ($P \leq 0.05$).

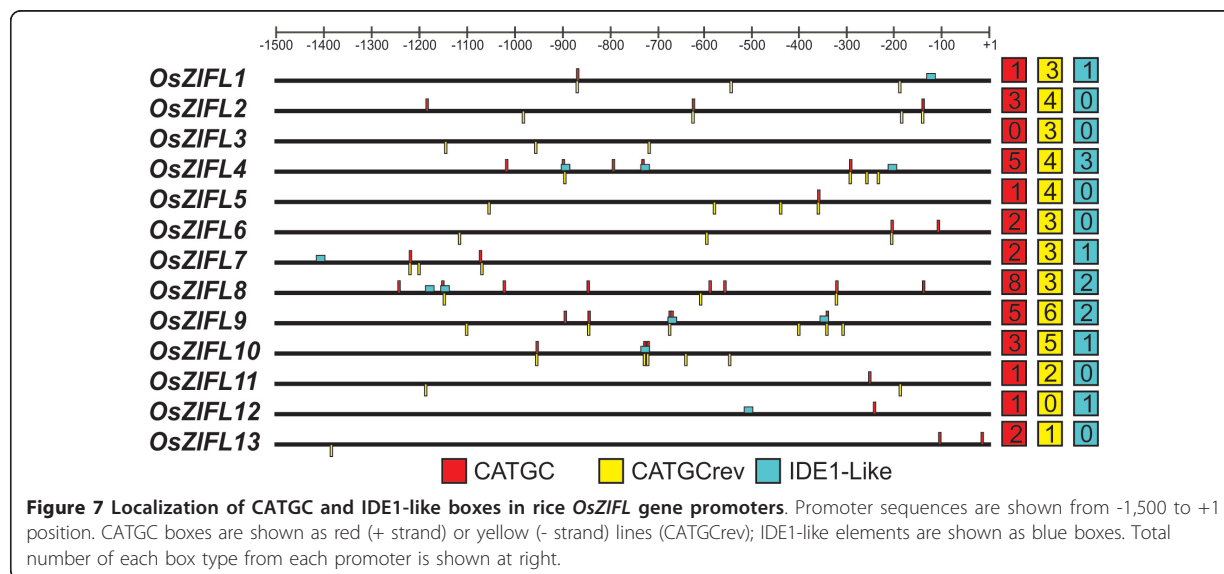


Figure 7 Localization of CATGC and IDE1-like boxes in rice *OsZIFL* gene promoters. Promoter sequences are shown from -1,500 to +1 position. CATGC boxes are shown as red (+ strand) or yellow (- strand) lines (CATGCreV); IDE1-like elements are shown as blue boxes. Total number of each box type from each promoter is shown at right.

compared to *Arabidopsis* promoters. This sequence is the core binding site of IDEF1 (iron-deficiency responsive element-binding factor 1), a transcription factor of the ABI3/VP1 family involved in Fe-deficiency response in rice [30,54]. As *Arabidopsis* is not closely related to rice and thus the motif frequency in promoters could vary between these species, we confirmed the enrichment by counting the average number of CATGC boxes in nearly 25,000 promoters of rice downloaded from Osiris (<http://www.bioinformatics2.wsu.edu/cgi-bin/Osiris/cgi/home.pl>) [55]. While the average number of the CATGC sequences in rice promoters was 3.24, in promoters of the thirteen *OsZIFL* genes it was 5.85 boxes per promoter. Some promoters are highly enriched for CATGC boxes, such as *OsZIFL2* (7 boxes), *OsZIFL10* (8 boxes), *OsZIFL4* (9 boxes) and *OsZIFL9* (10 boxes) (Figure 7). Genes that were not detected in our qPCR experiments such as *OsZIFL8* and *OsZIFL1* also have promoters enriched in CATGC boxes (11 and 6, respectively) (Figure 7). *OsZIFL5*, *OsZIFL6* and *OsZIFL7* promoters show 5 boxes each (Figure 7).

Since the CATGC box is the core motif of IDE1, we searched for IDE1-like sequences in promoters of *OsZIFL* genes following the method described by Kobayashi et al. [56]. We found eleven IDE1-like motifs distributed in seven gene promoters, *OsZIFL1*, *OsZIFL4*, *OsZIFL7*, *OsZIFL8*, *OsZIFL9*, *OsZIFL10* and *OsZIFL12* (Figure 7). *OsZIFL4* shows three sequences, two of them overlapping with CATGC boxes, while *OsZIFL8* and *OsZIFL9* show two IDE1-like motifs (Figure 7). Considering that the motif is 18 bp long, it is surprising to find such a high number of IDE1-like motifs in our promoter set. The enrichment for CATGC and IDE1-like

sequences in promoters of *OsZIFL* genes suggests that they are possibly regulated by Fe-deficiency.

Zn-excess and Fe-deficiency regulate *OsZIFL* expression mainly in rice roots

It has been demonstrated that *AtZIF1* is up-regulated by Zn-excess in roots and leaves of *Arabidopsis* plants, as well as by Fe-deficiency [34,57,58]. As promoters of *OsZIFL* genes are enriched for Fe-deficiency *cis*-elements, we submitted rice plants to Zn-excess (200 μM) for three days and to Fe-deficiency (no Fe added to nutrient solution) for seven days. *OsZIFL* mRNA expression level was evaluated by qPCR in roots and leaves from both experiments.

Several *OsZIFL* genes were up-regulated in roots of Zn-excess treated plants: *OsZIFL2*, *OsZIFL4*, *OsZIFL5*, *OsZIFL10*, *OsZIFL7* and *OsZIFL12* (Figure 8). Expression of *OsZIFL1*, *OsZIFL3*, *OsZIFL9* and of the duplicated pairs *OsZIFL6*-*OsZIFL11* and *OsZIFL8*-*OsZIFL13* was not detected. Expression of *OsZIFL4*, which is nearly root-specific (Figure 6C), is induced 3.5-fold by Zn-excess (Figure 8B). Both *OsZIFL5* and *OsZIFL10*, a duplicated pair, are also up-regulated by 2- and 3-fold, respectively (Figures 8C and 8D). *OsZIFL7* and *OsZIFL12* show different patterns of induction, with *OsZIFL7* induced by almost 14-fold in comparison to control levels (Figure 8E). *OsZIFL12*, although induced by 3-fold (Figure 8F). To confirm that our treatment was effective, we used *OsNAS1* and *OsIRO2* (Figures 8G and 8H), two genes up-regulated by Zn-excess in rice roots [59]. Therefore, the *OsZIFL* genes which are expressed in roots are up-regulated under Zn-excess.

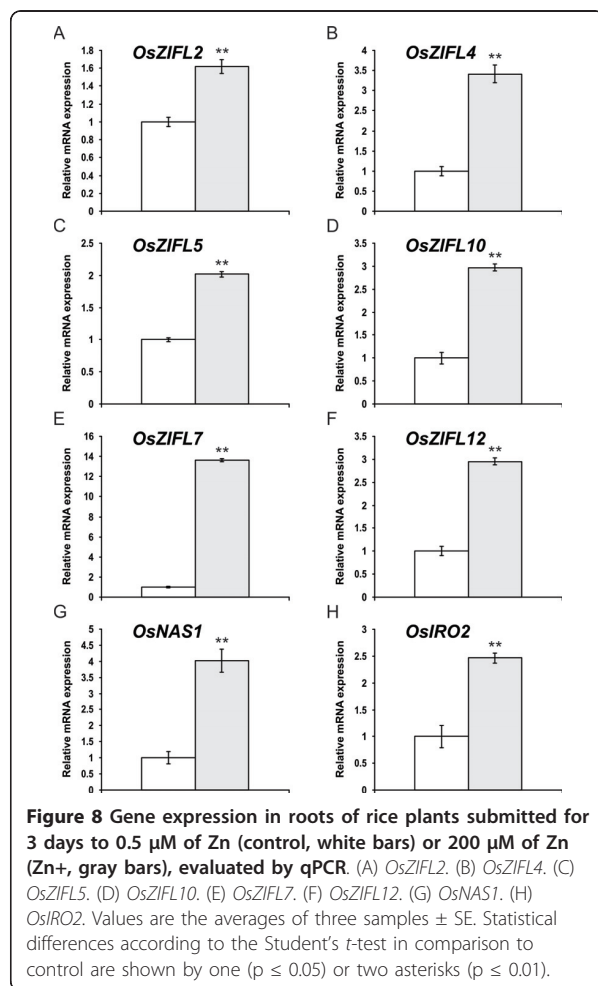


Figure 8 Gene expression in roots of rice plants submitted for 3 days to 0.5 μ M of Zn (control, white bars) or 200 μ M of Zn (Zn+, gray bars), evaluated by qPCR. (A) OsZIFL2. (B) OsZIFL4. (C) OsZIFL5. (D) OsZIFL10. (E) OsZIFL7. (F) OsZIFL12. (G) OsNAS1. (H) OsIRO2. Values are the averages of three samples \pm SE. Statistical differences according to the Student's *t*-test in comparison to control are shown by one ($p \leq 0.05$) or two asterisks ($p \leq 0.01$).

A very different expression pattern of *OsZIFL* genes was observed in leaves under Zn-excess: expression of *OsZIFL2*, *OsZIFL3*, *OsZIFL5* and *OsZIFL10* was not affected (Figures 9A, 9B, 9C and 9D). Only *OsZIFL7* and *OsZIFL12* mRNA levels were altered under Zn-excess: 1.4-fold and 3.3-fold higher than in the control treatment, respectively (Figures 9E and 9F). The *OsZIFL7* and *OsZIFL12* genes are a duplicated pair and are also up-regulated by Zn-excess in roots, suggesting a strong co-regulation under these conditions in both organs. However, most *OsZIFL* genes seem to be differentially regulated in leaves compared to roots when plants are under excessive Zn concentrations.

OsZIFL expression was also regulated in roots of plants under Fe-deficiency. Expression of *OsZIFL2* and *OsZIFL10* was not significantly increased by the treatment (Figures 10A and 10D). *OsZIFL4*, *OsZIFL5*, *OsZIFL7* and *OsZIFL12*, however, were up-regulated by 1.8 to 2-fold (Figures 10B, 10C, 10E and 10F). This

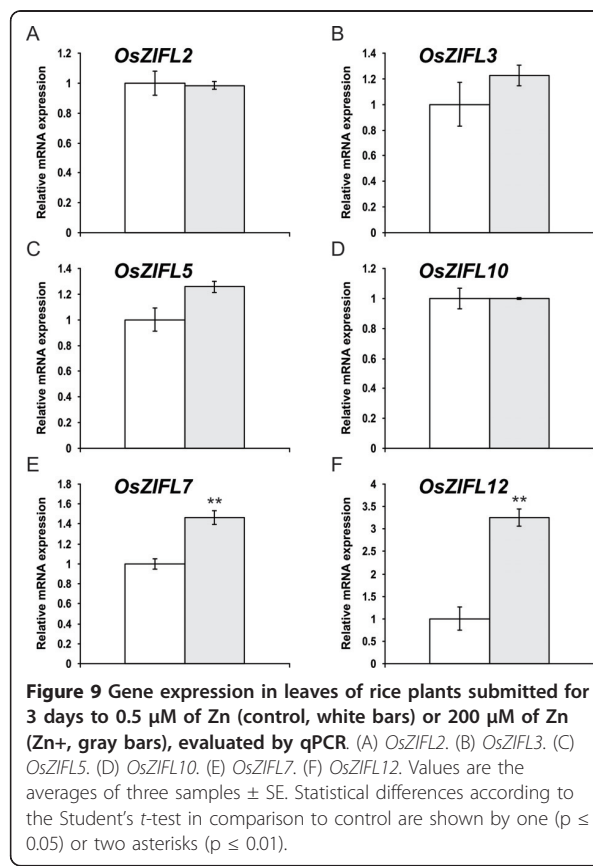


Figure 9 Gene expression in leaves of rice plants submitted for 3 days to 0.5 μ M of Zn (control, white bars) or 200 μ M of Zn (Zn+, gray bars), evaluated by qPCR. (A) OsZIFL2. (B) OsZIFL3. (C) OsZIFL5. (D) OsZIFL10. (E) OsZIFL7. (F) OsZIFL12. Values are the averages of three samples \pm SE. Statistical differences according to the Student's *t*-test in comparison to control are shown by one ($p \leq 0.05$) or two asterisks ($p \leq 0.01$).

effect occurred in parallel with increased expression of *OsIRT1* (2.8-fold), a gene already described as responsive to Fe-deficiency in rice roots [60,61]. This demonstrates that the plants were indeed under Fe-deficient conditions. Moreover, all four genes regulated by Fe-deficiency in roots were also induced by Zn-excess (Figure 8), confirming a trend for common responses to both stresses in this organ, as previously reported [59].

A completely different response to Fe-deficiency was observed in leaves. None of the *OsZIFL* genes showed up-regulation under this condition (Figure 11A-F), although expression of the *OsIRO2* gene, was up-regulated by 5.6-fold (Figure 11G). It is known that *OsIRO2* is induced by Fe-deficiency in leaves [62]. This is, however, similar to *OsZIFL* gene expression in leaves of Zn-excess-treated plants (Figure 9): although six *OsZIFL* genes were expressed, only *OsZIFL7* and *OsZIFL12* were up-regulated, while all other family members did not change their expression levels. Considering the results obtained with Zn-excess and Fe-deficiency, it is possible to suggest that transcriptional regulation of most *OsZIFL* genes is more important in roots than in leaves, regardless of the level of expression in control conditions.

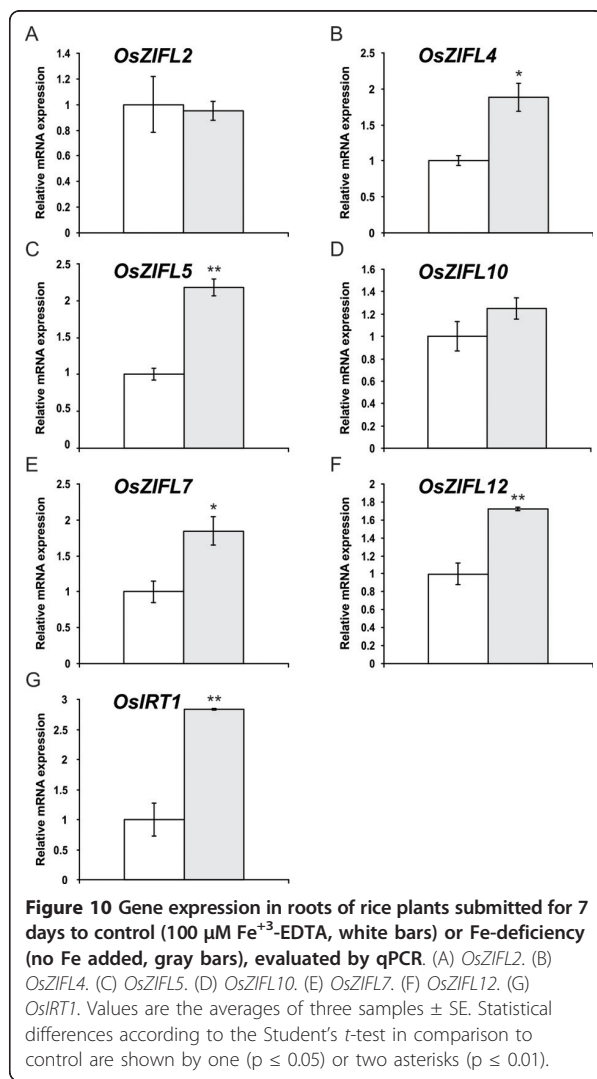


Figure 10 Gene expression in roots of rice plants submitted for 7 days to control (100 μ M Fe^{+3} -EDTA, white bars) or Fe-deficiency (no Fe added, gray bars), evaluated by qPCR. (A) *OsZIFL2*, (B) *OsZIFL4*, (C) *OsZIFL5*, (D) *OsZIFL10*, (E) *OsZIFL7*, (F) *OsZIFL12*, (G) *OsIRT1*. Values are the averages of three samples \pm SE. Statistical differences according to the Student's *t*-test in comparison to control are shown by one ($p \leq 0.05$) or two asterisks ($p \leq 0.01$).

OsZIFL duplicated pairs are co-expressed in specific plant organs and in response to stresses

To analyze the expression pattern of *OsZIFL* genes based on microarray meta-analysis, we used Genevestigator [63]. Affymetrix unique probes used for expression analyses of *OsZIFL2*, *OsZIFL3*, *OsZIFL5*, *OsZIFL7*, *OsZIFL8*, *OsZIFL10*, *OsZIFL12* and *OsZIFL13* are listed in Additional File 7. The available data on expression of *OsZIFL* genes in different organs of rice plants is shown in Figure 12. Clearly, the expression pattern within each one of the duplicated gene pairs *OsZIFL5*-*OsZIFL10* and *OsZIFL7*-*OsZIFL12* cluster together, indicating their overlapping expression. According to microarray data, *OsZIFL5* and *OsZIFL10* are highly expressed in seed tissues, while *OsZIFL7* and *OsZIFL12* are expressed in reproductive organs and shoot tissues (Figure 12). Similarly, our qPCR experiments showed higher expression

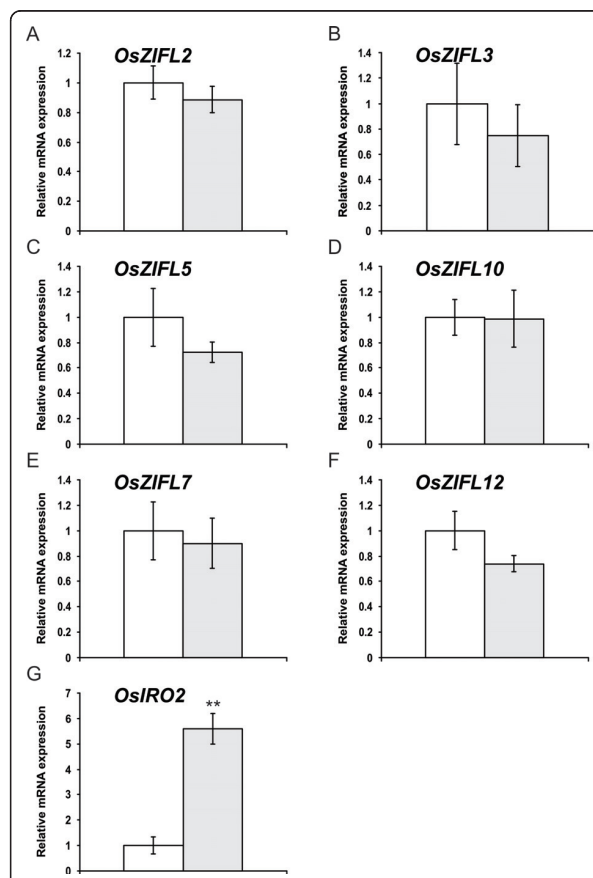
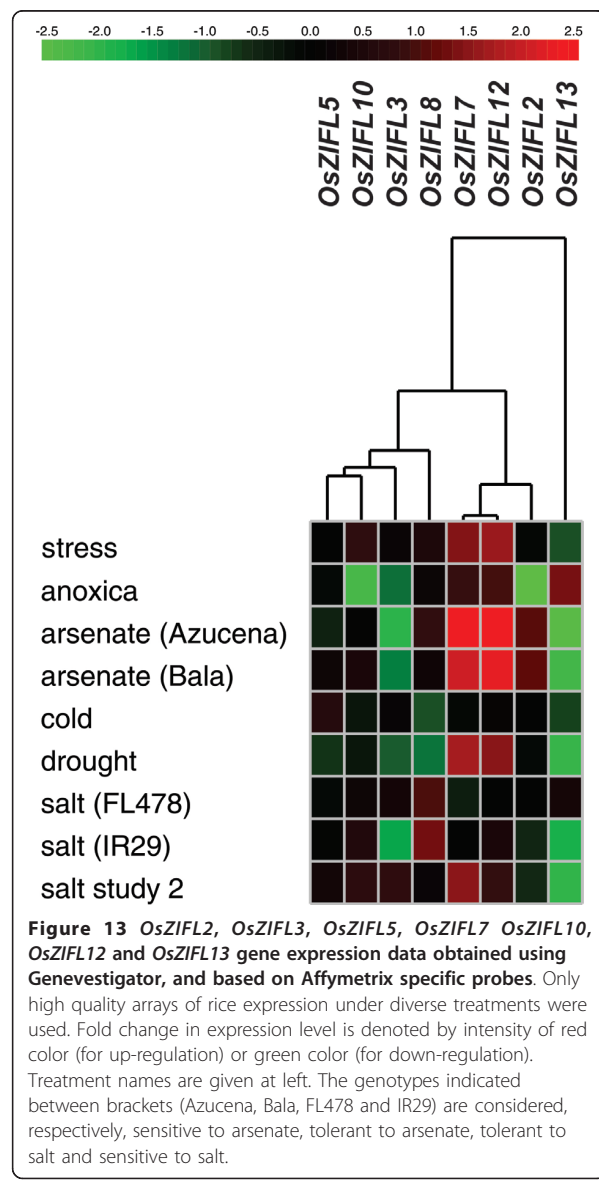
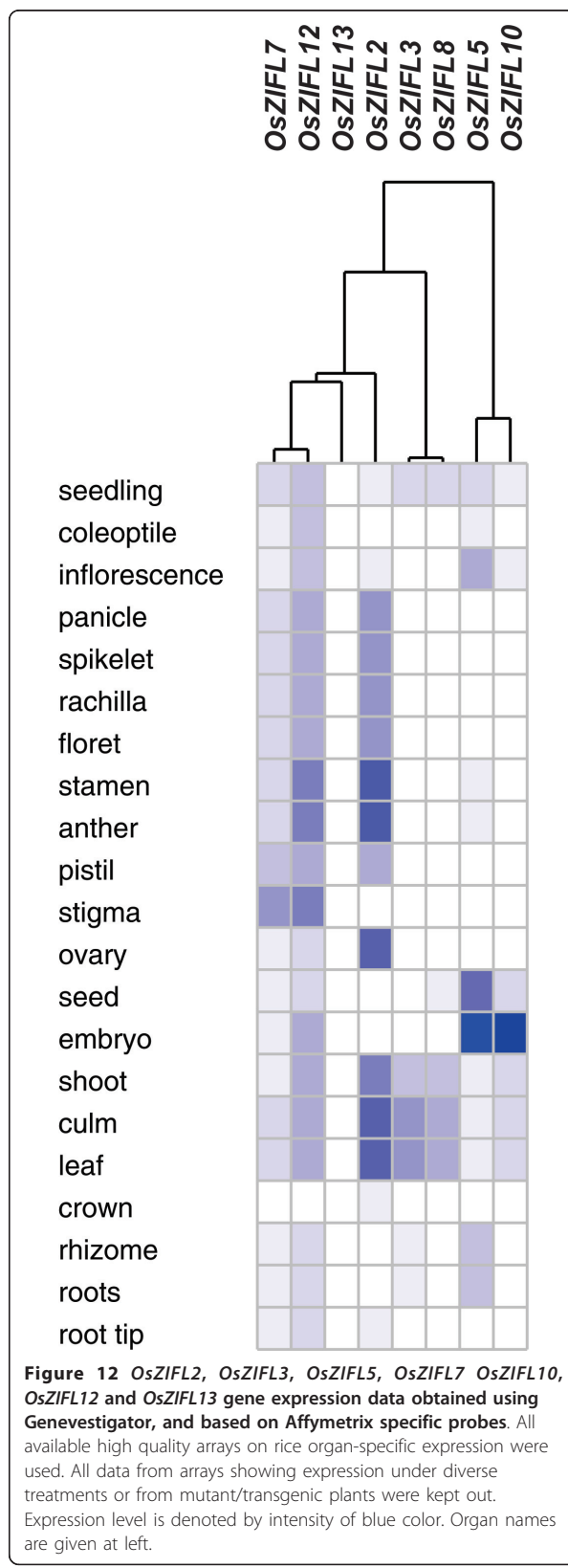


Figure 11 Gene expression in leaves of rice plants submitted for 7 days to control (100 μ M Fe^{+3} -EDTA, white bars) or Fe-deficiency (no Fe added, gray bars), evaluated by qPCR. (A) *OsZIFL2*, (B) *OsZIFL3*, (C) *OsZIFL5*, (D) *OsZIFL10*, (E) *OsZIFL7*, (F) *OsZIFL12*, (G) *OsIRO2*. Values are the averages of three samples \pm SE. Statistical differences according to the Student's *t*-test in comparison to control are shown by one ($p \leq 0.05$) or two asterisks ($p \leq 0.01$).

of both *OsZIFL7* and *OsZIFL12* in flag leaves and panicles and lower in roots (Figures 6G and 6H). The pair *OsZIFL8* and *OsZIFL13*, which had no detected expression in our qPCR experiments, was evaluated using specific probes. While *OsZIFL13* showed no expression, low expression of *OsZIFL8* was observed in shoot tissues. Although qPCR will never generate the large amount of data that is achieved by cDNA microarrays, PCR has the advantage of unparalleled sensitivity, and therefore slight discrepancies are expected [64].

OsZIFL duplicated pairs also show co-expression under stress conditions (Figure 13). *OsZIFL7* and *OsZIFL12* are highly up-regulated by arsenate in roots of an arsenate-tolerant (Bala) and an arsenate-sensitive (Azucena) cultivars (Figure 13) [65]. This suggests that these transporters could be responsive to general stress, as they are also up-regulated by Zn-excess and Fe-deficiency (Figures 8E



and 8F; 9E and 9F, 10E and 10F). *OsZIFL2* is also responsive to arsenate (Figure 13). *OsZIFL7* and *OsZIFL12* are also up-regulated under drought and salt stresses (Figure 13). *OsZIFL5* and *OsZIFL10* are mostly co-expressed, although no marked increase or decrease in expression was observed for both genes (Figure 13). The microarray results indicate a strong co-expression of the recently duplicated gene pairs *OsZIFL7*-*OsZIFL12* and *OsZIFL5*-*OsZIFL10*, in accordance with our qPCR data.

Discussion

ZIFL expansion through segmental duplication

Phenotypic variation is not necessarily the result of entirely new genes. Instead, redundancy generated through

gene duplication can be the source of evolutionary novelty. Plants are highly susceptible to duplication events, as most (if not all) have experienced whole-genome duplication events in their evolutionary past, as well as tandem and segmental duplications [66,67]. After duplication, gene copies can follow (1) neofunctionalization, where one copy maintains the ancestral function and the other can explore new evolutionary terrain; (2) pseudogenization, where one copy accumulates mutations and lose function while the other maintains the ancestral function; (3) subfunctionalization, in which deleterious mutations make one copy to be partially functional, but complementary to the other (i.e. in regard to the ancestral gene) [67,68]. As deleterious mutations are expected to be more common than beneficial ones, subfunctionalization is considered to be a more common fate for duplicated copies than neofunctionalization, and examples are already known [69,70]. These mutations are also more common in regulatory regions (i.e. promoters) than in functional motifs, where selective pressure is stronger; therefore, changes in expression patterns and/or changes in the responses to stimuli are probably more frequent [68].

In this work, we described the ZIFL protein family in plants, which is part of the MFS superfamily. We suggested that ZIFL proteins experienced an expansion in the monocot lineage, as we found three to four gene copies in dicots and eight up to thirteen in monocots, with all monocot paralogs grouping together (Figure 2). We further characterized the genomic organization of ZIFL genes in rice, and found that ten out of thirteen copies are located in a duplicated region of chromosomes 11 and 12 (Figure 3A). This region was first described as a recent segmental duplication, estimated from five to seven MYA [11,18]. This estimation was based on the high degree of similarity between terminal segments of both chromosomes (Figure 3). However, recent data showed that the duplication of this genomic segment is ancestral to the split of *S. bicolor*, *B. distachyon* and rice [14,19]. Wang et al. proposed that three rounds of unequal crossing-over events have produced the high similarity observed [9]. Thus, variation in sequence similarity within these regions reflects rather the antiquity of the unequal crossing-over events, than the date of segmental duplication as suggested earlier [11,18]. Gene conversion is also occurring at high frequencies within this region, further contributing for the maintenance of high similarity [9,13,15]. Using paralog pairs within the 3 Mb of chromosomes 11 and 12 from all species in the *Oryza* genus, a recent work demonstrated that concerted evolution is recurrent in this region for *Oryza* species [19]. Gene conversion was specifically found between *OsZIFL4* and *OsZIFL9* in *indica* rice, suggesting that concerted evolution has participated in the evolution of ZIFL genes [9].

We also demonstrated that the region where *S. bicolor* ZIFL genes are located in chromosome 8 is inverted in relation to its homologous region in rice chromosome 12 (Figures 3B and 3C). This inverted region was recently described for both *S. bicolor* and *B. distachyon*, encompassing 0.8 Mb [19]. *S. bicolor* ZIFL gene pairs are not as similar as rice paralogs, indicating that *S. bicolor* ZIFL genes probably did not undergo the same degree of concerted evolution as rice paralogs (i.e. unequal crossing-over and gene conversion). In agreement with that, Wang et al. used paralog quartets from rice and *S. bicolor* (i.e. a duplicated gene pair from rice and their homologs from *S. bicolor*) to search for gene conversions. They found that *OsZIFL4* and *OsZIFL9* went through whole gene conversion after the split between rice and *S. bicolor*, while *S. bicolor* homologs did not show conversion (in their supplemental table) [15]. Inversions are known to reduce the probability of recombination and to facilitate the maintenance of differences between interbreeding populations [71,72]. These results suggest that the inversion observed in *S. bicolor* reduced the probability of concerted evolution in the *SbZIFL* genes when compared to rice paralogs.

Sequence and expression analyses suggest new functional sites in OsZIFL proteins and insights about duplicated gene pairs

Our analysis on motif composition of OsZIFL proteins also revealed interesting features of this family in rice. Together with the exon-intron organization (Figure 4), motif composition of duplicated genes *OsZIFL8* and *OsZIFL13* and their partial duplicated copy *OsZIFL3* suggests that these genes are diverging in a higher rate when compared to other *OsZIFL* paralogs. They all show no ZIFL signature Cys motif C-P-G-C (Additional File 4). *OsZIFL3* and *OsZIFL8* also lack the MFS signature and *OsZIFL13* lacks both MFS and antiporter signatures (Additional File 4). *OsZIFL3* expression was detected in leaves, but at relatively low levels (Figure 6B). *OsZIFL8* and *OsZIFL13* transcripts were not detected in any of our qPCR experiments, and cDNAs corresponding to them are not present at the KOME database (<http://cdna01.dna.affrc.go.jp/PIPE/>). However, microarray metadata showed low expression of *OsZIFL8* in shoots, although no expression of *OsZIFL13* was detected in all plant organs evaluated (Figure 12). Further experiments should clarify if these genes are gaining new functions or accumulating mutations to become pseudogenes.

A variable region, which corresponds to a cytoplasmic loop, occupies a central position in the OsZIFL proteins (Figures 1B, 5A and Additional File 6). There is very low amino acid conservation within this loop. For this reason, we were able to find conserved motifs within the variable region only when using the whole ZIFL protein

dataset in our analyses (Figure 5B). Variable regions are often found in transporters [50,51]. In the ZIP family (Zinc-regulated/Iron-regulated transporter Proteins), a variable region is considered to be the metal-binding site, as these loops are rich in histidine residues [50,51]. Our motif analysis in the ZIFL variable region detected some residues in conserved positions. In the CDF family, substrate specificity was proposed to be determined by few amino acids, normally histidine (H) or aspartic acid (D), which are, respectively, positively and negatively charged [52]. In OsZIFL proteins, lysine (K) and glutamic acid (E), also positive and negative residues, seem to be conserved in the variable loop (Figure 4B), although aspartic acid (D) and leucine (L) are also frequent (Figure 5B). This region and its conserved residues emerge as candidates for mutagenesis studies to clarify their importance in substrate transport, although no substrate was proven to be transported by ZIFL proteins [34]. Moreover, we described conserved motifs specific to ZIFL proteins (Figure 1B), which also contain candidate residues for site-directed mutagenesis studies.

We characterized the expression of *OsZIFL* genes in rice vegetative and reproductive organs (Figure 6) and compared the expression patterns of three duplicated gene pairs, *OsZIFL4-OsZIFL9*, *OsZIFL5-OsZIFL10* and *OsZIFL7-OsZIFL12* (Figure 6). *OsZIFL4* and *OsZIFL9* are both expressed in panicles at R7 stage, but only *OsZIFL4* is expressed in roots (Figures 6C and 6D). This partial overlap suggests that their ancestral gene was at least expressed in panicles at R7 and in roots, as deleterious mutations could be subfunctionalizing *OsZIFL9* (i.e. turning into a panicle-specific gene) while *OsZIFL4* maintains both panicle and root expression. However, neofunctionalization of *OsZIFL4* cannot be discarded. In agreement with that, Throude et al. showed that, from 115 duplicated gene pairs, the vast majority have been neofunctionalized or subfunctionalized, as 88%, 89% and 96% of duplicates, respectively expressed in grain, leaf and root, show distinct expression patterns [73]. A recent work in rice showed that the average number of conserved motifs between duplicated gene pairs declines with increased expression diversity, partially supporting the subfunctionalization model [74]. This is in accordance with the observed divergent expression of *OsZIFL4* and *OsZIFL9* and their motif composition, because *OsZIFL9* has lost one N-terminal and two C-terminal motifs (Figure 5A). Expression patterns within the gene pairs *OsZIFL5-OsZIFL10* and *OsZIFL7-OsZIFL12* are similar (Figure 6), and both *OsZIFL5* and *OsZIFL10* have the same motif composition (Figure 5A). *OsZIFL12* has two C-terminal motifs which are lacking in *OsZIFL7* (Figure 5A), but expression of *OsZIFL7* and *OsZIFL12* is quite similar, as

both are up-regulated in roots and leaves under Zn-excess (Figures 8E, 8F, 9E and 9F) and in roots under Fe-deficiency (Figures 10E and 10F). Microarray data also shows that the *OsZIFL* duplicated pairs *OsZIFL5-OsZIFL10* and *OsZIFL7-OsZIFL12* are co-expressed in the same plant organs and under the same treatments (Figures 12 and 13). Yim et al. showed that duplicated gene pairs with high local similarity (HLS) segments show higher expression correlations than gene pairs without these segments [74]. This probably results in an increased likelihood of gene conversion in promoters of gene pairs harboring HLS [74]. As gene conversion is known to homogenize sequences in multigene families, this probably explains the similar expression patterns of *OsZIFL* pairs, although it is established that duplicated gene pairs tend to rapidly diverge in their expression patterns [12,13,75].

Expression of *OsZIFL* genes is involved in the partially overlapping pathways of Zn-excess and Fe-deficiency responses

Ten out of thirteen *OsZIFL* genes are found in two tandem groups of five genes in rice chromosomes 11 and 12, probably as a result of repeatedly tandem duplication events. This size of tandemly arrayed genes was estimated to be very rare, as only 7% of gene arrays in the rice genome have more than three genes [76]. Tandem duplication events have a tendency to be retained when involving genes for which fluctuation in copy number is unlikely to affect downstream genes, such as those at the end of or in flexible steps of pathways [76]. In *Arabidopsis* and rice, tandemly arrayed genes are enriched for membrane proteins and genes with function on abiotic and biotic stresses [76]. Moreover, tandemly arrayed genes often share regulatory *cis*-elements and tend to be expressed in a coordinated manner, as well as family members with HLS generated through gene conversion [74,77]. These observations are in accordance with the up-regulation of *OsZIFL* members under Zn-excess or Fe-deficiency, some of which show strong up-regulation upon stress imposition, mostly in roots (Figures 8, 9, 10 and 11). It also agrees with the enrichment observed for CATGC and IDE1-like elements in *OsZIFL* promoter sequences (Figure 7). Enrichment for the CATGC-box is related to Fe-deficiency responses in rice [30,78]. The rice specific gene *OsMIR* is strongly up-regulated by Fe-deficiency and shows 10 CATGC-boxes in its promoter sequence [78]. In another work, CATGC was shown to be enriched in promoters of genes regulated by OsIDEF1, an upstream transcription factor involved in the early response to Fe-deficiency [30]. Thus, *OsZIFL* genes which are responsive to Fe-deficiency are potentially under the same control network, although more data is necessary to confirm this

hypothesis. Moreover, a similar up-regulation pattern is also observed in the *Arabidopsis AtZIF1* gene, which is also responsive to both Zn-excess and Fe-deficiency [34,57,58]. This suggests that *OsZIFL* genes which are responsive to both stresses could have conserved regulatory sequences in comparison to *AtZIF1*.

Partial overlap between Zn-excess and Fe-deficiency response has been reported [59]. Zn-excess treated plants show much higher concentrations of Fe in roots, but slightly decreased Fe in shoots and inhibited expression of *OsFER1* [59]. This indicates that Zn-excess causes Fe-deficiency due to mislocalization of the available Fe [59]. On the other hand, Fe-deficiency can cause Zn-excess, as Fe regulated transporters such as *OsIRT1* are suggested to transport Zn and *Arabidopsis* plants under Fe-deficiency accumulate excessive Zn [39,79]. It was also demonstrated that 13.75% of the Zn-excess up-regulated genes in roots are also up-regulated by Fe-deficiency, further indicating an overlap between these stresses [59]. Excessive Zn was also shown to induce more genes in rice roots than in shoots, as 400 genes were induced in roots, while only 54 in shoots of *Arabidopsis* plants under Zn-excess [59].

OsIRO2, a bHLH (basic Helix-Loop-Helix) transcription factor induced by Fe-deficiency, is the regulator of Fe-deficiency responsive genes in roots, such as the genes *OsNAS1* (*nicotianamine synthase 1*), *OsNAS2*, *OsNAAT1* (*nicotianamine amino-transferase 1*), *OsDMAS1* (*deoxymugineic acid synthase 1*) and the DMA-Fe³⁺ transporter *OsYSL15* [80]. Expression of *OsIRO2* was shown to be up-regulated by and to control the induction of these genes under Zn-excess [59]. However, *OsIRT1*, a classical Fe-deficiency-regulated gene, is not regulated by *OsIRO2* [80], and is not up-regulated under Zn-excess [59]. These results indicate that *OsIRO2* is in the crosslink between Zn-excess and Fe-deficiency responses. The *OsIRO2* binding site CACGTGG is not found in *OsZIFL* promoters, but our qPCR data shows that *OsZIFL4*, *OsZIFL5*, *OsZIFL7* and *OsZIFL12* are up-regulated in roots by both stresses (Figures 8 and 10). Considering our results, it is possible to suggest that *OsZIFL* genes are part of the overlapping pathway that links Fe-deficiency and Zn-excess, although regulators different from *OsIRO2* may control their expression. One of these regulators could be IDEF1 [54].

Conclusions

As the first description of the *ZIFL* family in plants, this work is the basis for functional studies, especially in rice. We have shed light onto the unusual genomic distribution of *OsZIFL* genes, and made suggestions about the evolutionary forces that shaped the high degree of similarity between them. We also characterized in detail

the motif composition of rice *OsZIFL* genes and the expression patterns in different rice organs and under stress conditions. More functional data, such as loss-of-function mutants, sub cellular localization and ligand specificity, are necessary to uncover the specific roles of each protein and to know to what extent they are functionally redundant, as well as to clarify the roles of *OsZIFL* genes in the homeostasis of Zn and Fe in rice.

Methods

Plant material and treatments

Rice seeds of the Nipponbare cultivar were germinated for four days in petri dishes, soaked in distilled water at 28°C (two days in the dark, two days in the light). After germination, seedlings were transferred to holders positioned over plastic pots with five liters of nutrient solution (16 seedlings per pot) containing 700 μM K₂SO₄, 100 μM KCl, 100 μM KH₂PO₄, 2 mM Ca(NO₃)₂, 500 μM MgSO₄, 10 μM H₃BO₃, 0.5 μM MnSO₄, 0.5 μM ZnSO₄, 0.2 μM CuSO₄, 0.01 μM (NH₄)₆Mo₇O₂₄, and 100 μM Fe⁺³-EDTA. The pH of the nutrient solution was adjusted to 5.4. Plants were kept at 28°C ± 1°C under photoperiod of 16h/8h light/dark (150 μmol.m⁻².s⁻¹). Solutions were replaced every 3-4 days.

For expression analyses in vegetative organs, samples of roots, leaves and culms were collected at the four-leaf stage (approximately 30 days of growth). For expression analyses in reproductive organs, plants were grown in soil under flooded conditions in an experimental unit at IRGA (Instituto Rio-Grandense do Arroz), in Cachoeirinha, RS, Brazil (29°54'58.61"S 51°10'02.65"W), during the rice growing season (October 2007 to March 2008). Soil characteristics of this site were reported by Stein et al. [36]. Samples of flag-leaves and panicles were collected during R3 (panicle exertion), R5 (grain filling) and R7 (grain dry-down) stages, according to Counce et al. [81]. Laboratory grown plants at the four-leaf stage were submitted to Zn-excess or to Fe-deficiency. For Zn-excess, plants were kept in 200 μM of ZnSO₄ for 3 days. For Fe-deficiency, Fe⁺³-EDTA was omitted from nutrient solution and samples were collected after 7 days. In all experiments, three biological samples composed of at least three plants each were used for gene expression analyses.

Sequence retrieval and databases

Sequences of *Arabidopsis thaliana* AtZIF1 (AT5G13740), AtZIFL1 (AT5G13750) and AtZIFL2 (AT3G43790) proteins were downloaded from the TAIR database (The *Arabidopsis* Information Resource, <http://www.arabidopsis.org/>) and used as queries to search the rice genome at the TIGR Rice Genome database (<http://rice.plantbiology.msu.edu/>) for *ZIFL* sequences using tBLASTn and BLASTp. Sequences with an expected

value lower than 1×10^{-30} and harboring more than 30% of similarity considering 30% of the sequence were selected. Both *Arabidopsis* and rice sequences were then used as queries to survey the genomes of *Vitis vinifera*, *Populus trichocarpa*, *Sorghum bicolor*, *Brachypodium distachyon*, *Zea mays*, *Selaginella moellendorffii* and *Physcomitrella patens* at the Phytozome database (<http://www.phytozome.net/>), using the same criteria as above. All plant sequences found (plus the previously known *Arabidopsis* sequences) were aligned and used as an input to build an HMM profile using the HMMER package [82]. The ZIFL HMM profile consensus sequence was used to re-search the listed genomes. As new sequences were found, the procedure was repeated iteratively until no new sequence appeared. To visualize the ZIFL HMM profile and the conserved motifs we used LogoMat M [83]. Alignments of ZIFL profile to MFS_1 HMM profile were performed using LogoMat P [84]. Individual sequences were manually curated to discard those of poor quality or incomplete (not starting with methionine or not having a stop codon). Accession numbers, given nomenclature, chromosome and genomic positions and predicted number of transmembrane domains (TMs) of ZIF-like proteins are shown in Additional File 1. Two unannotated ZIFL genes from *Zea mays* were predicted using Egenesh (<http://www.softberry.com>) and their given nomenclature, chromosome and genomic positions, exon coordinates and predicted number of TMs are shown in Additional File 2.

Sequences from MFS_1 proteins from each monocot and dicot species analyzed in this work were retrieved using the same method as for ZIFL protein sequences. The consensus sequence generated from the HMM profile of MFS_1 (Pfam number PF07690) was used to search the genomes. All locus numbers of *MFS_1* genes used are given in Additional File 8.

Alignments and phylogenetic analyses

Sequence alignment and phylogenetic analyses for ZIFL proteins were performed using the MEGA (Molecular Evolutionary Genetics Analysis) 4.1 package [85]. Protein multiple alignments were obtained with ClustalW and phylogenetic trees were reconstructed with the neighbor-joining method and the following parameters: pairwise deletion option, 1,000 replicates of bootstrap and Poisson correction distance. The consensus tree shows only branches with a bootstrap consensus >50. Bayesian analysis was applied to generate a posterior probability distribution using the Metropolis-coupled Markov Chain Monte Carlo (MCMC) with MrBayes 3.0b4 [86,87]. The search was run for 1×10^6 generations, and every 100th tree was sampled. Posterior probabilities for each branch were calculated from the sampled trees. Sequence alignments of MFS_1 proteins

were performed using MEGA 4.1 package, and phylogenetic trees were reconstructed with the neighbor-joining method, following the same parameters described above.

For genomic alignments, we used a 100 kb region from rice chromosomes 11 and 12 and *S. bicolor* chromosomes 5 and 8 spanning the tandemly repeated ZIFL genes regions in both species. The graphic alignment tool for comparative sequence analysis (GATA) was used to align the sequences and visualize the results [88]. GATA uses BLASTn to compare a reference to a comparative sequence. A sliding window of predefined size slides through the reference sequence and aligns it to the comparative sequence. Matches are shown in black for forward hits (+/+) and in red for reverse hits (+/-). We used a window size of 24 and a lower cutoff score of 80. The default values were used for the other settings.

Exon-intron determination, motif finding and promoter analysis

For determining exon-intron organization, genomic and coding sequences (predicted, cDNA when available) were aligned. To search for conserved motifs in ZIF-like proteins, MEME (Motif EM for Motif Elicitation - <http://meme.nbcr.net/> [49]) was used, with the following parameters: zero or one motif per sequence, 6 and 300 amino acids as minimum and maximum sizes of motifs. Only motifs with expected value lower than 1×10^{-20} were considered. For motifs within the variable region, the e-value cutoff was increased to 1×10^{-10} due to high sequence divergence. The best possible match of each motif was searched in the InterPro database (<http://www.ebi.ac.uk/interpro/>). To identify the transmembrane domains of ZIFL proteins we used Conpred II (<http://bioinfo.si.hirosaki-u.ac.jp/~ConPred2/>), a consensus prediction method for obtaining transmembrane topology models. Promoter sequences from -1,500 bp to +1 bp of each rice ZIF-like gene were extracted from the TIGR Rice Genome database. Different strategies were used to find regulatory sequences within the promoters of *OsZIF-like* genes. POCO was used to compare the promoter dataset to the *Arabidopsis thaliana* clean background, the closest species available for this tool [53]. POCO was run with default settings, except for the pattern length selected as 5 bp. To confirm that over-represented motifs in comparison to *Arabidopsis* background are also over-represented when compared to rice background, the -1,500 bp to +1 bp promoter region of nearly 25,000 rice genes were downloaded from the Osiris database (<http://www.bioinformatics2.wsu.edu/cgi-bin/Osiris/cgi/home.pl/> [55]) and evaluated for average number of motifs.

Genevestigator

We used only specific Affymetrix probes for rice ZIF genes (Additional File 7) to analyze expression data

from GENEVESTIGATOR (<http://www.genevestigator.com>) [63]. Only high quality arrays were used.

RNA extraction and cDNA synthesis

Rice tissues were harvested from plants grown under laboratory or field conditions as described above. Total RNA was extracted using the Concert Plant RNA Reagent (Invitrogen®, Carlsbad, CA, USA) and treated with DNase I (Invitrogen®, Carlsbad, CA, USA). cDNA was prepared using the SMART PCR cDNA Synthesis Kit by Clontech® Laboratories (Mountain View, CA, USA), according to the manufacturer's instructions. First-strand cDNA synthesis was performed with oligo dT and reverse transcriptase (M-MLV, Invitrogen®, Carlsbad, CA, USA) using 1 µg of RNA.

Quantitative RT-PCR and data analysis

For quantitative RT-PCR analysis (qPCR), the synthesized first strand cDNA from each time point was diluted 100 times. qPCR was carried out in an Applied Biosystems StepOne real-time cycler. All primers (listed in Additional File 9) were designed to amplify 100-150 bp of the 3'-UTR of the genes and to have similar Tm values ($60 \pm 2^\circ\text{C}$). Reaction settings were composed of an initial denaturation step of 5 min at 94°C , followed by 40 cycles of 10 s at 94°C , 15 s at 60°C , 15 s at 72°C ; samples were held for 2 min at 60°C for annealing of the amplified products and then heated from 60 to 99°C with a ramp of $0.3^\circ\text{C}/\text{s}$ to provide the denaturing curve of the amplified products. qPCRs were carried out in 20 µl final volume composed of 10 µl of each reverse transcription sample diluted 100 times, 2 µl of 10X PCR buffer, 1.2 µl of 50 mM MgCl₂, 0.1 µl of 5 mM dNTPs, 0.4 µl of 10 µM primer pairs, 4.25 µl of water, 2.0 µl of SYBR green (1:10,000, Molecular Probe), and 0.05 µl of Platinum Taq DNA polymerase (5 U/µl, Invitrogen®, Carlsbad, CA, USA). Obtained data were analyzed using the comparative C_t (threshold cycle) method [89]. The PCR efficiency from the exponential phase (E) was calculated for each individual amplification plot using the LinRegPCR software [90]. In each plate, the average of PCR efficiency for each amplicon was determined and used in further calculations. C_t values for all genes were normalized to the C_t value of UBQ5 [91]. The equation $Q_0 \text{ target gene} / Q_0 \text{ UBQ5} = [(Eff_{UBQ5})^{Ct_{UBQ5}} / (Eff_{target gene})^{Ct_{target gene}}]$, where Q₀ corresponds to the initial amount of transcripts, was used for normalization [89]. Each data point corresponds to three true biological replicate samples.

Statistical analyses

When appropriate, data were subjected to ANOVA and means were compared by the Tukey HSD or Student's *t* test using the SPSS Base 12.0 for Windows (SPSS Inc., USA).

Abbreviations

CDF: cation diffusion facilitator; CDS: coding sequence; OsDMAS1: deoxymugineic acid synthase; DDC: duplication-degeneration-complementation; HLS: high local similarity; IDE1: iron-deficiency responsive element 1; IDEF1: iron-deficiency responsive element-binding factor 1; MFS: major facilitator superfamily; MYA: million years ago; NAAT1: nicotianamine amino transferase; NAS: nicotianamine synthase; ORF: open reading frame; ZIF: zinc-induced facilitator; ZIFL: zinc-induced facilitator-like; ZIP: zinc-regulated/iron-regulated transporter protein

Additional material

Additional File 1: ZIFL gene sequence information. Gene locus number, given name, chromosome number, genomic localization, strand, predicted coding sequence (CDS) and protein length, and predicted number of transmembrane domains (TM) are shown for each gene.

Additional File 2: Previously unannotated ZIFL genes. Gene locus number, given name, chromosome number, genomic localization, strand, predicted coding sequence (CDS) and protein length, exon positions and predicted number of transmembrane domains (TM) are shown for each gene.

Additional File 3: Phylogenetic trees of ZIFL and MFS_1 proteins.

Phylogenetic trees showing the separation of ZIFL proteins from the other MFS_1 sequences in each monocot and dicot species analyzed. (A) *Oryza sativa*, (B) *Sorghum bicolor*, (C) *Zea mays*, (D) *Brachypodium distachyon*, (E) *Arabidopsis thaliana*, (F) *Vitis vinifera*, (G) *Populus trichocarpa*.

Additional File 4: Conserved residues found in ZIFL protein sequences. Residues of cysteine (Cys) motif, histidine (His) motif, TM8-TM9 loop motif, and residues of MFS and antiporter signatures of each ZIFL protein are shown.

Additional File 5: Chromosomal positions of ZIFL genes.

Chromosomal positions of ZIFL genes in (A) *Oryza sativa*, *Sorghum bicolor* and *Brachypodium distachyon* chromosomes, and in (B) *Zea mays* chromosomes. Only ZIFL-containing chromosomes are shown. Non-ZIFL genes within ZIFL gene clusters were omitted.

Additional File 6: Alignment of OsZIFL protein sequences. Alignment was constructed using ClustalW. Conserved amino acids are marked in black or grayscale according to similarity level.

Additional File 7: Probes used in Genevestigator analyses and evaluation of specificity of rice ZIFL Affymetrix® microarray probes.

For each ZIFL gene locus number, all corresponding probes are listed. Each probe is classified as unique or not unique, and, in the second case, the number of the other locus matching to the probe is provided.

Additional File 8: Locus numbers of MFS_1 genes used in reconstruction of phylogenetic trees, in addition to ZIFL genes.

Locus numbers of MFS_1 genes used in the reconstruction of phylogenetic trees shown in Additional File 3, in addition to ZIFL genes (Additional File 1 and Additional File 2).

Additional File 9: Gene-specific primers used for quantitative RT-PCR. Sequences of PCR primers used in quantitative RT-PCR analyses of rice ZIFL gene expression.

Acknowledgements

This research was supported by CNPq (Conselho Nacional de Desenvolvimento Científico e Tecnológico, Brazil): research fellowship to JPF and scholarships to FKR, PKM and ERS. RAS was recipient of a scholarship

from CAPES (Coordenação de Aperfeiçoamento de Pessoal de Nível Superior, Brazil) and KLL from FAPERGS (Fundação de Apoio à Pesquisa do Rio Grande do Sul). The authors thank IRGA (Instituto Rio-Grandense do Arroz) for technical support.

Author details

¹Centro de Biotecnologia, Universidade Federal do Rio Grande do Sul, Av. Bento Gonçalves 9500, P.O.Box 15005, Porto Alegre, 91501-970, Brazil.

²Departamento de Botânica, Instituto de Biociências, Universidade Federal do Rio Grande do Sul, Av. Bento Gonçalves 9500, Porto Alegre, 91501-970, Brazil.

Authors' contributions

FKR designed the experiments and drafted the manuscript. FKR performed the alignments, phylogenetic, motif composition, promoter and microarray expression analyses, and participated in qPCR experiments. RAS, PKM, ERS and KLL performed qPCR experiments. FKR and RAS analyzed qPCR data. RAS helped drafting the manuscript. JPF conceived and coordinated the study and prepared the final manuscript. All authors read and approved the final manuscript.

Received: 4 February 2010 Accepted: 25 January 2011

Published: 25 January 2011

References

- Bowers JE, Chapman BA, Rong J, Paterson AH: Unravelling angiosperm genome evolution by phylogenetic analysis of chromosomal duplication events. *Nature* 2003, **422**:433-438.
- Jaillon O, Aury JM, Noel B, Pollicetti A, Clepet C, Casagrande A, Choisne N, Aubourg S, Vitulo N, Jubin C, Vezzi A, Legeai F, Hugueney P, Dasilva C, Hormer D, Mica E, Jublot D, Poulain J, Bruylants C, Billault A, Segurens B, Gouyvenoux M, Ugarte E, Cattonaro F, Anthouard V, Vico V, Del Fabbro C, Alaux M, Di Gaspero G, Dumas V, Felice N, Paillard S, Juman I, Morollo M, Scalabrin S, Canaguier A, Le Clainche I, Malacrida G, Durand E, Pesole G, Laucou V, Chatelet P, Merdinoglu D, Delledonne M, Pezzotti M, Lecharny A, Scarpelli C, Artiguenave F, Pé ME, Valle G, Morgante M, Caboche M, Adam-Blondon AF, Weissenbach J, Quétier F, Wincker P, French-Italian Public Consortium for Grapevine Genome Characterization: The grapevine genome sequence suggests ancestral hexaploidization in major angiosperm phyla. *Nature* 2007, **449**:463-467.
- Paterson AH, Bowers JE, Chapman BA: Ancient polyploidization predating divergence of the cereals, and its consequences for comparative genomics. *Proc Natl Acad Sci USA* 2004, **101**:9903-9908.
- Tang H, Bowers JE, Wang X, Paterson AH: Angiosperm genome comparisons reveal early polyploidy in the monocot lineage. *Proc Natl Acad Sci USA* 2010, **107**:472-477.
- Otto SP, Whitham J: Polyploid incidence and evolution. *Annu Rev Genet* 2010, **34**:401-437.
- Ohno S: *Evolution by gene duplication* New York: Springer; 1970.
- Force A, Lynch M, Pickett FB, Amores A, Yan Y, Postlethwait J: Preservation of duplicate genes by complementary, degenerative mutations. *Genetics* 1999, **151**:1531-1545.
- Chapman BA, Bowers JE, Feltus FA, Paterson AH: Buffering of crucial functions by paleologous duplicated genes may contribute cyclicity to angiosperm genome duplication. *Proc Natl Acad Sci USA* 2006, **103**:2730-2735.
- Wang X, Tang H, Bowers JE, Feltus FA, Paterson AH: Extensive concerted evolution of rice paralogs and the road to regaining independence. *Genetics* 2007, **177**:1753-1763.
- Lockton S, Gaut BS: Plant conserved non-coding sequences and parologue evolution. *Trends Genet* 2005, **21**:60-65.
- Wang X, Shi X, Hao B, Ge S, Luo J: Duplication and DNA segmental loss in the rice genome: implications for diploidization. *New Phytol* 2005, **165**:937-946.
- Gu Z, Nicolae D, Lu HH, Li WH: Rapid divergence in expression between duplicate genes inferred from microarray data. *Trends Genet* 2002, **18**:609-613.
- Xu S, Clark T, Zheng H, Vang S, Li R, Wong GK, Wang J, Zheng X: Gene conversion in the rice genome. *BMC Genomics* 2008, **9**:93.
- Paterson AH, Bowers JE, Bruggmann R, Dubchak I, Grimwood J, Gundlach H, Haberer G, Hellsten U, Mitros T, Poliakov A, Schmutz J, Spannagl M, Tang H, Wang X, Wicker T, Bharti AK, Chapman J, Feltus FA, Gowik U, Grigoriev IV, Lyons E, Maher CA, Martis M, Narechania A, Ottillar RP, Penning BW, Salamov AA, Wang Y, Zhang L, Carpe NC, Freeling M, Gingle AR, Hash CT, Keller B, Klein P, Kresovich S, McCann MC, Ming R, Peterson DG, Mehboob-ur-Rahman , Ware D, Westhoff P, Mayer KF, Messing J, Rokhsar DS: The *Sorghum bicolor* genome and the diversification of grasses. *Nature* 2009, **457**:551-556.
- Wang X, Tang H, Bowers JE, Paterson AH: Comparative inference of illegitimate recombination between rice and sorghum duplicated genes produced by polyploidization. *Genome Res* 2009, **19**:1026-1032.
- Yu J, Wang J, Lin W, Li S, Li H, Zhou J, Ni P, Dong W, Hu S, Zeng C, Zhang J, Zhang Y, Li R, Xu Z, Li S, Li X, Zheng H, Cong L, Lin L, Yin J, Geng J, Li G, Shi J, Liu J, Lv H, Li J, Wang J, Deng Y, Ran L, Shi X, Wang X, Wu Q, Li C, Ren X, Wang J, Wang X, Li D, Liu D, Zhang X, Ji Z, Zhao W, Sun Y, Zhang Z, Bao J, Han Y, Dong L, Ji J, Chen P, Wu S, Liu J, Xiao Y, Bu D, Tan J, Yang L, Ye C, Zhang J, Xu J, Zhou Y, Yu Y, Zhang B, Zhuang S, Wei H, Liu B, Lei M, Yu H, Li Y, Xu H, Wei S, He X, Fang L, Zhang Z, Zhang Y, Huang X, Su Z, Tong W, Li J, Tong Z, Li S, Ye J, Wang L, Fang L, Lei T, Chen C, Chen H, Xu Z, Li H, Huang H, Zhang F, Xu H, Li N, Zhao C, Li S, Dong L, Huang Y, Li L, Xi Y, Qi Q, Li W, Zhang B, Hu W, Zhang Y, Tian X, Jiao Y, Liang X, Jin J, Gao L, Zheng W, Hao B, Liu S, Wang W, Yuan L, Cao M, McDermott J, Samudrala R, Wang J, Wong GK, Yang H: The Genomes of *Oryza sativa*: a history of duplications. *PLoS Biol* 2009, **3**:e38.
- Salse J, Bolot S, Throude M, Jouffre V, Piegu B, Quraishi UM, Calcagno T, Cooke R, Delseny M, Feuillet C: Identification and characterization of shared duplications between rice and wheat provide new insight into grass genome evolution. *Plant Cell* 2008, **20**:11-24.
- Rice Chromosomes 11 and 12 Sequencing Consortium: The sequence of rice chromosomes 11 and 12, rich in disease resistance genes and recent gene duplications. *BMC Biol* 2005, **3**:20.
- Jacquemin J, Laudie M, Cooke R: A recent duplication revisited: phylogenetic analysis reveals an ancestral duplication highly-conserved throughout the *Oryza* genus and beyond. *BMC Plant Biology* 2009, **9**:146.
- Yu J, Hu S, Wang J, Wong GK, Li S, Liu B, Deng Y, Dai L, Zhou Y, Zhang X, Cao M, Liu J, Sun J, Tang J, Chen Y, Huang X, Lin W, Ye C, Tong W, Cong L, Geng J, Han Y, Li L, Li W, Hu G, Huang X, Li W, Li J, Liu Z, Li L, Liu J, Qi Q, Liu J, Li L, Li T, Wang X, Lu H, Wu T, Zhu M, Ni P, Han H, Dong W, Ren X, Feng X, Cui P, Li X, Wang H, Xu X, Zhai W, Xu Z, Zhang J, He S, Zhang J, Xu J, Zhang K, Zheng X, Dong J, Zeng W, Tao L, Ye J, Tan J, Ren X, Chen X, He J, Liu D, Tian W, Tian C, Xia H, Bao Q, Li G, Gao H, Cao T, Wang J, Zhao W, Li P, Chen W, Wang X, Zhang Y, Hu J, Wang J, Liu S, Yang J, Zhang G, Xiong Y, Li Z, Mao L, Zhou C, Zhu Z, Chen R, Hao B, Zheng W, Chen S, Guo W, Li G, Liu S, Tao M, Wang J, Zhu L, Yuan L, Yang H: A draft sequence of the rice genome (*Oryza sativa* L. ssp. *indica*). *Science* 2002, **296**:79-92.
- Goff SA, Ricke D, Lan TH, Presting G, Wang R, Dunn M, Glazebrook J, Sessions A, Oeller P, Varma H, Hadley D, Hutchison D, Martin C, Katagiri F, Lange BM, Moughamer T, Xia Y, Budworth P, Zhong J, Miguel T, Paszkowski U, Zhang S, Colbert M, Sun WL, Chen L, Cooper B, Park S, Wood TC, Mao L, Quail P, Wing R, Dean R, Yu Y, Zharkikh A, Shen R, Sahasrabudhe S, Thomas A, Cannings R, Gutin A, Pruss D, Reid J, Tavtigian S, Mitchell J, Eldredge G, Scholl T, Miller RM, Bhatnagar S, Adey N, Rubano T, Tusneem N, Robinson R, Feldhaus J, Macalma T, Oliphant A, Briggs S: A draft sequence of the rice genome (*Oryza sativa* L. ssp. *japonica*). *Science* 2002, **296**:92-100.
- Yuan Q, Ouyang S, Liu J, Suh B, Cheung F, Sultana R, Lee D, Quackenbush J, Buell CR: The TIGR rice genome annotation resource: annotating the rice genome and creating resources for plant biologists. *Nucleic Acids Res* 2003, **31**:229-233.
- Ohyanagi H, Tanaka T, Sakai H, Shigemoto Y, Yamaguchi K, Habara T, Fujii Y, Antonio BA, Nagamuro Y, Imanishi T, Ieko K, Itoh T, Gojobori T, Sasaki T: The Rice Annotation Project Database (RAP-DB): hub for *Oryza sativa* ssp. *japonica* genome information. *Nucleic Acids Res* 2006, **34** Database: D741-4.
- An G, Jeong DH, Jung KH, Lee S: Reverse genetic approaches for functional genomics of rice. *Plant Mol Biol* 2005, **59**:111-23.
- White PJ, Broadley MR: Biofortification of crops with seven mineral elements often lacking in human diets–iron, zinc, copper, calcium, magnesium, selenium and iodine. *New Phytol* 2009, **182**:49-84.
- Zhao FJ, McGrath SP: Biofortification and phytoremediation. *Curr Opin Plant Biol* 2009, **12**:373-80.

27. Walker EL, Connolly EL: Time to pump iron: iron-deficiency-signaling mechanisms of higher plants. *Curr Opin Plant Biol* 2008, 11:530-5.
28. Hänsch R, Mendel RR: Physiological functions of mineral micronutrients (Cu, Zn, Mn, Fe, Ni, Mo, B, Cl). *Curr Opin Plant Biol* 2009, 12:259-66.
29. Palmer CM, Guerinot ML: Facing the challenges of Cu, Fe and Zn homeostasis in plants. *Nat Chem Biol* 2009, 5:333-340.
30. Kobayashi T, Itai RN, Ogo Y, Kakei Y, Nakanishi H, Takahashi M, Nishizawa NK: The rice transcription factor IDEF1 is essential for the early response to iron deficiency, and induces vegetative expression of late embryogenesis abundant genes. *Plant J* 2009, 60:948-961.
31. Sperotto RA, Ricachenevsky FK, Duarte GL, Boff T, Lopes KL, Sperb ER, Grusak MA, Fett JP: Identification of up-regulated genes in flag leaves during rice grain filling and characterization of OsNAC5, a new ABA-dependent transcription factor. *Planta* 2009, 230:985-1002.
32. Wirth J, Poletti S, Aeschlimann B, Yakandawala N, Drosos B, Osorio S, Tohge T, Fernie AR, Günther D, Gruissem W, Sauter C: Rice endosperm iron biofortification by targeted and synergistic action of nicotianamine synthase and ferritin. *Plant Biotechnol J* 2009, 7:631-44.
33. Marschner H: *Mineral nutrition of higher plants* London: Academic Press; 1995.
34. Haydon MJ, Cobbett CS: A novel major facilitator superfamily protein at the tonoplast influences zinc tolerance and accumulation in Arabidopsis. *Plant Physiol* 2007, 143:1705-1719.
35. Kawachi M, Kobae Y, Mori H, Tomioka R, Lee Y, Maeshima M: A mutant strain *Arabidopsis thaliana* that lacks vacuolar membrane zinc transporter MTP1 revealed latent tolerance to excessive zinc. *Plant Cell Physiol* 2009, 50:1156-1170.
36. Stein RJ, Duarte GL, Spohr MG, Lopes SIG, Fett JP: Distinct physiological responses of two rice cultivars subjected to iron toxicity under field conditions. *Ann Appl Biol* 2009, 154:269-277.
37. Stein RJ, Ricachenevsky FK, Fett JP: Differential regulation of the two rice ferritin genes (OsFER1 and OsFER2). *Plant Sci* 2009, 177:563-569.
38. Eide D, Broderius M, Fett J, Guerinot ML: A novel iron-regulated metal transporter from plants identified by functional expression in yeast. *Proc Natl Acad Sci USA* 1996, 93:5624-5628.
39. Lee S, An G: Over-expression of OsIRT1 leads to increased iron and zinc accumulations in rice. *Plant Cell Environ* 2009, 32:408-416.
40. Aoyama T, Kobayashi T, Takahashi M, Nagasaki S, Usuda K, Kakei Y, Ishimaru Y, Nakanishi H, Mori S, Nishizawa NK: OsYSL18 is a rice iron(III)-deoxymugineic acid transporter specifically expressed in reproductive organs and phloem of lamina joints. *Plant Mol Biol* 2009, 70:681-92.
41. Lee S, Chiecko JC, Kim SA, Walker EL, Lee Y, Guerinot ML, An G: Disruption of OsYSL15 leads to iron inefficiency in rice plants. *Plant Physiol* 2009, 150:786-800.
42. Morrissey J, Baxter IR, Lee J, Li L, Lahner B, Grotz N, Kaplan J, Salt DE, Guerinot ML: The ferroportin metal efflux proteins function in iron and cobalt homeostasis in Arabidopsis. *Plant Cell* 2009, 21:3326-3338.
43. Morel M, Crouzet J, Gravot A, Auroy P, Leonhardt N, Navasseur A, Richaud P: AtHMA3, a P1B-ATPase allowing Cd/Zn/Cu/Pb vacuolar storage in Arabidopsis. *Plant Physiol* 2009, 149:894-904.
44. Simmons CR, Fridlander M, Navarro PA, Yalpani N: A maize defense-inducible gene is a major facilitator superfamily member related to bacterial multidrug resistance efflux antiporters. *Plant Mol Biol* 2003, 53:433-446.
45. Saier MH Jr, Beatty JT, Goffeau A, Harley KT, Heijne WH, Huang SC, Jack DL, Jähn PS, Lew K, Liu J, Pao SS, Paulsen IT, Tseng TT, Virk PS: The major facilitator superfamily. *J Mol Microbiol Biotechnol* 1999, 1:257-279.
46. Waters BM, Grusak MA: Quantitative trait locus mapping for seed mineral concentrations in two *Arabidopsis thaliana* recombinant inbred populations. *New Phytol* 2008, 179:1033-1047.
47. Tauris B, Borg S, Gregersen PL, Holm PB: A roadmap for zinc trafficking in the developing barley grain based on laser capture microdissection and gene expression profiling. *J Exp Bot* 2009, 60:1333-1347.
48. Gross J, Stein RJ, Fett-Neto AG, Fett JP: Iron homeostasis related genes in rice. *Genet Mol Biol* 2003, 26:477-497.
49. Bailey TL, Williams N, Misleh C, Li WW: MEME: discovering and analyzing DNA and protein sequence motifs. *Nucleic Acids Res* 2006, 34:W369-373.
50. López-Millán AF, Ellis DR, Grusak MA: Identification and characterization of several new members of the ZIP family of metal ion transporters in *Medicago truncatula*. *Plant Mol Biol* 2004, 54:583-96.
51. Yang X, Huang J, Jiang Y, Zhang HS: Cloning and functional identification of two members of the ZIP (Zrt, Irt-like protein) gene family in rice (*Oryza sativa* L.). *Mol Biol Rep* 2009, 36:281-287.
52. Montanini B, Blaudz D, Jeandroz S, Sanders D, Chalot M: Phylogenetic and functional analysis of the Cation Diffusion Facilitator (CDF) family: improved signature and prediction of substrate specificity. *BMC Genomics* 2007, 8:107.
53. Kankainen M, Holm L: POCO: discovery of regulatory patterns from promoters of oppositely expressed gene sets. *Nucleic Acids Res* 2005, 33: W427-31.
54. Kobayashi T, Ogo Y, Itai RN, Nakanishi H, Takahashi M, Mori S, Nishizawa NK: The transcription factor IDEF1 regulates the response to and tolerance of iron deficiency in plants. *Proc Natl Acad Sci USA* 2007, 104:19150-19155.
55. Morris RT, O'Connor TR, Wyrick JJ: Osiris: an integrated promoter database for *Oryza sativa* L. *Bioinformatics* 2008, 24:2915-2917.
56. Kobayashi T, Suzuki M, Inoue H, Itai RN, Takahashi M, Nakanishi H, Mori S, Nishizawa NK: Expression of iron-acquisition-related genes in iron-deficient rice is co-ordinately induced by partially conserved iron-deficiency-responsive elements. *J Exp Bot* 2005, 56:1305-1316.
57. Long TA, Tsukagoshi H, Busch W, Lahner B, Salt DE, Benfey PN: The bHLH Transcription Factor POPEYE Regulates Response to Iron Deficiency in *Arabidopsis* Roots. *Plant Cell* 2010, 22:2219-36.
58. Buckhout TJ, Yang TJ, Schmidt W: Early iron-deficiency-induced transcriptional changes in *Arabidopsis* roots as revealed by microarray analyses. *BMC Genomics* 2009, 10:147.
59. Ishimaru Y, Suzuki M, Ogo Y, Takahashi M, Nakanishi H, Mori S, Nishizawa NK: Synthesis of nicotianamine and deoxymugineic acid is regulated by OsIRO2 in Zn excess rice plants. *Soil Sci Plant Nutr* 2008, 54:417-423.
60. Buglio N, Yamaguchi H, Nishizawa NK, Nakanishi H, Mori S: Cloning an iron-regulated metal transporter from rice. *J Exp Bot* 2002, 53:1677-1682.
61. Ishimaru Y, Suzuki M, Tsukamoto T, Suzuki K, Nakazono M, Kobayashi T, Wada Y, Watanabe S, Matsuhashi S, Takahashi M, Nakanishi H, Mori S, Nishizawa NK: Rice plants take up iron as an Fe³⁺-phytosiderophore and as Fe²⁺. *Plant J* 2006, 45:335-346.
62. Ogo Y, Itai RN, Nakanishi H, Inoue H, Kobayashi T, Suzuki M, Takahashi M, Mori S, Nishizawa NK: Isolation and characterization of IRO2, a novel iron-regulated bHLH transcription factor in graminaceous plants. *J Exp Bot* 2006, 57:2867-2878.
63. Zimmermann P, Hennig L, Gruissem W: Gene-expression analysis and network discovery using Genevestigator. *Trends Plant Sci* 2005, 10:407-409.
64. Schmittgen TD, Livak KJ: Analyzing real-time PCR data by the comparative Ct method. *Nat Protoc* 2008, 3:1101-1108.
65. Norton GJ, Lou-Hing DE, Meharg AA, Price AH: Rice-arsenate interactions in hydroponics: whole genome transcriptional analysis. *J Exp Bot* 2008, 59:2267-2276.
66. Cui L, Wall PK, Leebens-Mack JH, Lindsay BG, Soltis DE, Doyle JJ, Soltis PS, Carlson JE, Arumuganathan K, Barakat A, Albert VA, Ma H, dePamphilis CW: Widespread genome duplications throughout the history of flowering plants. *Genome Res* 2007, 16:738-749.
67. Flagel LE, Wendel JF: Gene duplication and evolutionary novelty in plants. *New Phytol* 2009, 183:557-564.
68. Moore RC, Purugganan MD: The evolutionary dynamics of plant duplicate genes. *Curr Opin Plant Biol* 2005, 8:122-128.
69. Duarte JM, Cui L, Wall PK, Zhang Q, Zhang X, Leebens-Mack J, Ma H, Altman N, dePamphilis CW: Expression pattern shifts following duplication indicative of subfunctionalization and neofunctionalization in regulatory genes of *Arabidopsis*. *Mol Biol Evol* 2006, 23:469-478.
70. Ha M, Kim ED, Chen ZJ: Duplicate genes increase expression diversity in closely related species and allopolyploids. *Proc Natl Acad Sci USA* 2009, 106:2295-2300.
71. Hoffman AA, Rieseberg LH: Revisiting the impact of inversions in evolution: from population genetic markers to drivers of adaptive shifts and speciation? *Ann Rev Ecol Evol Syst* 2008, 39:21-42.
72. Feder JL, Nosil P: Chromosomal inversions and species differences: when are genes affecting adaptive divergence and reproductive isolation expected to reside within inversions? *Evolution* 2009, 63:3061-3075.
73. Throude M, Bolot S, Bosio M, Pont C, Sarda X, Quraishi UM, Bourgis F, Lessard P, Rogowsky P, Ghesquiere A, Murigneux A, Charmet G, Perez P,

- Salse J: Structure and expression analysis of rice paleo duplications. *Nucleic Acids Res* 2009, 37:1248-1259.
74. Yim WC, Lee BM, Jang CS: Expression diversity and evolutionary dynamics of rice duplicate genes. *Mol Genet Genomics* 2009, 281:483-493.
75. Blanc G, Wolfe KH: Functional divergence of duplicated genes formed by polyploidy during *Arabidopsis* evolution. *Plant Cell* 2004, 16:1679-1691.
76. Rizzon C, Ponger L, Gaut BS: Striking similarities in the genomic distribution of tandemly arrayed genes in *Arabidopsis* and rice. *PLoS Comput Biol* 2006, 2:e115.
77. Schmid M, Davison TS, Henz SR, Pape UJ, Demar M, Vingron M, Schölkopf B, Weigel D, Lohmann JU: A gene expression map of *Arabidopsis thaliana* development. *Nat Genet* 2005, 37:501-506.
78. Ishimaru Y, Bashir K, Fujimoto M, An G, Itai RN, Tsutsumi N, Nakanishi H, Nishizawa NK: Rice-specific mitochondrial iron-regulated gene (MIR) plays an important role in iron homeostasis. *Mol Plant* 2009, 2:1059-1066.
79. Cassin G, Mari S, Curie C, Briat JF, Czernic P: Increased sensitivity to iron deficiency in *Arabidopsis thaliana* overaccumulating nicotianamine. *J Exp Bot* 2009, 60:1249-1259.
80. Ogo Y, Itai RN, Nakanishi H, Kobayashi T, Takahashi M, Mori S, Nishizawa NK: The rice bHLH protein OsIRO2 is an essential regulator of the genes involved in Fe uptake under Fe-deficient conditions. *Plant J* 2007, 51:366-377.
81. Counce PA, Keisling TC, Mitchell AJ: A uniform, objective and adaptative system for expressing rice development. *Crop Sci* 2000, 40:436-443.
82. Eddy SR: Profile hidden Markov models. *Bioinformatics* 1998, 14:755-63.
83. Schuster-Böckler B, Schultz J, Rahmann S: HMM Logos for visualization of protein families. *BMC Bioinformatics* 2004, 5:7.
84. Schuster-Böckler B, Bateman A: Visualizing profile-profile alignment: pairwise HMM logos. *Bioinformatics* 2005, 21:2912-3.
85. Tamura K, Dudley J, Nei M, Kumar S: MEGA4: Molecular Evolutionary Genetics Analysis (MEGA) software version 4.0. *Mol Biol Evol* 2007, 24:1596-1599.
86. Huelsenbeck JP, Ronquist F: MRBAYES. Bayesian inference of phylogeny. *Bioinformatics* 2001, 17:754-755.
87. Ronquist F, Huelsenbeck JP: MrBayes 3: Bayesian phylogenetic inference under mixed models. *Bioinformatics* 2003, 19:1572-1574.
88. Nix DA, Eisen MB: GATA: a graphic alignment tool for comparative sequence analysis. *BMC Bioinformatics* 2005, 6:9.
89. Livak KJ, Schmittgen TD: Analysis of relative gene expression data using real-time quantitative PCR and the $2^{-\Delta\Delta C_t}$ method. *Methods* 2001, 25:402-408.
90. Ramakers C, Ruijter JM, Deprez RH, Moorman AF: Assumption-free analysis of quantitative real-time polymerase chain reaction (PCR) data. *Neurosci Lett* 2003, 339:62-6.
91. Jain M, Nijhawan A, Tyagi AK, Khurana JP: Validation of housekeeping genes as internal control for studying gene expression in rice by quantitative real-time PCR. *Biochem Biophys Res Commun* 2006, 345:646-651.

doi:10.1186/1471-2229-11-20

Cite this article as: Ricachenevsky et al.: ZINC-INDUCED FACILITATOR-LIKE family in plants: lineage-specific expansion in monocotyledons and conserved genomic and expression features among rice (*Oryza sativa*) paralogs. *BMC Plant Biology* 2011 11:20.

Submit your next manuscript to BioMed Central and take full advantage of:

- Convenient online submission
- Thorough peer review
- No space constraints or color figure charges
- Immediate publication on acceptance
- Inclusion in PubMed, CAS, Scopus and Google Scholar
- Research which is freely available for redistribution

Submit your manuscript at
www.biomedcentral.com/submit



Additional File 1. *ZIFL* gene sequence information.

Locus number	Gene name	Chromosome number	Genomic localization	Strand	CDS size (base pairs)	Protein size (amino acids)	TM domains
<i>Zea mays</i>							
GRMZM2G141081	<i>ZmZIFL2</i>	2	145779171 - 145783123	+	1,479	492	12
GRMZM2G115658	<i>ZmZIFL3</i>	2	145861576 - 145865621	-	1,509	502	12
GRMZM2G029219	<i>ZmZIFL4</i>	3	42872091 - 42879804	+	1,473	490	12
GRMZM2G161310	<i>ZmZIFL5</i>	3	45160852 - 45175101	-	1,347	448	12
GRMZM2G075594	<i>ZmZIFL6</i>	3	228297411 - 228302606	-	1,437	478	11
GRMZM2G022375	<i>ZmZIFL7</i>	4	185559013 - 185562973	+	1,497	498	12
GRMZM2G456923	<i>ZmZIFL9</i>	8	1809029 - 1814823	+	1,443	480	11
GRMZM2G311401	<i>ZmZIFL10</i>	10	3684222 - 3687765	-	1,278	425	10
<i>Oryza sativa</i>							
LOC_Os01g16260	<i>OsZIFL1</i>	1	9202963 - 9210788	-	1,461	486	12
LOC_Os01g17214	<i>OsZIFL2</i>	1	9888524 - 9901714	-	1,494	497	12
LOC_Os07g08300	<i>OsZIFL3</i>	7	4239045 - 4252498	+	1,071	356	8
LOC_Os11g04020	<i>OsZIFL4</i>	11	1617495 - 1622979	-	1,422	473	11
LOC_Os11g04030	<i>OsZIFL5</i>	11	1625475 - 1630422	-	1,413	470	11
LOC_Os11g04060	<i>OsZIFL6</i>	11	1640193 - 1644545	-	1,329	442	10
LOC_Os11g04104	<i>OsZIFL7</i>	11	1656864 - 1667363	-	1,515	504	11
LOC_Os11g04150	<i>OsZIFL8</i>	11	1680094 - 1687100	-	1,197	398	9
LOC_Os12g03830	<i>OsZIFL9</i>	12	1567001 - 1571324	-	1,233	410	10
LOC_Os12g03860	<i>OsZIFL10</i>	12	1583171 - 1588135	-	1,413	470	11
LOC_Os12g03870	<i>OsZIFL11</i>	12	1593733 - 1599962	-	1,398	465	10
LOC_Os12g03899	<i>OsZIFL12</i>	12	1605073 - 1615757	-	1,509	502	11
LOC_Os12g03950	<i>OsZIFL13</i>	12	1634122 - 1641673	-	870	289	7

AT5G13750	AtZIFL1 ^a	5	4438200 - 4441579	+	1,437	478	10
AT3G43790	AtZIFL2 ^a	3	15655384 - 15660086	+	1,455	484	11
<i>Populus trichocarpa</i>							
POPTR_0006s02710	PtZIFL1	scaffold_6	1722558 - 1728279	+	1,437	478	10
POPTR_0008s01110	PtZIFL2	scaffold_8	532910 - 538315	+	1,488	495	12
POPTR_0009s02680	PtZIFL3	scaffold_9	3436203 - 3443562	-	1,497	498	10
POPTR_0016s02500	PtZIFL4	scaffold_16	1231196 - 1238604	+	1,440	479	11
<i>Vitis vinifera</i>							
GSVIVT00023334001	VvZIFL1	8	10337395 - 10355258	-	1,431	476	11
GSVIVT00033966001	VvZIFL2	Un_random	126574785 - 126599999	+	1,413	470	11
GSVIVT00033971001	VvZIFL3	Un_random	126641091 - 126674624	+	1,467	488	11
GSVIVT00033972001	VvZIFL4	Un_random	126681308 - 126695478	-	1,647	548	11
GSVIVT00033975001	VvZIFL5	Un_random	126731215 - 126739779	-	1,464	487	10
<i>Selaginella moellendorffii</i>							
164091	SmZIFL1	scaffold_0	4058805 - 4064564	+	1,485	494	11
408219	SmZIFL2	scaffold_8	1448426 - 1450923	-	1,497	498	11
147893	SmZIFL3	scaffold_17	1505890 - 1508475	+	1,545	514	11
96275	SmZIFL4	scaffold_18	585495 - 587800	-	1,362	453	10
412524	SmZIFL5	scaffold_18	589633 - 592168	+	1,353	450	10
157948	SmZIFL6	scaffold_73	557939 - 560436	-	1,461	486	9
184037	SmZIFL7	scaffold_90	208963 - 214635	+	1,476	1476	11
<i>Physcomitrella patens</i>							
116273	PpZIFL1	scaffold_15	520309 - 525256	+	1,329	442	10
185929	PpZIFL2	scaffold_88	594417 - 600663	+	1,521	506	12

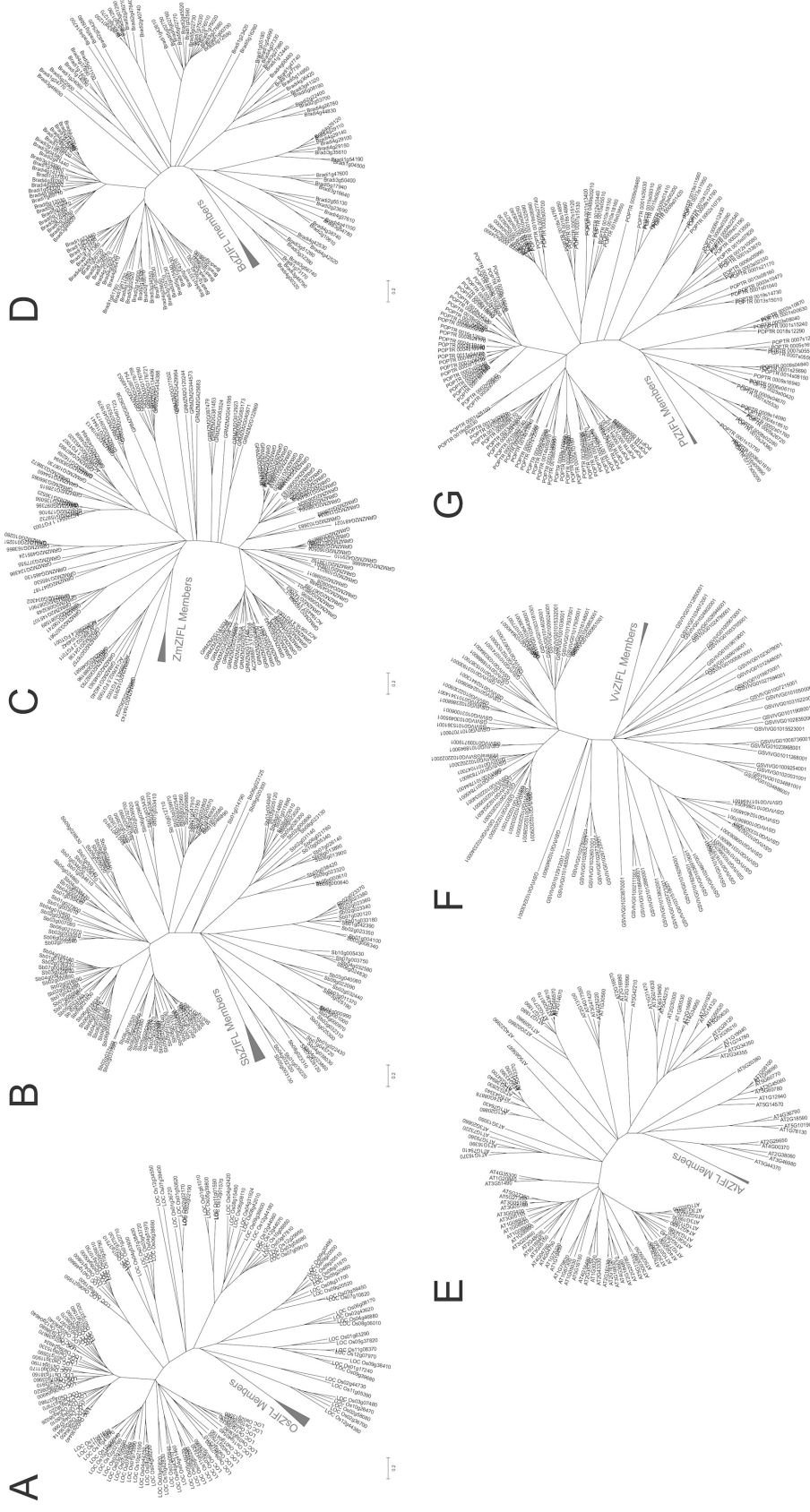
^a Previously annotated by Haydon and Cobbett [34]. CDS: predicted coding sequence. TM: transmembrane domains

Additional File 2. Previously unannotated *ZIFL* genes.

Gene name	Chromosome number	Locus localizations	Strand	CDS size (base pairs)	Protein size (amino acids)	Exon positions ^A	TM domains
<i>ZmZIFL1</i>	4	185583768 - 185587694	- (minus)	1560	519	185583768 - 185584010 - 185584053; 185584209 - 185584297; 185584395 - 185584439; 185584529 - 185584636; 185584719 - 185584804; 185585075 - 185585162; 185585499 - 185585699; 185585808 - 185585883; 185585964 - 185586028; 185586120 - 185586182; 185586266 - 185586319; 185586419 - 185586521; 185586664 - 185586766; 185586897 - 185586957; 185587095 - 185587137; 185587468 - 185587694	11
<i>ZmZIFL8</i>	1	199261494 - 199264659	+	1296	431	199261494 - 199261554; 199261765 - 199261867; 199261963 - 199262065; 199262156 - 199262209; 199262323 - 199262385; 199262473 - 199262522; 199262606 - 199262681; 199262864 - 199263064; 199263227 - 199263314; 199263493 - 199263578; 199263895 - 199264002; 199264057 - 199264126; 199264192 - 199264276; 199264391 - 199264434; 199264556 - 199264659	10

^A For the genes encoded by the minus strand, exon positions are given in the same order they appear in the genomic sequence.

CDS: predicted coding sequence. TM: transmembrane domains.



Additional File 3. Phylogenetic trees of ZIFL and MFS_1 proteins. Phylogenetic trees showing the separation of ZIFL proteins from the other MFS_1 sequences in each monocot and dicot species analyzed. (A) *Oryza sativa*, (B) *Sorghum bicolor*, (C) *Zea mays*, (D) *Vitis vinifera*, (E) *Populus trichocarpa*, (F) *Arabidopsis thaliana*, (G) *Brachypodium distachyon*

Additional File 4. Conserved residues found in ZIFL protein sequences.

Locus number	Gene name	Cys Motif ^a	His Motif ^b	TM8-TM9 Loop	MFS signature ^d	Antipporter signature ^e
<i>Zea mays</i>	<u>GRMZM2G141081</u>	ZmZIFL2	CPGC	PETLHKH	RILGPIKTSR	WGMAADRFGRK
	<u>GRMZM2G115658</u>	ZmZIFL3	CPGC	PETLHRH	KVILGPIKSSR	WGIAADRIGRK
	<u>GRMZM2G029219</u>	ZmZIFL4	CPGC	PETLHKH	KTVDHITLVR	WGIVADKYGRK
	<u>GRMZM2G161310</u>	ZmZIFL5	CPGC	PETLHFH	KYFGPPIKTFR	WGMFADKYGRK
	<u>GRMZM2G075594</u>	ZmZIFL6	CPGC	PETLHFH	RILGTIVNSAR	WGVTADRVGRK
	<u>GRMZM2G022375</u>	ZmZIFL7	CPGC	PETLHKH	KILGPVNSTR	WGVVADRVGRK
	<u>GRMZM2G456923</u>	ZmZIFL9	CPGC	PETLHFH	KYFGPIKTFR	WGMFADKYGRK
	<u>GRMZM2G311401</u>	ZmZIFL10	-	PETLHFH ^c	KYFGPVKIFR	WGIFADKYGRK
<i>Oryza sativa</i>	<u>LOC_Os01g16260</u>	OsZIFL1	CPGC	PETLHKH	KSVEPITLVR	WGIVADKYGRK
	<u>LOC_Os01g17214</u>	OsZIFL2	CPGC	PETLHMH	KYVGPIKPFR	WGIFADKYGRK
	<u>LOC_Os07g08300</u>	OsZIFL3	-	PETLHDL	KILGPINTSR	-
	<u>LOC_Os11g04020</u>	OsZIFL4	CPGC	PETLHKH	KELGSINSSR	WGIVADIGRK
	<u>LOC_Os11g04030</u>	OsZIFL5	CPGC	PETLHKH	KILGPINSTR	WGIVADIGRK
	<u>LOC_Os11g04060</u>	OsZIFL6	-	PETIHKH	KELGPIISLR	WGIVADIGRK
	<u>LOC_Os11g04104</u>	OsZIFL7	CPGC	PETLHKH	KVIGHIKASR	WGIAADIGRK
	<u>LOC_Os11g04150</u>	OsZIFL8	-	PETLHKH	KVILGIINTSR	-
	<u>LOC_Os12g03830</u>	OsZIFL9	-	PETLHKH	KELGSINSSR	--VADRIGRK
	<u>LOC_Os12g03860</u>	OsZIFL10	CPGC	PETLHKH	KILGPIHSIR	WGIVADIGRK
	<u>LOC_Os12g03870</u>	OsZIFL11	CPGC	PETIHKH	KELGPIISLR	WGIVADIGRK
	<u>LOC_Os12g03899</u>	OsZIFL12	CPGC	PETLHKH	KVIGHIKASR	WGIAADIGRK
	<u>LOC_Os12g03950</u>	OsZIFL13	-		KVILGIINTSR	-
<i>Sorghum bicolor</i>	<u>Sb03g010620</u>	SbZIFL1	CPGC	PETLHKH	KAVDHITLVR	WGIVADKYGRK
	<u>Sb03g011240</u>	SbZIFL2	CPGC	PETLHFH	KSFGPPIRPLR	WGIFADKYGRK

<i>Sb</i> 03g011330	<i>C</i> PGC	PETLH <small>FH</small>	R <small>Y</small> F <small>GPI</small> RPLR	WG <small>I</small> FADKYGRK	SLV <small>TSSVAAGL</small> VVGPAIG
<i>Sb</i> 03g011340	<i>C</i> PGC	-	K <small>Y</small> F <small>GPI</small> RPLR	WG <small>I</small> FADKYGRK	SLV <small>TSSRAIAF</small> VVGPAIG
<i>Sb</i> ZI <small>FL5</small>	<i>C</i> PGC	PETLH <small>FH</small>	K <small>Y</small> V <small>GPI</small> KTR	WG <small>M</small> FADKYGRK	SLV <small>TSSRAIALV</small> IGPAIG
<i>Sb</i> ZI <small>FL6</small>	<i>C</i> PGC	PETLH <small>FH</small>	K- <small>F</small> G <small>GPI</small> KTR	WG <small>M</small> FADKYGRK	SEV <small>TSSRAIALV</small> IGPSIG
<i>Sb</i> ZI <small>FL7</small>	<i>C</i> PGC	-	K <small>Y</small> F <small>GPI</small> RPLR	WG <small>I</small> FADK---	IKV <small>TSSRAIAF</small> VVGPAIG
<i>Sb</i> 03g023750	<i>C</i> PGC	OPGC	-	KVILGP <small>INSTR</small>	SVV <small>STAWGMCVIT</small> GPALG
<i>Sb</i> 05g002050	<i>C</i> PGC	OPGC	-	KVILGP <small>IKSSR</small>	SLV <small>STAWGIGLI</small> IGPALG
<i>Sb</i> 05g002060	<i>C</i> PGC	OPGC	-	QETLH <small>TH</small>	--VGTAWGIGLIIGPALG
<i>Sb</i> 05g002070	<i>C</i> PGC	OPGC	-	KILGP <small>VSTSSR</small>	SLISTSWAIGLILGPSIG
<i>Sb</i> 05g008475	<i>C</i> PGC	OPGC	-	KVILGP <small>VNASR</small>	TLVSTSWAICLIIIGPAIG
<i>Sb</i> 08g001400	<i>C</i> PGC	OPGC	-	PETLH <small>KKH</small>	--VNTAWALGLIVGPALG
<i>Sb</i> 08g001410	<i>C</i> PGC	OPGC	-	PETI <small>HKH</small>	SIVSTAWGLGLIVGPSSIG
<i>Sb</i> 08g008410	<i>C</i> PGC	OPGC	-	PETLH <small>TH</small>	
<i>Brachypodium distachyon</i>					
<i>Bradi2g10020</i>	<i>Bd</i> ZI <small>FL11</small>	PETLH <small>KKH</small> ^c	K <small>SIEP</small> I ALVR	WG <small>VVADKY</small> GRK	SLISSSRIGLIVGPALG
<i>Bradi2g10030</i>	<i>Bd</i> ZI <small>FL2</small>	PETLH <small>KKH</small>	-	WG <small>VVADKY</small> GRK	SLISSSRIGLIVGPALG
<i>Bradi2g10800</i>	<i>Bd</i> ZI <small>FL3</small>	PETLHMH	KYAGL <small>IKPFR</small>	WG <small>M</small> FADKYGRK	SLV <small>TSSRAIALV</small> VGPAIG
<i>Bradi4g26340</i>	<i>Bd</i> ZI <small>FL4</small>	PETLHNH	GVLGP <small>INTSR</small>	WG <small>M</small> IADRIGRK	SLV <small>STS</small> SWAIGLIVGPTIG
<i>Bradi4g26350</i>	<i>Bd</i> ZI <small>FL5</small>	PETLHNH	-	WG <small>VVADKY</small> GRK	SLV <small>TSSRAIALV</small> VGPAIG
<i>Bradi4g26370</i>	<i>Bd</i> ZI <small>FL6</small>	PETLHNH	KVLG <small>HVRSSQ</small>	WG <small>VVADKY</small> GRK	SLVSTAWGIGLIIGPALG
<i>Bradi4g26380</i>	<i>Bd</i> ZI <small>FL7</small>	PETLHMH	RYLG <small>SIISSR</small>	WG <small>VVADKY</small> GRK	SVVSTGWGIGLVAGPAIG
<i>Bradi4g43580</i>	<i>Bd</i> ZI <small>FL8</small>	PESLH <small>KKH</small>	KIFGP <small>TNLTR</small>	WG <small>MVADRY</small> GRK	STVNNTAWMIGLIIIGPAIG
<i>Bradi4g43590</i>	<i>Bd</i> ZI <small>FL9</small>	PETI <small>HKH</small>	KFLGP <small>VISAR</small>	WG <small>VVADRY</small> GRK	SVVNTAWGFGLVIGPALG
<i>Bradi4g43620</i>	<i>Bd</i> ZI <small>FL0</small>	-	PETI <small>HKH</small>	WG <small>VVADRY</small> GRK	SVVNTAWGVGLVIGPALG
<i>Arabidopsis thaliana</i>					
<i>AT5G13740</i>	-	CPGC	RLLGP <small>VIVTR</small>	WG <small>IVADRY</small> GRK	SAVSTAWGIGLIIIGPALG
<i>AT5G13750</i>	-	SSGC	RLLGP <small>IIVTR</small>	WG <small>LVADRY</small> GRK	SAVSTAWGIGLIIIGPALG
<i>AT3G43790</i>	-	CPGC	PSVGLLAVTR	WGKLADRYGRK	SVVSTSRGIGLIIIGPALG
<i>Populus trichocarpa</i>					
<i>POPTR_0006s02710</i>	<i>Pt</i> ZI <small>FL11</small>	CPGC	RNFGP <small>VIVSR</small>	WG <small>M</small> IADRIGRK	SIISTSWGIGLIVGPALG
<i>Pt</i> ZI <small>FL10</small>	PETLH <small>SH</small>	PETLH <small>SH</small>			

<u>POPTR_0008s01110</u>	<i>PzIFL2</i>	CPGC	RILGPIPVHQ	STVSTAWGLGLIIGPAIG
<u>POPTR_0009s02680</u>	<i>PzIFL3</i>	CPGC	PETLHMH	SVVSTSRGICMIIIGPAIG
<u>POPTR_0016s02500</u>	<i>PzIFL4</i>	CPGC	PETIHNA	SIISTSWGIGLVIGPAIG
<i>Vitis vinifera</i>				
<u>GSVIVT00023334001</u>	<i>VvZIFL1</i>	CPGC	QETLHH	RILGPVMVSR
<u>GSVIVT100033966001</u>	<i>VvZIFL2</i>	CPGC	QETLHH	KLLGPIIICR
<u>GSVIVT00033971001</u>	<i>VvZIFL3</i>	CPGC	QETLHH	KLLGPIIICR
<u>GSVIVT100033972001</u>	<i>VvZIFL4</i>	CSGC	PETLHH	RFLGPVMIICR
<u>GSVIVT00033975001</u>	<i>VvZIFL5</i>	CSGC	PETLHH	RFLGPVMIICR
<i>Selaginella moellendorffii</i>				
<u>164091</u>	<i>SmZIFL1</i>	CPGC	PETLHRK	RMVGPPIRACR
<u>408219</u>	<i>SmZIFL2</i>	CPGC	PETLHRK	RLLGPPIRACR
<u>147893</u>	<i>SmZIFL3</i>	CPGC	PETLHKD	KWLGPPIRLTR
<u>96275</u>	<i>SmZIFL4</i>	CPGC	PETLHKH	NMLGPPIFMR
<u>412524</u>	<i>SmZIFL5</i>	CPGC	PETLHH	RRLGPAMVTR
<u>157948</u>	<i>SmZIFL6</i>	CPGC	PETLHKH	RLIGAIRSSCR
<u>184037</u>	<i>SmZIFL7</i>	CPGC	PETLHKH	RLIGAIRSYR
<i>Physcomitrella patens</i>				
<u>116273</u>	<i>PpZIFL1</i>	-	-	NWMGAVILVSR
<u>185929</u>	<i>PpZIFL2</i>	CPGC	-	HWMGAVILVSR
				WGMMVADRYGRV
				WGMAASDRYGRK
				SIVGTVWGLGLIIGPAMGG
				SIVGTVWGLGLIIGPAMGG

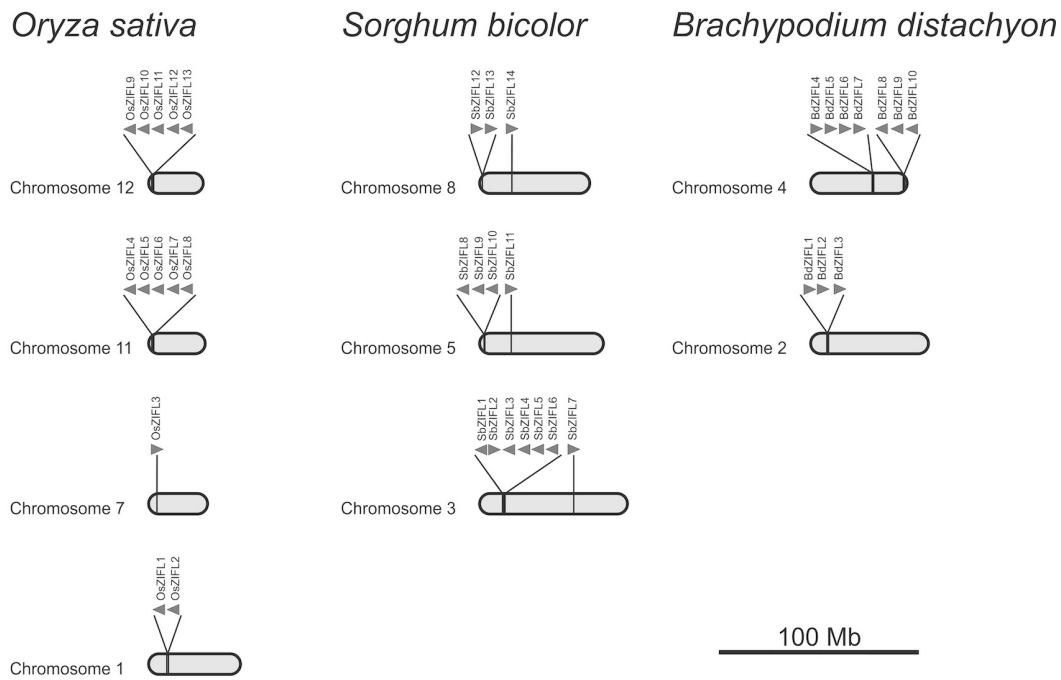
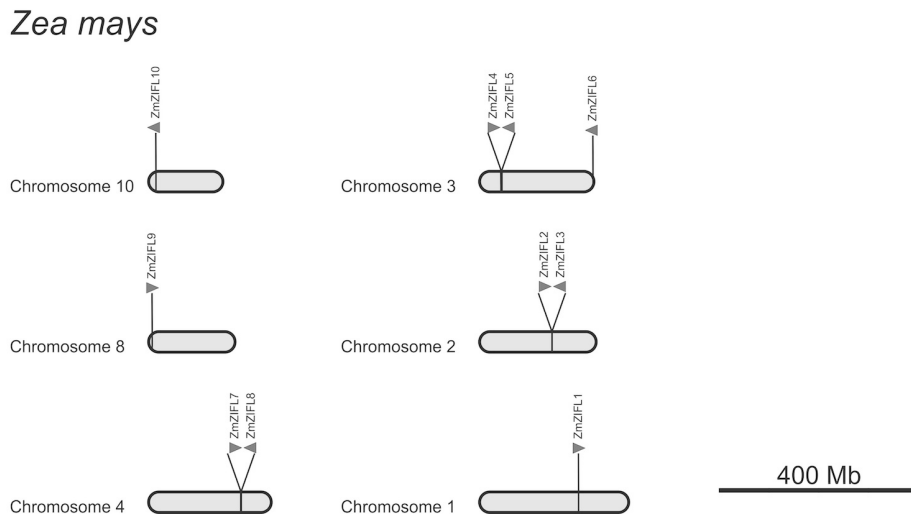
^a Only the most frequent C-P-G-C residues are highlighted.

^b Only the most frequent P-E-T-L-H-x-H residues are highlighted.

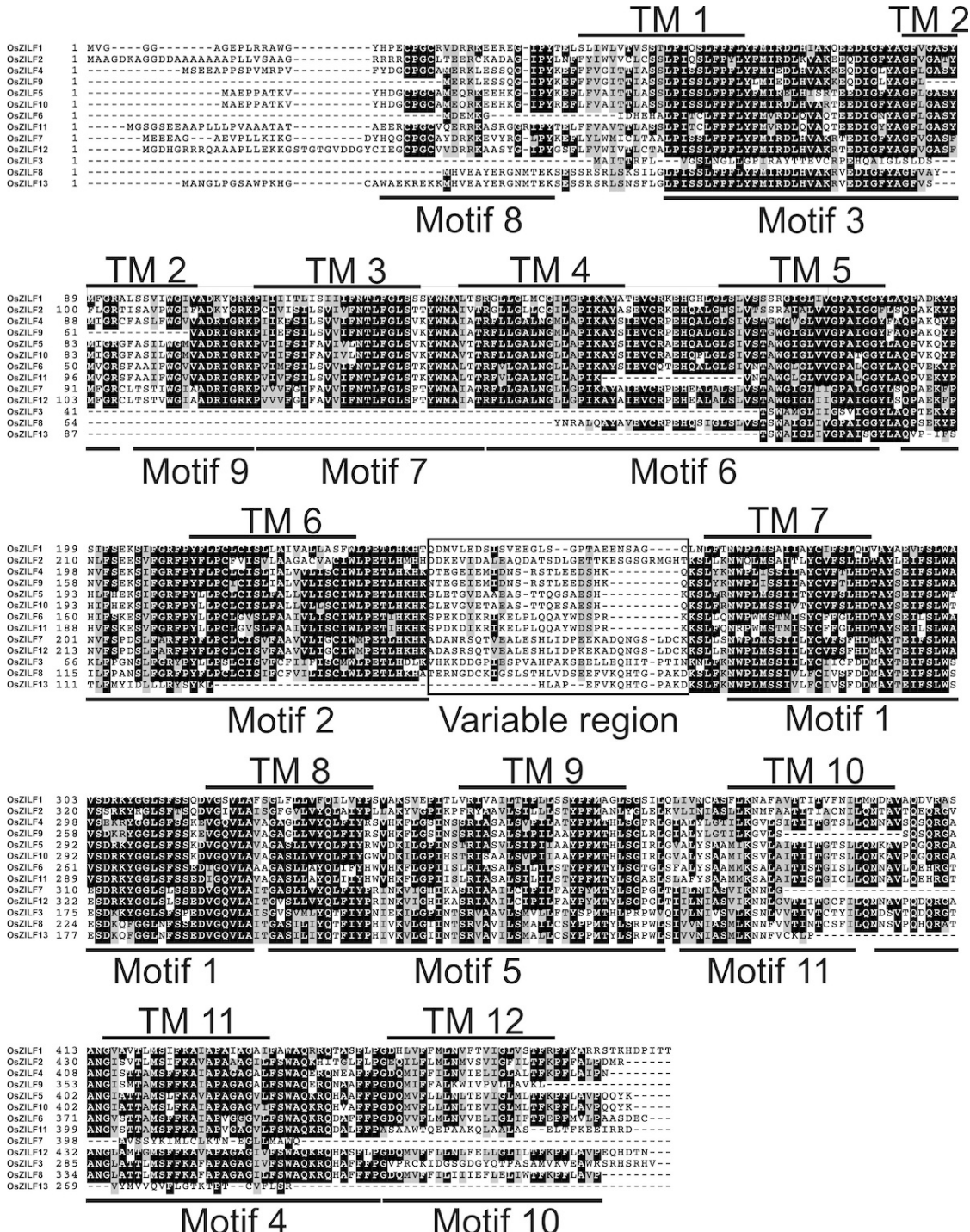
^c There is a sequence gap between the first and second positions.

^d Only the canonical MFS G-x(3)-D-[RK]-x-G-R-[RK] residues are highlighted.

^e Only the Antipporter S-x(8)-G-x(3)-G-P-x(2)-G-G residues are highlighted.

A**B**

Additional File 5. Chromosomal positions of ZIFL genes. Chromosomal positions of ZIFL genes in (A) *Oryza sativa*, *Sorghum bicolor* and *Brachypodium distachyon* chromosomes, and in (B) *Zea mays* chromosomes. Only ZIFL-containing chromosomes are shown. Non-ZIFL genes within ZIFL gene clusters were omitted.



Additional File 6. Alignment of OsZIFL protein sequences. Alignment was constructed using ClustalW. Conserved amino acids are marked in black or grayscale according to similarity level.

Additional File 7. Probes used in Genevestigator analyses and evaluation of specificity of rice ZIFL Affymetrix® microarray probes.

Gene	Probe	Specificity	Other match
LOC_Os01g16260	Os.10292.1.S1_at Os.39764.1.S1_at Os.39764.1.S1_x_at	Not unique Not unique Not unique	LOC_Os01g16250 LOC_Os01g16250 LOC_Os01g16250
LOC_Os01g17214	Os.17416.1.S1_at* OsAffx.22176.1.S1_x_at*	Unique (<i>OsZIFL2</i>) Unique	- -
LOC_Os07g08300	Os.16958.1.S1_at	Unique (<i>OsZIFL3</i>)	-
LOC_Os11g04020	Os.18707.1.S1_at	Not unique	LOC_Os12g03830
LOC_Os11g04030	Os.6142.1.S1_s_at	Unique (<i>OsZIFL5</i>)	-
LOC_Os11g04104	Os.18177.1.S1_at Os.9752.2.S1_x_at Os.9752.3.S1_x_at	Unique (<i>OsZIFL7</i>) Not unique Not unique	- LOC_Os12g03899 LOC_Os12g03899
LOC_Os11g04150	OsAffx.19478.1.S1_at OsAffx.19478.2.S1_s_at	Unique (<i>OsZIFL8</i>) Not unique	- LOC_Os12g03950
LOC_Os12g03830	No probe		
LOC_Os12g03860	Os.21635.1.S1_at	Unique (<i>OsZIFL10</i>)	-
LOC_Os12g03899	Os.9752.1.S1_a_at Os.9752.2.S1_x_at Os.9752.3.S1_x_at	Unique (<i>OsZIFL12</i>) Not unique Not unique	- LOC_Os11g04104 LOC_Os11g04104
LOC_Os12g03950	OsAffx.19478.2.S1_at OsAffx.19478.2.S1_s_at	Unique (<i>OsZIFL13</i>) Not unique	- LOC_Os11g04150

* Distinct probes for the same gene, with the same expression pattern.

Probes used in Figures 12 and 13 are indicated by the respective ZIFL gene names between brackets (third column).

Additional File 9: Gene-specific primers used for quantitative RT-PCR.

Gene name ^a	Forward Primer 5' → 3'	Reverse Primer 5' → 3'
<i>OsZIFL1</i>	GAAGAAGCACGAAGCACGAT	AAAAATGGGGTCTACATCAGA
<i>OsZIFL2</i>	GCCCTGGATTCTAACCTGCAA	TGGTTCGGAGTTCAAGACAGA
<i>OsZIFL3</i>	GATCTGGAGTTGTGCCAATA	TCATATGGCGAAGGAAAGAA
<i>OsZIFL4</i>	TGTGATTGAATTAATTGGACTTGC	GGGGTGCTATTCCAGCTTCT
<i>OsZIFL5</i>	TTGTAGCAGAGTGTAGAACATGC	GCAGAACAAAAAGAAGAACACC
<i>OsZIFL6</i>	TGCCCTTCTTCTTCAGGTG	GCCGCAGGTAAACACCATAAA
<i>OsZIFL7</i>	CTGTGAAGCGAAGGCATATAA	TATACAAGCATAAGGAGGTACCAA
<i>OsZIFL8</i>	ATCAAAGAGCAACCGCAAAT	CGAAAACAGAATGCCTGCTC
<i>OsZIFL9</i>	TGCCCTAAAATGGATTGTCC	CAATGTTGATCTGACCCCAA
<i>OsZIFL10</i>	TTACAGTGAGTAATAAGTATGGCTTG	AAAGCAGAACAAAATCCAACAGA
<i>OsZIFL11</i>	CCCTCTTCTTCAGCTTCA	TTAGTCCCAGCGTATCTCCT
<i>OsZIFL12</i>	CGCTGTGTGAAGCAAAGGTA	GCTTGATTCTTGGGACAGA
<i>OsZIFL13</i>	CTCAAGACCTTGGTTGTCCA	CCATGTACACCGGTAGTTGC

^a Gene names in bold are of *OsZIFL* genes which show expression in at least one qPCR experiment.

Capítulo 2

**Manuscrito a ser submetido para publicação ao periódico
Plant Physiology (Fator de Impacto JCR 2011 = 6.535)**

Elemental profiling of rice FOX lines leads to characterization of a new Zn transporter and uncovers a function for Zn accumulation in trichomes of *Arabidopsis thaliana*

Felipe K. Ricachenevsky¹, Tracy Punshon², Brett Lahner³, Elena Yakubova³, Maria Hindt², Danku J⁴, Sichul Lee², David E. Salt^{3,4}, Janette P. Fett^{1,5}, Mary Lou Guerinot^{2*}

¹Centro de Biotecnologia, Universidade Federal do Rio Grande do Sul, Brazil.

²Department of Biological Sciences, Dartmouth College, USA.

³Department of Horticulture and Landscape Architecture, Purdue University, USA.

⁴Institute of Biological and Environmental Sciences, University of Aberdeen, UK.

⁵Departamento de Botânica, Universidade Federal do Rio Grande do Sul, Brazil.

*** Corresponding author:** Dartmouth College, Department of Biological Sciences, Life Sciences Center, 78 College St. 03755, New Hampshire, United States.

Email: mary.lou.guerinot@dartmouth.edu.

Abstract

Iron (Fe) and zinc (Zn) are essential micronutrients for almost all living organisms. However, deficiencies of both elements impair proper development in both humans and plants. Rice (*Oryza sativa* L.) is the staple food for nearly half of the world's population, but a poor source of metals like Fe and Zn. In this context, biofortification is a very cost-effective solution for improvement of the nutritional quality of crops. To improve our knowledge on proteins related to metal homeostasis, we screened *Arabidopsis thaliana* lines expressing rice genes (rice FOX lines) by elemental profiling. Among the most interesting results, we found two lines with 25% higher Zn concentrations in shoots that express OsZIP7, a putative Fe/Zn transporter. OsZIP7 was shown to be localized at the plasma membrane and to transport Zn but not Fe or Cd in yeast mutant complementation assays. OsZIP7 expression in *A. thaliana* increased translocation of Zn from roots to shoots and sensitivity to high Zn in culture media. OsZIP7-expressing lines showed increased Zn concentrations in their seeds. We showed by synchrotron X-ray fluorescence (SXRF) that expression of OsZIP7 changed the dynamics of Zn accumulation at the base of trichomes. We demonstrated that Zn accumulation in trichomes occurs at the base of the trichome cell, and not at the subjacent socket cells. By performing high resolution imaging of sectioned trichomes, we showed that Zn is very likely to be accumulating at the extracellular spaces. By comparing natural accessions of *A. thaliana*, we showed that high Zn accumulation in trichomes is correlated with high Zn concentrations in leaves. These results indicate that in *A. thaliana*, contrary to Zn hyperaccumulators such as *A. halleri*, detoxification of excessive Zn in trichomes is a mechanism used for metal tolerance. Moreover, we demonstrated the feasibility of using heterologous expression of genes from crops in *A. thaliana* as a fast method for gene characterization.

1. Background

Iron (Fe) and zinc (Zn) are two essential micronutrients for plant nutrition and development. Fe is necessary in key reactions such as chlorophyll synthesis, electron transfer in chloroplasts and mitochondria and many others, while Zn is a catalytic or structural co-factor in a large number of enzymes and regulatory proteins, including transcription factors (Marschner 1995, Maret 2009). However, both can become toxic when in concentrations above a certain threshold: Fe participates in Fenton chemistry, generating reactive oxygen species, while Zn competes with other ions for binding sites (Briat 2002, Clemens 2001). Thus, plants have to maintain Fe and Zn concentration within a narrow range for proper function.

For humans, Fe deficiency is the most widespread mineral nutritional disorder, while Zn deficiency is the second. Anemia affects 30% or around 2 billion people worldwide (WHO - <http://www.who.int/nutrition/topics/ida/en/>) and conservative estimates suggest that 25% of the human population is at risk of becoming Zn deficient (Maret and Sandstead 2006). Most staple foods, including rice (*Oryza sativa*), present low concentrations of both Fe and Zn in edible tissues (Gómez-Galera et al 2010). A monotonous diet composed mainly of milled cereal grains is especially common among poor populations, and the majority of people suffering from micronutrient deficiencies live in poverty. Biofortification, the increase of mineral concentrations in edible portions of crops before harvesting, has been proposed as a cost-effective solution for micronutrient malnutrition (White and Broadley 2005). In agreement with that, the Copenhagen Consensus (<http://www.copenhagenconsensus.com>) has ranked food supplementation with Zn and fortification with Fe first and third as best cost-benefit balance solution for pressing challenges in the world, while biofortification ranked fifth (Gómez-Galera et al 2010).

In order to devise genetic manipulation strategies for increasing micronutrients concentrations in seeds, it is necessary to understand how plants uptake, distribute and store Fe and Zn within their tissues, and which proteins are involved in each step. Although we have learned much in the past few years about Fe and Zn homeostasis, most of the work has been done in the model plant *Arabidopsis thaliana* (for reviews, see

Conte and Walker 2011, Sinclair and Kramer 2012, Hindt and Guerinot 2012). Rice is one of the most important cultivated plants, and is the staple food for nearly half of the world's population (<http://www.fao.org/rice2004/en/rice-us.htm>). It is also a model organism, especially for monocots, with two varieties (*indica* and *japonica*) with fully sequenced genomes (Yu et al 2002, IRGSP 2005), several resources for gene and genome function characterization such as insertional mutants (Wang et al 2012), established transformation procedure (Sallaud et al 2003), and comprehensive cDNA collections (Kikuchi et al 2003). Although many tools are available, the speed of gene function characterization in rice is still slower compared to faster cycling plants, like *A. thaliana*. Recently, an *A. thaliana* collection of lines over-expressing rice genes (hereafter Rice FOX – Full-length Over-eXpressor Arabidopsis lines) was developed, comprising more than 30,000 independent lines (Kondou et al 2009, Sakurai et al 2011). These lines have been successfully used for characterization of genes associated with several processes in plants (Dobouzet et al 2011, Yokotani et al 2008, Yokotani et al 2009, Higuchi-Takeuchi et al 2011, Anders 2012, Albinsky et al 2010), but not to the regulation of the ionome.

The ionome is defined as all the mineral nutrients and trace elements found in an organism (Lahner et al 2003, Salt et al 2008). High-throughput elemental profiling in plants has become feasible recently, measuring element concentrations in tissues of mutagenized plants compared to their wild types or among natural variation (Lahner et al 2003, Baxter et al 2012) using mainly volume-averaged methods like inductively-coupled plasma mass spectrometry (ICP-MS; Salt et al 2008). ICP-MS screening has been successfully used to identify genes that regulate the ionome (Borghi et al 2011, Chao et al 2012). These methods, although highly reliable and of relative low-cost, lack the spatial resolution necessary to approach how plants control tissue or cell-specific element localization, as in the metal-enriched areas in trichomes of some species (Kupper et al 2000, Ager et al 2003, Sarret et al 2009). Trichomes from Arabidopsis species are non-glandular, unicellular structures that differentiate from epidermal cells. The function of non-glandular trichomes is water loss reduction, UV protection, reduction of photosynthesis through reflectance, and others (Wagner et al 2004, and references therein). Arabidopsis trichomes are also a model for *de novo* patterning and development,

and the genetic basis of trichome cell differentiation is being dissected for a long time (Ishida et al 2008, Grebe 2012).

Some authors have used synchrotron X-ray fluorescence (SXRF) and other synchrotron radiation-base techniques to explore metal localization in trichomes of the hyperaccumulator *A. halleri* (Kupper et al 2000, Zhao et al 2000, Sarret et al 2002, Sarret et al 2009) and of non-hyperaccumulators *A. lyrata* and *A. thaliana* (Ager et al 2003, Isaure et al 2006, Sarret et al 2009). SXRF is an alternative for spatially resolved quantification of elements that allow sub-ppm (parts per million - $\mu\text{g.g}^{-1}$) detection of transition metals at a spatial resolution of 100 nm (Punshon et al 2009). As examples, SXRF was used to identify the function of vacuolar iron transporter 1 (VIT1) and of Ca^{+2} transporters CAX1 and CAX3 in *A. thaliana* embryo and seed element localization (Kim et al 2006; Punshon et al 2012). It was also used to demonstrate differences in Zn accumulation in the hyperaccumulator *A. halleri* and the non-hyperaccumulator *A. lyrata* (Sarret et al 2009), and to show that Ni and Co-hyperaccumulator *Alyssum murale* uses different mechanisms to store exceeding metals within leaf tissues (Tappero et al 2007).

This work demonstrates the feasibility of using *Arabidopsis thaliana* heterologously expressing cDNAs for fast characterization of genes involved in regulation of the ionome. We functionally characterized a Zn plasma membrane transporter from rice that changes the dynamics of Zn accumulation in *A. thaliana* leaves. High resolution SXRF analyses of Zn accumulation in trichomes strongly suggest extracellular localization of the metal. Moreover, we established a correlation between trichome Zn accumulation and total Zn abundance using *A. thaliana* natural accessions, suggesting a detoxification mechanism based on trichome metal accumulation.

2. Results

2.1 Rice FOX lines selection

In order to make informed selection of Rice FOX lines, we first searched the rice genome (<http://rice.plantbiology.msu.edu/>) for all predicted proteins that have similarity to proteins described in the literature as having a role in Fe and Zn homeostasis in plants in the literature. This included the transporter families ZIP (Zinc-Regulated/ Iron-

Regulated Transporter Protein; Eide et al 1996), YSL (Yellow Stripe-Like; Inoue et al 2009, Lee et al 2009), ZIFL (Zinc-Induced Facilitator-Like; Haydon and Cobbett 2007, Ricachenevsky et al 2011), MTP (Metal Tolerance Protein; Gustin et al 2011), NRAMP (Natural Resistance Associated Macrophage Protein; Sasaki et al 2012), OPT (Oligopeptide Transporter; Stacey et al 2008) and VIT (Vacuolar Iron Transporter; Zhang et al 2012). We also searched for other proteins with a role in metal homeostasis, as FER (Ferritins; Stein et al 2009), PCS (Phytochelatin Synthase; Brunetti et al 2011), transcription factors of the NAC stress-related subfamily (Nuruzzaman et al 2010, Sperotto et al 2009) and IRO2 (Ogo et al 2006), enzymes of the phytosiderophore biosynthetic pathway (Deoxymugineic acid synthase – DMAS; Bashir et al 2006), and genes that, when mutated in *A. thaliana*, changed the ionomics profile (www.ionomicshub.org; Baxter et al 2007). All rice gene products showing at least 30% similarity with query sequences were compiled and used as query to search the Rice FOX Database (<http://ricefox.psc.riken.jp/>; Sakurai et al 2011). The lines found that contain one of the query genes were selected for further analyses. The complete set had 51 lines and 30 genes, from 16 different gene families (Supplemental Table 1).

2.2 Elemental analysis of Rice FOX lines

In order to gain information about the changes in ionomics profile caused by the expression of a rice transgene, all lines had the elements Li, Mg, P, S, K, Ca, Fe, Co, Ni, Cu, Zn, As, Rb, Sr, Mo, and Cd quantified by ICP-MS in leaves after 6 weeks of growth. It should be noted that plants analyzed were T2 seeds, meaning they are expected to segregate the transgene. However, effects on the ionome should be dominant considering they are caused by the transgene and not by insertion into *A. thaliana* genome. We observed several statistically significant differences in elemental accumulation, either increasing or decreasing its concentrations (Table 1). As for many genes we have independent lines, we were interested in alterations that were (1) statistically significant, (2) consistent between two or more lines expressing the same transgene, and (3) greater than 20%. As examples, three lines expressing OsVIT2 showed a consistent 29% to 44% decrease in As accumulation, while two lines expressing OsPCS1 showed 20% to 24% increase in Cd (Table 1). Interestingly, two lines expressing OsZIP7 showed a consistent

25% increase in Zn concentration (Fig 1). As we were focusing in putative Fe and Zn transporters, we decided to further characterize this gene.

2.3 OsZIP7 can complement yeast cells defective in Zn uptake

To determine which metals OsZIP7 transports, we expressed its full-length coding sequence in different yeast strains. When introduced in the Zn uptake-defective *zrt1zrt2* mutant, OsZIP7 was able to rescue growth in low Zn media to the same extent as the positive control AtIRT1 (Fig. 2A). However, in the Fe uptake-defective strain *fet3fet4*, OsZIP7 did not restore growth in low Fe media (Fig. 2B), indicating that OsZIP7 transports Zn but not Fe. This is in contrast with a previous report that showed OsZIP7 as a Fe transporter (Yang et al 2009). Also, we transformed the wild-type strain BY4743 and tested whether OsZIP7 transports Cd. When growing in media containing 20 µM Cd, both OsZIP7 and empty vector-transformed yeast were able to grow, while AtIRT1-transformed cells did not grow well. This phenotype was even stronger in media containing 50 µM Cd (Fig 2C). Therefore, we concluded that OsZIP7 transports Zn but not Fe or Cd in yeast.

2.4 OsZIP7 is localized to the plasma membrane in *A. thaliana* protoplasts

An OsZIP7-YFP construct was generated to determine the subcellular localization of OsZIP7. *A. thaliana* protoplasts were either transfected with OsZIP7-YFP alone or co-transfected with AHA2-RFP. As shown in Fig 3, YFP signal was observed in a pattern that indicated plasma membrane localization. When co-transfected with AHA2-RFP construct, a known plasma membrane protein (Kim et al 2001), YFP and RFP signals were co-localized (Fig 3). As OsZIP7 complemented *zrt1zrt2* mutant, which lacks two ZIP plasma membrane transporters (MacDiarmid et al 2000), plasma membrane localization is in agreement with the yeast complementation assays.

2.5 Expression of OsZIP7 in *Arabidopsis* leads to enhanced Zn sensitivity and disruption of Zn root-to-shoot partitioning

To gain more information on OsZIP7 function, we tested the two independent lines in media containing Zn at toxic levels. When OsZIP7-over-expressing (OE) lines

were grown at control conditions, we observed similar growth compared to their segregating wild types (WT; Fig 4A). However, at 100 μ M Zn, both lines started to show decreased growth. At 200 μ M Zn, OsZIP7-OE lines are stunted, with short roots and small shoots (Fig 4A). We also quantified root length and shoot fresh weight of WT and OsZIP7-OE lines. Root length was 30-35% decreased in OsZIP7-OE lines in both 100 μ M and 200 μ M Zn, while shoot fresh weight was about 40% decreased in 100 μ M Zn and 60-65% in 200 μ M Zn (Fig 4B and 4C).

Roots and shoots of WT and OsZIP7-OE plants grown at control conditions, 50 μ M (the highest non-toxic Zn condition), 100 μ M or 200 μ M were analyzed by ICP-MS. In shoots, Zn concentration was slightly but significantly higher in OsZIP7-OE plants in all Zn concentrations, except in control conditions (Fig 5A). However, the opposite effect was observed in roots, where Zn concentration was lower in OsZIP7-OE plants compared to WT in all concentrations except for control conditions (Fig 5B). In 200 μ M Zn, OsZIP7-OE Zn concentrations were around 40% of WT. When we compared the shoot-to-root ratio, it was clear that OsZIP7 expression was leading to increased root-to-shoot translocation of Zn (Fig 5C), indicating that correct Zn partitioning in OsZIP7-OE plants is lost. Interestingly, OsZIP7 expression-derived Zn accumulation also led to changes in Fe concentrations, as roots of OsZIP7-OE plants accumulated more Fe at 100 μ M and 200 μ M Zn, and shoots at 200 μ M Zn (Supplemental Fig 1).

2.6 Seeds of plants expressing OsZIP7 accumulate more Zn

As Zn shoot/root partitioning changed in plants expressing OsZIP7, we asked what would be the effect of the transgene on seed Zn concentration and localization within the seed tissues. We first used synchrotron X-ray fluorescence (SXRF) microtomography to directly visualize metals in the seeds. Zn was clearly more abundant in OsZIP7-OE seeds compared to WT, and the distribution pattern was very similar (Fig 6A). Localization of K, Ca, Mn, Fe and Cu was also unchanged, with slight variations (Fig 6B). To confirm these results, we performed ICP-MS elemental quantification of WT and OsZIP7-OE seeds. Zn concentrations in seeds of both OsZIP7-OE lines were 20-25% higher than in WT (Fig 6C). The magnitude of increase in seeds is similar to what was observed in leaves of soil-growing plants (Fig 1). We also observed a small but

consistent decrease in Cd concentration, a trait that is desirable for biofortification purposes (Supplemental Fig 2). All other elements were either unchanged or inconsistently changed in only one line, in agreement with a Zn-specific transport activity of OsZIP7. These results demonstrate that OsZIP7 expression in *A. thaliana* increased Zn concentration in seeds.

2.7 OsZIP7 constitutive expression leads to alteration in Zn dynamic accumulation in leaves

We used SXRF 2D mapping of leaves of WT and OsZIP7-OE plants. In all experiments, we compared the detached 7th true leaf of each plant grown under the same conditions of the previous experiment (Fig 4). When grown under control conditions, in WT Zn was evenly distributed throughout the leaf surface, except for higher concentrations areas in hydathodes and closer to the petiole detachment site (Fig 7A). Differently, in OsZIP7-OE Zn was observed in highly concentrated small areas, in a punctuated pattern at the leaf surface. When Zn maps were overlaid with Ca maps, which accumulate in trichome papillae (Esch et al 2003), it was clear that Zn was accumulating at the base of trichomes in leaves of OsZIP7-OE plants (Fig 7B). When plants were grown on media with 50 μ M or 100 μ M Zn, the punctuated pattern associated with the base of trichomes was observed in both WT and OsZIP7-OE leaves (Fig 7C-7F). Interestingly, Zn abundance appeared to be slightly higher in each trichome base on OsZIP7-OE leaves compared to WT in both conditions. Furthermore, the trichome-less *glabra-1* mutant (Hülskamp et al 1994) leaf of plants growing at the same conditions in all Zn concentrations showed an evenly distributed Zn pattern, confirming the association of Zn concentration areas with trichomes (Fig 7).

Next, we used region of interest (ROI) analysis to quantify the total Zn abundance per trichome in each mapped leaf. The OsZIP7-OE leaf from control conditions has the lowest Zn abundance per trichome (Fig 8). When comparing WT and OsZIP7-OE leaves from plants growing at 100 μ M Zn, trichomes of the OsZIP7-OE had higher Zn abundances (Fig 8). In leaves of plants growing at 50 μ M Zn, the difference was not statistically significant; however, the distribution of Zn abundances clearly showed more trichomes with high Zn abundance in OsZIP7-OE than in WT (Fig 8). These results

showed that OsZIP7 expression in *A. thaliana* leaves lead to alterations in Zn accumulation dynamics at the base of trichomes.

2.8 High resolution SXRF imaging of trichomes suggest extracellular Zn localization in trichome cells

To gain more information on the site of high Zn accumulation at the base of trichomes, we used high-resolution SXRF 2D mapping of fresh trichomes. Plants growing at 50 μ M Zn were chosen because both WT and OsZIP7-OE leaves accumulate Zn in trichomes under these conditions (Fig 7C and 7D). Imaging of WT trichome showed that Zn was accumulating in a ring-shaped pattern around the base of the trichome (Fig 9A and 9B). In OsZIP7-OE trichome, the Zn ring was also evident, but Zn accumulation was also observed up the trichome stalk (Fig 9C and 9D). These results suggested that Zn was accumulating from the base region towards the upper region of the trichome. Although the experiment was performed in media amended with enough Zn that plants would accumulate the metal in trichomes but low in other micronutrients, high resolution imaging allowed the visualization of Fe, Cu and Mn at the base of trichomes (Supplemental Fig 3A-F). This indicates that other metals might be accumulated at the same site as Zn, possibly using a similar mechanism.

Next, we asked if the trichome cell or the surrounding socket cells at the base of the trichome were the ones accumulating Zn. To answer that question, we used SXRF to map longitudinally sectioned leaves of OsZIP7-OE plants growing on control or 50 μ M Zn, including the trichome base. In the control leaf, the trichome cell showed the highest abundance of Zn, compared to socket cells or epidermal cells (Fig 10B). In 50 μ M Zn leaf trichome, we expected to observe an order of magnitude higher Zn abundance, based on our previous experiment (Fig 7A and 7C). Clearly, the trichome cell showed markedly higher Zn abundance, while socket cells and epidermal cells had only marginal variations (Fig 10C-E), demonstrating that the trichome single cell is the site of Zn accumulation. When we decreased the maximum pixel abundance scale to see low count pixels, we observed stretches containing low Zn abundance inside the trichome cell, indicating the possible localization of the cytoplasm (Gutierrez-Alcala et al 2000; Fig 10E). This

indicates that the high Zn accumulation site is the apoplast of the trichome, and not inside the cell.

2.9 Variations in leaf Zn concentration change accumulation at the base of trichomes in *A. thaliana* natural accessions

Our previous experiments showed that OsZIP7 expression in *A. thaliana* led to increased Zn concentration in leaves, as well as higher Zn accumulation at the base of trichomes (Fig 5 and Fig 7). We then asked if the ability to accumulate varying Zn concentration in leaves would also affect Zn abundance in trichomes of these leaves. To test our hypothesis, we first compared data for Zn concentrations in leaves of 349 *A. thaliana* natural accessions at the iHub database (www.ionomicshub.org; Baxter et al 2007), and selected the accessions with highest and lowest Zn concentrations as measured by ICP-MS. We mapped leaves of the accessions with the highest and the lowest Zn concentrations, Kn-0 and Fab-2, respectively (Fig 11, Table 2). Col-0 was also included as a reference accession. We observed that Fab-2 leaf had several trichomes with no Zn, and some with very low Zn abundance (Fig 11C and 11D). On the other hand, Kn-0 showed higher Zn abundance in its trichomes when compared to Col-0 (Fig 11A, 11B, 11E and 11F). We confirmed these observations by performing ROI analyses of the trichome base region in each leaf (Fig 11G).

Next, we mapped another 13 accessions within the list of ten highest or lowest Zn concentrations in leaves, analyzing a total of 16 accessions (Table 2). By using ROI analyses, we were able to determine the percentage of Zn, from the total found in each leaf, that was at the base of trichome or elsewhere at the leaf surface. When we correlated the mean counts per pixel (an indicator of leaf Zn concentration) with the percentage of Zn in trichomes, we saw a strong positive correlation between the two variables (Fig 12). These results show that *A. thaliana* accessions with higher Zn concentrations in leaves accumulate more Zn at the base of trichomes, which in turn suggest that translocation of Zn to trichomes might have a role in Zn detoxification.

3. Discussion

3.1 Coupling Rice FOX lines and ionomics profiling is a fast method for molecular characterization of metal-related genes from rice

Several proteins have been described as having a role in metal homeostasis in plants, including transporters, transcription factors and enzymes (for a review, see Conte and Walker 2011, Hindt and Guerinot 2012, Sinclair and Kramer 2012). However, most was done in the model plant *A. thaliana*, leaving many genes from crops with no molecular function assigned. There is a pressing need to translate the information from models to agronomically important plants. In rice, an important crop and a model for monocots with several available resources for functional genomics (Wang et al 2012), there are still many proteins with unknown function.

Rice FOX lines were already successfully used to describe proteins that confer resistance to fungal and bacterial pathogens (Dobouzet et al 2011), tolerance to abiotic stresses (Yokotani et al 2008, Yokotani et al 2009), enzyme characterization (Higuchi-Takeuchi et al 2011, Anders 2012) and in metabolomics profiling (Albinsky et al 2010). Our work highlights the feasibility of using the Rice FOX lines ionomics profiling for characterization of metal-related genes from heterologous systems. Our screen shows examples of interesting proteins, such as OsPCS1, that might be studied in depth to understand their role in the regulation of the ionome. As constitutive expression of a gene in a heterologous system may overcome regulatory mechanisms that might modulate protein activity (i.e., post-transcriptional regulation) or put the protein in a different environment, it could lead to previously uncharacterized roles for known proteins. One possible example is OsVIT2, a vacuolar Fe, Zn and Mn transporter (Zhang et al 2012): three FOX lines showed a consistent decrease in As (Table 1), which raises the possibility that OsVIT2 might have a role in As transport. Although that could be a side effect, more comprehensive screens with Rice FOX lines show potential for interesting new findings. As a proof-of-concept, we described in detail one transporter that increased Zn concentrations in leaves, OsZIP7.

3.2 OsZIP7 is a Zn influx plasma membrane transporter

Described ZIP proteins in plants are mostly localized to the plasma membrane (Ishimaru et al 2005, Ishimaru et al 2006, Lin et al 2009, Lee et al 2010a, Lee et al

2010b), as was observed for OsZIP7. There are only a few exceptions: AtIRT2, localized to intracellular punctate bodies in protoplasts (Vert et al 2009), and the founding member of the ZIP family AtIRT1, recently described as being localized at the trans-Golgi network/early endosomes, cycling between the plasma membrane to transport cations and the vacuole for turnover (Barberon et al 2011). ZIP transporters are also known for having variable substrate specificity. AtIRT1 is able to transport Zn^{+2} , Fe^{2+} , Mn^{2+} , Cd^{2+} , Co^{2+} , Ni^{2+} and Fe^{3+} (Korshunova et al 1999) while its rice ortholog OsIRT1 transports Fe^{2+} , Zn^{2+} and Cd^{2+} at least (Ishimaru et al 2006, Lee and An 2009). AtIRT2 and AtIRT3 transport Fe^{2+} and Zn^{+2} , but not Mn^{2+} or Cd^{2+} (Vert et al 2001, Lin et al 2009). Others like OsZIP4, OsZIP5 and OsZIP8 appear to be Zn-specific transporters (Ishimaru et al 2005, Lee et al 2010a, Lee et al 2010b).

OsZIP7 was reported earlier as an Fe transporter with no ability to transport Zn, based on complementation of the Fe uptake yeast mutant *fet3fet4* (Yang et al 2009). However, our results clearly showed that OsZIP7 is a Zn transporter that does not transport Fe. Expression of OsZIP7 in *A. thaliana* led to alteration in sensitivity to Zn excess, changes in Zn accumulation in leaves and seeds. Although it is known that *A. thaliana* plants physiologically respond to Fe status without noticeable alteration in Fe concentrations (Baxter et al 2008), based on our yeast mutant complementation assays, it is very unlikely that OsZIP7 has Fe transport activity.

OsZIP7 expression in *A. thaliana* led to increased translocation of Zn to the shoots (Fig 5). ZIP transporters generally transport metal from the extracellular space into the cytoplasm. In the hyperaccumulator *A. halleri*, increased root-to-shoot translocation is caused by triplication and stronger promoter activity of the Zn efflux transporter HMA4, which results in extra xylem loading of Zn (Hanikenne et al 2008). In addition, it is also known that several ZIP genes are highly expressed in *A. halleri* roots compared to the non-hyperaccumulator *A. thaliana* (Talke et al 2006), indicating that both uptake and xylem loading are more efficient in the hyperaccumulator *A. halleri*. Heterologous expression of OsZIP7 under the control of a constitutive promoter is probably increasing Zn uptake in roots, and *A. thaliana* orthologs HMA4/HMA2 (Hussain et al 2004) proteins may be loading the metal in the xylem. As the genetic structure necessary for Zn tolerance of *A. halleri* that includes the vacuolar Zn detoxification protein MTP1

(Shahzad et al 2010) is not present in *A. thaliana*, Zn becomes toxic when in high concentration in media for OsZIP7-OE plants due to high Zn translocation to shoots.

Yang et al (2009) showed that OsZIP7 expression is induced by Fe deficiency in rice using a semi-quantitative RT-PCR method (Yang et al 2009). However, microarray-based data showed that OsZIP7 was induced by Zn deficiency (Ishimaru et al 2005, Ishimaru et al 2007, Widodo et al 2010) and inhibited by Fe deficiency (Zheng et al 2009, in their Supplemental Table 1) in roots and shoots of rice plants. OsZIP7 was found highly expressed in shoots of rice plants over-expressing OsZIP4 (Ishimaru et al 2007). OsZIP4-OE plants accumulate high concentrations of Zn in roots, but are severely Zn-deficient in shoots (Ishimaru et al 2007), again suggesting that OsZIP7 expression is responsive to Zn concentration. Taken together, the evidence suggests that OsZIP7 expression is driven by the Zn status in both roots and shoots.

3.3 Zn accumulates at the base of trichomes in *A. thaliana*, possibly at the extracellular space

We demonstrated that *A. thaliana* accumulates Zn at the base of the trichome in leaves. It has been known that trichomes accumulate several different elements, like Pb, Zn and Cd in *Nicotiana tabacum* (Martell 1974, Sarret et al 2006, Isaure et al 2010), Cd in *Brassica juncea* (Salt et al. 1995), Mn in *Helianthus annuus* (Blamey et al. 1986), Ni in the Ni-hyperaccumulator *Alyssum lesbiacum* (Kramer et al. 1997, Küpper et al 2001). In the Zn hyperaccumulator/hypertolerant *A. halleri*, it was extensively shown that the base of trichomes accumulates the highest concentrations of Zn in leaves (Küpper et al 2000, Zhao et al 2000, Sarret et al 2002, Sarret et al 2009). Despite the high concentrations, trichomes do not account for the majority of Zn in leaves: a comparison with non-hyperaccumulator *A. lyrata* showed that Zn in trichomes of *A. halleri* are 10% of the total, while *A. lyrata* trichomes have 20% (Sarret et al 2009). These data agree with our findings in *A. thaliana*, ranging from 4% to 23% (Fig 12).

We found that Zn accumulates mostly at the base of the trichome cell and not at subjacent socket cells (Fig 10). Localization in the trichome cell is more obvious in *A. halleri*, as the ring is localized more distally on the trichome stalk (Küpper et al 2000, Sarret et al 2009). In *A. lesbiacum*, Ni has similar distribution along the stalk, and it is

suggested that they could be inside the vacuoles (Küpper et al 2001). SXRF mapping of *A. halleri* leaves also led to the suggestion that vacuoles are the main storage site of Cd and Zn, based on observed shrinkage of the Cd/Zn-rich areas that would be due to vacuole water loss (Hokura et al 2006). However, our results of SXRF on intact, fresh trichomes of WT and OsZIP7-OE leaves showed Zn in a ring shape at the base of trichome and going towards the stalk (Fig 9). This Zn distribution is more consistent with an extracellular than a vacuolar localization, which would presumptively give a more round, U-bottom shaped, filled with Zn image, and not as ring-shaped as observed. In agreement with that, sectioned trichomes showed Zn at edges of the cell (Fig 10), suggesting again that Zn is at the apoplastic space.

Another possible explanation is that the Zn localization observed in sectioned trichomes is cytoplasmic, where the cytoplasm would be compressed against the cell wall by the vacuole. That seems unlikely, as cytoplasm would show stretches crossing the central vacuole besides a thin peripheral layer adjacent to the cell wall (Gutierrez-Alcalá et al 2000). It is possible to see cytoplasm-resembling stretches in some sections that do not match the high Zn areas (Fig 10D and 10E). Moreover, the high Zn areas are also observed at the interface of the trichome with mesophyll and socket cells, and at the superior side of socket cells (Fig 10D and 10E). We would expect a more confined distribution within the trichome if Zn accumulation was inside the cell.

Previous work has shown that Cd accumulating at the base of trichomes was predominantly bound to O and N ligands in both *A. thaliana* and *A. halleri* (Isaure et al 2006, Fukuda et al 2008). Based on that, these authors proposed that Cd is associated with the cell wall in trichomes (Isaure et al 2006). In *A. halleri*, Zn was also shown to bind mainly to carboxyl and/or hydroxyl groups (Sarret et al 2002). Moreover, phosphate, thiol and silanol groups can be excluded as Zn ligands (Sarret et al 2009). These results, together with our observations, strongly suggest that Zn observed in the apoplastic space is bound to the cell wall in *A. thaliana* trichomes. Moreover, it is interesting to note that the non-hyperaccumulator *A. lyrata* has more Zn bound to cell wall (40% of the Zn in trichomes) compared to hyperaccumulator *A. halleri* (20%; Sarret et al 2009).

3.4 Trichomes might have a role in metal detoxification

In this work, we have shown that natural accessions of *A. thaliana* accumulate varying abundances of Zn in their trichomes (Fig 11). We have also demonstrated that this is correlated with Zn concentration in leaves: the more Zn an accession accumulates in the whole leaf, the more Zn is accumulated in trichomes (Fig 12). These data indicate that trichome metal accumulation might have a role in metal detoxification in *A. thaliana*.

Sarret et al (2009) showed, when comparing leaf SXRF maps of hyperaccumulator *A. halleri* and non-hyperaccumulator *A. lyrata*, that both species have high Zn accumulation at the base of trichomes. However, Zn concentration in mesophyll cells increases 30-fold upon exposure of *A. halleri* plants to high Zn media, whereas trichomes concentration increases by 3-fold. It was also shown that Zn accumulates more in the mesophyll in *A. halleri* compared to veins, whereas the opposite is observed in *A. lyrata* (Sarret et al 2009). These results indicated that, despite their high Zn concentrations, trichomes are not responsible for the Zn hyperaccumulation/hypertolerance traits in *A. halleri*. In tobacco (*Nicotiana tabacum*), the role of trichomes in heavy metal excretion was well documented, showing that both Zn and Cd are secreted from trichome heads in 20-150 μm crystallized grains, where metals are present in Ca-containing compounds (Choi et al 2001, Sarret et al 2006, Isaure et al 2010). However, these glandular, multicellular trichomes, are very different from the unicellular, non-glandular trichomes as found in *Arabidopsis* species (Yang and Ye 2012).

In *A. thaliana*, it has already been shown that Cd and Mn accumulate at the base of trichomes (Ager et al 2003, Isaure et al 2006). Interestingly, it was also shown that, in transgenic lines that accumulate varying concentrations of Cd, trichome concentrations vary in a similar way: the more Cd in leaves, the more Cd in trichomes (Ager et al 2003). As only two lines were analyzed, no correlation analysis was performed. This is consistent with what we observed for Zn in trichomes of natural accessions (Fig 11 and Fig 12).

In a recent work, Huguet et al (2012) found that *A. halleri* trichomes accumulate Cd as shown by ^{109}Cd autoradiography. Cd-enrichment in trichomes was clearly visible at three weeks of exposure time, but after nine weeks, they could hardly be observed on the autoradiographs. These data were interpreted as Cd being first accumulated in trichomes,

reaching a plateau, and increasing continuously in concentration in leaf tissues. As a consequence, trichomes would not be distinguished in autoradiographs from older leaves (Huguet et al 2012). They suggest that Cd sequestration in trichome cells could be a short-term response to metal excess, which becomes marginal upon continuous exposure, when leaf tissue genes controlling hyperaccumulation/hypertolerance traits would be necessary (Huguet et al 2012). In agreement with that, *A. lyrata* was shown to have more Zn (20%) than *A. halleri* (10%) in trichomes (Sarret et al 2009). Thus, trichome Cd sequestration and possibly detoxification might be more important in the non-tolerant and non-accumulators *A. thaliana* and *A. lyrata*.

Based on our findings, we propose that, differently from what is seen in hyperaccumulators, trichome Zn accumulation is important to avoid metal toxicity in leaves of the non-hyperaccumulator species *A. thaliana*. As the concentrations found in the environment by *A. thaliana* are much lower than for *A. halleri*, the short-term buffering capacity of trichomes would be enough for Zn not to accumulate in excessive concentrations in leaf cells. Zn abundance in trichomes appears to be more related to total leaf concentrations than with genetic background driven trichome cell-specific accumulation. In *B. juncea*, experiments where mass flow is decreased by application of ABA to induce stomata closure showed that Cd accumulation in leaves is dependent of transpiration, although root uptake is not affected (Salt et al 1995). This raised the question whether metal accumulation in trichomes is dependent on transpiration rates. In this model, transpiration would be driving Zn to trichomes, and leaves with higher concentration simply would have more Zn to be transported by mass flow. However, we observed differences in the percentage of the total Zn that is found in trichomes (Fig 12). If the genotype was controlling total leaf Zn concentration and mass flow was controlling trichome accumulation, we would expect similar percentages from total Zn in trichomes even if the absolute number differed. As this is not the case, an active transport mechanism should be driving Zn accumulation in trichomes, possibly carried out by a broad spectrum transporter.

4. Materials and Methods

4.1 Plant materials and growth conditions

For ionomics profile screening, Rice FOX lines and Col-0 wild-type seeds were sown on moist soil (Promix; Premier Horticulture, Québec, Canada) with non-essential elements (As, Cd, Co, Li, Ni and Se) added at subtoxic concentrations in a 20-row tray. After three days at 4°C for stratification, trays were kept in a climate-controlled with 10 hours of light ($90 \mu\text{mol.m}^{-2}\text{s}^{-1}$)/14 h dark, humidity of 60% and temperature ranging from 19 to 22°C. Twelve plants of each genotype, including wild-type Col-0, were cultivated for 6 weeks, and were bottom-watered twice a week with modified 0.25X Hoagland solution in which Fe was replaced by 10 μM Fe-HBED ($\text{N,N}'\text{-di(2-hydroxybenzyl)ethylenediamine-N,N}'\text{-diacetic acid monohydrochloride hydrate}$; Strem Chemicals, Inc., Newburyport, MA, USA).

For growth in axenic conditions, seeds were sterilized for 15 minutes in 25% and 0.05% SDS, washed 5 times in sterile H_2O and stratified at 4°C for three days. Sterile 0.1% agar was used to suspend seeds and sow using a pipette in full strength Gamborg's B5 media with vitamins, 1mM MES (2-(N-morpholino)ethanesulfonic acid), 2% sucrose and 0.6% agar. After 5 days, seedlings were transferred to minimal media containing 2 mM MES, 2 mM $\text{Ca}(\text{NO}_3)_2 \cdot 4\text{H}_2\text{O}$, 0.75 mM K_2SO_4 , 0.65 mM $\text{MgSO}_4 \cdot 7\text{H}_2\text{O}$, 0.1 mM KH_2PO_4 , 10 μM H_3BO_3 , 0.1 μM MnSO_4 , 50 nM CuSO_4 , 5 nM $(\text{NH}_4)_6\text{Mo}_7\text{O}_{24}$ and 50 μM Fe-EDTA. ZnSO_4 was added to a final concentration of 50 nM in control conditions, or at indicated concentrations. Seedlings were analyzed after 15 days of growth and plates were kept at 22°C with 16 hours of light/ 8 hours of dark in growth chambers.

For ICP-MS analyses of seed samples, plants were grown on soil in a growth room at 22°C with 16 hours of light/ 8 hours of dark, and bottom-waterted until maturity. Five plants of each genotype had their seeds collected and analyzed by ICP-MS as above.

4.2 Elemental analyses by ICP-MS

Elemental concentration analyses in leaf samples of Rice FOX lines were performed as described (Lahner et al 2003). One to two leaves (~2 to 4 mg dry weight) were harvested from *A. thaliana* plants grown for 6 weeks, leaves were rinsed with 18 MΩ water and placed into Pyrex digestion tubes. Samples were placed into an oven at 92°C to dry for 20 hours. Subsequently, all samples were digested with 0.7 ml

concentrated nitric acid (OmniTrace; VWR Scientific Products) and diluted to 6.0 ml with 18 MΩ water. After samples and controls were prepared, elemental analysis was performed with an ICP-MS (Elan DRCe; PerkinElmer) for Li, B, Na, Mg, P, K, Ca, Mn, Fe, Co, Ni, Cu, Zn, As, Se, Mo and Cd. All samples were normalized to calculated weights, as determined with a heuristic algorithm using the best-measured elements, the weights of seven weighed samples and the solution concentrations, detailed at www.ionomicshub.org. Data was normalized across different trays using Col-0 samples, present in each tray as a control. Percentage of difference for each element was obtained comparing medians of each element in each genotype to Col-0 median from the same tray. All data is publicly available at www.ionomics.org for download.

For ICP-MS analyses of shoots and rootsof axenically grown plants, metals were desorbed from samples on ice with cold 5 mM CaSO₄, 1 mM MES, pH 5.7, for 10 min, cold 5 mM CaSO₄, 10 mM EDTA, 1 mM MES, pH 5.7, for 5 min, then washed twice with cold ultrapure water (Haydon et al. 2012). Samples processing was performed as above. Five samples ($n = 5$) for each genotype in each condition were analyzed, as each sample was composed of a pool of 54 plants (for OsZIP7-OE lines under 200 μM) or 18 plants (for all other plants).

4.3 Protoplast preparation and subcellular localization

For protoplast preparation, *A. thaliana* Col-0 plants were grown in soil in a growth chamber at 22°C with 12 hours of light/ 12 hours of dark. After a month, around 25 leaves were detached and had their abaxial epidermis removed following digestion by the tape-sandwich method (Wu et al 2009). Macerozyme and cellulase treatment and protoplast recovery were performed as described (Yoo et al 2007).

For subcellular localization, the OsZIP7 coding sequence lacking the stop codon was amplified using specific primers (Supplementa Table 2) and cloned in pENTR/D-TOPO entry vector. Subsequently, LR recombination was performed into a vector containing a C-terminal fusion with YFP, pEarleyGate101, generating pEarleyGate101-OsZIP7. High concentrations of the final construct were prepared using PureYield™ Plasmid Midiprep from Promega®. AtAHA2-RFP construct (Kim et al 2001) was used as plasma membrane localization control.

Protoplast transfection was performed as described (Yoo et al 2007). Because of the large size of pEarleyGate101-OsZIP7 construct, 20 µg of DNA were used. For AtAHA2-RFP, standard 10 µg were used. For visualization of YFP and RFP signals after 16-20 hours, we used a Nikon Eclipse Ti inverted microscope stand, and image capture and processing was performed with Nikon Elements software.

4.4 Yeast mutants complementation

For yeast complementation experiments, a full-length version of OsZIP7 was amplified using specific primers (Supplemental Table 1) and cloned into pDR195 vector using XhoI and BamHI sites. As a control, AtIRT1 was amplified and cloned into pDR195 using XhoI and BamHI sites as well.

Yeast strains DY1457 (MAT_a ade6 can1 his3 leu2 trp1 ura3), ZHY3 (MAT_a ade6 can1 his3 leu2 trp1 ura3 zrt1::LEU2 zrt2::HIS3) and DEY1453 (MAT_{a/MAT_a} ade2/ADE2 can1/can1 his3/his3 leu2/leu2 trp1/trp1 ura3/ura3 fet3-2::HIS3/fet3-2::HIS3 fet4-1::LEU2/fet4-1::LEU2) were grown in YPD media pH 5.3 (DEY1453 was grown in pH 4 to increase Fe availability) and transformed with pDR195, pDR195-OsZIP7, or pDR195-AtIRT1 by the LiOAc/PEG (Gietz and Schiestl 2007). Selection of transformants was performed in SD media without uracil (SD – ura: 6.7 g/L yeast nitrogen base without amino acids, supplemented with 2% glucose, 0.1% casamino acids, 0.01% adenine, and 0.01% tryptophan), pH 5.3. Colonies were grown overnight in liquid SD -ura media, diluted to OD₆₀₀ 1.0, 0.1, 0.01 and 0.001, and spotted onto plates. For Cd toxicity test, SD -ura was amended with CdCl₂ in given concentrations. For Zn deficiency test, no Zn was added, and 10 µM ZnCl₂ was added to control plates. For Fe deficiency test, pH was raised to 6.0, and compared to control plates at pH 5.3. Pictures were taken after 3 to 5 days of growth.

4.5 Preparation of samples for high-resolution two-dimensional SXRF raster scanning of trichomes

The 7th true leaf of 20 days-old plants grown in MM 50 µM Zn were placed in fixative solution (a mixture of 3% glutaraldehyde and 4% paraformaldehyde in 0.4 M sodium cacodylate) under gentle vacuum overnight. Samples were rinsed in a solution of

0.2 M sodium cacodylate and 2.5 mM CaCl₂, pH 7.2, followed by distilled water, and then dehydrated in an ethanol series (30%, 50%, 70%, 95%, and 100% for 30 min each), with the final step repeated three times over the course of 1 h. Leaf samples were then immersed in three changes of 100% ethanol for 10 min each, followed by LR White resin:ethanol mixtures of 1:3, 1:2, and 1:1 (twice) for 1 h each, after which they were stored at 4°C in 1:1 LR White resin:ethanol overnight. Samples were warmed to room temperature and moved to a 2:1 LR White resin:ethanol solution over 4 h, before immersing in two changes of 100% LR White solution for 1 h each. Samples were stored at 4°C overnight and then warmed to room temperature the following day before immersing in three changes of 100% LR White resin over a 4-h period. Leaf samples were transferred to flat embedding molds using a toothpick to achieve the correct orientation, before polymerizing for 24 h.

Embedding molds were constructed following the methods described by Palmieri and Kiss (2005). Custom molds were created to provide flat embedding chambers that exclude oxygen from contacting the embedding medium. We chose 0.254-mm and 0.381-mm polycarbonate films (McMaster-Carr). These polycarbonate films were cut using a scalpel to fit standard 25 × 3 × 75 mm² glass microscope slides. The slides were precleaned with 100% ethanol and wiped with lint-free Kim wipes. To facilitate specimen removal, the slide was treated with an antistick agent (Fluoroglide spray; Electron Microscopy Sciences) prior to adhering the gasket to the slide. This was applied three times and then polished to remove lubricity. Silicone adhesive was then added to one side of the gasket and pressed onto the slide so an airtight seal was formed. Silicone adhesive was cured at room temperature for 24 h or in a 60°C oven for 1 h and allowed to cool before use.

LR White and leaf samples were added until the chamber was slightly overfilled and the liquid formed a convex surface, and then an Aclar strip (Ted Pella) was cut to a slightly larger width than the slide and placed on top of the chamber to shield the LR White from oxygen. One end of the Aclar strip was placed onto the edge of the chamber and the rest was rolled down onto the resin so that any excess resin spilled over the side and prevented air bubbles from being trapped underneath. The specimens were polymerized at 60°C for 24 h. After polymerization, the Aclar was removed and

specimens were excised with a razor blade while the slide was still warm. Initial samples were cut to between 1 and 5 μm thick with a microtome and a glass knife and allowed to adhere to silicone nitride windows.

4.6 Synchrotron X-Ray Fluorescence (SXRF)

For microtomography of seed, tomograms were collected at the bending magnet beamline X26A at the National Synchrotron Light Source, Brookhaven National Laboratory. X-ray fluorescence measurements were conducted using a 12-keV monochromatic X-ray beam, which was tuned using a Si(111) channel-cut monochromator. Monochromatic x-rays were focused to a beam size of $5 \times 8 \mu\text{m}$ using rhodium-coated, silicon Kirkpatrick-Baez microfocusing mirrors. Incident beam energy was monitored using an ion chamber upstream of the focusing optics. X-ray fluorescence spectra were collected with a Vortex-EX silicon-drift detector (SII Nanotechnology) with an active area of 50 mm^2 . X-ray transmission through the sample was recorded simultaneously using a p-type, intrinsic, n-type photodiode.

Individual seeds were attached to a 100- μm -diameter silicon fiber using Devcon 5-min epoxy resin, with the micropyle uppermost. The fiber was inserted into a Huber 1001 goniometer, centered, and mounted on a xyz θ stage. During fluorescence microtomography, the seed samples were translated horizontally through the focused X-ray microbeam in step sizes ranging from 5 to 7 μm and then rotated at intervals of between 0.8° to 1.1° angular steps, repeating the translation through a total of 180° . Full-energy dispersive spectra were collected at each pixel with a dwell time of 250 ms per pixel. Two-dimensional sinograms (plot of intensity against θ) were computationally reconstructed using fast Fourier transform-based Gridrec software developed by Brookhaven National Laboratory (Dowd et al, 1999), which is controlled by the Interactive Data Language programming software (Research Systems) to provide images of the cross-sectional internal metal distribution.

Elemental abundances (weight fraction) were calculated for the fluorescence measurements, adapted from McNear et al (2005). We used an assumed object density of 1.2 g cm^{-3} for *Arabidopsis* seed, a measured voxel size of $3.887 \times 10^{-8} \text{ cm}^3$ (reconstructed pixel area \times beam height), and the average Fe response from the sample to

calculate the Fe content of a whole tomogram. This Fe abundance was used as a fixed value for input into the NRLXRF program (Naval Research Laboratory X-Ray Fluorescence; Criss, 1977), from which abundances for K, Ca, Mn, Ni, Fe, and Zn were calculated. The concentration precision is typically $\pm 15\%$ and $\pm 10\%$ (1σ) for individual and mean values, respectively. A thin-film standard reference material (SRM 1833) was measured prior to the collection of each data set to establish sensitivities (counts per s per μg per cm^2) for Fe.

Micro-focused leaf 2D maps were collected at multiple runs at beamline 2-3 at Stanford Synchrotron Radiation Lightsource (SSRL). Beam line 2-3 used a water-cooled double crystal monochromator with either a Si(220), $f=0$ or Si(111) crystal and a Vortex single element detector. The beam was focused using a Pt-coated Kirkpatrick-Baez mirror pair (Xradia Inc., Pleasanton, CA, USA) and tuned to 11000 eV. All maps were collected from the 7th true leaf. Elemental mapping was performed in 7 μm steps with a 50 ms dwell time for whole leaf maps, and in 2 μm steps and 50 ms dwell time for trichome 2D mapping. The XRF maps were analyzed using the Microanalysis Toolkit (http://home.comcast.net/~sam_webb/smak.html). To determine total abundance of elements in whole leaf maps and in individual trichomes, region of interest (ROI) analysis was performed. Background counts in each trichome ROI was calculated by multiplying the mean counts per pixel in the whole leaf map by the number of pixels in ROI, and then subtracting this value from the total abundance. Percentage of elements in trichomes was calculated by the sum of total abundance in each trichome divided by total abundance in whole leaf map.

For high-resolution imaging of trichomes, scanning X-ray fluorescence microscopy was performed at Beamline 2-ID-D of the Advanced Photon Source at the Argonne National Laboratory (Cai et al, 2000). Incident X-rays of 10 keV were chosen to excite elements from P to Zn. A Fresnel zone plate focused the X-ray beam to a spot size of $0.2 \times 0.2 \mu\text{m}$ on the sample, which was raster scanned (Yun et al, 1999) at resolutions of 0.6 μm step in the trichome plus mesophyll map, with dwell times ranging from 0.5 to 1 s per pixel. X-ray fluorescence from the sample was captured with an energy-dispersive silicon drift detector. Data is expressed as normalized fluorescence counts.

4.7 Statistical analyses

When appropriate, data were subjected to ANOVA and means were compared by the Tukey HSD or Student's t-test using the JMP 10.0 for Mac (SAS Inc., USA).

5. References

- Ager FJ, Ynsa MD, Dominguez Solis JR, Lopez Martin MC, Gotor C, Romero LC (2003) Nuclear micro-probe analysis of *Arabidopsis thaliana* leaves. Nuclear Instruments and Methods in Physics Research Section B 210: 401–406.
- Albinsky D, Kusano M, Higuchi M, Hayashi N, Kobayashi M, Fukushima A, Mori M, Ichikawa T, Matsui K, Kuroda H, Horii Y, Tsumoto Y, Sakakibara H, Hirochika H, Matsui M, Saito K (2010) Metabolomic screening applied to rice FOX *Arabidopsis* lines leads to the identification of a gene-changing nitrogen metabolism. Mol Plant 3: 125-142.
- Anders N, Wilkinson MD, Lovegrove A, Freeman J, Tryfona T, Pellny TK, Weimar T, Mortimer JC, Stott K, Baker JM, Defoin-Platel M, Shewry PR, Dupree P, Mitchell RA (2012) Glycosyl transferases in family 61 mediate arabinofuranosyl transfer onto xylan in grasses. Proc Natl Acad Sci USA 109: 989-993.
- Barberon M, Zelazny E, Robert S, Conéjero G, Curie C, Friml J, Vert G (2011) Monoubiquitin-dependent endocytosis of the iron-regulated transporter 1 (IRT1) transporter controls iron uptake in plants. Proc Natl Acad Sci USA 108: E450-8.
- Bashir K, Inoue H, Nagasaka S, Takahashi M, Nakanishi H, Mori S, Nishizawa NK (2006) Cloning and characterization of deoxymugineic acid synthase genes from graminaceous plants. J Biol Chem 281: 32395-32402.
- Baxter I, Ouzzani M, Orcun S, Kennedy B, Jandhyala SS, Salt DE (2007) Purdue ionomics information management system. An integrated functional genomics platform. Plant Physiol 143: 600-611.
- Baxter IR, Vitek O, Lahner B, Muthukumar B, Borghi M, Morrissey J, Guerinot ML, Salt DE (2008) The leaf ionome as a multivariable system to detect a plant's physiological status. Proc Natl Acad Sci USA 105: 12081-12086.
- Baxter I, Hermans C, Lahner B, Yakubova E, Tikhonova M, Verbruggen N, Chao DY, Salt DE (2012) Biodiversity of mineral nutrient and trace element accumulation in *Arabidopsis thaliana*. PLoS One 7: e35121.
- Blamey FPC, Joyce DC, Edwards DG, Asher CJ (1986) Role of trichomes in sunflower tolerance to manganese toxicity. Plant Soil 91: 171-180

- Borghi M, Rus A, Salt DE (2011) Loss-of-function of Constitutive Expresser of Pathogenesis Related Genes5 affects potassium homeostasis in *Arabidopsis thaliana*. PLoS One 6: e26360.
- Briat JF (2002) Metal ion-activated oxidative stress and its control. In: Inze, D, Van Montagu, M (eds.) Oxidative Stress in Plants. Taylor & Francis, London, pp. 171–190.
- Brunetti P, Zanella L, Proia A, De Paolis A, Falasca G, Altamura MM, Sanità di Toppi L, Costantino P, Cardarelli M (2011) Cadmium tolerance and phytochelatin content of *Arabidopsis* seedlings over-expressing the phytochelatin synthase gene AtPCS1. J Exp Bot 62: 5509-5519.
- Cai Z, Lai B, Yun W, Ilinski P, Legnini D, Maser J, Rodrigues W (2000) A hard x-ray scanning microprobe for fluorescence imaging and microdiffraction at the Advanced Photon Source. Am Inst Physics Proc 507: 472–477.
- Chao DY, Silva A, Baxter I, Huang YS, Nordborg M, Danku J, Lahner B, Yakubova E, Salt DE (2012) Genome-wide association studies identify heavy metal ATPase3 as the primary determinant of natural variation in leaf cadmium in *Arabidopsis thaliana*. PLoS Genet 8: e1002923.
- Choi YE, Harada E, Wada M, Tsuboi H, Morita Y, Kusano T, Sano H (2001) Detoxification of cadmium in tobacco plants: formation and active excretion of crystals containing cadmium and calcium through trichomes. Planta 213: 45-50.
- Clemens S (2001) Developing tools for phytoremediation: towards a molecular understanding of plant metal tolerance and accumulation. Int J Occup Med Environ Health 14: 235-239.
- Conte SS, Walker EL (2011) Transporters contributing to iron trafficking in plants. Mol Plant 4: 464-476.
- Criss JW (1977) NRLXRF, A FORTRAN Program for X-Ray Fluorescence Analysis. Naval Research Laboratory, Washington, DC.
- Dowd BA, Campbell GH, Marr RB, Nagarkar VV, Tipnis SVLA, Siddons DP (1999) Developments in synchrotron x-ray computed microtomography at the National Synchrotron Light Source. Proc SPIE 3772: 224–236.

- Dubouzet JG, Maeda S, Sugano S, Ohtake M, Hayashi N, Ichikawa T, Kondou Y, Kuroda H, Horii Y, Matsui M, Oda K, Hirochika H, Takatsuji H, Mori M (2011) Screening for resistance against *Pseudomonas syringae* in rice-FOX Arabidopsis lines identified a putative receptor-like cytoplasmic kinase gene that confers resistance to major bacterial and fungal pathogens in Arabidopsis and rice. *Plant Biotechnol J* 9: 466-485.
- Eide D, Broderius M, Fett J, Guerinot ML (1996) A novel iron-regulated metal transporter from plants identified by functional expression in yeast. *PNAS* 93: 5624-5628.
- Esch JJ, Chen M, Sanders M, Hillestad M, Ndkium S, Idelkope B, Neizer J, Marks MD (2003) A contradictory GLABRA3 allele helps define gene interactions controlling trichome development in Arabidopsis. *Development* 130: 5885-5894.
- Fukuda N, Hokura A, Kitajima N, Terada Y, Saito H, Abed T, Nakai A. 2008. Micro X-ray fluorescence imaging and micro X-ray absorption spectroscopy of cadmium hyper-accumulating plant, *Arabidopsis halleri* ssp. *gummifera*, using high-energy synchrotron radiation. *Journal of Analytical Atomic Spectrometry* 23:1068–1075.
- Gietz RD, Schiestl RH (2007) High-efficiency yeast transformation using the LiAc/SS carrier DNA/PEG method. *Nat Protoc* 2: 31-34.
- Gómez-Galera S, Rojas E, Sudhakar D, Zhu C, Pelacho AM, Capell T, Christou P (2010) Critical evaluation of strategies for mineral fortification of staple food crops. *Transgenic Res* 19: 165-80.
- Grebe M (2012) The patterning of epidermal hairs in Arabidopsis - updated. *Curr Opin Plant Biol* 15: 31-37.
- Gustin JL, Zanis MJ, Salt DE (2011) Structure and evolution of the plant cation diffusion facilitator family of ion transporters. *BMC Evol Biol* 11:76.
- Gutierrez-Alcalá G, Gotor C, Meyer AJ, Fricker M, Vega JM, Romero LC (2000) Glutathione biosynthesis in Arabidopsis trichome cells. *Proc Natl Acad Sci USA* 97: 11108-11113.
- Hanikenne M, Talke IN, Haydon MJ, Lanz C, Nolte A, Motte P, Kroymann J, Weigel D, Krämer U (2008) Evolution of metal hyperaccumulation required cis-regulatory changes and triplication of HMA4. *Nature* 453: 391-395.

Haydon MJ, Cobbett CS (2007) A novel major facilitator superfamily protein at the tonoplast influences zinc tolerance and accumulation in Arabidopsis. *Plant Physiol* 143: 1705-1719.

Higuchi-Takeuchi M, Ichikawa T, Kondou Y, Matsui K, Hasegawa Y, Kawashima M, Sonoike K, Mori M, Hirochika H, Matsui M (2011) Functional analysis of two isoforms of leaf-type ferredoxin-NADP(+) oxidoreductase in rice using the heterologous expression system of Arabidopsis. *Plant Physiol* 157: 96-108.

Hindt MN, Guerinot ML (2012) Getting a sense for signals: regulation of the plant iron deficiency response. *Biochim Biophys Acta* 1823: 1521-1530.

Hokura A, Onuma R, Kitajima N, Terada Y, Saito H, Abe T, Yoshida S, Nakai I (2006) 2-D X-ray Fluorescence Imaging of Cadmium Hyperaccumulating Plants by Using High-energy Synchrotron Radiation X-ray Microbeam. *Chem Lett* 35: 1246-1247.

Huguet S, Bert V, Laboudigue A, Barthès V Isaure MP, Llorens I, Schat H, Sarret G (2012) Cd speciation and localization in the hyperaccumulator *Arabidopsis halleri*. *Environ Exp Bot* 82: 54–65

Hülskamp M, Misra S, Jürgens G (1994) Genetic dissection of trichome cell development in *Arabidopsis*. *Cell* 76: 555-566.

Hussain D, Haydon MJ, Wang Y, Wong E, Sherson SM, Young J, Camakaris J, Harper JF, Cobbett CS (2004) P-type ATPase heavy metal transporters with roles in essential zinc homeostasis in *Arabidopsis*. *Plant Cell* 16: 1327-1339.

IRGSP - International Rice Genome Sequencing Project. (2005) The map-based sequence of the rice genome. *Nature* 436: 793-800.

Inoue H, Kobayashi T, Nozoye T, Takahashi M, Kakei Y, Suzuki K, Nakazono M, Nakanishi H, Mori S, Nishizawa NK (2009) Rice OsYSL15 is an iron-regulated iron(III)-deoxymugineic acid transporter expressed in the roots and is essential for iron uptake in early growth of the seedlings. *J Biol Chemistry* 284: 3470–3479.

Isaure MP, Fayard B, Sarret G, Pairis S, Bourguignon J. 2006. Localization and chemical forms of cadmium in *Arabidopsis thaliana*. *Spectrochimica Acta Part B* 61: 1242–1252.

Isaure MP, Sarret G, Harada E, Choi YE, Marcus MA, Fakra SC, Geoffroy N, Pairis S, Susini J, Clemens S, Manceau A (2010) Calcium promotes cadmium elimination as vaterite grains by tobacco trichomes. *Geochim Cosmochim Acta* 74: 5817–5834.

Ishida T, Kurata T, Okada K, Wada T (2008) A genetic regulatory network in the development of trichomes and root hairs. *Annu Rev Plant Biol* 59: 365-386.

Ishimaru Y, Masuda H, Suzuki M, Bashir K, Takahashi M, Nakanishi H, Mori S, Nishizawa NK (2007) Overexpression of the OsZIP4 zinc transporter confers disarrangement of zinc distribution in rice plants. *J Exp Bot* 58: 2909-2915.

Ishimaru Y, Suzuki M, Kobayashi T, Takahashi M, Nakanishi H, Mori S, Nishizawa NK (2005) OsZIP4, a novel zinc-regulated zinc transporter in rice. *J Exp Bot* 56: 3207-3214.

Ishimaru Y, Suzuki M, Tsukamoto T, Suzuki K, Nakazono M, Kobayashi T, Wada Y, Watanabe S, Matsuhashi S, Takahashi M, Nakanishi H, Mori S, Nishizawa NK (2006) Rice plants take up iron as an Fe³⁺-phytosiderophore and as Fe²⁺. *Plant J* 45: 335-346.

Kikuchi S, Satoh K, Nagata T, Kawagashira N, Doi K, Kishimoto N, Yazaki J, Ishikawa M, Yamada H, Ooka H, Hotta I, Kojima K, Namiki T, Ohneda E, Yahagi W, Suzuki K, Li CJ, Ohtsuki K, Shishiki T; Foundation of Advancement of International Science Genome Sequencing & Analysis Group, Otomo Y, Murakami K, Iida Y, Sugano S, Fujimura T, Suzuki Y, Tsunoda Y, Kurosaki T, Kodama T, Masuda H, Kobayashi M, Xie Q, Lu M, Narikawa R, Sugiyama A, Mizuno K, Yokomizo S, Niikura J, Ikeda R, Ishibiki J, Kawamata M, Yoshimura A, Miura J, Kusumegi T, Oka M, Ryu R, Ueda M, Matsubara K; RIKEN, Kawai J, Carninci P, Adachi J, Aizawa K, Arakawa T, Fukuda S, Hara A, Hashizume W, Hayatsu N, Imotani K, Ishii Y, Itoh M, Kagawa I, Kondo S, Konno H, Miyazaki A, Osato N, Ota Y, Saito R, Sasaki D, Sato K, Shibata

K, Shinagawa A, Shiraki T, Yoshino M, Hayashizaki Y, Yasunishi A (2003) Collection, mapping, and annotation of over 28,000 cDNA clones from japonica rice. *Science* 301: 376-379.

Kim DH, Eu YJ, Yoo CM, Kim YW, Pih KT, Jin JB, Kim SJ, Stenmark H, Hwang I (2001) Trafficking of phosphatidylinositol 3-phosphate from the trans-Golgi network to the lumen of the central vacuole in plant cells. *Plant Cell* 13: 287-301.

Kim SA, Punshon T, Lanzirotti A, Li L, Alonso JM, Ecker JR, Kaplan J, Guerinot ML (2006) Localization of iron in *Arabidopsis* seed requires the vacuolar membrane transporter VIT1. *Science* 314: 1295-1298.

Kondou Y, Higuchi M, Takahashi S, Sakurai T, Ichikawa T, Kuroda H, Yoshizumi T, Tsumoto Y, Horii Y, Kawashima M, Hasegawa Y, Kuriyama T, Matsui K, Kusano M, Albinsky D, Takahashi H, Nakamura Y, Suzuki M, Sakakibara H, Kojima M, Akiyama K, Kurotani A, Seki M, Fujita M, Enju A, Yokotani N, Saitou T, Ashidate K, Fujimoto N, Ishikawa Y, Mori Y, Nanba R, Takata K, Uno K, Sugano S, Natsuki J, Dubouzet JG, Maeda S, Otake M, Mori M, Oda K, Takatsuji H, Hirochika H, Matsui M (2009) Systematic approaches to using the FOX hunting system to identify useful rice genes. *Plant J* 57: 883-894.

Korshunova YO, Eide D, Clark WG, Guerinot ML, Pakrasi HB (1999) The IRT1 protein from *Arabidopsis thaliana* is a metal transporter with a broad substrate range. *Plant Mol Biol* 40: 37-44.

Krämer U, Grime GW, Smith JAC, Hawes CR, Baker AJM (1997) Micro-PIXE as a technique for studying nickel localization in leaves of the hyperaccumulator plant *Alyssum lesbiacum*. *Nuclear Instruments & Methods in Physics Research* 346-350.

Kumar G, Kushwaha HR, Panjabi-Sabharwal V, Kumari S, Joshi R, Karan R, Mittal S, Singla-Pareek SL, Pareek A (2012) Clustered metallothionein genes are co-regulated in rice and ectopic expression of OsMT1e-P confers multiple abiotic stress tolerance in tobacco via ROS scavenging. *BMC Plant Biol* 12: 107.

Küpper H, Lombi E, Zhao FJ, McGrath SP (2000) Cellular compartmentation of cadmium and zinc in relation to other elements in the hyperaccumulator *Arabidopsis halleri*. *Planta* 212: 75-84.

Küpper H, Lombi E, Zhao FJ, Wieshammer G, McGrath SP (2001) Cellular compartmentation of nickel in the hyperaccumulators *Alyssum lesbiacum*, *Alyssum bertolonii* and *Thlaspi goesingense*. *J Exp Bot* 52: 2291-2300.

Lahner B, Gong J, Mahmoudian M, Smith EL, Abid KB, Rogers EE, Guerinot ML, Harper JF, Ward JM, McIntyre L, Schroeder JI, Salt DE (2003) Genomic scale profiling of nutrient and trace elements in *Arabidopsis thaliana*. *Nat Biotechnol* 21: 1215-1221.

Lee S, An G (2009) Over-expression of OsIRT1 leads to increased iron and zinc accumulations in rice. *Plant Cell Environ* 32: 408-416.

Lee S, Chiecko JC, Kim SA, Walker EL, Lee Y, Guerinot ML, An G (2009) Disruption of OsYSL15 leads to iron inefficiency in rice plants. *Plant Physiology* 150: 786-800.

Lee S, Jeong HJ, Kim SA, Lee J, Guerinot ML, An G (2010b) OsZIP5 is a plasma membrane zinc transporter in rice. *Plant Mol Biol* 73: 507-517.

Lee S, Kim SA, Lee J, Guerinot ML, An G (2010a) Zinc deficiency-inducible OsZIP8 encodes a plasma membrane-localized zinc transporter in rice. *Mol Cells* 29: 551-558.

Lee S, Moon JS, Ko TS, Petros D, Goldsbrough PB and Korban SS (2003) Overexpression of *Arabidopsis* phytochelatin synthase paradoxically leads to hypersensitivity to cadmium stress. *Plant Physiol* 131: 656 – 663.

Lin YF, Liang HM, Yang SY, Boch A, Clemens S, Chen CC, Wu JF, Huang JL, Yeh KC (2009) *Arabidopsis* IRT3 is a zinc-regulated and plasma membrane localized zinc/iron transporter. *New Phytol* 182: 392-404.

MacDiarmid CW, Gaither LA, Eide D (2000) Zinc transporters that regulate vacuolar

zinc storage in *Saccharomyces cerevisiae*. *EMBO J* 19: 2845-2855.

Marschner, H (1995) Mineral Nutrition of Higher Plants, 2nd Edition. Academic Press, Boston, 674 p.

Maret W, Sandstead HH (2006). Zinc requirements and the risks and benefits of zinc supplementation. *J Trace Elem Med Biol* 20: 3–18.

Maret W (2009) Molecular aspects of human cellular zinc homeostasis: redox control of zinc potentials and zinc signals. *Biometals* 22:149–157.

Martell EA (1974) Radioactivity of tobacco trichomes and insoluble cigarette smoke particles. *Nature* 249: 215-217

Meyberg M, Krohn S, Bruemmer B, Kristen U (1991) Ultrastructure and secretion of glandular trichomes of tobacco leaves. *Flora Jena* 185: 357-363

McNear D, Peltier E, Everhart J, Chaney R, Sutton S, Newville M, Sparks DL (2005) Application of quantitative fluorescence and absorption-edge computed microtomography to image metal compartmentalization in *Alyssum murale*. *Environ Sci Technol* 39: 2210–2218

Morrissey J, Baxter IR, Lee J, Li L, Lahner B, Grotz N, Kaplan J, Salt DE, Guerinot ML (2009) The ferroportin metal efflux proteins function in iron and cobalt homeostasis in *Arabidopsis*. *Plant Cell* 21: 3326-3338.

Nuruzzaman M, Manimekalai R, Sharoni AM, Satoh K, Kondoh H, Ooka H, Kikuchi S (2010) Genome-wide analysis of NAC transcription factor family in rice. *Gene* 465: 30-44.

Ogo Y, Itai RN, Nakanishi H, Inoue H, Kobayashi T, Suzuki M, Takahashi M, Mori S, Nishizawa NK (2006) Isolation and characterization of IRO2, a novel iron-regulated bHLH transcription factor in graminaceous plants. *J Exp Bot* 57: 2867-2878.

OsVIT2 is known as a vacuolar transporter of Fe, Zn and Mn (Zhang et al 2012), but not of As. PCS proteins, on the other hand, are involved in Cd detoxification, although over-expression or heterologous expression of PCS genes often gives controversial results (Pomponi et al 2006); Lee et al 2003; Wojas et al 2005).

Palmieri M, Kiss JZ (2005) A novel technique for flat-embedding cryofixed plant specimens in LR white resin. *Microsc Res Tech* 68: 80–84.

Pomponi M, Censi V, Girolamo DV, Paolis DA, Toppi SS, Aromolo R and Costantino P, et al. Overexpression of *Arabidopsis* phytochelatin synthase in tobacco plants enhances Cd²⁺ tolerance and accumulation but not translocation to the shoot. *Planta* 2006, 223: 180–190.

Punshon T, Guerinot ML, Lanzirotti A (2009) Using synchrotron X-ray fluorescence microprobes in the study of metal homeostasis in plants. *Ann Bot* 103: 665-672.

Punshon T, Hirschi K, Yang J, Lanzirotti A, Lai B, Guerinot ML (2012) The role of CAX1 and CAX3 in elemental distribution and abundance in *Arabidopsis* seed. *Plant Physiol* 158: 352-362.

Ricachenevsky FK, Sperotto RA, Menguer PK, Sperb ER, Lopes KL, Fett JP (2011) ZINC-INDUCED FACILITATOR-LIKE family in plants: lineage-specific expansion in monocotyledons and conserved genomic and expression features among rice (*Oryza sativa*) paralogs. *BMC Plant Biol* 11:20.

Sakurai T, Kondou Y, Akiyama K, Kurotani A, Higuchi M, Ichikawa T, Kuroda H, Kusano M, Mori M, Saitou T, Sakakibara H, Sugano S, Suzuki M, Takahashi H, Takahashi S, Takatsujii H, Yokotani N, Yoshizumi T, Saito K, Shinozaki K, Oda K, Hirochika H, Matsui M (2011) RiceFOX: a database of *Arabidopsis* mutant lines overexpressing rice full-length cDNA that contains a wide range of trait information to facilitate analysis of gene function. *Plant Cell Physiol* 52: 265-273.

Sallaud C, Meynard D, van Boxtel J, Gay C, Bès M, Brizard JP, Larmande P, Ortega D, Raynal M, Portefaix M, Ouwerkerk PB, Rueb S, Delseney M, Guiderdoni E (2003) Highly efficient production and characterization of T-DNA plants for rice (*Oryza*

sativa L.) functional genomics. *Theor Appl Genet* 106: 1396-1408.

Salt DE, Prince RC, Pickering IJ, Raskin I (1995) Mechanisms of cadmium mobility and accumulation in Indian mustard. *Plant Physiol* 109: 427-433.

Salt DE, Baxter I, Lahner B (2008) Ionomics and the study of the plant ionome. *Annu Rev Plant Biol* 59: 709-733.

Sarret G, Harada E, Choi YE, Isaure MP, Geoffroy N, Fakra S, Marcus MA, Birschwilks M, Clemens S, Manceau A (2006) Trichomes of tobacco excrete zinc as zinc-substituted calcium carbonate and other zinc-containing compounds. *Plant Physiol* 141: 1021-1034.

Sarret G, Willems G, Isaure MP, Marcus MA, Fakra SC, Frérot H, Pairis S, Geoffroy N, Manceau A, Saumitou-Laprade P (2009) Zinc distribution and speciation in *Arabidopsis halleri* x *Arabidopsis lyrata* progenies presenting various zinc accumulation capacities. *New Phytol* 184: 581-595.

Satoh-Nagasawa N, Mori M, Nakazawa N, Kawamoto T, Nagato Y, Sakurai K, Takahashi H, Watanabe A, Akagi H (2012) Mutations in rice (*Oryza sativa*) heavy metal ATPase 2 (OsHMA2) restrict the translocation of zinc and cadmium. *Plant Cell Physiol* 53: 213-224.

Shahzad Z, Gosti F, Frérot H, Lacombe E, Roosens N, Saumitou-Laprade P, Berthomieu P. The five AhMTP1 zinc transporters undergo different evolutionary fates towards adaptive evolution to zinc tolerance in *Arabidopsis halleri*. *PLoS Genet* 6: e1000911.

Sinclair SA, Krämer U (2012) The zinc homeostasis network of land plants. *Biochim Biophys Acta* 1823: 1553-1567.

Sperotto RA, Ricachenevsky FK, Duarte GL, Boff T, Lopes KL, Sperb ER, Grusak MA, Fett JP (2009) Identification of up-regulated genes in flag leaves during rice grain filling and characterization of OsNAC5, a new ABA-dependent transcription factor. *Planta* 230: 985-1002.

- Stein RJ, Ricachenevsky FK, Fett JP (2009) Differential regulation of the two rice ferritin genes (OsFER1 and OsFER2). *Plant Science* 177: 563-569.
- Talke IN, Hanikenne M, Krämer U (2006) Zinc-dependent global transcriptional control, transcriptional deregulation, and higher gene copy number for genes in metal homeostasis of the hyperaccumulator *Arabidopsis halleri*. *Plant Physiol* 142: 148-167.
- Tappero R, Peltier E, Gräfe M, Heidel K, Ginder-Vogel M, Livi KJ, Rivers ML, Marcus MA, Chaney RL, Sparks DL (2007) Hyperaccumulator *Alyssum murale* relies on a different metal storage mechanism for cobalt than for nickel. *New Phytol* 175: 641-654.
- Vert G, Briat JF, Curie C (2009) *Arabidopsis IRT2* gene encodes a root-periphery iron transporter. *Plant J* 26: 181-189.
- Wagner GJ, Wang E, Shepherd RW (2004) New approaches for studying and exploiting an old protuberance, the plant trichome. *Ann Bot* 93: 3-11.
- Wang N, Long T, Yao W, Xiong L, Zhang Q, Wu C (2012) Mutant Resources for the Functional Analysis of the Rice Genome Mol Plant doi:10.1093/mp/sss142
- White PJ, Broadley MR (2005) Biofortifying crops with essential mineral elements. Trends Plant Sci 10: 586-593.
- Wojas S, Clemens S, Hennig J, Sklodowska A, Kopera E, Schat H and Bal W, et al. Overexpression of phytochelatin synthase in tobacco: distinctive effects of AtPCS1 and CePCS genes on plant response to cadmium. *J Exp Bot* 2008, 59: 2205 – 2219.
- Wu FH, Shen SC, Lee LY, Lee SH, Chan MT, Lin CS (2009) Tape-Arabidopsis Sandwich - a simpler Arabidopsis protoplast isolation method. *Plant Methods* 5:16.
- Yang X, Huang J, Jiang Y, Zhang HS (2009) Cloning and functional identification of two members of the ZIP (Zrt, Irt-like protein) gene family in rice (*Oryza sativa* L.). *Mol Biol Rep* 36: 281-287.

Yang C, Ye Z (2012) Trichomes as models for studying plant cell differentiation. *Cell Mol Life Sci.* doi: 10.1007/s00018-012-1147-6.

Yokotani N, Ichikawa T, Kondou Y, Matsui M, Hirochika H, Iwabuchi M, Oda K (2008) Expression of rice heat stress transcription factor OsHsfA2e enhances tolerance to environmental stresses in transgenic Arabidopsis. *Planta* 227: 957-967.

Yokotani N, Ichikawa T, Kondou Y, Matsui M, Hirochika H, Iwabuchi M, Oda K (2009) Tolerance to various environmental stresses conferred by the salt-responsive rice gene ONAC063 in transgenic Arabidopsis. *Planta* 229: 1065-1075.

Yoo SD, Cho YH, Sheen J (2007) Arabidopsis mesophyll protoplasts: a versatile cell system for transient gene expression analysis. *Nat Protoc* 2: 1565-1572.

Yu J, Hu S, Wang J, Wong GK, Li S, Liu B, Deng Y, Dai L, Zhou Y, Zhang X, Cao M, Liu J, Sun J, Tang J, Chen Y, Huang X, Lin W, Ye C, Tong W, Cong L, Geng J, Han Y, Li L, Li W, Hu G, Huang X, Li W, Li J, Liu Z, Li L, Liu J, Qi Q, Liu J, Li L, Li T, Wang X, Lu H, Wu T, Zhu M, Ni P, Han H, Dong W, Ren X, Feng X, Cui P, Li X, Wang H, Xu X, Zhai W, Xu Z, Zhang J, He S, Zhang J, Xu J, Zhang K, Zheng X, Dong J, Zeng W, Tao L, Ye J, Tan J, Ren X, Chen X, He J, Liu D, Tian W, Tian C, Xia H, Bao Q, Li G, Gao H, Cao T, Wang J, Zhao W, Li P, Chen W, Wang X, Zhang Y, Hu J, Wang J, Liu S, Yang J, Zhang G, Xiong Y, Li Z, Mao L, Zhou C, Zhu Z, Chen R, Hao B, Zheng W, Chen S, Guo W, Li G, Liu S, Tao M, Wang J, Zhu L, Yuan L, Yang H (2002) A draft sequence of the rice genome (*Oryza sativa* L. ssp. *indica*). *Science* 296: 79-92.

Yun W, Lai B, Cai Z, Maser J, Legnini D, Gluskin E, Chen Z, Krasnoperova AA, Vladimirska Y, Cerrina F, Di Fabrizio E, Gentili M (1999) Nanometer focusing of hard x-rays by phase zone plates. *Rev Sci Instrum* 70: 2238–2241.

Zhang Y, Xu YH, Yi HY, Gong JM (2012) Vacuolar membrane transporters OsVIT1 and OsVIT2 modulate iron translocation between flag leaves and seeds in rice. *Plant J* 72: 400-410.

- Zhao FJ, Lombi E, Breedon T, McGrath SP (2000) Zinc hyperaccumulation and cellular distribution in *Arabidopsis halleri*. *Plant Cell Environ* 23: 507-514
- Zheng L, Huang F, Narsai R, Wu J, Giraud E, He F, Cheng L, Wang F, Wu P, Whelan J, Shou H (2009) Physiological and transcriptome analysis of iron and phosphorus interaction in rice seedlings. *Plant Physiol* 151: 262-274.

Table 1. Ionomics profile of Rice FOX lines^a. Given number are percentage of difference when comparing WT and Rice FOX line median for each element.

Line	Gene	Li	Na	Mg	P	S	K	Ca	Fe	Co	Ni	Cu	Zn	As	Rb	Si	Mo	Cd	
K02538	OsiR02	20.75	25.69	5.24	5.33	3.40	-2.94	6.57	-3.52	4.38	9.79	11.47	-21.84	14.85	13.23	-2.39	10.55		
K15412	OsiR02	21.98	19.43	8.97	12.11	-3.19	0.42	4.77	5.94	-16.51	2.01	6.02	-37.93	26.21	13.80	-7.88	22.95		
K02642	OSDMASI	13.00	2.11	0.85	5.62	8.80	-2.04	-0.63	-0.17	-8.12	-3.99	6.18	9.40	-19.77	13.57	1.54	3.78	0.43	
K01905	OSDMASI	37.46	32.09	17.11	3.40	-2.54	4.55	13.90	5.73	12.55	12.32	0.66	19.63	-25.01	7.05	5.68	22.74	4.36	
K14626	OsvT12	17.39	31.74	17.17	11.59	11.59	-8.55	-5.43	16.96	9.25	0.22	15.96	-0.77	3.76	-44.69	19.00	1.21	25.55	
K30225	OsvT12	23.46	28.77	11.08	6.22	-8.80	-8.23	11.83	0.42	4.58	16.19	2.66	12.54	-33.10	8.80	1.80	16.97	-12.64	
K32631	OsvT12	29.45	30.19	15.88	8.78	-7.37	-8.10	9.86	-1.95	-0.67	9.76	0.23	11.13	-20.38	3.85	21.93	-25.02	14.21	
K32620	OsfER2	7.01	24.53	6.23	1.17	-12.55	9.33	8.21	-1.24	10.05	7.63	3.86	7.53	-26.31	-8.72	16.69	12.85	8.63	
OsvRAMP1	OsvRAMP1	-0.80	21.30	2.13	5.37	-18.31	1.55	3.08	1.05	4.62	7.19	8.12	-12.02	-24.74	10.81	16.74	-11.89	4.99	
OsvRAMP6	OsvRAMP6	-7.94	10.28	-2.44	6.07	-10.65	7.37	-3.91	-12.41	19.31	-1.78	0.76	15.35	8.34	12.88	-6.15	-13.48	6.85	
OsvRAMP6	OsvRAMP6	-10.73	18.91	5.87	4.96	-12.01	10.25	3.10	2.00	17.25	-1.12	0.00	8.77	-14.25	6.66	5.62	10.98	-20.19	15.47
OsvRAMP7	OsvRAMP7	4.51	45.82	15.54	8.19	7.72	13.40	1.97	22.86	8.87	-0.46	6.12	-35.71	-14.20	9.75	21.26	2.26	8.40	
OsvRAMP7	OsvRAMP7	-16.12	11.24	1.48	5.54	-11.69	8.38	-3.09	-5.6	45.96	3.76	-2.73	4.13	-18.79	-23.86	20.87	11.25	-16.62	0.94
QZ1D6	QZ1D6	-4.13	31.20	5.30	-3.61	-24.75	-0.95	8.84	-0.50	13.15	12.61	11.53	6.53	-27.33	23.14	-1.35	23.16	-4.76	7.00
K21926	OsZIP16	-19.27	15.88	3.08	8.65	-18.96	13.77	6.34	6.65	5.76	12.80	1.54	2.43	-18.05	14.99	18.78	-19.54	-5.34	7.00
K3648	OsZIP16	-18.09	23.57	-0.52	0.05	-8.36	-1.00	4.74	-2.48	-2.95	10.50	2.10	4.09	-7.97	-20.22	1.75	8.57	1.93	-6.56
K36532	OsZIP16	-10.05	5.43	0.83	13.88	-5.32	-15.69	4.17	-1.76	-11.47	20.48	3.20	24.32	-28.43	-1.90	8.41	8.37	-11.27	0.94
K11313	OsZIP17	-12.57	12.57	0.68	2.34	-10.65	7.37	-3.91	-12.41	19.31	-1.78	0.76	15.35	8.25	15.95	-11.05	-17.71	13.08	
K27616	OsZIP18	-5.11	17.29	-1.58	-0.56	-6.22	-8.31	3.40	-1.02	2.13	2.69	2.69	2.63	-13.95	-11.05	-4.78	7.31	6.08	9.17
K15088	OsZIP18	-17.06	17.29	-1.58	-0.56	-6.22	-8.31	3.40	-1.02	2.13	2.69	2.69	2.63	-13.95	-11.05	-4.78	7.31	6.08	9.17
K34166	OsZIP18	-1.73	5.38	-2.52	2.07	-3.41	-0.59	-0.07	-5.42	10.32	5.10	2.09	7.46	-6.98	12.59	7.10	4.32	10.44	4.53
K34306	OsZIP18	-11.24	11.24	1.48	5.54	-11.69	8.38	-3.09	-5.6	45.96	3.76	-2.73	4.13	-18.79	-23.86	20.87	11.25	-16.62	0.94
K21926	OsZIP18	-11.27	5.48	0.50	2.60	-2.74	0.72	4.54	-3.70	-6.63	1.93	0.50	6.20	21.99	-12.50	7.30	8.70	2.03	-9.48
K09221	OsZIP14	-23.68	33.17	5.78	-2.84	-12.62	-15.04	9.99	-3.49	16.55	9.59	-4.86	11.74	-28.55	-27.96	-6.95	17.85	8.67	8.67
K18128	OsZIP14	5.86	21.83	3.97	-0.11	-13.47	-15.04	15.36	-5.57	4.38	2.13	3.53	11.87	-27.53	-7.04	-4.20	16.33	2.10	16.21
K28632	OsyS1L6	5.82	16.10	0.03	7.85	-9.33	-4.71	-1.48	-3.99	27.40	-0.02	2.64	3.41	-13.67	8.80	2.80	-4.62	3.76	3.76
K32237	OsyS1L7	4.24	4.10	1.33	6.37	-4.10	0.77	5.80	-5.38	12.30	-5.31	2.80	3.79	-22.67	-13.90	11.90	4.23	1.51	12.13
K37642	OsyS1L7	18.30	19.70	3.77	7.50	-14.62	-5.00	8.33	-10.70	31.89	-1.79	1.23	4.41	-18.78	-18.78	13.19	-1.51	8.90	4.53
K29309	OsyS1L12	1.67	10.51	-0.82	14.39	1.86	2.61	1.13	-3.98	23.34	-10.12	-4.74	-3.76	-13.39	-13.25	18.99	0.68	-15.41	1.86
OsyS1L13	OsyS1L13	0.97	18.04	8.28	-15.34	-0.93	14.81	-6.67	6.97	7.29	8.09	12.50	-30.85	-29.09	-1.12	19.51	4.04	12.24	
K06540	OsyS1L13	9.72	22.90	9.79	-8.08	-16.54	-17.14	16.29	-8.84	21.30	10.78	-0.56	24.82	-19.70	-6.53	22.05	4.09	9.42	
K02304	OsFDL4	-6.72	14.36	-8.49	21.62	2.40	-3.52	-2.31	-3.73	19.02	1.74	-0.41	-5.41	-14.43	-18.73	18.73	14.90	-13.90	24.06
K16426	OsPcS1	-0.39	13.83	-6.46	20.01	7.53	1.34	-5.76	-10.39	12.02	-1.10	-1.10	-5.54	-19.09	21.40	5.65	-6.85	15.55	15.55
K21701	OsZF1E4	3.90	-1.51	-10.85	14.21	17.47	0.31	-7.05	-5.79	0.65	-1.67	-7.87	-3.48	1.16	20.36	29.78	1.31	-1.51	12.13
K35343	OsZF1F5	2.31	-4.66	-2.42	8.35	5.94	-1.22	-0.68	-6.10	-11.97	-1.17	-1.67	0.99	-6.62	15.40	11.87	4.41	4.08	6.44
OszIFL5	OszIFL5	-8.64	30.67	-3.76	21.58	-9.14	13.58	-5.18	-5.18	12.24	-0.63	-31.24	-9.99	43.67	13.02	-4.30	4.57	4.57	
K21705	OszIFL7	-1.89	-3.95	-8.15	9.30	12.05	2.46	-4.88	-2.81	10.21	-0.35	-9.13	-4.92	-0.43	28.59	16.81	-0.59	-2.56	0.97
K24919	OszIFL12	5.88	-0.76	11.17	10.57	13.90	4.65	-4.16	-2.03	5.02	2.97	-2.68	-1.30	3.11	24.78	28.68	5.70	6.62	15.97
K29419	OszIFL12	4.60	25.79	16.22	8.01	-15.17	-11.60	14.54	-2.03	12.05	13.71	1.30	-26.11	-32.33	-20.16	-2.34	20.14	-15.66	11.36
K30332	OsoPT13	-0.02	9.53	7.62	2.81	-3.18	-14.26	8.04	0.44	-6.82	9.83	-1.60	7.22	-27.49	-10.66	-8.49	18.19	13.51	15.06
K07130	OsmTP1	-11.18	30.17	21.87	13.29	-17.81	-10.87	13.76	0.66	8.89	49.03	1.70	34.77	-41.82	-28.56	2.22	29.74	11.81	31.06
K07728	OsmTP1	5.11	29.30	17.74	-3.16	-23.68	-23.51	10.53	4.23	40.80	-0.76	7.78	33.39	-32.66	-17.75	44.47	15.69	30.28	
K27745	OsmTP1	6.38	18.43	6.42	1.84	-1.47	-2.67	4.97	-1.15	-11.78	14.10	-1.22	1.13	-12.20	-1.41	3.61	14.89	-2.49	3.12
K20149	ONAC103	-0.13	30.81	18.44	14.68	-23.24	-6.33	17.80	9.02	-3.74	24.81	5.80	20.18	-51.93	-21.47	30.84	-2.37	14.44	14.44
K21349	ONAC40NAC068	9.47	14.37	-1.02	0.74	-8.50	-1.50	4.27	4.97	8.72	38.35	13.77	22.80	-29.82	-13.22	-9.76	15.27	-23.48	-1.25
K21218	LOC_Os03g01120	1.02	28.89	22.77	-0.11	-1.73	-11.31	-11.50	6.46	-0.56	-4.47	-0.10	0.13	0.57	-27.49	-5.01	-2.43	9.80	4.75
K05312	LOC_Os03g04080	10.21	29.28	5.39	15.96	-10.00	-21.04	0.81	-1.58	7.36	-2.18	-4.61	-6.14	-13.83	11.07	10.45	1.47	13.71	1.47
K14749	LOC_Os03g04080	26.33	25.29	22.28	2.56	-23.02	-2.03	3.43	1.33	35.27	6.49	1.02	-7.46	-30.59	-13.41	-0.59	20.64	-2.89	13.60
K18320	LOC_Os03g04080	26.33	25.29	22.28	2.56	-23.02	-2.03	3.43	1.33	35.27	6.49	1.02	-7.46	-30.59	-13.41	-0.59	20.64	-2.89	13.60
K23746	LOC_Os02g7880	7.52	-1.12	-8.07	11.60	11.83	8.78	-8.22	-4.86	7.54	-7.10	14.60	-6.89	9.01	1.51	-7.93	5.51	15.31	6.02
K31942	LOC_Os06g2890	16.33	0.09	-8.07	11.60	11.83	8.78	-8.22	-4.86	7.54	-7.10	14.60	-6.89	9.01	1.51	-7.93	5.51	15.31	6.02
K17446	LOC_Os06g48700	-6.08	3.47	0.12	7.53	5.16	5.16	-8.92	-8.92	7.53	-11.21	5.72	-31.13	-31.13	-31.13	-9.60	14.01	-5.71	13.93
K21120	LOC_Os06g48700	12.80	26.39	5.02	-0.59	-1.02	5.30	-1.47	1.64	9.81	-1.46	3.55	1.19	-1.46	3.82	9.02	-1.03	-2.57	-0.04

Decreased compared to WT

Increased compared to WT

All highlighted percentage differences are statistically significant (p≤ 0.05).

Table 2. Natural accession of *A. thaliana* used in this work.

Group	Accession	Zn concentration by ICP-MS ^a
Low Zn accessions	Fab-2	41.15
	Rev-2	70.44
	Pn-0	78.6
	Ste-3	79.31
	TAD 01	79.51
	T1060	80.03
	Shahdara	84.3
	Mc-0	84.54
	Wag-3	85.13
	TOU-E-11	87.79
Reference accession	Col-0	131.92
High Zn accessions	ZdrI 2-25	178.39
	Ull2-5	181.23
	Ob-1	182.69
	PHW-13	196.65
	Ors-2	196.76
	NC-6	201.48
	Uod-7	205.2
	Na-1	205.38
	Sav-0	238.5
	Kn-0	254.53

^a Data downloaded from the ionomics Atlas (<http://www.ionomicshub.org/ionomicsatlas/>).

Supplemental Table 1. Rice FOX lines used in this work.

Number	Line Number	Gene	KOME cDNA Number	Locus number
1	K02538	OsIRO2	J023035P08	LOC_Os01g72370
2	K15412	OsIRO2	J033041D19	LOC_Os01g72370
3	K02642	OsDMAS1	J033064L19	LOC_Os03g13390
4	K01905	OsDMAS1	J033064L19	LOC_Os03g13390
5	K14626	OsVIT2	J023101O19	LOC_Os09g23300
6	K30225	OsVIT2	J023101O19	LOC_Os09g23300
7	K36331	OsVIT2	J023101O19	LOC_Os09g23300
8	K32620	OsFER2	J033088E01	LOC_Os12g01530
9	K30712	OsNRAMP1	J033132H19	LOC_Os07g15460
10	K18030	OsNRAMP6	J013089K10	LOC_Os01g31870
11	K34146	OsNRAMP6	J013164K10	LOC_Os01g31870
12	K13416	OsNRAMP7	J023095G02	LOC_Os12g39180
13	K34306	OsNRAMP7	J023095G02	LOC_Os12g39180
14	K21926	OsZIP6	J033138E20	LOC_Os05g07210
15	K33648	OsZIP6	J033138E20	LOC_Os05g07210
16	K36532	OsZIP6	J033138E20	LOC_Os05g07210
17	K11313	OsZIP7	J023087M13	LOC_Os05g10940
18	K27616	OsZIP7	J023087M13	LOC_Os05g10940
19	K11508	OsZIP8	J013157C18	LOC_Os02g10230
20	K37429	OsZIP8	J013157C18	LOC_Os02g10230
21	K09221	OsZIP14	J033089E10	LOC_Os08g36420
22	K18128	OsZIP14	J033089E10	LOC_Os08g36420
23	K08632	OsYSL6	J013070E15	LOC_Os04g32050
24	K32237	OsYSL7	J023003B17	LOC_Os02g02450
25	K37642	OsYSL7	J023003B17	LOC_Os02g02450
26	K20105	OsYSL12	J023023O07	LOC_Os04g44320
27	K29309	OsYSL13	J013096O22	LOC_Os04g44300
28	K06540	OsYSL13	J013096O22	LOC_Os04g44300
29	K02304	OsFRDL4	J013001B22	LOC_Os12g01580
30	K16426	OsPCS1	J013081H24	LOC_Os06g01260
31	K26346	OsPCS1	J023112B16	LOC_Os06g01260
32	K21701	OsZIFL4	J023019M18	LOC_Os11g04020
33	K35343	OsZIFL5	J013072J11	LOC_Os11g04030
34	K04142	OsZIFL5	J013072J11	LOC_Os11g04030
35	K21705	OsZIFL7	J023109G16	LOC_Os11g04104

36	K24919	OsZIFL12	J033105E18	LOC_Os12g03899
37	K29419	OsZIFL12	J033105E18	LOC_Os12g03899
38	K30332	OsOPT3	J013116J20	LOC_Os06g03560
39	K07130	OsMTP1	J023117P18	LOC_Os05g03780
40	K07728	OsMTP1	J023117P18	LOC_Os05g03780
41	K27745	OsMTP1	J023117P18	LOC_Os05g03780
42	K20149	ONAC103	J013157G23	LOC_Os07g48450
43	K21349	OsNAC4/ONAC068	J033069M07	LOC_Os01g60020
44	K21218	LOC_Os08g01120 ^A	J033145N05	LOC_Os08g01120
45	K05312	LOC_Os03g60480 ^B	J023043H06	LOC_Os03g60480
46	K14729	LOC_Os03g60480 ^B	J023043H06	LOC_Os03g60480
47	K18320	LOC_Os03g60480 ^B	J023043H06	LOC_Os03g60480
48	K23746	LOC_Os02g07880 ^C	J013098C06	LOC_Os02g07880
49	K31942	LOC_Os08g12890 ^C	J023108H08	LOC_Os08g12890
50	K17446	LOC_Os06g48700 ^C	J023006H21/ J013124K03	LOC_Os06g48700/ LOC_Os05g3326
51	K21120	LOC_Os06g48700 ^C	J023006H21	LOC_Os06g48700

^A Homologous to At2g25680 (MOT1)

^B Homologous to At5g02600 (FN mutant 13631)

^C Homologous to At4g31350 (similar ionomics profile to dir10)

Supplemental Table 2. Primers used in this work.

Primer name	Sequence 5' è 3'	Purpose
AtIRT1_XhoI_F	AATCTCGAGATGAAAACAATCTCCTCGTACTCA	Cloning AtIRT1 in pDR195
AtIRT1_BamHI_R	AATGGATCCTTAAGCCCATTGGCGATAA	Cloning AtIRT1 in pDR195
OsZIP7_XhoI_F	AATCTCGAGATGGAGCGGGTCGTGCAGT	Cloning OsZIP7 in pDR195
OsZIP7_BamHI_R	AATGGATCCTCAGGCCAGATTGCAAG	Cloning OsZIP7 in pDR195
OsZIP7_pENTR_F	CACCATGGAGCGGTTCTGCAGT	Cloning OsZIP7 in pENTR
OsZIP7_pENTR_NS_R	GGCCCAGATTGCAAGGGAT	Cloning OsZIP7 in pENTR
OsZIP7_Nterm_F	GGTCGTGCAGTTCTTGAGG	Expression in FOX lines
OsZIP7_Nterm_R	GTGCAGCATGTGGACGAA	Expression in FOX lines
OsZIP7_Cterm_F	CTCTAGTGGTGGAGGGCATC	Expression in FOX lines
OsZIP7_Cterm_R	GCAAGGGATGACATGGAGAG	Expression in FOX lines

6. Legends to Figures

Figure 1. The OsZIP7-OE lines accumulate higher Zn in leaves. Zn concentrations of Col-0, K11313-OsZIP7 and K27616-OsZIP7 were determined by ICP-MS. Black line represents the median, box edges 1st and 3rd quartile and bars minimum and maximum values. One-way ANOVA and Tukey HSD were performed to show significant changes ($n = 12$).

Figure 2. Functional complementation of yeast mutant strains. Empty pDR195 vector, pDR195-OsZIP7 or pDR195-AtIRT1 constructs were transformed into yeast cells. Liquid cultures were diluted as indicated before plating. (A) Zn-uptake defective strain *zrt1zrt2* growing under Zn-sufficient (10 μ M Zn) or Zn-deficient (no Zn added) transformed with each construct. (B) Fe-uptake defective strain *fet3fet4* growing under Fe-sufficient (pH 5.3) or Fe-deficient (pH 6.0) transformed with each construct. (C) Wild-type strain BY4347 growing under control, 20 μ M or 50 μ M Cd conditions, transformed with each construct.

Figure 3. Subcellular localization of OsZIP7-YFP construct in *A. thaliana* mesophyll protoplast after transient transformation. The upper images show Figure OsZIP7-YFP transformed protoplast, and YFP signal at the plasma membrane. Mid and lower images show protoplasts co-transformed with OsZIP-OE and plasma membrane marker AHA2-RFP. Both signals are observed at the plasma membrane. Imaging was performed with a Nikon Eclipse Ti inverted microscope stand, and image capture and processing was performed with Nikon Elements software.

Figure 4. *A. thaliana* OsZIP7-OE lines show higher sensitivity to excessive Zn. (A) Seeds were sowed on Gamborg's B5 with vitamins plus 2% sucrose. After 5 days, seedlings were transferred to minimal media containing the indicated concentrations of Zn. Pictures were taken after 15 days of treatment. Left: WT; Center: OsZIP7-OE1; Right: OsZIP7-OE2. Shoot fresh weight (B) and root length (C) measurements were performed to quantify the changes observed. Red lines show the longest root for each line. Significant differences by t-test are shown (* = $p < 0.05$; ** = $p < 0.01$).

Figure 5. OsZIP7-OE plants show changes in Zn root to shoot translocation. (A) Zn concentration in shoots (A) and roots (B) of Col-0 and OsZIP7-OE plants grown under control, 50 μ M, 100 μ M e 200 μ M Zn conditions ($n = 5$). (C) Shoot-to-root ratio. Significant differences by t-test are shown (* = $p < 0.05$; ** = $p < 0.01$).

Figure 6. Seeds of OsZIP7-OE lines show higher abundance of Zn. (A) Zn SXRF tomogram of Col-0 and OsZIP7-OE. Tomograms were obtained using 250 ms dwell time, 7 μ m step size, at beamline X26A at the National Synchrotron Light Source (NSLS). (B) ICP- MS Zn concentrations in Col-0 and OsZIP7-OE lines. Significant differences by one-way ANOVA and Tukey HSD are shown ($n = 5$).

Figure 7. 2D SXRF leaf maps of Col-0, OsZIP7-OE and *glabrous-1* mutant. Leaves of 20 days-old plants were detached, placed on metal-free tape and scanned. Data was collected using 50 ms dwell time, 7 μ m step size at beamline 2-3 of SSRL (Stanford Synchrotron Radiation Lightsource). Maps show Zn localization in leaves of plants grown under control (A), 50 μ M Zn (C) and 100 μ M Zn (E), and Zn and Ca overlay of leaves from plants grown under control (B), 50 μ M Zn (D) and 100 μ M Zn (F).

Figure 8. Quantification of Zn total abundance in individual trichomes of maps from leaves shown in Figure 7. Total Zn abundance in trichomes was quantified using Region of Interest (ROI) analysis of leaves from OsZIP7-OE plants grown under control, and Col-0 and OsZIP7-OE plants grown under 50 μ M Zn and 100 μ M Zn. Significant differences by one-way ANOVA and Tukey HSD are shown.

Figure 9. High resolution 2D SXRF maps of fresh individual trichomes. Leaves of 20 days-old plants were detached, placed on metal-free tape and scanned. Data was collected using 50 ms dwell time, 2 μ m step size at beamline 2-3 of SSRL (Stanford Synchrotron Radiation Lightsource). Maps show localization of Zn in trichomes of Col-0 (A) and OsZIP7-OE (C), and Zn and Ca localization overlay of Col-0 (B) and OsZIP7-OE (D). Plants were grown under 50 μ M Zn-containing media.

Figure 10. High resolution SXRF maps of resin-embedded, sectioned trichomes. Leaves of 20 days-old plants of OsZIP7-OE plants were detached and included in silica nitrate

windows as described in methods. Data was collected at 2-ID-D beamline at APS (Advanced Photon Source). (A) Light microscope image of a sectioned trichome. Zn localization is shown in a trichome from a plant grown under control conditions (B) or under 50 μ M Zn (C). The Zn localization map of a second trichome from a plant grown under 50 μ M Zn is shown in high maximum pixel abundance scale in (D) and in low maximum pixel abundance scale in (E). Arrows in (C) and (D) show regions where Zn seems to “leak” from trichome cell to surrounding cells. Arrows in (E) show stretches resembling cytoplasm in trichome cells.

Figure 11. Zn abundance in trichomes of *A. thaliana* accessions with contrasting total leaf Zn concentrations. Leaves of 20 days-old plants growing under 50 μ M Zn were detached, placed on metal-free tape and scanned. (A) to (F) 2D SXRF leaf maps Zn and Zn and Ca overlay of Col-0 (A-B); Fab-2 (low Zn accession) (C-D); and Kn-0 (high Zn accession) (E-F). Data was collected using 50 ms dwell time, 7 μ m step size size at beamline 2-3 of SSRL (Stanford Synchrotron Radiation Lightsource). (G) Zn quantification in individual trichomes of the corresponding accessions. Total Zn abundance in trichomes was quantified using Region of Interest (ROI) analysis of leaves shown in Fig.7. Significant differences by one-way ANOVA and Tukey HSD are shown.

Figure 12. Correlation of the percentage of the total Zn in trichomes with mean Zn counts in whole leaf of 16 *Arabidopsis* accessions (as shown in Table 3). ROI analyses determined mean counts per pixel in whole leaf maps. Pearson correlation was used to show significance of the correlation. ($R = 0.6871, p < 0.05$).

7. Legends to Supplemental Figures

Supplemental Figure 1. Metal concentrations in shoots (A-D) and roots (E-H) of Col-0 and OsZIP7-OE plants grown under control, 50 μ M, 100 μ M e 200 μ M Zn conditions ($n = 5$). Concentrations of Mn (A, E), Fe (B, F), Cu (C, G) and Cd (D, H) are shown. Significant differences by t-test are shown (* = $p < 0.05$; ** = $p < 0.01$).

Supplemental Figure 2. Metal concentrations in seeds of Col-0 and OsZIP7-OE plants

(n = 5). Concentrations of Mn (A), Fe (B), Cu (C) and Cd (D) are shown. Significant differences by t-test are shown (* = p<0,05; ** = p < 0,01).

Supplemental Figure 3. High resolution 2D SXRF maps of fresh individual trichomes. Leaves of 20 days-old plants were detached, placed on metal-free tape and scanned. Data was collected using 50 ms dwell time, 2 μ m step size at beamline 2-3 of SSRL (Stanford Synchrotron Radiation Lightsource). Maps show localization of Fe (A, B), Mn (C, D), Cu (E, F) and K (G, H) in trichomes of Col-0 (A, C, E, G) and OsZIP7-OE (B, D, F, H) Plants were grown under 50 μ M Zn-containing media.

Figure 1

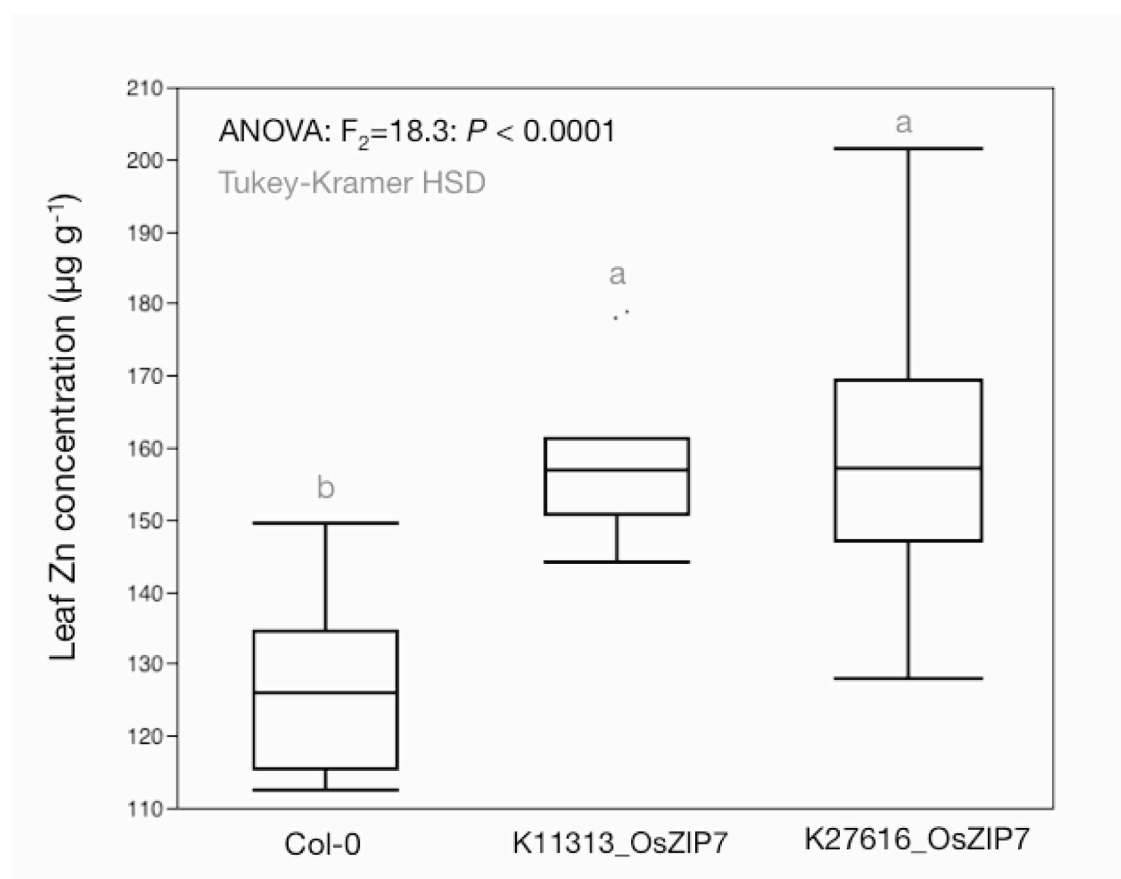


Figure 2

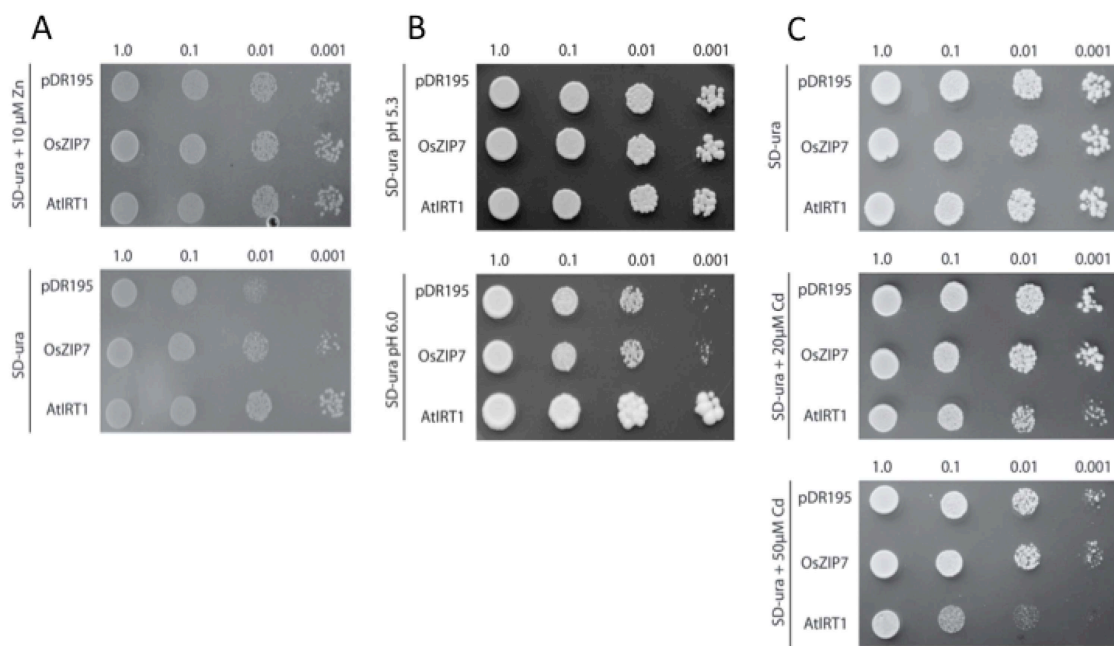


Figure 3

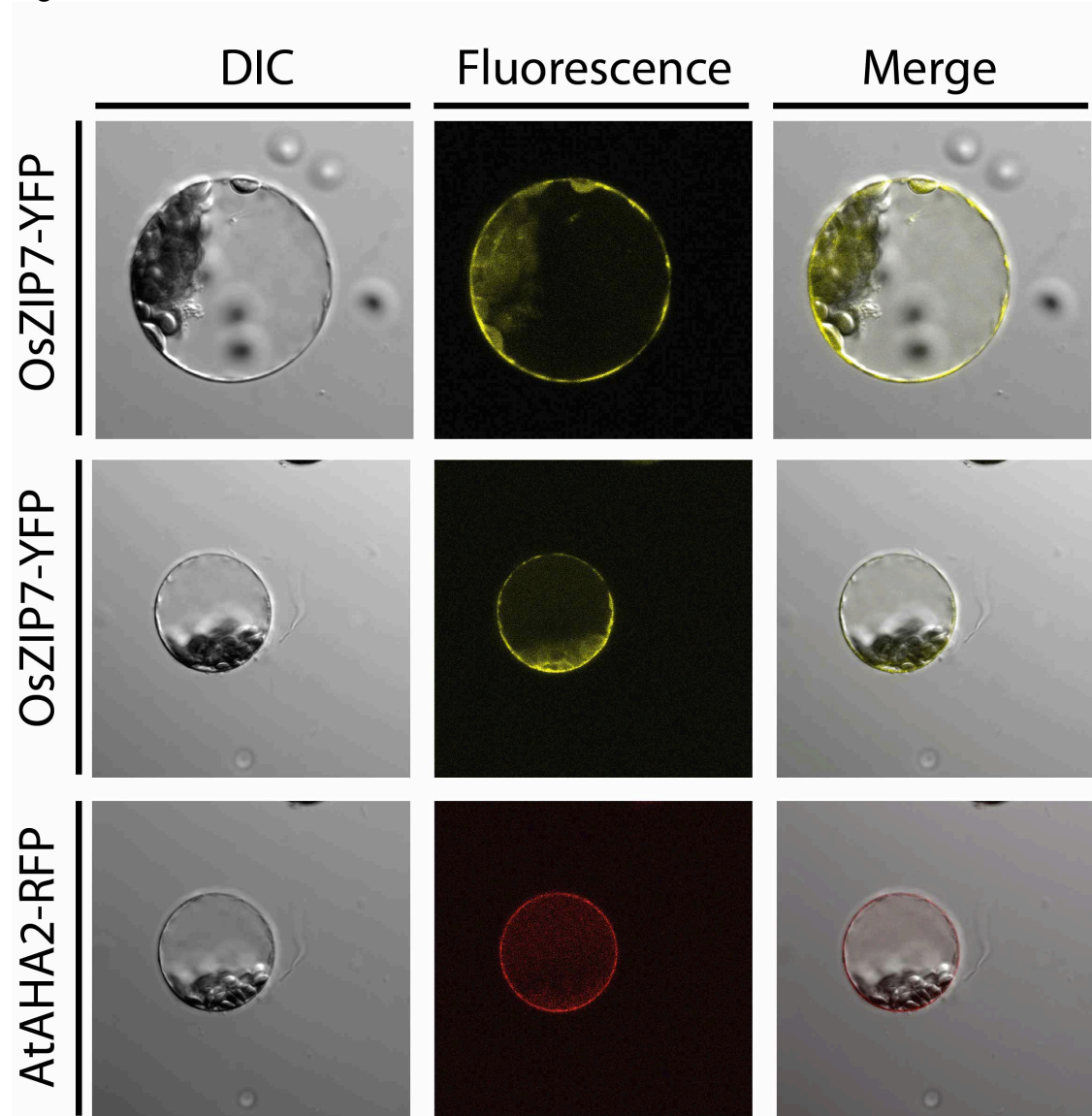


Figure 4

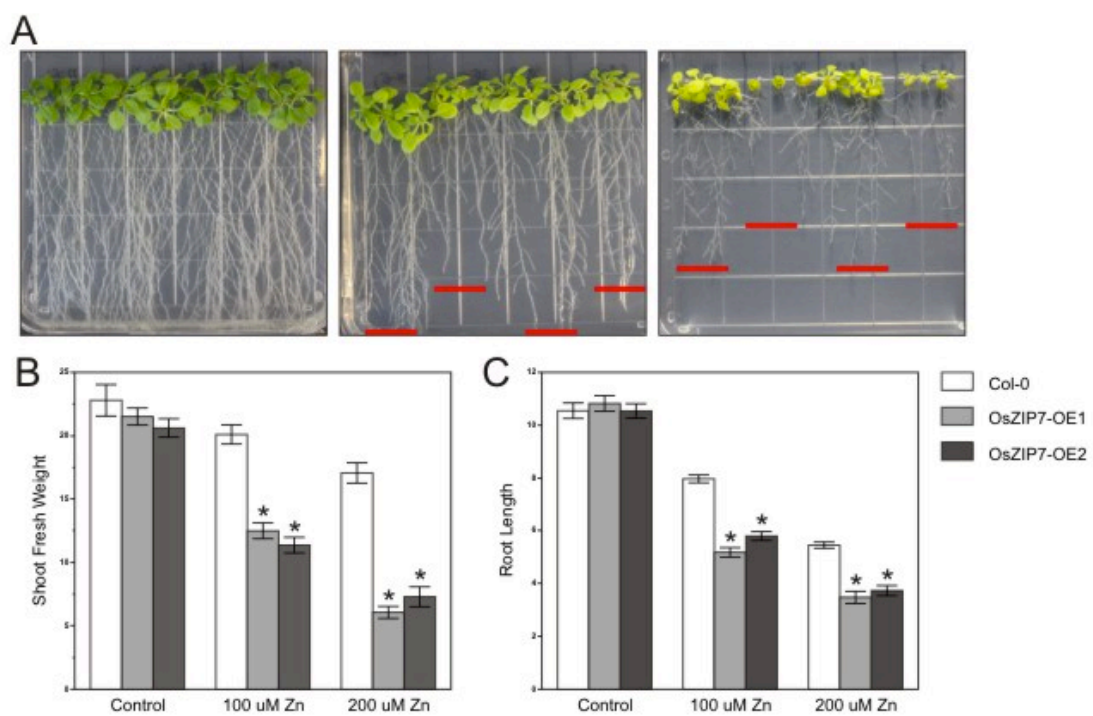


Figure 5

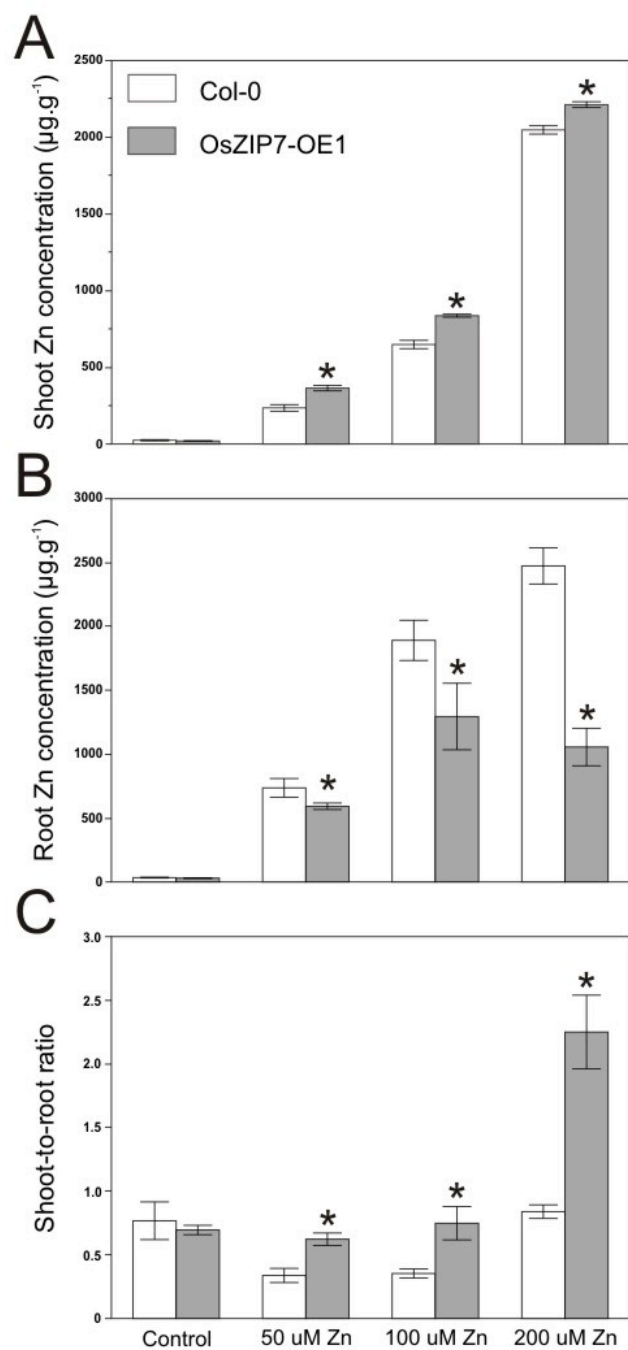


Figure 6

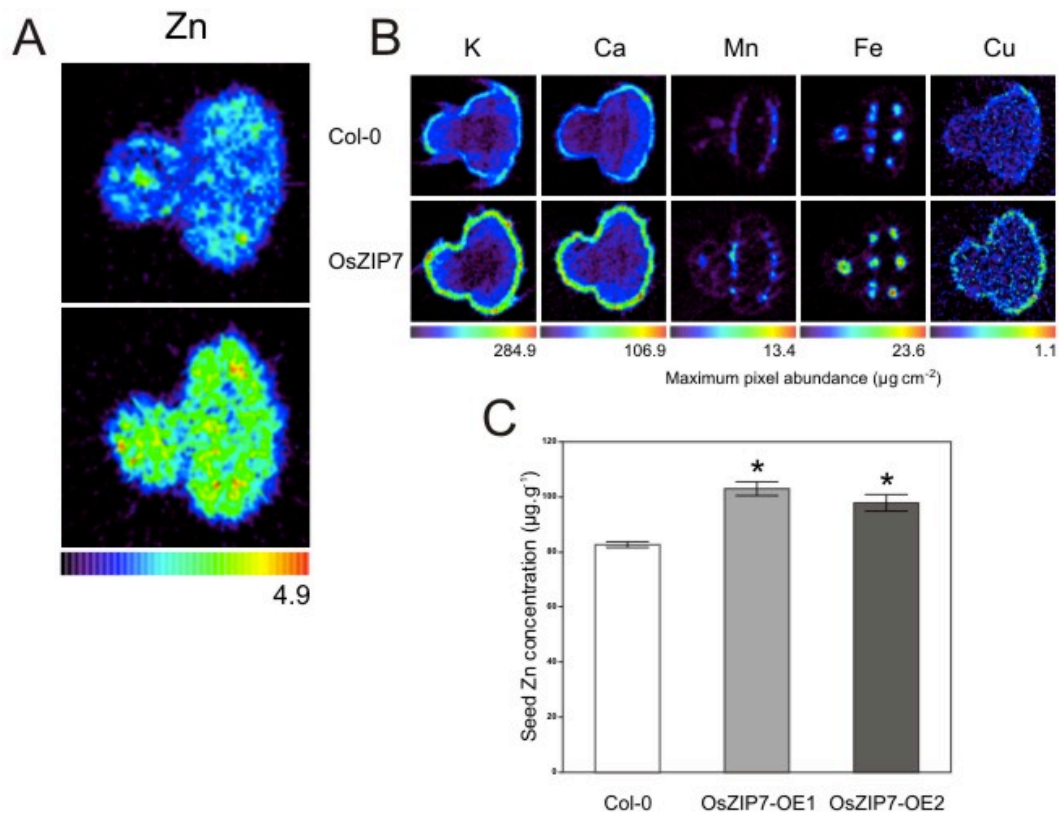


Figure 7

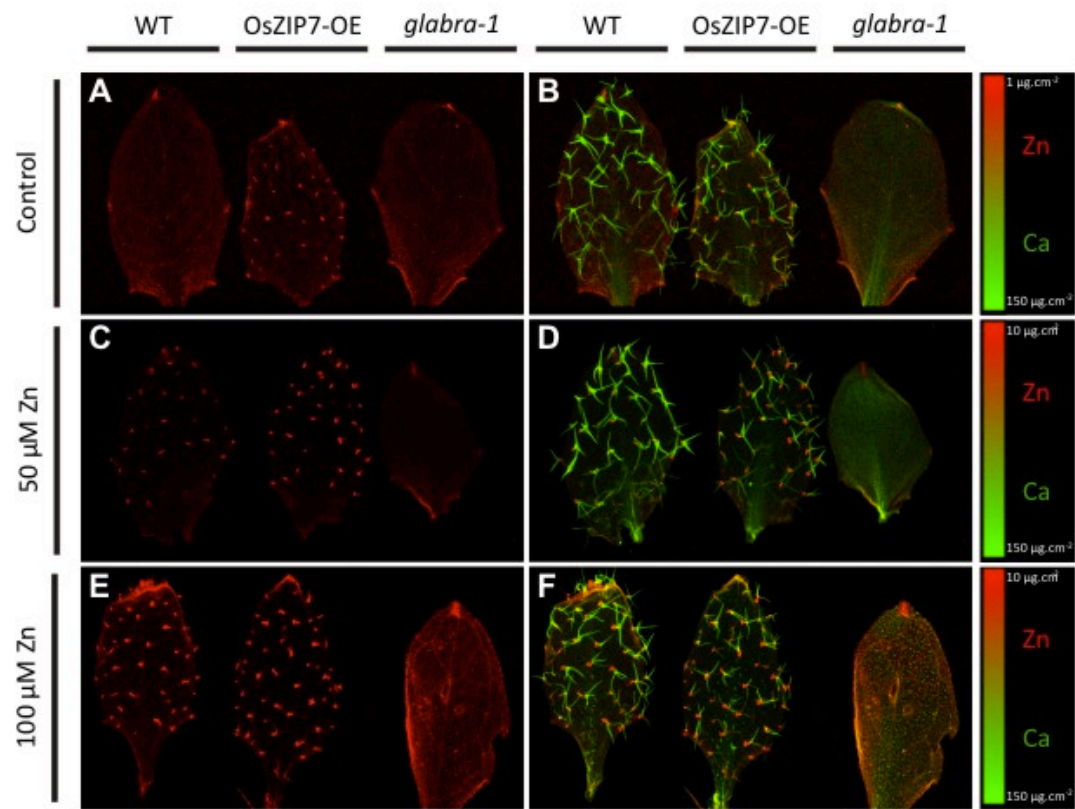


Figure 8

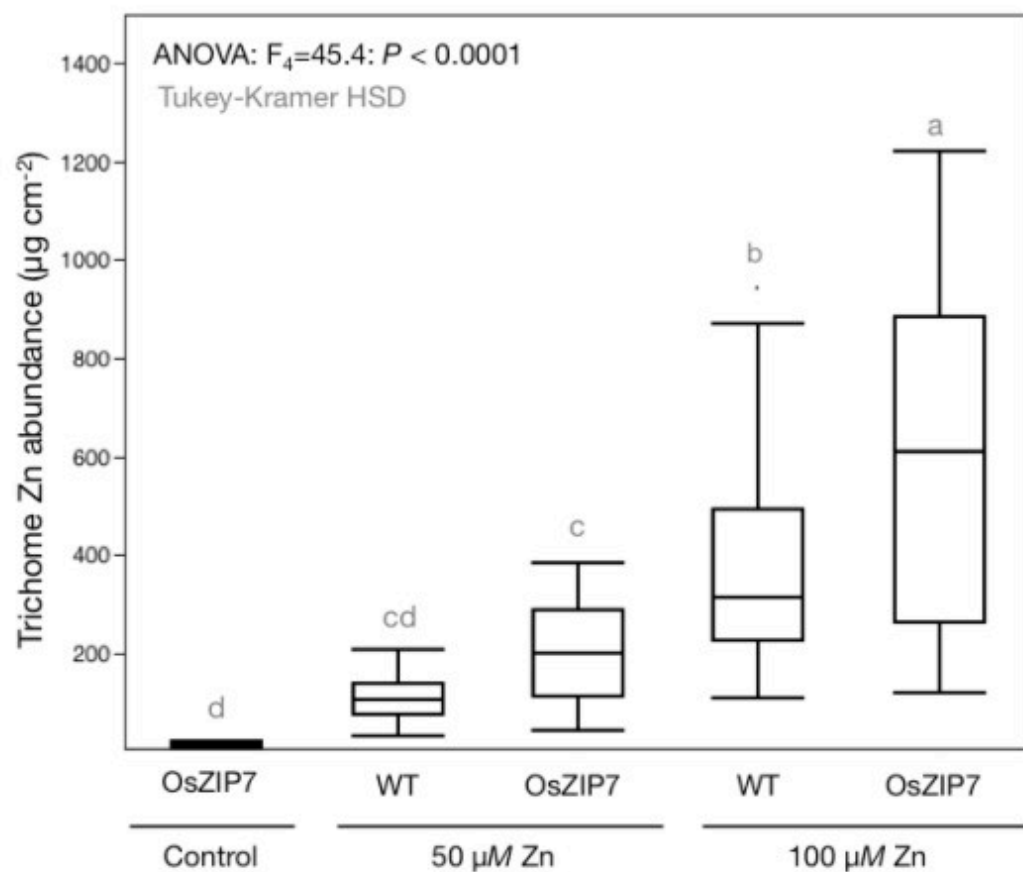


Figure 9

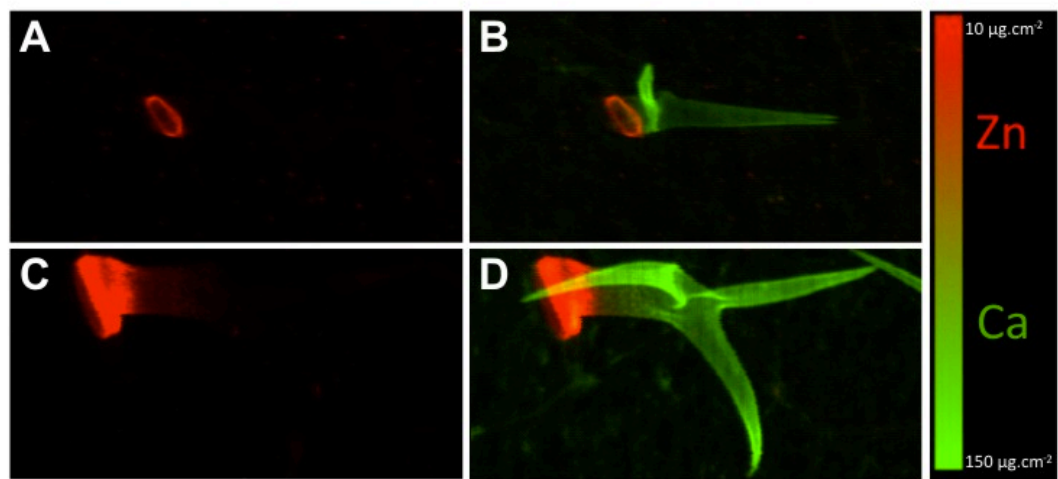


Figure 10

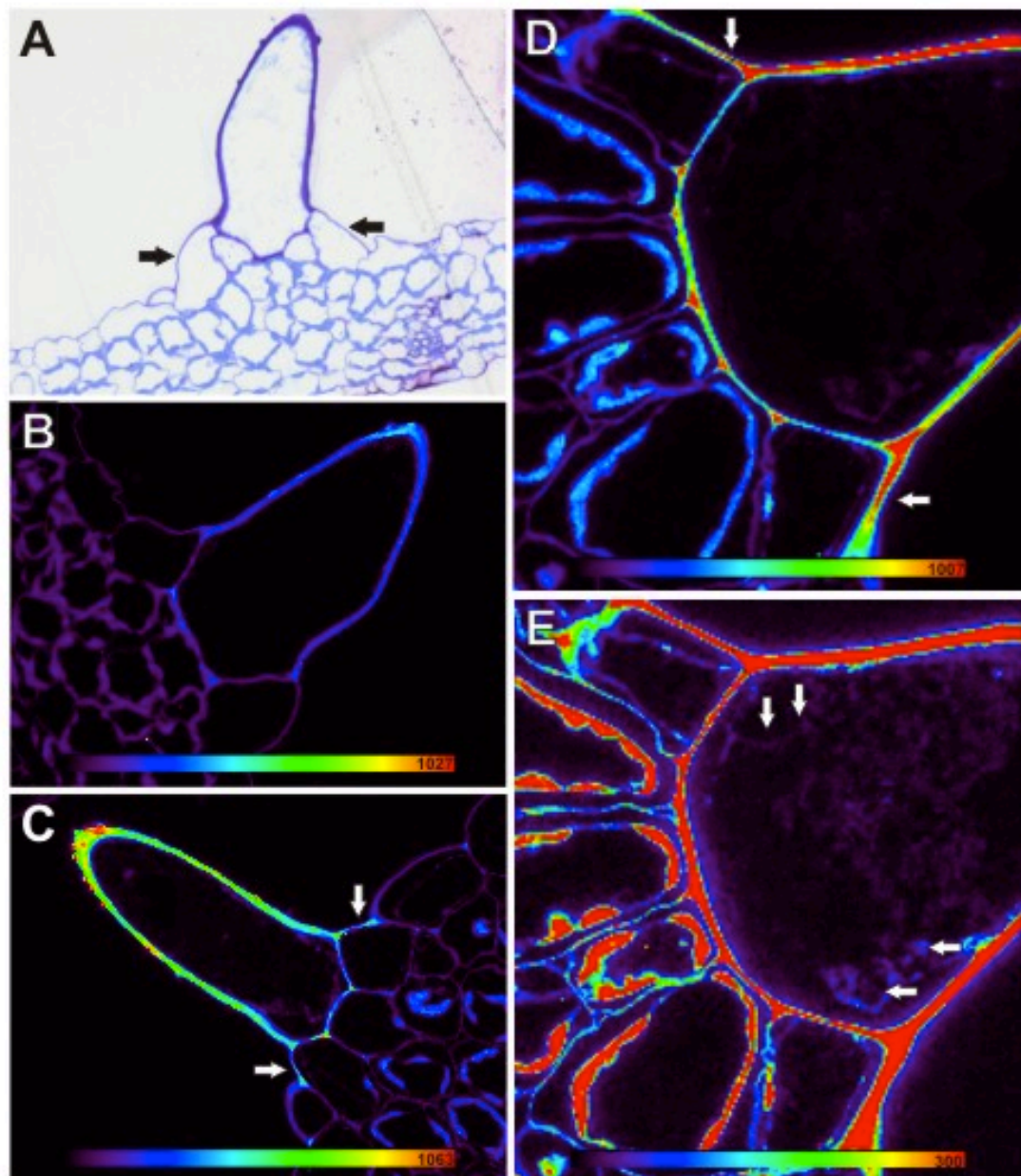


Figure 11

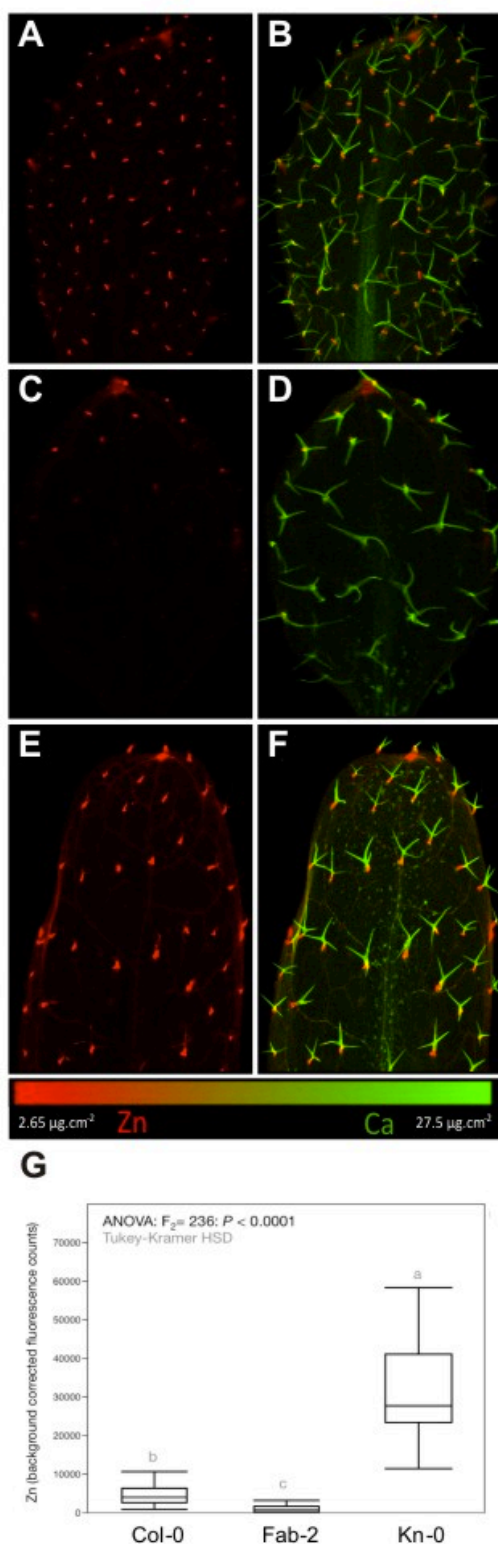
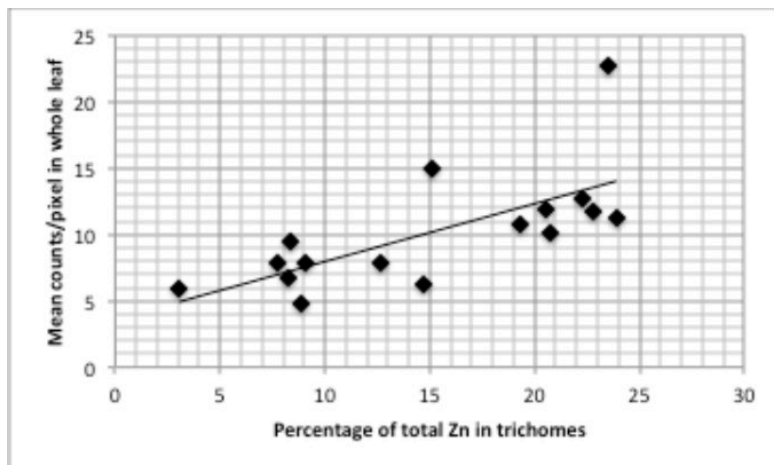
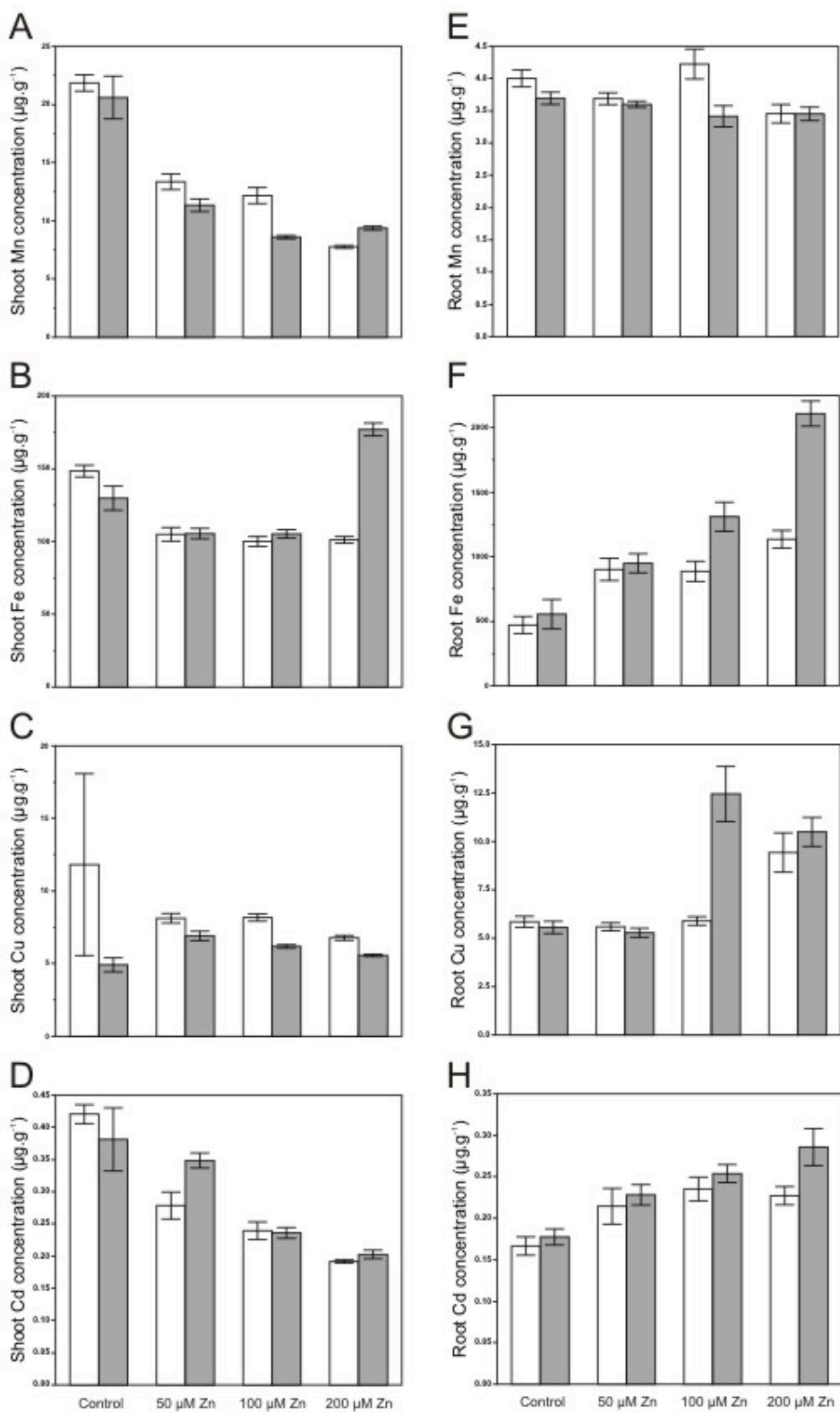


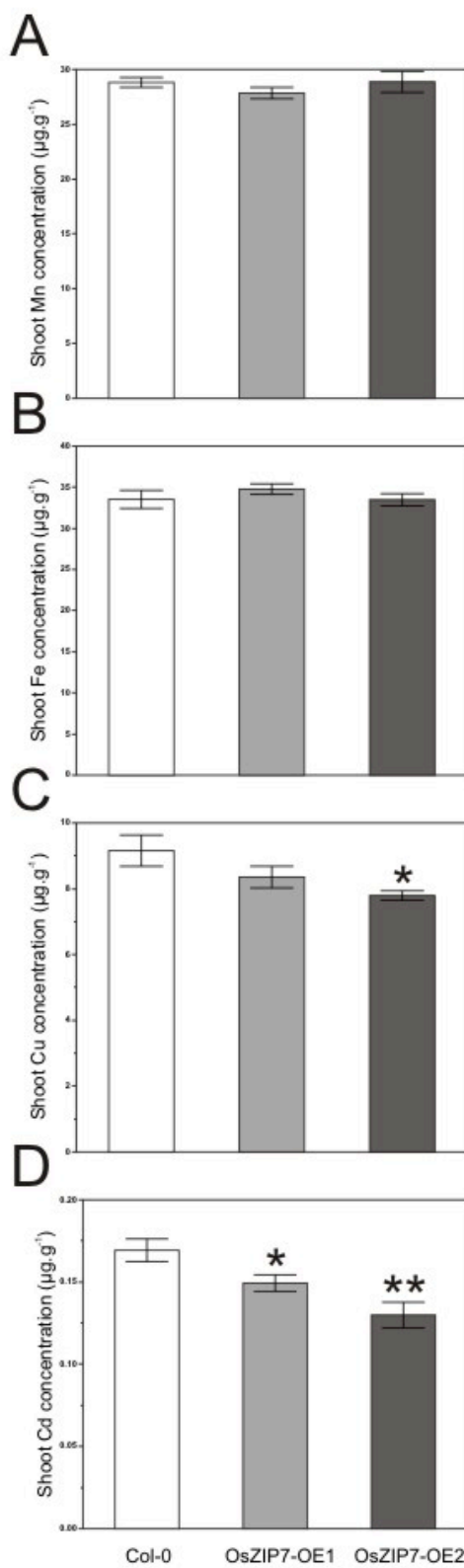
Figure 12



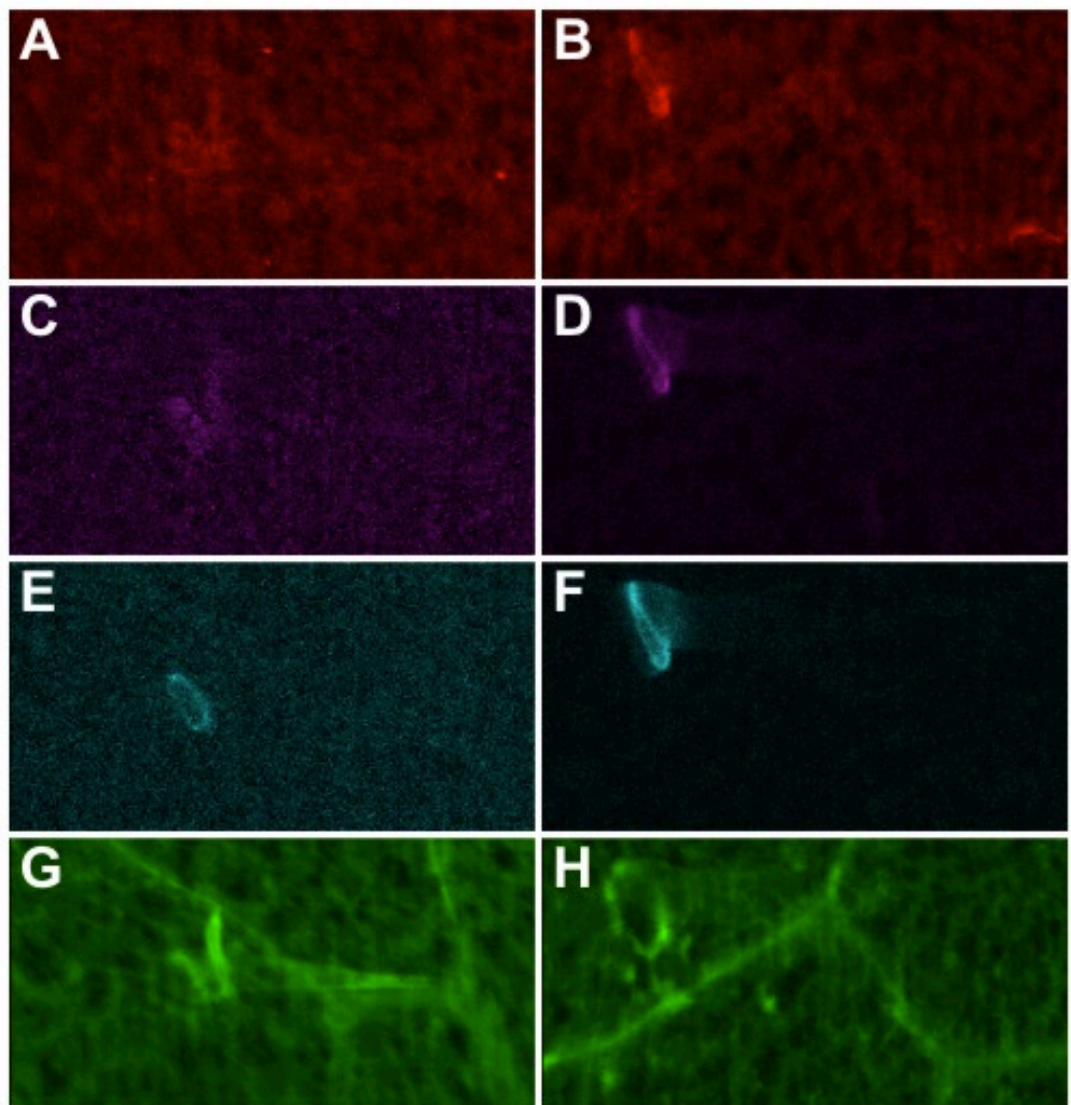
Supplemental Figure 1



Supplemental Figure 2



Supplemental Figure 3



Considerações Finais

1. Utilizando *A. thaliana* para transferir conhecimento de uma planta modelo para uma planta cultivada

A compreensão dos mecanismos responsáveis pela aquisição, distribuição e manutenção correta dos níveis de Fe e Zn em plantas ainda é incipiente, assim como pouco sabemos sobre os genes envolvidos nesses mecanismos. Até o momento, a maior parte do conhecimento adquirido é oriunda de trabalhos com a planta-modelo *Arabidopsis thaliana*, devido à rapidez de cultivo, estrutura genética conhecida, grande quantidade de mutantes disponíveis, facilidade na obtenção de plantas transgênicas e protocolos bem estabelecidos, tanto para estudos genéticos quanto bioquímicos (Ledford 2010, www.arabidopsis.org). *A. thaliana* não é uma planta de importância agronômica. Porém tem grande importância no desenvolvimento da genética e bioquímica vegetal, sendo importante para posterior transferência do conhecimento adquirido para plantas cultivadas, como arroz, trigo e milho. Destas, o arroz é a planta que mais se aproxima de ter as mesmas ferramentas disponíveis para a planta-modelo, estimulando iniciativas de cooperação como o *Rice 2020*, que visa coordenar esforços científicos para descrever a função de todos os genes presentes no genoma do arroz até 2020, similar ao projeto *Arabidopsis 2010* encerrado recentemente (Ledford 2010, Wang et al 2012).

Neste trabalho, foram utilizadas duas abordagens para a caracterização de genes relacionados à homeostase de Fe e Zn em plantas: na primeira, identificamos os homólogos do gene já descrito de *A. thaliana*, *AtZIF1*, que estão presentes no genoma de arroz e de outras gramíneas. Essa família gênica, denominada de *ZIF-Like*, passou por eventos de duplicação em monocotiledôneas, resultando em expansão linhagem-específica. Também caracterizamos o efeito de duplicações no número de cópias de genes *ZIFL* no genoma de arroz, além de demonstrar a regulação destes genes por excesso de Zn e deficiência de Fe. Na segunda abordagem, utilizamos linhagens de *A. thaliana* expressando genes de arroz, permitindo a análise simultânea do perfil ionômico de 51 linhagens independentes. Caracterizamos o transportador de arroz OsZIP7, localizado na membrana plasmática, e que altera a dinâmica de acúmulo de Zn em folhas de *A. thaliana*. Também demonstramos que o Zn é acumulado na base dos tricomas das

folhas, provavelmente no apoplasto, e que esse acúmulo funciona como mecanismo de detoxificação de Zn em excesso na planta-modelo.

2. A nomenclatura *OsZIFL4* deve ser adotada em detrimento à *TOM1*

Baseado em similaridade de sequência, identificamos genes da família *ZIFL* em genomas de oito espécies, que até o momento contava com apenas um membro caracterizado (Haydon e Cobbett 2007, Ricachenevsky et al 2011). Concomitantemente, foi publicada uma descrição completa da função da proteína OsZIFL4, denominada pelos autores como *TOM1* (Nozoye et al 2011). *TOM1* é essencial para a secreção de DMA na rizosfera pelas raízes, etapa inicial da estratégia II de aquisição de Fe e, por muito tempo, considerada a última proteína a ser identificada para a elucidação deste mecanismo (Nozoye et al 2011). Em concordância com os nossos resultados, transcritos de *TOM1* acumulam em resposta à deficiência de Fe em raízes, presumivelmente para aumentar a secreção de PS nessas condições.

Embora os dois trabalhos tenham sido publicados independentemente, o que justificaria a utilização de nomenclaturas distintas, a sequência codificante de *OsZIFL4/TOM1* é bastante similar à do gene *AtZIF1*, descrito anteriormente (Haydon e Cobbett 2007). *AtZIF1* e seus parálogos em *A. thaliana* *AtZIFL1* e *AtZIFL2* são comparadas com *TOM1* em uma análise filogenética em Nozoye et al (2011). Porém, mesmo fazendo referência à similaridade a genes *ZIF*, a nomenclatura *TOM* é adotada, inclusive para outros dois parálogos em arroz, *TOM2* e *TOM3* (em nosso trabalho, *OsZIFL5* e *OsZIFL7*). Assim, entendemos que a nomeclatura *OsZIFL4* deve ser adotada na literatura para este gene, assim como para os outros genes *OsZIFL* descritos em Ricachenevsky et al (2011). Em concordância com a nossa proposição, o banco de dados do genoma de arroz *Rice Annotation Project DataBase* (RAP-DB; <http://rapdb.dna.affrc.go.jp/>; Sakai et al 2013) associou o nome *OsZIFL4* ao *locus Os11g0134900*, que corresponde *locus LOC_Os11g04020* da base de dados utilizada no nosso trabalho (TIGR; <http://rice.plantbiology.msu.edu/>). A nomenclatura proposta por Ricachenevsky et al (2011) também foi associada aos *loci* de todos os genes *ZIFL* descritos.

3. As proteínas ZIFL possivelmente possuem funções no efluxo de moléculas da família NA/DMA em plantas de arroz

Inicialmente, a caracterização do mutante *zifl* de *A. thaliana* indicava que a proteína AtZIF1 estava ligada à homeostase de Zn, transportando para dentro do vacúolo Zn ligado a um quelante, Zn livre ou um quelante livre (Haydon e Cobbett 2007). Recentemente, um trabalho demonstrou que AtZIF1 está envolvida no transporte de NA para dentro do vacúolo em células de raízes, o que contribui para a detoxificação de Zn absorvido em excesso por AtIRT1 durante a resposta à deficiência de Fe (Haydon et al 2012). NA é o precursor de DMA, o PS secretado por OsZIFL4 (Figura 2). Interessantemente, OsZIFL4 não transporta NA, indicando que embora tenham afinidade por substratos similares, as duas proteínas possivelmente distinguem entre as moléculas de NA e DMA. Enquanto AtZIF1 está localizada no tonoplasto, OsZIFL4 é uma proteína de membrana (Haydon e Cobbett 2007, Nozoye et al 2011). Baseado nesses dados, é possível inferir que as proteínas ZIFL tem função no efluxo de moléculas semelhantes às da família NA/DMA, retirando-as do citoplasma, seja para o meio extracelular, como no caso de OsZIFL4/TOM1, ou para dentro do vacúolo como AtZIF1.

Nossos resultados demonstram que outros genes *ZIFL* são regulados por deficiência de Fe e/ou ao excesso de Zn, como o par de parálogos *OsZIFL7* e *OsZIFL12*, que respondem aos dois estresses em raízes (Ricachenevsky et al 2011, capítulo 1, Fig 8 e 10). Embora não seja uma premissa para o seu envolvimento na homeostase de metais, a regulação sugere que estas proteínas podem ter papel no transporte de NA ou DMA através de membranas e impacto direto na homeostase de metais. A função de DMA na aquisição de Fe por plantas de estratégia II foi extensivamente descrita; porém, sabe-se também que o Zn é mais eficientemente translocado para as folhas quando complexado a DMA, em comparação a Zn⁺² livre (Suzuki et al 2008), indicando que a molécula pode ter funções ainda não conhecidas no transporte de Fe e Zn.

Além disso, é possível que haja redundância parcial de função, com mais de uma proteína ZIFL atuando na secreção de PS. Quando analisamos a relação filogenética para identificar os ortólogos de *OsZIFL4* em outras gramíneas, os genes *SbZIFL14* e *BdZIFL7*

de sorgo e *Brachypodium* são os mais próximos (Ricachenevsky et al 2011; capítulo 1, Fig 2). No entanto, não há genes de milho no agrupamento. O gene mais próximo é *ZmZIFL7*, que está agrupado com o par *OsZIFL5/OsZIFL10*. Como milho sabidamente secreta PS, pode-se especular que *ZmZIFL7* é o candidato a desempenhar função da secreção, o que sugeriria que *OsZIFL5/OsZIFL10* também podem atuar de maneira semelhante. Experimentos determinando a localização subcelular das proteínas ZIFL, a identificação de seus substratos por meio de experimentos com oócitos de *Xenopus laevis* e/ou leveduras (Nozoye et al 2011, Haydon et al 2012), e o isolamento de mutantes com perda de função, deverão elucidar a função das proteínas ZIFL de maneira mais clara.

4. O uso de linhagens FOX permite a identificação de genes envolvidos na homeostase de metais de maneira rápida

Na segunda abordagem, nós utilizamos linhagens de *A. thaliana* super-expressando cDNAs de arroz para identificar genes cuja atividade altera o ionoma. A expressão de genes heterólogos é muito empregada no estudo de transportadores para identificar substratos, como nos experimentos de complementação de fenótipo de leveduras mutantes (Capítulo 2, Fig 2). Embora devamos ser cuidadosos ao inferir a função de uma proteína de arroz expressa em *A. thaliana*, nossos resultados demonstram, por mais de um método, que OsZIP7 é um transportador de Zn de membrana plasmática, indicando que a análise inicial do perfil ionômico das linhagens expressando OsZIP7, que mostra aumento nas concentrações de Zn, é robusta. As análises foram conduzidas em plantas T2 provenientes diretamente da base de dados RiceFOX, e os resultados foram obtidos após 7 semanas a partir do início do experimento. Assim, demonstramos não apenas o potencial das linhagens FOX na identificação de genes de arroz envolvidos na regulação do ionoma, mas também a capacidade de obtenção de dados de forma rápida. Esse potencial já foi descrito para a busca de genes envolvidos em outros processos (Yokotani et al 2009, Albinsky et al 2010, Dubouzet et al 2011, Anders et al 2012). Além de *A. thaliana* apresentar as vantagens já mencionadas, existe uma quantidade maior de informação sobre o ionoma desta planta-modelo, como o perfil de alteração em elementos que corresponde ao estado fisiológico de deficiência de Fe (Baxter et al 2008),

permitindo que alterações causadas por genes de arroz possam ser mais facilmente interpretadas, o que facilita a identificação de fenótipos.

5. Localização e dinâmica de acúmulo de Zn em tricomas de *A. thaliana* indicam um novo mecanismo de detoxificação em não-hiperacumuladores

Nossos achados demonstram que o acúmulo de Zn nos tricomas de *A. thaliana* é dependente da concentração de Zn nas folhas: tanto diferentes ecotipos quanto linhagens expressando OsZIP7, ambos com quantidades maiores de Zn nas folhas, apresentam uma porcentagem maior de Zn nos tricomas. Uma vez que as concentrações de Zn no ambiente em que plantas de *A. thaliana* se desenvolvem são relativamente baixos (Krämer 2010, Sinclair e Krämer 2012), é possível que o acúmulo em tricomas seja eficiente para tamponar variações de baixa escala, porém potencialmente tóxicas. Em hiperacumuladores como *A. halleri*, esse mecanismo inicial seria insuficiente para detoxificar Zn em quantidades elevadas, sendo necessário o acúmulo em células do mesófilo. Em concordância com o mecanismo proposto, experimentos preliminares com mutantes glabros de *A. thaliana* sugerem que a ausência de tricomas aumenta a sensibilidade da planta ao excesso de Zn (Ricachenevsky et al, dados não-publicados).

Provavelmente, as características de hipertolerância/hiperacumulação de *A. halleri* estão baseadas em dois mecanismos principais: eficiência na translocação de Zn por meio dos transportadores de efluxo do pericílio do tipo HMA, que carregam o xilema e levam à hiperacumulação em parte aérea (Hanikenne et al 2008); e detoxificação nas folhas, provavelmente baseada na função de transportadores vacuolares do tipo MTP em células do mesófilo, que acumulam Zn no vacúolo de forma não tóxica, levando à hipertolerância (Shahzad et al 2010). Para ambos os mecanismos, há maior número de cópias dos genes e/ou maior expressão no genoma de *A. halleri* do que em *A. thaliana* (Hanikenne et al 2008, Shahzad et al 2010).

No entanto, é provável que o mecanismo de detoxificação em vacúolo também seja importante em *A. thaliana*, já que a concentração de Zn em ecotipos distintos tem correlação positiva com a expressão de *AtMTP1* (Conn et al 2012). Assim, é possível especular um cenário no qual tanto o mecanismo de acúmulo de Zn nos tricomas quanto em vacúolos de células do mesófilo sejam importantes quando a concentração de Zn

atinge níveis potencialmente tóxicos. Mesmo em *A. halleri*, que também é hipertolerante/hiperacumuladora de Cd, Huguet et al (2012) sugere que em baixas concentrações a detoxificação de Cd nos tricomas pode ser o primeiro mecanismo utilizado, enquanto que o acúmulo no mesófilo passa a ter importância apenas em concentrações mais altas.

Referências Gerais

- Abou-khalifa AAB, Misra AN, Salem AEAKM (2008) Effect of leaf cutting on physiological traits and yield of two rice cultivars. *African Journal of Plant Science*, 2: 147-150.
- Ager FJ, Ynsa MD, Dominguez Solis JR, Lopez Martin MC, Gotor C, Romero LC (2003) Nuclear micro-probe analysis of *Arabidopsis thaliana* leaves. *Nuclear Instruments and Methods in Physics Research Section B* 210: 401–406.
- Alberts IL, Nadassy K, Wodak SJ (1998) Analysis of zinc binding sites in protein crystal structures. *Protein Science*, 7: 1700–1716.
- An L, Zhou Z, Yan A, Gan Y (2011) Progress on trichome development regulated by phytohormone signaling. *Plant Signal Behav* 6: 1959-1962.
- Anders N, Wilkinson MD, Lovegrove A, Freeman J, Tryfona T, Pellny TK, Weimar T, Mortimer JC, Stott K, Baker JM, Defoin-Platel M, Shewry PR, Dupree P, Mitchell RA (2012) Glycosyl transferases in family 61 mediate arabinofuranosyl transfer onto xylan in grasses. *Proc Natl Acad Sci USA* 109: 989-93.
- Anderson GJ, McLaren GD, editors. *Iron physiology and patho-physiology in humans*. New York, NY : Humana Press, 2012.
- Andreini C, Banci L, Bertini I, Rosato A (2006) Counting the zinc-proteins encoded in the human genome. *J Proteome Res* 5: 196-201.
- Arabidopsis Genome Initiative (2000) Analysis of the genome sequence of the flowering plant *Arabidopsis thaliana*. *Nature* 408: 796-815.
- Arosio P, Ingrassia R, Cavadini P (2009) Ferritins: a family of molecules for iron storage, antioxidation and more. *Biochim Biophys Acta* 1790: 589-599.
- Arrivault S, Senger T, Krämer U (2006) The *Arabidopsis* metal tolerance protein AtMTP3 maintains metal homeostasis by mediating Zn exclusion from the shoot under Fe deficiency and Zn oversupply. *Plant J* 46: 861–879.
- Arulanantham AR, Rao IM, Terry N (1990) Limiting factors in photosynthesis. VI. Regeneration of ribulose 1,5-biphosphate limits photosynthesis at low photochemical capacity. *Plant Physiology* 93: 1466-1475.

- Atwell S, Huang YS, Vilhjálmsson BJ, Willems G, Horton M, Li Y, Meng D, Platt A, Tarone AM, Hu TT, Jiang R, Muliyati NW, Zhang X, Amer MA, Baxter I, Brachi B, Chory J, Dean C, Debieu M, de Meaux J, Ecker JR, Faure N, Kniskern JM, Jones JD, Michael T, Nemri A, Roux F, Salt DE, Tang C, Todesco M, Traw MB, Weigel D, Marjoram P, Borevitz JO, Bergelson J, Nordborg M (2010) Genome-wide association study of 107 phenotypes in *Arabidopsis thaliana* inbred lines. *Nature* 465: 627-631.
- Barak P, Helmke PA (1993) The chemistry of zinc. In: Robson, A (ed.) Zinc in Soils and Plants. Kluwer Academic Publishers, Dordrecht, 208 p.
- Barker AV, Pilbeam DJ eds. (2007) Handbook of Plant Nutrition, Taylor & Francis, Boca Raton, 613 p.
- Bashir K, Inoue H, Nagasaka S, Takahashi M, Nakanishi H, Mori S, Nishizawa NK (2006) Cloning and characterization of deoxymugineic acid synthase genes from graminaceous plants *J Biol Chem* 281:32395–32402.
- Bashir K, Ishimaru Y, Shimo H, Nagasaka S, Fujimoto M, Takanashi H, Tsutsumi N, An G, Nakanishi H, Nishizawa NK (2011) The rice mitochondrial iron transporter is essential for plant growth. *Nat Commun* 2:322.
- Baxter I, Ouzzani M, Orcun S, Kennedy B, Jandhyala SS, Salt DE (2007) Purdue ionomics information management system. An integrated functional genomics platform. *Plant Physiol* 143: 600-611.
- Baxter IR, Vitek O, Lahner B, Muthukumar B, Borghi M, Morrissey J, Guerinot ML, Salt DE (2008a) The leaf ionome as a multivariable system to detect a plant's physiological status. *Proc Natl Acad Sci USA* 105: 120811208–6.
- Baxter I, Muthukumar B, Park HC, Buchner P, Lahner B, Danku J, Zhao K, Lee J, Hawkesford MJ, Guerinot ML, Salt DE (2008b) Variation in molybdenum content across broadly distributed populations of *Arabidopsis thaliana* is controlled by a mitochondrial molybdenum transporter (MOT1). *PLoS Genet* 4: e1000004.
- Baxter I, Hosmani PS, Rus A, Lahner B, Borevitz JO, Muthukumar B, Mickelbart MV, Schreiber L, Franke RB, Salt DE (2009) Root suberin forms an extracellular barrier that affects water relations and mineral nutrition in *Arabidopsis*. *PLoS Genet* 5: e1000492.

- Baxter I, Hermans C, Lahner B, Yakubova E, Tikhonova M, Verbruggen N, Chao DY, Salt DE (2012) Biodiversity of mineral nutrient and trace element accumulation in *Arabidopsis thaliana*. PLoS One 7: e35121.
- Becher M, Talke IN, Krall L, Krämer U (2004) Cross-species microarray transcript profiling reveals high constitutive expression of metal homeostasis genes in shoots of the zinc hyperaccumulator *Arabidopsis halleri*. Plant J. 37: 251–268.
- Blamey FPC, Joyce DC, Edwards DG, Asher CJ (1986) Role of trichomes in sunflower tolerance to manganese toxicity. Plant Soil 91: 171-180
- Briat JF (2002) Metal ion-activated oxidative stress and its control. In: Inze, D, Van Montagu, M (eds.) Oxidative Stress in Plants. Taylor & Francis, London, pp. 171–190.
- Briat JF, Curie C Gaymard F (2007) Iron utilization and metabolism in plants. Current Opinion in Plant Biology 10: 276–282.
- Broadley MR, White PJ, Hammond JP, Zelko I, Lux A (2007) Zinc in plants. New Phytologist, 173: 677-702.
- Brown TA (2006) Genomes, 3rd edition. Garland Science, Manchester, 750 p.
- Buescher E, Achberger T, Amusan I, Giannini A, Ochsenfeld C, Rus A, Lahner B, Hoekenga O, Yakubova E, Harper JF, Guerinot ML, Zhang M, Salt DE, Baxter IR (2010) Natural genetic variation in selected populations of *Arabidopsis thaliana* is associated with ionic differences. PLoS One 5: e11081.
- Cardoso MZ (2008) Herbivore handling of a Plants trichome: The case of *Heliconius charithonia* (L.) (Lepidoptera: Nymphalidae) and *Passiflora lobata* (Killip) Hutch. (Passifloraceae) Neotrop Entomol 37:247–252.
- Carey AM, Norton GJ, Deacon C, Scheckel KG, Lombi E, Punshon T, Guerinot ML, Lanzirotti A, Newville M, Choi Y, Price AH, Meharg AA (2011) Phloem transport of arsenic species from flag leaf to grain during grain filling. New Phytol 192: 87-98.
- Carey AM, Scheckel KG, Lombi E, Newville M, Choi Y, Norton GJ, Price AH, Meharg AA (2012) Grain accumulation of selenium species in rice (*Oryza sativa* L.). Environ Sci Technol 46:5557-5564.
- Chao DY, Silva A, Baxter I, Huang YS, Nordborg M, Danku J, Lahner B, Yakubova E, Salt DE (2012) Genome-wide association studies identify heavy metal ATPase3 as

the primary determinant of natural variation in leaf cadmium in *Arabidopsis thaliana*. PLoS Genet 8: e1002923.

- Chauveau O, Eggers L, Raquin C, Silvério A, Brown S, Couloux A, Cruaud C, Kaltchuk-Santos E, Yockteng R, Souza-Chies TT, Nadot S, Cheng L, Wang F, Shou H, Huang F, Zheng L, He F, Li J, Zhao FJ, Ueno D, Ma FJ, Wu P (2007) Mutation in nicotianamine aminotransferase stimulated the Fe(II) acquisition system and led to iron accumulation in rice. Plant Physiol 145: 1647–1657 (2011) Evolution of oil-producing trichomes in *Sisyrinchium* (Iridaceae): insights from the first comprehensive phylogenetic analysis of the genus. Ann Bot 107: 1287-1312.
- Cobbett C, Goldsbrough P (2002) Phytochelatins and metallothioneins: roles in heavy metal detoxification and homeostasis. Annu Rev Plant Biol 53: 159–182.
- Conn SJ, Berninger P, Broadley MR, Gillham M (2012) Exploiting natural variation to uncover candidate genes that control element accumulation in *Arabidopsis thaliana*. New Phytol 193: 859-66.
- Connolly EL, Fett JP, Guerinot ML (2002) Expression of the IRT1 metal transporter is controlled by metals at the levels of transcript and protein accumulation. Plant Cell. 14: 1347–1357.
- Cousins RJ (2006) Mammalian zinc transport, trafficking, and signals, J Biol Chem 281: 24085–24089.
- Curie C, Cassin G, Couch D, Divol F, Higuchi K, Le Jean M, Misson J, Schikora A, Czernic P, Mari S (2009) Metal movement within the plant: contribution of nicotianamine and yellow stripe 1-like transporters. Ann Bot 103: 1-11.
- Curie C, Panaviene Z, Loulergue C, Dellaporta SL, Briat JF, Walker EL (2001) Maize yellow stripe1 encodes a membrane protein directly involved in Fe(III) uptake. Nature 409: 346–349.
- Deinlein U, Weber M, Schmidt H, Rensch S, Trampczynska A, Hansen TH, Husted S, Schjoerring JK, Talke IN, Krämer U, Clemens S (2012) Elevated nicotianamine levels in *Arabidopsis halleri* roots play a key role in zinc hyperaccumulation. Plant Cell 24: 708-723.
- Desbrosses-Fonrouge AG, Voigt K, Schröder A, Arrivault S, Thomine S, Krämer U (2005) *Arabidopsis thaliana* MTP1 is a Zn transporter in the vacuolar membrane

which mediates Zn detoxification and drives leaf Zn accumulation. FEBS Lett 579: 4165–4174.

- Distelfeld A, Pearce SP, Avni R, Scherer B, Uauy C, Piston F, Slade A, Zhao R, Dubcovsky J (2012) Divergent functions of orthologous NAC transcription factors in wheat and rice. *Plant Mol Biol* 78: 515-24.
- Donner E, Punshon T, Guerinot ML, Lombi E (2012) Functional characterisation of metal(loid) processes in planta through the integration of synchrotron techniques and plant molecular biology. *Anal Bioanal Chem* 402: 3287-3298.
- Drakakaki G, Christou P, Stöger E (2005) Constitutive expression of soybean ferritin cDNA in transgenic wheat and rice results in increased iron levels in vegetative tissues but not in seeds. *Transgenic Res* 9: 445-452.
- Dufner-Beattie J, Huang ZL, Geiser J, Xu W, Andrews GK (2005) *Mol Cell Biol* 25:5607–5615.
- Dufner-Beattie J, Huang ZL, Geiser J, Xu W, Andrews GK (2006) *Genesis* 44:239–251.
- Durrett TP, Gassmann W, Rogers EE (2007) The FRD3-mediated efflux of citrate into the root vasculature is necessary for efficient iron translocation. *Plant Physiol* 144: 197-205.
- Duy D, Stübe R, Wanner G, Philipp K (2011) The chloroplast permease PIC1 regulates plant growth and development by directing homeostasis and transport of iron. *Plant Physiol* 155: 1709-1722.
- Duy D, Wanner G, Meda AR, von Wirén N, Soll J, Philipp K (2007) PIC1, an ancient permease in *Arabidopsis* chloroplasts mediates iron transport. *Plant Cell* 19: 986-1006.
- Eide D, Broderius M, Fett J, Guerinot ML (1996) A novel iron-regulated metal transporter from plants identified by functional expression in yeast. *Proc Natl Acad Sci USA* 93: 5624–5628.
- Eren E, Arguello JM (2004) *Arabidopsis* HMA2, a divalent heavy metal- transporting PIB-type ATPase, is involved in cytoplasmic Zn²⁺ homeostasis. *Plant Physiol* 136: 3712–3723.

- Erenoglu EB, Kutman UB, Ceylan Y, Yildiz B, Cakmak I (2011) Improved nitrogen nutrition enhances root uptake, root-to-shoot translocation and remobilization of zinc ((65) Zn) in wheat. *New Phytol* 189: 438-448.
- Freeman JL, Marcus MA, Fakra SC, Devonshire J, McGrath SP, Quinn CF, Pilon-Smits EA (2012) Selenium Hyperaccumulator Plants *Stanleya pinnata* and *Astragalus bisulcatus* Are Colonized by Se-Resistant, Se-Excluding Wasp and Beetle Seed Herbivores. *PLoS One* 7: e50516.
- Fukada T, Civic N, Furuichi T, Shimoda S, Mishima K, Higashiyama H, Idaira Y, Asada Y, Kitamura H, Yamasaki S, Hojyo S, Nakayama M, Ohara O, Koseki H, Dos Santos HG, Bonafe L, Ha-Vinh R, Zankl A, Unger S, Kraenzlin ME, Beckmann JS, Saito I, Rivolta C, Ikegawa S, Superti-Furga A, Hirano T (2008) The zinc transporter SLC39A13/ZIP13 is required for connective tissue development; its involvement in BMP/TGF-beta signaling pathways. *PLoS One* 3: e3642.
- Fukada T, Kambe T (2011) Molecular and genetic features of zinc transporters in physiology and pathogenesis. *Metalomics* 3: 662-674.
- Fukada T, Yamasaki S, Nishida K, Murakami M, Hirano T (2011) Zinc homeostasis and signaling in health and diseases: Zinc signaling. *J Biol Inorg Chem* 16: 1123-1134.
- Goff SA, Ricke D, Lan TH, Presting G, Wang R, Dunn M, Glazebrook J, Sessions A, Oeller P, Varma H, Hadley D, Hutchison D, Martin C, Katagiri F, Lange BM, Moughamer T, Xia Y, Budworth P, Zhong J, Miguel T, Paszkowski U, Zhang S, Colbert M, Sun WL, Chen L, Cooper B, Park S, Wood TC, Mao L, Quail P, Wing R, Dean R, Yu Y, Zharkikh A, Shen R, Sahasrabudhe S, Thomas A, Cannings R, Gutin A, Pruss D, Reid J, Tavtigian S, Mitchell J, Eldredge G, Scholl T, Miller RM, Bhatnagar S, Adey N, Rubano T, Tusneem N, Robinson R, Feldhaus J, Macalma T, Oliphant A, Briggs S (2002) A draft sequence of the rice genome (*Oryza sativa* L. ssp. *japonica*). *Science* 296: 92-100.
- Gómez-Galera S, Rojas E, Sudhakar D, Zhu C, Pelacho AM, Capell T, Christou P (2010) Critical evaluation of strategies for mineral fortification of staple food crops. *Transgenic Research* 19: 165-180.
- Goto F, Yoshihara T, Shigemoto N, Toki S, Takaiwa F (1999) Iron fortification of rice seed by the soybean ferritin gene. *Nat Biotechnol* 17:282-286.

- Grebe M (2012) The patterning of epidermal hairs in *Arabidopsis*--updated. *Curr Opin Plant Biol* 15: 31-37.
- Green L, Rogers EE (2004) FRD3 controls iron localization in *Arabidopsis*. *Plant Physiol* 136: 2523-2531.
- Grotz N, Fox T, Connolly E, Park W, Guerinot ML, Eide D (1998) Identification of a family of zinc transporter genes from *Arabidopsis* that respond to zinc deficiency. *Proc. Natl. Acad. Sci. USA* 95: 7220-7224.
- Grusak MA (1994) Iron transport to developing ovules of *Pisum sativum*. I. Seed import characteristics and phloem iron-loading capacity of source regions. *Plant Physiol* 104: 649-655.
- Gu H, Zhu P, Jiao Y, Meng Y, Chen M (2011) PRIN: a predicted rice interactome network. *BMC Bioinformatics* 12:161.
- Guerinot ML, Yi Y (1994) Iron: Nutritious, Noxious, and Not Readily Available. *Plant Physiol* 104: 815-820.
- Guo WJ, Meetam M, Goldsbrough PB (2008) Examining the specific contributions of individual *Arabidopsis* metallothioneins to copper distribution and metal tolerance. *Plant Physiology* 146: 1697-706.
- Hanikenne M, Talke IN, Haydon MJ, Lanz C, Nolte A, Motte P, Kroymann J, Weigel D, Krämer U (2008) Evolution of metal hyperaccumulation required cis-regulatory changes and triplication of HMA4. *Nature* 453: 391-395.
- Haydon MJ, Cobbett CS (2007) A novel major facilitator superfamily protein at the tonoplast influences zinc tolerance and accumulation in *Arabidopsis*. *Plant Physiol.* 143: 1705-1719.
- Haydon MJ, Kawachi M, Wirtz M, Hillmer S, Hell R, Krämer U (2012) Vacuolar nicotianamine has critical and distinct roles under iron deficiency and for zinc sequestration in *Arabidopsis*. *Plant Cell* 24: 724-737.
- Helmy M, Tomita M, Ishihama Y (2011) OryzaPG-DB: rice proteome database based on shotgun proteogenomics. *BMC Plant Biol* 11:63.
- Higuchi K, Suzuki K, Nakanishi H, Yamaguchi H, Nishizawa NK, Mori S (1999) Cloning of nicotianamine synthase genes, novel genes involved in the biosynthesis of phytosiderophores. *Plant Physiol* 119: 471-480

Higuchi K, Watanabe S, Takahashi M, Kawasaki S, Nakanishi H, Nishizawa NK, Mori S (2001) Nicotianamine synthase gene expression differs in barley and rice under Fe-deficient conditions. *Plant J* 25: 159–167.

Hokura A, Onuma R, Kitajima N, Terada Y, Saito H, Abe T, Yoshida S, Nakai I (2006) 2-D X-ray Fluorescence Imaging of Cadmium Hyperaccumulating Plants by Using High-energy Synchrotron Radiation X-ray Microbeam. *Chem Lett* 35: 1246-1247.

Huang X, Kurata N, Wei X, Wang ZX, Wang A, Zhao Q, Zhao Y, Liu K, Lu H, Li W, Guo Y, Lu Y, Zhou C, Fan D, Weng Q, Zhu C, Huang T, Zhang L, Wang Y, Feng L, Furuumi H, Kubo T, Miyabayashi T, Yuan X, Xu Q, Dong G, Zhan Q, Li C, Fujiyama A, Toyoda A, Lu T, Feng Q, Qian Q, Li J, Han B (2012) A map of rice genome variation reveals the origin of cultivated rice. *Nature* 490: 497-501.

Huguet S, Bert V, Laboudigue A, Barthès V Isaure MP, Llorens I, Schat H, Sarret G (2012) Cd speciation and localization in the hyperaccumulator *Arabidopsis halleri*. *Environ Exp Bot* 82: 54–65.

Hussain D, Haydon MJ, Wang Y, Wong E, Sherson SM, Young J, Camakaris J, Harper JF, Cobbett CS (2004) P-type ATPase heavy metal transporters with roles in essential zinc homeostasis in *Arabidopsis*. *Plant Cell* 16: 1327–1339.

IBGE - Instituto Brasileiro de Geografia e Estatística. Levantamento Sistemático da Produção Agrícola. Disponível em:
http://www.ibge.gov.br/home/estatistica/indicadores/agropecuaria/lspa/default_publ_completa.shtml.

Inoue H, Higuchi K, Takahashi M, Nakanishi H, Mori S, Nishizawa NK (2003) Three rice nicotianamine synthase genes, OsNAS1, OsNAS2, and OsNAS3 are expressed in cells involved in long-distance transport of iron and differentially regulated by iron. *Plant J* 36: 366–381.

Inoue H, Kobayashi T, Nozoye T, Takahashi M, Kakei Y, Suzuki K, Nakazono M, Nakanishi N, Mori S, Nishizawa NK (2009) Rice OsYSL15 is an iron-regulated

iron(III)-deoxymugineic acid transporter expressed in the roots and is essential for iron uptake in early growth of the seedlings. *J Biol Chem* 284: 3470–3479.

IRGSP - International Rice Genome Sequencing Project. (2005) The map-based sequence of the rice genome. *Nature* 436: 793-800.

Isaure MP, Sarret G, Harada E, Choi YE, Marcus MA, Fakra SC, Geoffroy N, Pairis S, Susini J, Clemens S, Manceau A (2010) Calcium promotes cadmium elimination as vaterite grains by tobacco trichomes. *Geochim Cosmochim Acta* 74: 5817–5834.

Ishimaru Y, Kakei Y, Shimo H, Bashir K, Sato Y, Sato Y, Uozumi N, Nakanishi H, Nishizawa NK (2011) A rice phenolic efflux transporter is essential for solubilizing precipitated apoplastic iron in the plant stele. *J Biol Chem* 286: 24649–24655.

Ishimaru Y, Kim S, Tsukamoto T, Oki H, Kobayashi T, Watanabe S, Matsuhashi S, Takahashi M, Nakanishi H, Mori S, Nishizawa NK (2007) Mutational reconstructed ferric chelate reductase confers enhanced tolerance in rice to iron deficiency in calcareous soil *Proc Natl Acad Sci USA* 104: 7373–7378.

Ishimaru Y, Masuda H, Bashir K, Inoue H, Tsukamoto T, Takahashi M, Nakanishi H, Aoki N, Hirose T, Ohsugi R, Nishizawa NK (2010) Rice metal-nicotianamine transporter, OsYSL2, is required for the long-distance transport of iron and manganese *Plant J* 62: 379–390.

Ishimaru Y, Masuda H, Suzuki M, Bashir K, Takahashi M, Nakanishi H, Mori S, Nishizawa NK (2007) Overexpression of the OsZIP4 zinc transporter confers disarrangement of zinc distribution in rice plants. *J Exp Bot.* 58: 2909–2915.

Ishimaru Y, Suzuki M, Kobayashi T, Takahashi M, Nakanishi H, Mori S, Nishizawa NK (2005) OsZIP4, a novel zinc-regulated zinc transporter in rice. *J Exp Bot.* 56: 3207–3214.

Ishimaru Y, Suzuki M, Tsukamoto T, Suzuki K, Nakazono M, Kobayashi T, Wada Y, Watanabe S, Matsuhashi S, Takahashi M, Nakanishi H, Mori S, Nishizawa NK (2006) Rice plants take up iron as a Fe³⁺-phytosiderophore and as Fe²⁺. *Plant J* 45: 335–346.

Jeong J, Cohu C, Kerkeb L, Pilon M, Connolly EL, Guerinot ML (2008) Chloroplast Fe(III) chelate reductase activity is essential for seedling viability under iron limiting conditions. Proc Natl Acad Sci USA 105: 10619-10624.

Johnson AA, Kyriacou B, Callahan DL, Carruthers L, Stangoulis J, Lombi E, Tester M (2011) Constitutive overexpression of the OsNAS gene family reveals single-gene strategies for effective iron- and zinc-biofortification of rice endosperm. PLoS One. 6: e24476.

Jung KH, Dardick C, Bartley LE, Cao P, Phetsom J, Canlas P, Seo YS, Shultz M, Ouyang S, Yuan Q, Frank BC, Ly E, Zheng L, Jia Y, Hsia AP, An K, Chou HH, Rocke D, Lee GC, Schnable PS, An G, Buell CR, Ronald PC (2008) Refinement of light-responsive transcript lists using rice oligonucleotide arrays: evaluation of gene-redundancy. PLoS One 3: e3337.

Kawachi M, Kobae Y, Mori H, Tomioka R, Lee Y, Maeshima M (2009) A mutant strain *Arabidopsis thaliana* that lacks vacuolar membrane zinc transporter MTP1 revealed the latent tolerance to excessive zinc. Plant Cell Physiol 50: 1156–1170.

Kennedy G, Burlingame B (2003) Analysis of food composition data on rice from a plant genetic resources perspective. Food Chemistry 80: 589–596.

Kikuchi S, Satoh K, Nagata T, Kawagashira N, Doi K, Kishimoto N, Yazaki J, Ishikawa M, Yamada H, Ooka H, Hotta I, Kojima K, Namiki T, Ohneda E, Yahagi W, Suzuki K, Li CJ, Ohtsuki K, Shishiki T; Foundation of Advancement of International Science Genome Sequencing & Analysis Group, Otomo Y, Murakami K, Iida Y, Sugano S, Fujimura T, Suzuki Y, Tsunoda Y, Kurosaki T, Kodama T, Masuda H, Kobayashi M, Xie Q, Lu M, Narikawa R, Sugiyama A, Mizuno K, Yokomizo S, Niikura J, Ikeda R, Ishibiki J, Kawamata M, Yoshimura A, Miura J, Kusumegi T, Oka M, Ryu R, Ueda M, Matsubara K; RIKEN, Kawai J, Carninci P, Adachi J, Aizawa K, Arakawa T, Fukuda S, Hara A, Hashizume W, Hayatsu N, Imotani K, Ishii Y, Itoh M, Kagawa I, Kondo S, Konno H, Miyazaki A, Osato N, Ota Y, Saito R, Sasaki D, Sato K, Shibata K, Shinagawa A, Shiraki T, Yoshino M, Hayashizaki Y, Yasunishi A (2003) Collection, mapping, and annotation of over 28,000 cDNA clones from japonica rice.

Science 301: 376-379.

Kim AM, Bernhardt ML, Kong BY, Ahn RW, Vogt S, Woodruff TK, O'Halloran TV (2011) Zinc sparks are triggered by fertilization and facilitate cell cycle resumption in mammalian eggs. ACS Chem Biol 6: 716-23.

Kim SA, Punshon T, Lanzilotti A, Li L, Alonso JM, Ecker JR, Kaplan J, Guerinot ML (2006) Localization of iron in Arabidopsis seed requires the vacuolar membrane transporter VIT1. Science 314: 1295-1298.

Klatte M, Schuler M, Wirtz M, Fink-Straube C, Hell R, Bauer P (2009) The analysis of Arabidopsis nicotianamine synthase mutants reveals functions for nicotianamine in seed iron loading and iron deficiency responses. Plant Physiol 150: 257-271.

Kobae Y, Uemura T, Sato MH, Ohnishi M, Mimura T, Nakagawa T, Maeshima M (2004) Zinc transporter of Arabidopsis thaliana AtMTP1 is localized to vacuolar membranes and implicated in zinc homeostasis. Plant Cell Physiol 45: 1749–1758.

Kobayashi T, Suzuki M, Inoue H, Itai RN, Takahashi M, Nakanishi H, Mori S, Nishizawa NK (2005) Expression of iron-acquisition-related genes in iron-deficient rice is co-ordinately induced by partially conserved iron-deficiency-responsive elements. J Exp Bot 56: 1305–1316.

Koike S, Inoue H, Mizuno D, Takahashi M, Nakanishi H, Mori S, Nishizawa NK (2004) OsYSL2 is a rice metal-nicotianamine transporter that is regulated by iron and expressed in the phloem. Plant J 39: 415–424.

Kopittke PM, de Jonge MD, Menzies NW, Wang P, Donner E, McKenna BA, Paterson D, Howard DL, Lombi E (2012a) Examination of the distribution of arsenic in hydrated and fresh cowpea roots using two- and three-dimensional techniques. Plant Physiol 159: 1149-1158.

Kopittke PM, Lombi E, McKenna BA, Wang P, Donner E, Webb RI, Blamey FP, de Jonge MD, Paterson D, Howard DL, Menzies NW (2012b) Distribution and speciation of Mn in hydrated roots of cowpea at levels inhibiting root growth. Physiol

Plant doi: 10.1111/j.1399-3054.2012.01674.x.

Korshunova YO, Eide D, Clark WG, Guerinot ML, Pakrasi HB (1999) The IRT1 protein from *Arabidopsis thaliana* is a metal transporter with a broad substrate range. *Plant Mol Biol*. 40: 37–44.

Krämer U, Grime GW, Smith JAC, Hawes CR, Baker AJM (1997) Micro-PIXE as a technique for studying nickel localization in leaves of the hyperaccumulator plant *Alyssum lesbiacum*. *Nuclear Instruments & Methods in Physics Research* 130:346–350.

Krämer U (2010) Metal hyperaccumulation in plants. *Annu Rev Plant Biol* 61: 517–534.

Küpper H, Jie Zhao F, McGrath SP (1999) Cellular compartmentation of zinc in leaves of the hyperaccumulator *thlaspi caerulescens*. *Plant Physiol* 119: 305-12.

Küpper H, Lombi E, Zhao FJ, McGrath SP (2000) Cellular compartmentation of cadmium and zinc in relation to other elements in the hyperaccumulator *Arabidopsis halleri*. *Planta* 212: 75-84.

Küpper H, Lombi E, Zhao FJ, Wieshammer G, McGrath SP (2001) Cellular compartmentation of nickel in the hyperaccumulators *Alyssum lesbiacum*, *Alyssum bertolonii* and *Thlaspi goesingense*. *J Exp Bot* 52: 2291-2300.

Küry S, Dréno B, Bézieau S, Giraudet S, Kharfi M, Kamoun R, Moisan JP (2002) Identification of SLC39A4, a gene involved in acrodermatitis enteropathica. *Nat Genet* 31: 239-240.

Lahner B, Gong J, Mahmoudian M, Smith EL, Abid KB, Rogers EE, Guerinot ML, Harper JF, Ward JM, McIntyre L, Schroeder JI, Salt DE (2003) Genomic scale profiling of nutrient and trace elements in *Arabidopsis thaliana*. *Nat Biotechnol* 21: 1215-1221.

Lan HX, Wang ZF, Wang QH, Wang MM, Bao YM, Huang J, Zhang HS (2012) Characterization of a vacuolar zinc transporter OZT1 in rice (*Oryza sativa* L.). *Mol*

- Lanquar V, Lelièvre F, Bolte S, Hamès C, Alcon C, Neumann D, Vansuyt G, Curie C, Schröder A, Krämer U, Barbier-Bryggo H, Thomine S (2005) Mobilization of vacuolar iron by AtNRAMP3 and AtNRAMP4 is essential for seed germination on low iron. *EMBO J* 24: 4041-4051.
- Laue G, Preston CA, Baldwin IT (2000) Fast track to the trichome: Induction of N-acyl nornicotines precedes nicotine induction in *Nicotiana repanda*. *Planta* 210:510–514.
- Ledford H (2010) Plant biologists fear for cress project. *Nature* 464: 154.
- Lee S, An G (2009) Over-expression of OsIRT1 leads to increased iron and zinc accumulations in rice. *Plant Cell Environ* 32: 408–416.
- Lee S, Chiecko JC, Kim SA, Walker EL, Lee Y, Guerinot ML, An S (2009a) Disruption of OsYSL15 leads to iron inefficiency in rice plants. *Plant Physiol* 150: 786–800.
- Lee S, Jeon US, Lee SJ, Kim YK, Persson DP, Husted S, Schjørring JK, Kakei Y, Masuda H, Nishizawa NK, An G (2009b) Iron fortification of rice seeds through activation of the nicotianamine synthase gene. *Proc Natl Acad Sci USA* 106: 22014–22019.
- Lee S, Jeong HJ, Kim SA, Lee J, Guerinot ML, An G (2010b) OsZIP5 is a plasma membrane zinc transporter in rice. *Plant Mol Biol* 73: 507-17.
- Lee S, Kim SA, Lee J, Guerinot ML, An G (2010a) Zinc deficiency-inducible OsZIP8 encodes a plasma membrane-localized zinc transporter in rice. *Mol Cells* 29: 551-8.
- Lee S, Persson DP, Hansen TH, Husted S, Schjoerring JK, Kim YS, Jeon US, Kim YK, Kakei Y, Masuda H, Nishizawa NK, An G (2011) Bio-available zinc in rice seeds is increased by activation tagging of nicotianamine synthase. *Plant Biotechnol J* 9: 865–873.
- Lemaire K, Ravier MA, Schraenen A, Creemers JW, Van de Plass R, Granvik M, Van Lommel L, Waelkens E, Chimienti F, Rutter GA, Gilon P, in't Veld PA, Schuit FC (2009) Insulin crystallization depends on zinc transporter ZnT8 expression, but is not

required for normal glucose homeostasis in mice. Proc Natl Acad Sci USA 106: 14872-14877.

Li LY, Cai QY, Yu DS, Guo CH (2011) Overexpression of AtFRO6 in transgenic tobacco enhances ferric chelate reductase activity in leaves and increases tolerance to iron-deficiency chlorosis. Mol Biol Rep 38: 3605-3613.

Lin YF, Aarts MG (2012) The molecular mechanism of zinc and cadmium stress response in plants. Cell Mol Life Sci 69:3187-3206.

Lin YF, Liang HM, Yang SY, Boch A, Clemens S, Chen CC, Wu JF, Huang JL, Yeh KC (2009) Arabidopsis IRT3 is a zinc-regulated and plasma membrane localized zinc/iron transporter. New Phytol. 182: 392-404.

Liu X, Lu T, Yu S, Li Y, Huang Y, Huang T, Zhang L, Zhu J, Zhao Q, Fan D, Mu J, Shangguan Y, Feng Q, Guan J, Ying K, Zhang Y, Lin Z, Sun Z, Qian Q, Lu Y, Han B (2007) A collection of 10,096 indica rice full-length cDNAs reveals highly expressed sequence divergence between *Oryza sativa* indica and japonica subspecies. Plant Mol Biol 65: 403-415.

López-Millán AF, Ellis DR, Grusak MA (2004) Identification and characterization of several new members of the ZIP family of metal ion transporters in *Medicago truncatula*. Plant Mol Biol. 54: 583-596.

Lucca P, Hurrell R, Potrykus I (2001) Genetic engineering approaches to improve the bioavailability and the level of iron in rice grains. Theor Appl Genet 21: 184S–190S.

Maret W, Sandstead HH (2006) Zinc requirements and the risks and benefits of zinc supplementation. J Trace Elem Med Biol 20: 3–18.

Marks MD (1997) Molecular genetic analysis of trichome development in arabidopsis. Annu Rev Plant Physiol Plant Mol Biol 48:137-163.

Marschner, H (1995) Mineral Nutrition of Higher Plants, 2nd Edition. Academic Press, Boston, 674 p.

Martell EA (1974) Radioactivity of tobacco trichomes and insoluble cigarette smoke

particles. *Nature* 249: 215-217

McDermid JM, Lönnerdal B (2012) Iron. *Adv Nutr* 3: 532-533.

McKie AT, Marciani P, Rolfs A, Brennan K, Wehr K, Barrow D, Miret S, Bomford A, Peters TJ, Farzaneh F, Hediger MA, Hentze MW, Simpson RJ (2000) A novel duodenal iron-regulated transporter, IREG1, implicated in the basolateral transfer of iron to the circulation. *Mol Cell* 5: 299-309.

Mims MP, Prchal JT (2005) Divalent metal transporter 1. *Hematology* 10: 339-45.

Mizuno D, Higuchi K, Sakamoto T, Nakanishi H, Mori S, Nishizawa NK (2003) Three nicotianamine synthase genes isolated from maize are differentially regulated by iron nutritional status. *Plant Physiol* 132: 1989–1997.

Moreau S, Thomson RM, Kaiser BN, Trevaskis B, Guerinot ML, Udvardi MK, Puppo A, Day DA (2002) GmZIP1 encodes a symbiosis-specific zinc transporter in soybean. *J Biol Chem* 277: 4738-4746.

Mori S, Nishizawa N, Hayashi H, Chino M, Yoshimura E, Ishihara J (1991) Why are young rice plants highly susceptible to iron deficiency? *Plant Soil* 130: 143–156.

Morrissey J, Guerinot ML (2009) Iron uptake and transport in plants: the good, the bad, and the ionome. *Chem Rev* 109: 4553-4567.

Murata Y, Ma JF, Yamaji N, Ueno D, Nomoto K, Iwashita T (2006) A specific transporter for iron(III)-phytosiderophore in barley roots. *Plant J* 46: 563–572.

Nakanishi H, Okumura N, Umehara Y, Nishizawa NK, Chino M, Mori S (1993) Expression of a gene specific for iron deficiency (Ids3) in the roots of *Hordeum vulgare*. *Plant Cell Physiol* 34: 401–410.

Nakanishi H, Yamaguchi H, Sasakuma T, Nishizawa NK, Mori S (2000) Two dioxygenase genes, Ids3 and Ids2, from *Hordeum vulgare* are involved in the biosynthesis of mugineic acid family phytosiderophores. *Plant Mol Biol* 44: 199–207.

Negishi T, Nakanishi H, Yazaki J, Kishimoto N, Fujii F, Shimbo K, Yamamoto K, Sakata K, Sasaki T, Kikuchi S, Mori S, Nishizawa NK (2002) cDNA microarray analysis of gene expression during Fe-deficiency stress in barley suggests that polar transport of vesicles is implicated in phytosiderophore secretion in Fe-deficient barley roots. *Plant J* 30: 83–94.

Nishio JN, Taylor SE, Terry N (1985) Changes in thylakoid galactolipids and proteins during iron nutrition-mediated chloroplast development. *Plant Physiology* 77: 705–711.

Nishiyama R, Kato M, Nagata S, Yanagisawa S, Yoneyama T (2012) Identification of Zn-nicotianamine and Fe-2'-Deoxymugineic acid in the phloem sap from rice plants (*Oryza sativa L.*). *Plant Cell Physiol.* 53: 381–390.

Nishizawa N, Mori S (1987) The particular vesicle appearing in barley root cells and its relation to mugineic acid secretion. *J Plant Nutr* 10: 1013–1020.

Nocito FF, Lancilli C, Dendena B, Lucchini G, Sacchi GA (2011) Cadmium retention in rice roots is influenced by cadmium availability, chelation and translocation. *Plant Cell Environ.* 34: 994–1008.

Norton GJ, Pinson SR, Alexander J, McKay S, Hansen H, Duan GL, Rafiqul Islam M, Islam S, Stroud JL, Zhao FJ, McGrath SP, Zhu YG, Lahner B, Yakubova E, Guerinot ML, Tarpley L, Eizenga GC, Salt DE, Meharg AA, Price AH (2012) Variation in grain arsenic assessed in a diverse panel of rice (*Oryza sativa*) grown in multiple sites. *New Phytol* 193: 650–664.

Nozoye T, Nagasaka S, Kobayashi T, Takahashi M, Sato Y, Sato Y, Uozumi N, Nakanishi N, Nishizawa NK (2011) Phytosiderophore efflux transporters are crucial for iron acquisition in graminaceous plants. *J Biol Chem* 286: 5446–5454.

Okumura N, Nishizawa NK, Umehara Y, Ohata T, Nakanishi H, Yamaguchi T, Chino M, Mori S (1994) A dioxygenase gene (*Ids2*) expressed under iron deficiency conditions in the roots of *Hordeum vulgare*. *Plant Mol Biol* 25: 705–719

- Pfeiffer WH, McClafferty B (2008) Biofortification: breeding micronutrient- dense crops. *Breeding Major Food Staples*: Blackwell Publishing Ltd. 61–91.
- Prasad AS (2003). Zinc deficiency: Has been known of for 40 years but ignored by global health organisations. *BMJ* 326: 409–10.
- Prasad AS (2012) Discovery of human zinc deficiency: 50 years later. *J Trace Elem Med Biol* 26: 66-69.
- Qu le Q, Yoshihara T, Ooyama A, Goto F, Takaiwa F (2005) Iron accumulation does not parallel the high expression level of ferritin in transgenic rice seeds. *Planta* 222: 225-233.
- Ramesh SA, Shin R, Eide DJ, Schachtman DP (2003) Differential metal selectivity and gene expression of two zinc transporters from rice. *Plant Physiol.* 133: 126-134.
- Reddy MB, Hurrell RF, Juillerat MA, Cook JD (1996) The influence of different protein sources on phytate inhibition of nonheme-iron absorption in humans. *Am J Clin Nutr* 63:203-207.
- Rellán-Álvarez R, Sierra JGM, Orduna J, Orera I, Rodríguez-Castrillón JA, García-Alonso JI, Abadía J, Álvarez-Fernández A (2010) Identification of a tri-iron(III), tri-citrate complex in the xylem sap of iron-deficient tomato resupplied with iron: new insights into plant iron long-distance transport. *Plant Cell Physiol* 51: 91-102.
- Ren Y, Liu Y, Chen H, Li G, Zhang X, Zhao J (2012) Type 4 metallothionein genes are involved in regulating Zn ion accumulation in late embryo and in controlling early seedling growth in *Arabidopsis*. *Plant Cell Environ.* 35: 770-789.
- Ricachenevsky FK, Sperotto RA, Menguer PK, Sperb ER, Lopes KL, Fett JP (2011) ZINC-INDUCED FACILITATOR-LIKE family in plants: lineage-specific expansion in monocotyledons and conserved genomic and expression features among rice (*Oryza sativa*) paralogs. *BMC Plant Biology* 11: 20.
- Robinson NJ, Procter CM, Connolly EL, Guerinot ML (1999) A ferric-chelate reductase for iron uptake from soils. *Nature* 397: 694–697.
- Rogers EE, Eide DJ, Guerinot ML (2000) Altered selectivity in an *Arabidopsis* metal transporter. *Proc Natl Acad Sci USA*. 97: 12356-12360.
- Rogers EE, Guerinot ML (2002) FRD3, a member of the multidrug and toxin efflux family, controls iron deficiency responses in *Arabidopsis*. *Plant Cell* 14: 1787-1799.

- Römhild V, Marschner H (1990) Genotypical differences among graminaceous species in release of phytosiderophores and uptake of iron phytosiderophores. *Plant Soil* 22: 147–153.
- Sahrawat KL (2000) Elemental composition of the rice plant as affected by iron toxicity under field conditions. *Communications in Soils Science and Plant Analysis* 31: 2819-2827.
- Sakaguchi T, Nishizawa N, Nakanishi H, Yoshimura E, Mori S (1999) The role of potassium in the secretion of mugineic acids family phytosiderophores from iron-deficient barley roots. *Plant Soil* 215: 221–227.
- Sakai H, Lee SS, Tanaka T, Numa H, Kim J, Kawahara Y, Wakimoto H, Yang CC, Iwamoto M, Abe T, Yamada Y, Muto A, Inokuchi H, Ikemura T, Matsumoto T, Sasaki T, Itoh T (2013) Rice Annotation Project Database (RAP-DB): An integrative and interactive database for rice genomics. *Plant Cell Physiol* doi: doi: 10.1093/pcp/pcs183.
- Sakurai T, Kondou Y, Akiyama K, Kurotani A, Higuchi M, Ichikawa T, Kuroda H, Kusano M, Mori M, Saitou T, Sakakibara H, Sugano S, Suzuki M, Takahashi H, Takahashi S, Takatsujii H, Yokotani N, Yoshizumi T, Saito K, Shinozaki K, Oda K, Hirochika H, Matsui M (2011) RiceFOX: a database of *Arabidopsis* mutant lines overexpressing rice full-length cDNA that contains a wide range of trait information to facilitate analysis of gene function. *Plant Cell Physiol* 52: 265-273.
- Salt DE, Prince RC, Pickering IJ, Raskin I (1995) Mechanisms of cadmium mobility and accumulation in Indian mustard. *Plant Physiol* 109: 427-433.
- Salt DE, Baxter I, Lahner B (2008) Ionomics and the study of the plant ionome. *Annu Rev Plant Biol* 59: 709-733.
- Santi S, Schmidt W (2008) Laser microdissection-assisted analysis of the functional fate of iron deficiency-induced root hairs in cucumber. *J Exp Bot* 59: 697-704.
- Santi S, Schmidt W (2009) Dissecting iron deficiency-induced proton extrusion in *Arabidopsis* roots. *New Phytol* 183: 1072–1084.
- Sarret G, Harada E, Choi YE, Isaure MP, Geoffroy N, Fakra S, Marcus MA, Birschwilks M, Clemens S, Manceau A (2006) Trichomes of tobacco excrete zinc as zinc-

substituted calcium carbonate and other zinc-containing compounds. *Plant Physiol* 141: 1021-1034.

Sarret G, Willems G, Isaure MP, Marcus MA, Fakra SC, Frérot H, Pairis S, Geoffroy N, Manceau A, Saumitou-Laprade P (2009) Zinc distribution and speciation in *Arabidopsis halleri* x *Arabidopsis lyrata* progenies presenting various zinc accumulation capacities. *New Phytol* 184: 581-595.

Sato Y, Namiki N, Takehisa H, Kamatsuki K, Minami H, Ikawa H, Ohyanagi H, Sugimoto K, Itoh JI, Antonio BA, Nagamura Y. RiceFREN: a platform for retrieving coexpressed gene networks in rice (2012a) *Nucleic Acids Res.* DOI: 10.1093/nar/gks1122.

Sato Y, Takehisa H, Kamatsuki K, Minami H, Namiki N, Ikawa H, Ohyanagi H, Sugimoto K, Antonio BA, Nagamura Y (2012b) RiceXPro Version 3.0: expanding the informatics resource for rice transcriptome. *Nucleic Acids Res.* DOI: 10.1093/nar/gks1125.

Satoh-Nagasawa N, Mori M, Nakazawa N, Kawamoto T, Nagato Y, Sakurai K, Takahashi H, Watanabe A, Akagi H (2012) Mutations in rice (*Oryza sativa*) heavy metal ATPase 2 (OsHMA2) restrict the translocation of zinc and cadmium. *Plant Cell Physiol.* 53: 213-224.

Shanmugam V, Lo JC, Wu CL, Wang SL, Lai CC, Connolly EL, Huang JL, Yeh KC (2011) Differential expression and regulation of iron-regulated metal transporters in *Arabidopsis halleri* and *Arabidopsis thaliana* - the role in zinc tolerance. *New Phytol* doi: 10.1111/j.1469-8137.2010.03606.x.

Shanmugam V, Tsednee M, Yeh KC (2012) ZINC TOLERANCE INDUCED BY IRON 1 reveals the importance of glutathione in the cross-homeostasis between zinc and iron in *Arabidopsis thaliana*. *Plant J* 69: 1006-1017.

Shayeghi M, Latunde-Dada GO, Oakhill JS, Laftah AH, Takeuchi K, Halliday N, Khan Y, Warley A, McCann FE, Hider RC, Frazer DM, Anderson GJ, Vulpe CD, Simpson RJ, McKie AT (2005) Identification of an intestinal heme transporter. *Cell* 122:789-

Shahzad Z, Gosti F, Frérot H, Lacombe E, Roosens N, Saumitou-Laprade P, Berthomieu P (2010) The five AhMTP1 zinc transporters undergo different evolutionary fates towards adaptive evolution to zinc tolerance in *Arabidopsis halleri*. PLoS Genet 6: e1000911.

Schilmiller A, Shi F, Kim J, Charbonneau AL, Holmes D, Daniel Jones A, Last RL (2010) Mass spectrometry screening reveals widespread diversity in trichome specialized metabolites of tomato chromosomal substitution lines. Plant J 62: 391-403.

Simmons AT, Gurr GM, McGrath D, Martin PM, Nicol HI (2004) Entrapment of *Helicoverpa armigera* (Hübner) (Lepidoptera: Noctuidae) on glandular trichomes of *Lycopersicon* species. Aust J Entomol 43:196–200.

Sinclair SA, Krämer U (2012) The zinc homeostasis network of land plants. Biochim Biophys Acta 1823: 1553-1567.

Sperotto RA, Boff T, Duarte GL, Santos LS, Grusak MA, Fett JP (2010) Identification of putative target genes to manipulate Fe and Zn concentrations in rice grains. J Plant Physiol 167: 1500-1506.

Sperotto RA, Ricachenevsky FK, Duarte GL, Boff T, Lopes KL, Sperb ER, Grusak MA, Fett JP (2009) Identification of up-regulated genes in flag leaves during rice grain filling and characterization of OsNAC5, a new ABA-dependent transcription factor. Planta 230: 985-1002.

Sperotto RA, Ricachenevsky FK, Waldow Vde A, Fett JP (2012a) Iron biofortification in rice: it's a long way to the top. Plant Sci 190: 24-39.

Sperotto RA, Vasconcelos MW, Grusak MA, Fett JP (2012b) Effects of different Fe supplies on mineral partitioning and remobilization during the reproductive development of rice (*Oryza sativa* L.). Rice 5: 27.

Spiller SC, Terry N (1980) Limiting factors of photosynthesis II: iron stress diminishes photochemical capacity by reducing the number of photosynthetic units. *Plant Physiology* 65: 121-125.

Stacey MG, Patel A, McClain WE, Mathieu M, Remley M, Rogers EE, Gassmann W, Blevins DG, Stacey G (2008) The Arabidopsis AtOPT3 protein functions in metal homeostasis and movement of iron to developing seeds. *Plant Physiol* 146:589-601.

Takahashi M, Yamaguchi H, Nakanishi H, Shioiri T, Nishizawa NK, Mori S (1999) Cloning two genes for nicotianamine aminotransferase, a critical enzyme in iron acquisition (Strategy II) in graminaceous plants. *Plant Physiol* 121: 947–956.

Takahashi R, Ishimaru Y, Shimo H, Ogo Y, Senoura T, Nishizawa NK, Nakanishi H (2012) The OsHMA2 transporter is involved in root-to-shoot translocation of Zn and Cd in rice. *Plant Cell Environ* 35: 1948-1957.

Takizawa R, Nishizawa N, Nakanishi H, Mori S (1996) Effect of iron deficiency on S-adenosyl-methionine synthetase in barley roots J. *Plant Nutr* 19:1189–1200.

Talke IN, Hanikenne M, Krämer U (2006) Zinc-dependent global transcriptional control, transcriptional deregulation, and higher gene copy number for genes in metal homeostasis of the hyperaccumulator *Arabidopsis halleri*. *Plant Physiol.* 142: 148-167.

Tanaka T, Antonio BA, Kikuchi S, Matsumoto T, Nagamura Y, Numa H, Sakai H, Wu J, Itoh T, Sasaki T, Aono R, Fujii Y, Habara T, Harada E, Kanno M, Kawahara Y, Kawashima H, Kubooka H, Matsuya A, Nakaoka H, Saichi N, Sanbonmatsu R, Sato Y, Shinso Y, Suzuki M, Takeda J, Tanino M, Todokoro F, Yamaguchi K, Yamamoto N, Yamasaki C, Imanishi T, Okido T, Tada M, Ikeo K, Tateno Y, Gojobori T, Lin YC, Wei FJ, Hsing YI, Zhao Q, Han B, Kramer MR, McCombie RW, Lonsdale D, O'Donovan CC, Whitfield EJ, Apweiler R, Koyanagi KO, Khurana JP, Raghuvanshi S, Singh NK, Tyagi AK, Haberer G, Fujisawa M, Hosokawa S, Ito Y, Ikawa H, Shibata M, Yamamoto M, Bruskiewich RM, Hoen DR, Bureau TE, Namiki N, Ohyanagi H, Sakai Y, Nobushima S, Sakata K, Barrero RA, Sato Y, Souvorov A,

Smith-White B, Tatusova T, An S, An G, OOta S, Fuks G, Fuks G, Messing J, Christie KR, Lieberherr D, Kim H, Zuccolo A, Wing RA, Nobuta K, Green PJ, Lu C, Meyers BC, Chaparro C, Piegu B, Panaud O, Echeverria M (2008) The Rice Annotation Project Database (RAP-DB): 2008 update. Nucleic Acids Res 36: D1028-33.

Tappero R, Peltier E, Gräfe M, Heidel K, Ginder-Vogel M, Livi KJ, Rivers ML, Marcus MA, Chaney RL, Sparks DL (2007) Hyperaccumulator *Alyssum murale* relies on a different metal storage mechanism for cobalt than for nickel. New Phytol 175: 641-654.

Terry N, Low G (1982) Leaf chlorophyll content and its relation to the intracellular location of iron. Journal of Plant Nutrition 5: 301–310.

Uauy C, Distelfeld A, Fahima T, Blechl A, Dubcovsky J (2006) A NAC Gene regulating senescence improves grain protein, zinc, and iron content in wheat. Science 314: 1298-301.

van de Mortel JE, Almar Villanueva L, Schat H, Kwekkeboom J, Coughlan S, Moerland PD, Ver Loren van Themaat E, Koornneef M, Aarts MG (2006) Large expression differences in genes for iron and zinc homeostasis, stress response, and lignin biosynthesis distinguish roots of *Arabidopsis thaliana* and the related metal hyperaccumulator *Thlaspi caerulescens*. Plant Physiol. 142: 1127-1147.

Vasconcelos M, Datta K, Oliva N, Khalekuzzaman M, Torrizo L, Krishnan S, Oliveira M, Goto F, Datta SD (2003) Enhanced iron and zinc accumulation in transgenic rice with the ferritin gene. Plant Sci 164: 371–378.

Verret F, Gravot A, Auroy P, Preveral S, Forestier C, Vavasseur A, Richaud P (2005) Heavy metal transport by AtHMA4 involves the N-terminal degenerated metal binding domain and the C-terminal His11 stretch. FEBS Lett. 579: 1515-1522.

Vert G, Briat JF, Curie C (2001) *Arabidopsis IRT2* gene encodes a root-periphery iron transporter. Plant J. 26: 181-189.

- Vert G, Grotz N, Dédaldéchamp F, Gaymard F, Guerinot ML, Briat JF, Curie C (2002) IRT1, an *Arabidopsis* transporter essential for iron uptake from the soil and for plant growth. *Plant Cell* 14: 1223-1233.
- Wang K, Zhou B, Kuo YM, Zemansky J, Gitschier J (2002) A novel member of a zinc transporter family is defective in acrodermatitis enteropathica. *Am J Hum Genet* 71: 66-73.
- Wang N, Long T, Yao W, Xiong L, Zhang Q, Wu C (2012) Mutant Resources for the Functional Analysis of the Rice Genome. *Mol Plant*. DOI: 10.1093/mp/ssl142.
- Waters BM, Chu HH, Didonato RJ, Roberts LA, Eisley RB, Lahner B, Salt DE, Walker EL (2006) Mutations in *Arabidopsis* yellow stripe-like1 and yellow stripe-like3 reveal their roles in metal ion homeostasis and loading of metal ions in seeds. *Plant Physiol* 141:1446-58.
- Waters BM, Grusak MA (2008a) Whole-plant mineral partitioning throughout the life cycle in *Arabidopsis thaliana* ecotypes Columbia, Landsberg erecta, Cape Verde Islands, and the mutant line *ysl1ysl3*. *J Exp Bot* 177:389-405.
- Waters BM, Grusak MA (2008b) Quantitative trait locus mapping for seed mineral concentrations in two *Arabidopsis thaliana* recombinant inbred populations. *New Phytol* 179: 1033-1047.
- Waters BM, Uauy C, Dubcovsky J, Grusak MA (2009) Wheat (*Triticum aestivum*) NAM proteins regulate the translocation of iron, zinc, and nitrogen compounds from vegetative tissues to grain. *J Exp Bot* 60: 4263-4274.
- Weinhold A, Baldwin IT (2011) Trichome-derived O-acyl sugars are a first meal for caterpillars that tags them for predation. *Proc Natl Acad Sci USA* 108: 7855-7859.
- White PJ, Broadley MR (2005) Biofortifying crops with essential mineral elements. *Trends Plant Sci* 10: 586-593.
- Wirth J, Poletti S, Aeschlimann B, Yakandawala N, Drosse B, Osorio S, Tohge T, Fernie AR, Günther D, Gruissem W, Sautter C (2009) Rice endosperm iron biofortification by targeted and synergistic action of nicotianamine synthase and ferritin. *Plant Biotechnol J* 7: 631-644.

Yang X, Huang J, Jiang Y, Zhang HS (2009) Cloning and functional identification of two members of the ZIP (Zrt, Irt-like protein) gene family in rice (*Oryza sativa* L.). *Mol Biol Rep.* 36: 281-287.

Yang X, Huang J, Jiang Y, Zhang HS (2009) Cloning and functional identification of two members of the ZIP (Zrt, Irt-like protein) gene family in rice (*Oryza sativa* L.). *Mol Biol Rep.* 36: 281-287.

Yazaki J, Kishimoto N, Ishikawa M, Endo D, Kojima K, MicroArray Center, Kikuchi S. The Rice Expression Database (RED): gateway to rice functional genomics (2002) *Trends in Plant Science* (12):563-564

Yokosho K, Yamaji N, Ueno D, Mitani N, Ma JF (2009) OsFRDL1 is a citrate transporter required for efficient translocation of iron in rice. *Plant Physiol* 149: 297-305.

Yokotani N, Ichikawa T, Kondou Y, Maeda S, Iwabuchi M, Mori M, Hirochika H, Matsui M, Oda K (2009) Overexpression of a rice gene encoding a small C2 domain protein OsSMCP1 increases tolerance to abiotic and biotic stresses in transgenic Arabidopsis. *Plant Mol Biol* 71: 391-402.

Yoneyama T, Gosho T, Kato M, Goto S, Hayashi H (2010) Xylem and phloem transport of Cd, Zn and Fe into the grains of rice plants (*Oryza sativa* L.) grown in continuously flooded Cd-contaminated soil. *Soil Sc Plant Nutr* 56: 445–453.

Yu J, Hu S, Wang J, Wong GK, Li S, Liu B, Deng Y, Dai L, Zhou Y, Zhang X, Cao M, Liu J, Sun J, Tang J, Chen Y, Huang X, Lin W, Ye C, Tong W, Cong L, Geng J, Han Y, Li L, Li W, Hu G, Huang X, Li W, Li J, Liu Z, Li L, Liu J, Qi Q, Liu J, Li L, Li T, Wang X, Lu H, Wu T, Zhu M, Ni P, Han H, Dong W, Ren X, Feng X, Cui P, Li X, Wang H, Xu X, Zhai W, Xu Z, Zhang J, He S, Zhang J, Xu J, Zhang K, Zheng X, Dong J, Zeng W, Tao L, Ye J, Tan J, Ren X, Chen X, He J, Liu D, Tian W, Tian C, Xia H, Bao Q, Li G, Gao H, Cao T, Wang J, Zhao W, Li P, Chen W, Wang X, Zhang Y, Hu J, Wang J, Liu S, Yang J, Zhang G, Xiong Y, Li Z, Mao L, Zhou C, Zhu Z, Chen R, Hao B, Zheng W, Chen S, Guo W, Li G, Liu S, Tao M, Wang J, Zhu L, Yuan L, Yang H (2002) A draft sequence of the rice genome (*Oryza sativa* L. ssp.

indica). *Science* 296: 79-92.

Yu D, Danku JM, Baxter I, Kim S, Vatamaniuk OK, Vitek O, Ouzzani M, Salt DE (2012) High-resolution genome-wide scan of genes, gene-networks and cellular systems impacting the yeast ionome. *BMC Genomics* 13: 623.

Yuan L, Yang S, Liu B, Zhang M, Wu K (2012) Molecular characterization of a rice metal tolerance protein, OsMTP1. *Plant Cell Rep.* 31: 67-79.

Zhang Q, Li J, Xue Y, Han B, Deng XW (2008) Rice 2020: a call for an international coordinated effort in rice functional genomics. *Mol Plant* 1:715-9.

Zhang WH, Zhou Y, Dibley KE, Tyerman SD, Furbank RT, Patrick JW (2007) Nutrient loading of developing seeds. *Funct Plant Biol* 34: 314-331.

Zhang Y, Xu YH, Yi HY, Gong JM (2012) Vacuolar membrane transporters OsVIT1 and OsVIT2 modulate iron translocation between flag leaves and seeds in rice. *Plant J* 72: 400-410.

Zhao H, Eide D (1996a) The yeast ZRT1 gene encodes the zinc transporter protein of a high-affinity uptake system induced by zinc limitation. *Proc. Natl. Acad. Sci. USA* 93: 2454–2458.

Zhao H, Eide D (1996b) The ZRT2 gene encodes the low affinity zinc transporter in *Saccharomyces cerevisiae*. *J. Biol. Chem.* 271: 23203–23210.

Apêndice 1

Artigos publicados no período do doutorado fora do escopo da tese

1. Sperotto RA, Ricachenevsky FK, Duarte GL, Boff T, Lopes KL, Sperb ER, Grusak MA, Fett JP (2009) Identification of up-regulated genes in flag leaves during rice grain filling and characterization of OsNAC5, a new ABA-dependent transcription factor. *Planta* 230: 985-1002. JCR = 3.
2. Stein RJ, Ricachenevsky FK, Fett JP (2009) Differential regulation of the two rice ferritin genes (OsFER1 and OsFER2). *Plant Science* 177: 563-569. JCR = 2.945.
3. Ricachenevsky FK, Sperotto RA, Menguer PK, Fett JP (2010) Identification of Fe-excess-induced genes in rice shoots reveals a WRKY transcription factor responsive to Fe, drought and senescence. *Molecular Biology Reports*, 37: 3735-3745. JCR = 2.929.
4. Sperotto RA, Ricachenevsky FK, Stein RJ, Waldow VA, Fett JP (2010) Iron stress in plants: dealing with deprivation and overload. *Plant Stress* 4: 57-69. Sem fator de impacto.
5. Bruno AN, Carneiro-Ramos MS, Buffon A, Pochmann D, Ricachenevsky FK, Barreto-Chaves ML, Sarkis JJ (2011) Thyroid hormones alter the adenine nucleotide hydrolysis in adult rat blood serum. *Biofactors* 37: 40-45. JCR = 2.959.
6. de Almeida MR, Ruedell CM, Ricachenevsky FK, Sperotto RA, Pasquali G, Fett-Neto AG (2011) Reference gene selection for quantitative reverse transcription-polymerase chain reaction normalization during in vitro adventitious rooting in *Eucalyptus globulus* Labill. *BMC Molecular Biology* 11:73. JCR = 2.857.
7. Sperotto RA*, Ricachenevsky FK*, Waldow Vde A*, Fett JP (2012) Iron biofortification in rice: it's a long way to the top. *Plant Science* 190: 24-39. *Primeira autoria compartilhada. JCR = 2.945.

Apêndice 2

Artigos submetidos no período do doutorado fora do escopo da tese

1. Menguer PK, Farthing E, Peaston KA, Ricachenevsky FK, Fett JP, Williams LE. Functional analysis of the rice vacuolar zinc transporter OsMTP1. Submetido para o periódico “The Journal of Experimental Botany”. JCR = 5.364.
2. Ricachenevsky FK^{*}, Menguer PK^{*}, Sperotto RA^{*}, Fett JP. Roles of plant Metal Tolerance Proteins (MTP) in metal storage and potential use in biofortification strategies. Submetido para o periódico “Frontiers in Plant Physiology”. *Primeira autoria compartilhada. Sem fator de impacto.
3. Ricachenevsky FK, Menguer PK, Sperotto RA. kNACKing on heaven’s door: how important are NAC transcription factors for leaf senescence and Fe/Zn remobilization to the seeds? Submetido para o periódico “Frontiers in Plant Physiology”. Sem fator de impacto.
4. Ricachenevsky FK^{*}, Menguer PK^{*}, Sperotto RA, Fett JP. You’ve got to hide your Zn away: Zn homeostasis, hyperaccumulators, non-accumulators and possible applications in plant biotechnology. Aceito como capítulo no livro “Biotechnological Applications for Environmental Protection”, Springer, New York. *Primeira autoria compartilhada. Sem fator de impacto.
5. Sperotto RA^{*}, Ricachenevsky FK^{*}, Waldow VA, Müller A, Dressler V, Fett JP. Rice grain Fe, Mn and Zn accumulation: how important are flag leaves and seed number? Submetido para o periódico “Plant, Soil and Environment”. *Primeira autoria compartilhada. JCR = 1.078.

Apêndice 3

Curriculum vitae resumido (até março de 2013)

1. Dados Pessoais

Nome: Felipe Klein Ricachenevsky

Local e data de nascimento: Cruz Alta/RS – Brasil, 11/04/1983.

Endereço professional: Universidade Federal do Rio Grande do Sul – Av. Bento Gonçalves, 9500, Laboratório de Fisiologia Vegetal. Porto Alegre –RS – Brasil

Endereço eletrônico: e-mail para contato : felipecruzalta@yahoo.com.br.

2. Formação Acadêmica

2001 – 2005: Graduação em Ciências Biológicas. Universidade Federal do Rio Grande do Sul, UFRGS, Porto Alegre, Brasil.

2005 – 2007: Mestrado em Biologia Celular e Molecular no Centro de Biotecnologia, UFRGS, Porto Alegre, Brasil.
Orientadora: Janette Palma Fett

2009 – 2013: Aluno de Doutorado do curso de Pós-Graduação em Biologia Celular e Molecular do Centro de Biotecnologia, UFRGS, Porto Alegre, Brasil, com estágio-sanduíche no Dartmouth College, EUA.
Orientadora: Janette Palma Fett

3. Atuação Profissional

Universidade Federal do Rio Grande do Sul (UFRGS):

05/2001 – 03/2002: Aluno de iniciação científica no projeto “Estudo de Ornitina Descarboxilase de *Anastrepha fraterculus*”, sob orientação da Prof. Dra. Alice Kalisz de Oliveira.

03/2002 – 09/2003: Aluno de iniciação científica no projeto “Biologia Molecular de Cestódeos”, sob orientação do Prof. Dr. Henrique Bunselmeyer Ferreira.

09/2003 – 10/2004: Aluno de iniciação científica no projeto “Atividade de ecto-nucleotidases em sistema nervoso central e circulatório em modelos de hipo- e hipertireoidismo”, sob orientação do Prof. Dr. João José Freiras Sarkis.

03/2005 – 03/2007: Aluno de Mestrado no laboratório de Fisiologia Vegetal, estando envolvido no projeto “Homeostase de ferro em arroz” sob orientação da Prof. Dra. Janette Palma Fett.

03/2007 – 03/2008: Colaborador no laboratório de Fisiologia Vegetal, estando envolvido no projeto “Homeostase de ferro em arroz” sob orientação da Prof. Dra. Janette Palma Fett.

03/2008 – 03/2009: Bolsista de desenvolvimento técnico no laboratório de Fisiologia Vegetal, estando envolvido no projeto “Identificação de análise da expressão de genes importantes para a translocação de ferro para o grão de arroz”, sob orientação da Prof. Dra. Janette Palma Fett.

03/2009 – atual: Aluno de Doutorado no laboratório de Fisiologia Vegetal, estando envolvido no projeto “Caracterização de linhagens de *Arabidopsis thaliana* super-expressando genes de arroz (*Oryza sativa*) possivelmente relacionados com a homeostase de ferro e zinco”, sob orientação da Prof. Dra. Janette Palma Fett.

Universidade de Cruz Alta:

03/2007 – 10/2007: Atuou como professor das disciplinas de “Bioquímica I” e “Bioquímica II” na Faculdade de Veterinária, ministrando um total de 13 horas-aula semanais.

Universidade Estadual de Campinas (UNICAMP):

04/2010-04/2010: Estágio de curta duraçāoo no laboratório do Prof. Dr. Marcelo Menossi, realizando experimentos do projeto “Localização subcelular de Ferritinhas de arroz”, sob orientação da Prof. Dra Janette Palma Fett.

Purdue University, EUA:

06/2010 – 08/2010: Aluno de doutorado estagiando no Salt Lab, estando envolvido no projeto “Caracterização de linhagens de *Arabidopsis thaliana* super-expressando genes de arroz (*Oryza sativa*) possivelmente relacionados com a homeostase de ferro e zinco”, sob orientação do Dr. David E. Salt.

Dartmouth College, EUA:

03/2011 – 06/2012: Aluno de doutorado-sanduíche no Guerinot Lab , estando envolvido no projeto “Caracterização de linhagens de *Arabidopsis thaliana* super-expressando genes de arroz (*Oryza sativa*) possivelmente relacionados com a homeostase de ferro e zinco”, sob orientação da Dra. Mary Lou Guerinot.

Stanford Linear Accelerator Center (SLAC), EUA:

12/2011 – 06/2012: Usuário do Stanford Sychrotron Radiation Lightsource (SSRL), trabalhando nas linhas de luz 2-3 e 10-2 periodicamente para realização de experimentos relacionados ao projeto “Caracterização de linhagens de *Arabidopsis thaliana* super-expressando genes de arroz (*Oryza sativa*) possivelmente relacionados com a homeostase de ferro e zinco”, sob orientação das Dra. Mary Lou Guerinot e da Dra. Tracy Punshon.

Brookhaven National Laboratory (BNL), EUA:

10/2011 – atual: Usuário do National Synchrotron Light Source (NSLS), trabalhando nas linhas de luz X26A e X27A periodicamente para realização de experimentos relacionados ao projeto “Caracterização de linhagens de *Arabidopsis thaliana* super-expressando genes de arroz (*Oryza sativa*) possivelmente relacionados com a homeostase de ferro e zinco”, sob orientação das Dra. Mary Lou Guerinot e da Dra. Tracy Punshon. Desde 2012, possui projeto próprio, intitulado

“Dynamics of zinc localization and storage in *Arabidopsis thaliana* leaves”, aprovado e possibilitando a obtenção de tempo de uso da linha de luz X27A no NSLS.

4. Prêmios e Títulos

- 2010:** Regulação epigenética em plantas (Carga horária: 80h). Universidade Federal do Rio de Janeiro.
- 2009:** Curso de Bioinformática. (Carga horária: 40h). Universidade de São Paulo.
- 2009:** Alinhamento de Sequências e Filogenética. (Carga horária: 24h). Pontifícia Universidade Católica do Rio Grande do Sul.
- 2009:** Modelagem e Dinâmica Molecular. (Carga horária: 24h). Pontifícia Universidade Católica do Rio Grande do Sul.
- 2008:** Noções e Aplicações em Bioinformática. (Carga horária: 40h). Empresa Brasileira de Pesquisa Agropecuária.
- 2006:** Sistema Gateway de Clonagem. (Carga horária: 20h). Universidade Federal do Rio Grande do Sul, UFRGS, Brasil.
- 2005:** Introdução à Genômica Funcional. (Carga horária: 88h). Instituto de Biologia Molecular do Paraná.
- 2004:** Extensão universitária em Técnicas Histológicas. (Carga horária: 45h). Universidade Federal do Rio Grande do Sul, UFRGS, Brasil.
- 2003:** Extensão universitária em Terapia Gênica. (Carga horária: 20h). Universidade Federal do Rio Grande do Sul, UFRGS, Brasil.
- 2003:** Bioquímica do Câncer. (Carga horária: 6h). Sociedade Brasileira de Bioquímica e Biologia Molecular.
- 2003:** DNA microarrays e sua aplicação. (Carga horária: 3h). Sociedade Brasileira de Genética.
- 2002:** Extensão universitária em Biologia Molecular Básica. (Carga horária: 20h). Universidade Federal do Rio Grande do Sul, UFRGS, Brasil.
- 2001:** Extensão universitária em Manipulação e Diagnóstico Genético de Embriões. (Carga horária: 20h).

5. Prêmios e Títulos

2009 – Co-autor do terceiro melhor trabalho publicado pelos alunos do PPGBCM/UFRGS no ano de 2009.

2010 – Co-autor do quinto melhor trabalho publicado pelos alunos do PPGBCM/UFRGS no ano de 2010.

2011 – Autor do terceiro melhor trabalho publicado por alunos do PPGBCM/UFRGS no ano de 2011.

2013 – Recebeu o “2013 ASPB Travel Award” da American Society of Plant Biologist, para participação no congresso “Plant Biology 2013” em Providence, RI, EUA.

6. Artigos Publicados

1. **Ricachenevsky FK**, Sperotto RA, Waldow VA, Fett JP (2012) Iron biofortification in rice: It's a long way to the top. *Plant Science* 190: 24-39. **JCR 2011 = 2,945**.
2. **Ricachenevsky FK**, Sperotto RA, Menguer PK, Sperb ER, Lopes KL Fett JP (2011) ZINC-INDUCED FACILITATOR-LIKE family in plants: lineage-specific expansion in monocotyledons and conserved genomic and expression features among rice (*Oryza sativa*) paralogs. *BMC Plant Biology* 11: 20. **JCR 2011 = 3,445**.
3. Bruno AN, Carneiro-Ramos MS, Buffon A, Pochmann D, **Ricachenevsky FK**, Barreto-Chaves MLM, Sarkis JJF (2011) Thyroid hormones alter the adenine nucleotide hydrolysis in adult rat blood serum. *BioFactors* 37: 40-45. **JCR 2011 = 4,933**.
4. de Almeida MR, Ruedell CM, **Ricachenevsky FK**, Sperotto RA, Pasquali G, Fett-Neto AG (2010) Reference gene selection for quantitative reverse transcription-polymerase chain reaction normalization during in vitro adventitious rooting in *Eucalyptus globulus* Labill. *BMC Molecular Biology* 11: 73. **JCR 2011 = 2,857**.
5. **Ricachenevsky FK**, Sperotto RA, Menguer PK, Fett JP (2010) Identification of Fe-excess-induced genes in rice shoots reveals a WRKY transcription factor responsive to Fe, drought and senescence. *Molecular Biology Reports* 37: 3735-3745. **JCR 2011 = 2,929**.

6. Sperotto RA, **Ricachenevsky FK**, Stein RJ, Waldow VA, Fett JP (2009) Iron stress in plants: dealing with deprivation and overload. *Plant Stress* 4: 57-69. **Ainda sem fator de impacto.**
7. Sperotto RA, **Ricachenevsky FK**, Duarte GL, Boff T, Lopes KL, Sperb ER, Grusak MA, Fett JP (2009) Identification of up-regulated genes in flag leaves during rice grain filling and characterization of OsNAC5, a new ABA-dependent transcription factor. *Planta*. 230: 985-1002. **JCR 2011 = 3.**
8. Stein RJ, **Ricachenevsky FK**, Fett JP (2009) Differential regulation of the two rice ferritin genes (OsFER1 and OsFER2). *Plant Science*. 177: 563-569. **JCR 2011 = 2,945.**
9. Sperotto RA, **Ricachenevsky FK**, Fett JP (2007) Iron deficiency in rice shoots: identification of novel induced genes using RDA and possible relation to leaf senescence. *Plant Cell Reports*. 26: 1399-1411. **JCR 2011 = 2,274.**
10. Bruno AN, **Ricachenevsky FK**, Pochmann D, Bonan CD, Battastini A, Barreto-Chaves MLM, Sarkis JJF (2005) Hypothyroidism changes adenine nucleotide hydrolysis in synaptosomes from hippocampus and cerebral cortex of rats in different phases of development. *International Journal of Developmental Neuroscience*. 23: 37-44. **JCR 2011 = 2,418.**
11. Bruno AN, Pochmann D, **Ricachenevsky FK**, Bonan CD, Barreto-Chaves MLM, Sarkis JJF (2005) 5'-nucleotidase activity is altered by hypo- and hyperthyroidism in platelets from adult rats. *Platelets*. 16: 25-30. **JCR 2011 = 1,847.**
12. Bruno AN, Diniz GP, **Ricachenevsky FK**, Pochmann D, Bonan CD, Barreto-Chaves MLM, Sarkis JJF (2005) Hypo-and hyperthyroidism affect the ATP, ADP and AMP hydrolysis in rat hippocampal and cortical slices. *Neuroscience Research*. 52: 61-68. **JCR 2011 = 2,25.**
13. Bizarro CV, Bengtson M ; **Ricachenevsky FK**, Zaha A, Sogayar MC, Ferreira HB (2005) Differentially expressed sequences from a cestode parasite reveals conserved developmental genes in platyhelminthes. *Molecular and Biochemical Parasitology*. 144: 114-118. **JCR 2011 = 2,551.**
14. Bruno AN, Pochmann D, **Ricachenevsky FK**, Fontella FU, Bonan CD, Dalmaz C, Barreto-Chaves MLM, Sarkis JJF (2005) Nociceptive Response and Adenine Nucleotide Hydrolysisin Synaptosomes Isolated from Spinal Cord of Hypothyroid Rats. *Neurochemical Research*. 30: 1155-1161. **JCR 2011 = 2,24.**

7. Resumos Publicados em Anais de Congressos

1. **Ricachenevsky FK**, Punshon T, Lahner B, Yakubova E, Lee S, Salt DE, Guerinot ML, Fett JP. Arabidopsis thaliana lines over-expressing rice cDNAs led to functional characterization of a new ZIP transporter and new insights about Zn distribution in leaves. **16th International Symposium on Iron Nutrition and Interactions in Plants**, Amherst, MA, EUA, 2012.
2. **Ricachenevsky FK**, Lahner B, Yakubova E, Salt DE, Guerinot ML, Fett JP. Arabidopsis thaliana overexpressors as a fast system for characterization of metal-related genes from rice (*Oryza sativa*). **Gordon Research Conference on Cell Biology of Metals**, Newport, RI, EUA, 2012.
3. **Ricachenevsky FK**, Punshon T, Lahner B, Yakubova E, Lee S, Salt DE, Guerinot ML, Fett JP. Coupling Arabidopsis heterologous expression, ionomics profiling and synchrotron radiation-based techniques for rapid characterization of metal-related genes from rice (*Oryza sativa*). **6th International Crop Science Congress**, Bento Gonçalves, 2012.
4. **Ricachenevsky FK**, Menguer PK, Lopes KL, Turchetto-Zolet AC, Margis R, Fett JP. Evolution of Vacuolar Iron Transporter 1 (VIT1) proteins in plants and functional characterization of rice paralogs. **6th International Crop Science Congress**, Bento Gonçalves, 2012.
5. Fett JP, Sperotto RA, **Ricachenevsky FK**, Menguer PK, Santos LS, Stein RJ, Boff T. Multiple approaches trying to understand iron and zinc homeostasis in rice plants. **II Simpósio Brasileiro de Genética Molecular de Plantas**, Ilhéus 2011.
6. **Ricachenevsky FK**, Sperotto RA, Menguer PK, Sperb ER, Lopes KL, Fett JP. ZINC-INDUCED FACILITATOR-LIKE family in plants: lineage-specific expansion in monocotyledons and conserved genomic and expression features among rice (*Oryza sativa*) paralogs. **III Simpósio Brasileiro de Genética Molecular de Plantas**, Ilhéus, 2011.
7. Martello CL, Menguer PK, **Ricachenevsky FK**, Fett JP. Análises sobre a família gênica VIT em plantas e caracterização dos genes OsVIT1 e OsVIT2 por meio de transformação de levedura. **XXIII Salão de Iniciação Científica da UFRGS**, Porto Alegre, 2011.
8. Santos LS, Menguer PK, **Ricachenevsky FK**, Lopes KL, Sperotto RA, Fett JP. Expression analysis of the vacuolar metal transporter OsNRAMP7. **8th International Symposium on Rice Functional Genomics**, Bento Gonçalves, 2010.

9. Menguer PK, **Ricachenevsky FK**, Lopes KL, Santos LS, Sperotto RA, Fett JP. Differential regulation of two putative rice vacuolar iron transporter genes (OsVIT1 and OsVIT2). **8th International Symposium on Rice Functional Genomics**, Bento Gonçalves, 2010.
10. **Ricachenevsky FK**, Sperotto RA, Vieira GF, Grunwald MS, Fett JP. Identification of iron-excess-induced genes in rice shoots and possible regulatory role for OsWRKY80. **II Simpósio Brasileiro de Genética Molecular de Plantas**, Búzios, 2009.
11. Fett JP, Sperotto RA, Duarte GL, **Ricachenevsky FK**, Waldow VA, Stein RJ. Iron allocation to the rice grain: multiple approaches in search of key genes. **II Simpósio Brasileiro de Genética Molecular de Plantas**, Búzios, 2009.
12. Sperotto RA, **Ricachenevsky FK**, Duarte GL, Boff T, Lopes KL, Sperb ER, Grusak MA, Fett JP. Rice grain filling: identification of novel induced genes and characterization of OsNAC5. **II Simpósio Brasileiro de Genética Molecular de Plantas**, Búzios, 2009.
13. Lopes KL, Sperotto RA, Duarte GL, Sperb ER, **Ricachenevsky FK**, Boff T, Fett JP. Possível função do gene OsNAC5 em processos de senescência em plantas de arroz. **XX Salão de Iniciação Científica**, Porto Alegre, 2008.
14. **Ricachenevsky FK**, Sperotto RA, Ferreira HB, Fett JP. Construction of cDNA libraries containing sequences up- and down-regulated by iron excess in rice (*Oryza sativa*) shoots. **XXXV Reunião Anual da Sociedade Brasileira de Bioquímica e Biologia Molecular**, Águas de Lindóia, 2006.
15. **Ricachenevsky FK**, Sperotto RA, Fett JP. Isolamento de seqüências de arroz envolvidas na resposta ao excesso de ferro através de RDA (Representational Difference Analysis). **52º Congresso Brasileiro de Genética**, Foz do Iguaçu, 2006.
16. Sperotto RA, **Ricachenevsky FK**, Fett JP. Identificação de novos genes ativados por deficiência de ferro em partes aéreas de arroz (*Oryza sativa L. indica*). **52º Congresso Brasileiro de Genética**, Foz do Iguaçu, 2006.
17. **Ricachenevsky FK**, Sperotto RA, Grunwald, MS, Fett JP. Isolamento e confirmação da expressão diferencial de seqüências de arroz (*Oryza sativa*) envolvidas na resposta ao excesso de ferro. **VIII Reunião Anual do Programa de Pós-Graduação em Biologia Celular e Molecular do Centro de Biotecnologia da UFRGS**, Porto Alegre, 2006.
18. Sperotto RA, **Ricachenevsky FK**, Fett JP. Identificação de novos genes responsivos à deficiência de ferro em raízes de plantas de arroz (*Oryza sativa ssp. indica*). **VIII**

**Reunião Anual do Programa de Pós-Graduação em Biologia Celular e Molecular
do Centro de Biotecnologia da UFRGS, Porto Alegre, 2006.**

19. Sperotto RA, **Ricachenevsky FK**, Fett JP. Expressão gênica diferencial em raízes de plantas de arroz (*Oryza sativa L. ssp. indica*) sob deficiência de ferro. **57º Congresso Nacional de Botânica**, Gramado, 2006.
20. Grunwald, MS, **Ricachenevsky FK**, Fett JP. Confirmação da expressão gênica diferencial em resposta ao excesso de ferro em partes aéreas de plantas de arroz através de RT-PCR semi-quantitativo. **XVIII Salão de Iniciação Científica da UFRGS**, Porto Alegre, 2006.
21. de Rosso AF, da Cruz RP, **Ricachenevsky FK**. Avaliação de genótipos de arroz para tolerância ao frio nos estádios de germinação e plântula. In: IV Congresso Brasileiro de Arroz Irrigado, 2005, Santa Maria. **IV Congresso Brasileiro de Arroz Irrigado**, 2005.
22. **Ricachenevsky FK**, Fett JP. Isolamento de seqüências diferencialmente expressas em resposta ao excesso de ferro em plantas de arroz através da técnica de Representative Difference Analysis (RDA). **VII Reunião Anual do Programa de Pós-Graduação em Biologia Celular e Molecular do Centro de Biotecnologia da UFRGS**, Porto Alegre, 2005.
23. **Ricachenevsky FK**, Bruno AN, Pochmann D, Barreto-Chaves ML, Sarkis JJF. Hipó- e hipertireoidismo afetam a atividade de ecto-nucleotidases de fatias de hipocampo e de córtex cerebral de ratos adultos. **XVI Salão de Iniciação Científica da UFRGS**, Porto Alegre, 2004.
24. **Ricachenevsky FK**, Bruno AN, Pochmann D, Barreto-Chaves ML, Bonan CD, Sarkis JJF. Hypo- and hyperthyroidism affects nucleotidase activity from brain hippocampal and cortical slices of adult rats. **XXXII Reunião Anual da Sociedade Brasileira de Bioquímica e Biologia Molecular**, Caxambú, 2004.
25. Bruno AN, **Ricachenevsky FK**, Pochmann D, Barreto-Chaves ML, Bonan CD, Sarkis JJF. 5'-nucleotidase activity is altered by hypo- and hyperthyroidism in platelets from adult rats. **XXXII Reunião Anual da Sociedade Brasileira de Bioquímica e Biologia Molecular**, Caxambú, 2004.
26. **Ricachenevsky FK**, Bruno AN, Pochmann D, Bonan CD, Battastini AM, Barreto-Chaves ML, Sarkis JJF. Hypothyroidism changes adenine nucleotide hydrolysis in synaptosomes from hippocampus and cerebral cortex of rats in different phases of development. **XIX Reunião Anual da Federação das Sociedades de Biologia Experimental - FeSBE**, Águas de Lindóia, 2004.

27. Böhmer AE, Bruno AN, **Ricachenevsky FK**, Pochmann D, Barreto-Chaves ML, Sarkis JJF. 5'-nucleotidase activity is altered by hypo- and hyperthyroidism in platelets from adult rats. **XIX Reunião Anual da Federação das Sociedades de Biologia Experimental - FeSBE**, Águas de Lindóia, 2004.
28. Bruno AN, **Ricachenevsky FK**, Pochmann D, Barreto-Chaves ML, Sarkis JJF. Hipó- e hipertireoidismo afetam as atividades ecto-nucleotidásicas em fatias de hipocampo de ratos adultos. **XIX Reunião Anual da Federação das Sociedades de Biologia Experimental - FeSBE**, Águas de Lindóia, 2004.
29. Leke R, **Ricachenevsky FK**, Oses JP, Bruno AN, Sarkis JJF, Souza DO, Portela LV. Decrease in nucleotidase activities in serum and cerebral córtex slices after methotrexate treatment. **XIX Reunião Anual da Federação das Sociedades de Biologia Experimental - FeSBE**, Águas de Lindóia, 2004.
30. Bruno AN, Pochmann D, **Ricachenevsky FK**, Urruth F, Barreto-Chaves ML, Sarkis JJF. Hipotireoidismo afeta a resposta nociceptiva e a hidrólise de nucleotídeos da adenina em sinaptossomas de medula espinhal de ratos em diferentes fases do desenvolvimento. **XIX Reunião Anual da Federação das Sociedades de Biologia Experimental - FeSBE**, Águas de Lindóia, 2004.
31. **Ricachenevsky FK**, Bizarro CV, Volweiss A, Bengtson MH, Sogayar MC, Zaha A, Ferreira HB. Isolamento de seqüências diferencialmente expressas em duas fases do ciclo vital do platelminto Mesocestoides corti. **XV Salão de Iniciação Científica**, Porto Alegre, 2003.
32. Volweiss A, Bizarro CV, **Ricachenevsky FK**, Bengtson MH, Sogayar MC, Zaha A, Ferreira HB. Validação de bibliotecas de cDNA subtraídas de Mesocestoides corti (Platyhelminthes, Cestoda). **XV Salão de Iniciação Científica**, Porto Alegre, 2003.
33. Bizarro CV, Volweiss A, **Ricachenevsky FK**, Sogayar MC, Zaha A, Ferreira HB. Isolation of differentially expressed genes during the strobilization of Mesocesoides corti (Platyhelminthes, Cestoda). **XXXII Reunião Annual da Sociedade Brasileira de Bioquímica e Biologia Molecular**, Caxambú, 2003.
34. **Ricachenevsky FK**, Bizarro CV, Volweiss A, Zaha A, Ferreira HB. Caracterização de seqüências expressadas diferencialmente em duas fases do ciclo vital do platelminto Mesocestoides corti. **49º Congresso Brasileiro de Genética**, Águas de Lindóia, 2003.
35. **Ricachenevsky FK**, Bizarro CV, Ferreira HB, Zaha A. Seqüenciamento e análise in silico de genes expressados diferencialmente em duas fases do ciclo vital do

platelminto *Mesocestoides corti*. **XIV Salão de Iniciação Científica**, Porto Alegre, 2002.

36. Cardoso VV, **Ricachenevsky FK**, Prestes PR, Oliveira AK, Moreira JCF. Changes in ornithine decarboxilase activity during *Anastrepha fraterculus* (Wied) development. **XXXI Reunião Anual da Sociedade Brasileira de Bioquímica e Biologia Molecular**, Caxambú, 2002.

8. Apresentação de Trabalho em Congressos

1. **Ricachenevsky FK**. *Arabidopsis thaliana* lines over-expressing rice cDNAs led to functional characterization of a new ZIP transporter and new insights about Zn distribution in leaves. **16th International Symposium on Iron Nutrition and Interactions in Plants**, Amherst, MA, EUA, 2012.
2. **Ricachenevsky FK**, Punshon T, Lahner B, Yakubova E, Lee S, Salt DE, Guerinot ML, Fett JP. Coupling *Arabidopsis* heterologous expression, ionomics profiling and synchrotron radiation-based techniques for rapid characterization of metal-related genes from rice (*Oryza sativa*). **6th International Crop Science Congress**, Bento Gonçalves, 2012.
3. **Ricachenevsky FK**, Menguer PK, Lopes KL, Turchetto-Zolet AC, Margis R, Fett JP. Evolution of Vacuolar Iron Transporter 1 (VIT1) proteins in plants and functional characterization of rice paralogs. **6th International Crop Science Congress**, Bento Gonçalves, 2012.
4. **Ricachenevsky FK**. Ionomics derived research – use of *A. thaliana* FOX lines for rice ionomics research. **First Annual iHUB Meeting 2012**. St Louis, Missouri, Estados Unidos.

9. Revisor de Periódico

1. International Research Journal of Plant Science (IRJPS), 2010 – atual.
2. Journal of Plant Breeding and Crop Science (JPBCS), 2011 – atual.
3. International Journal of Plant Physiology and Biochemistry (IJPPB), 2013 – atual.